Université de Montréal

RAS Small GTPase Signalling to the Enigmatic RASSF Death Effectors

par

Dhanaraman Seetharaman Thillai Villalan

Département de biologie moléculaire

Institut de Recherche en Immunologie et en Cancérologie (IRIC)

Faculté de Médecine

Thèse présentée à la Faculté des médecine en vue de l'obtention du grade de

Ph.D. en biologie moléculaire option biologie des systèmes

Avril 2020

Résumé

Les petites GTPases RAS alternent entre une forme inactive liée au GDP et une forme active liée au GTP. Ce mécanisme permet aux protéines RAS de transmettre les signaux des récepteurs se trouvant à la surface cellulaire vers divers réseaux de signalisation en aval. La protéine RAS joue un rôle important dans plusieurs fonctions biologiques, notamment la prolifération cellulaire, la survie cellulaire et même l'apoptose. Les mutations des gènes de la famille RAS sont retrouvées dans environ un tiers des tumeurs. HRAS, KRAS et NRAS, les trois principaux homologues de la protéine RAS, sont principalement mutées au niveau des codons 12, 13 ou 61. Les mutations avec un effet de gain de fonction au niveau de ces codons rendent ces protéines RAS constitutivement actives et sont à l'origine des signaux hyperprolifératifs. Depuis la découverte de la protéine RAS, de nombreuses "protéines effectrices RAS" agissant en aval ont été identifiées. Le rôle biologique de la plupart de ces effecteurs RAS est lié à la prolifération et à la survie des cellules. Cependant, au cours des deux dernières décennies une nouvelle famille d'effecteurs RAS, les protéines RASSF, a été découverte comme ayant une fonction pro-apoptotique.

Les protéines suppresseures de tumeurs de la famille RASSF sont fréquemment inhibées dans les cellules cancéreuses humaines. Il existe 10 homologues de RASSF (RASSF1-10) chez humain, chacun comprenant un domaine d'association RAS (RA) impliqué dans la liaison avec les GTPases RAS. Plusieurs RASSF comportent également les domaines SARAH (Salvador-RASSF-Hippo), connus pour interagir avec les kinases Hippo contenant aussi les domaines SARAH. On ne sait toutefois pas si toutes les protéines RASSF sont de véritables effecteurs RAS. Il a été démontré qu'un seul membre de la famille RASSF, appelé RASSF5, s'associe directement à HRAS et cette interaction a été validée par des études cristallographiques à rayons X. Dans la première partie de cette thèse, je démontre qu'aucun autre membre de la famille RASSF n'interagit directement avec KRAS. En me servant de la modélisation par l'homologie du domaine RA hautement apparenté de RASSF1, j'ai identifié les acides aminés essentiels pour l'interaction avec la GTPase. Je démontre que la substitution d'un seul acide aminé dans la protéine RASSF1 permet l'interaction avec KRAS, et je pose l'hypothèse que ce résidu, ayant divergé au cours de l'évolution, a modifié la spécificité de RASSF1 pour les petites GTPases.

En utilisant une approche informatique, nous avons prédit six GTPases candidates que pourraient interagir avec RASSF1 : GEM, REM1, REM2, RASL12, ERAS et DIRAS3. J'ai validé les interactions avec plusieurs GTPases RGK (GEM, REM1, REM2) et j'ai démontré que la co-expression des GTPases RGK avec RASSF1 active la voie Hippo. Ainsi, je propose un nouveau lien entre ces GTPases peu étudiées et la régulation de la voie de signalisation Hippo.

Dans la deuxième partie de ma thèse, je tente de rediriger la signalisation de prolifération cellulaire de KRAS (RAF/MAPK) vers une signalisation impliquant les effecteurs pro-apoptotiques (RASSF-Hippo). Pour y parvenir, j'ai conçu des mutations dans KRAS dans le but d'augmenter son affinité pour RASSF5 et d'affaiblir son interaction avec BRAF. Comme deuxième stratégie, j'ai remplacé les résidus divergents de l'effecteur RASSF1 par les résidus correspondants de RASSF5 et j'ai démontré que cette variante de RASSF1 est capable de lier KRAS. Diverses approches biophysiques et biochimiques ont été utilisées pour valider KRAS et RASSF1 mutés, impliquées dans cette signalisation redirigée. Les études de co-localisation montrent que ces mutants interagissent avec leurs nouveaux partenaires comme prévu. D'autre part, je démontre par les expériences intracellulaires que KRAS modifiée ne lie plus BRAF tout en interagissant fortement avec RASSF5 et RASSF1, et que les mutants établis activent la voie Hippo. Ainsi, j'ai développé deux approches qui nous aideront à étudier la signalisation de KRAS dans la voie pro-apoptotique impliquant RASSF en absence de l'activation de la voie des MAP kinases.

Les données présentées ici nous permettent de mieux comprendre la manière dont les protéines RASSF ont divergé au cours de l'évolution; cette divergence leur empêchant d'interagir avec les RAS. Ces données fournissent également une stratégie innovante pour rediriger les signaux RAS vers les effecteurs RASSF, qui pourrait être utilisée comme nouvelle stratégie dans les études cliniques utilisant RAS comme cible thérapeutique.

Mots-clés: RAS GTPase, RGK GTPase, RASSF1, RASSF5, RAF, Apoptosis, signalisation Hippo

Abstract

RAS small GTPases function as molecular switches to transduce signals from cell surface receptors to various downstream signalling networks. The RAS protein has roles in multiple biological functions, including cell proliferation, survival, and even apoptosis. Mutations in *RAS* genes are present in up to 30% of all human tumors. The three major RAS homologs HRAS, KRAS, and NRAS are each found mutated, predominantly at codons 12, 13 or 61. Gain-of-function mutations at these codons render these RAS proteins constitutively active and thereby produce hyperproliferative signals. Since the discovery of RAS, numerous downstream 'RAS effector proteins' have been identified. The biological role of most identified RAS effectors relates to cell proliferation and survival, however, in the past two decades a new family of RAS effectors, RASSF proteins, were discovered to have a pro-apoptotic function.

The RASSF family of tumor suppressors proteins are frequently downregulated in human cancer cells. There are 10 RASSF homologs (RASSF1-10) in humans, each comprising a RAS association (RA) domain presumed to bind RAS GTPases. RASSF also encode SARAH (Salvador-RASSF-Hippo) domain, known to interact with SARAH-containing Hippo kinases. It is not clear whether all the RASSF proteins are true RAS effectors. Only a single family member, RASSF5, has been shown to directly associate with HRAS and this interaction has been completely validated by X-Ray crystallographic studies. In the first part of this thesis, I demonstrate that no other RASSF family members directly interact with KRAS. I used homology modelling of the highly related RASSF1 RA domain to identify amino acids crucial to GTPase binding. I show that a single amino acid substitution in RASSF1 enables interaction with KRAS, and hypothesize that this evolutionarily diverged residue has altered RASSF1 specificity for small GTPases. Using an informatics approach, we predicted six candidate GTPases that could interact with RASSF1: GEM, REM1, REM2, RASL12, ERAS and DIRAS3. I validated interactions with several RGK GTPases (GEM, REM1, REM2) and show that co-expression of RGK GTPases with RASSF1 activates the Hippo pathway. Thus, I show a novel link between these unstudied GTPases to Hippo pathway regulation.

In the second part of my thesis I attempt to rewire KRAS signalling from cell proliferation pathways (RAF/MAPK) to pro-apoptotic effectors (RASSF-Hippo). To achieve

this, I designed mutations in KRAS that augmented its affinity for RASSF5 and weakened interaction with BRAF. As a second strategy, I reverted evolutionarily diverged residues in the RASSF1 effector to corresponding residues in RASSF5 and demonstrate that this variant now binds KRAS. Various biophysical and biochemical approaches were used to validate both the KRAS and RASSF1 rewired mutants, and co-localization studies show that these mutants interact with their new binding partners as predicted. Further, I demonstrate that our rewired KRAS no longer binds BRAF *in cells* but interacts strongly with RASSF5 and rewired RASSF1, and that the rewiring mutants activate the Hippo pathway. Thus, I have developed two rewiring approaches that will help us to study KRAS signalling towards pro-apoptotic RASSF pathway in the absence of strong MAP kinase activation.

The data presented here provide several novel insights into how RASSF proteins diverged through evolution and are not all direct effectors of RAS. In addition, I present an innovative rewiring strategy to couple RAS signals towards RASSF effectors which can be a clinical tactic to target RAS oncogenesis.

Keywords: RAS GTPase, RGK GTPase, RASSF1, RASSF5, RAF, Apoptosis, Hippo signalling

Acknowledgements

Several people made a significant contribution to my Ph.D. studies without them this journey would not have been accomplished. First of all, I would like to thank my research supervisor, Dr. Matthew James Smith, for providing me with the opportunity to work in his lab with an outstanding project. Throughout my studies, I always found him supportive and positive and he offered me the freedom to explore various avenues of the project.

I want to extend my sincere thanks to the committee members, Dr. Marc Therrien, Dr. Alain Verreault, for providing constructive comments on the committee meetings. I am also grateful to other researchers at IRIC for their valuable help during my stay at IRIC. Especially Drs. Pierre Thibault and Claude Perreault for their guidance in the master's project and Drs. Martine Raymond and Benjamin Kwok for scientific and academic assistance. I would also like to thank Dr. Damien D'Amours for my initial Ph.D. studies in his lab.

I am grateful to academic staff for IRIC and UdeM for their timely assistance whenever required. I would also like to thank the funding committee of IRIC, UdeM, FRQNT and SICI for providing me with the fellowships and tuition fees exemptions during my studies.

Special thanks to all the co-authors for their help and comments to prepare the manuscripts. I owe a special thanks to all the IRIC platforms, especially, Christian Charbonneau, for his help with Microscopy.

My special thanks to all the present and past lab members for their scientific and non-scientific help and discussions. First, Dr. Ryan Killoran for his help with NMR experiments, scientific advice and proofreading of my manuscripts. Special thanks to Swati Singh for all her help in choosing the right lab for my Ph.D. studies, scientific and non-scientific decisions. I am thankful to Marilyn and Valerie for sharing their scientific expertise, reagents and assisting me in experiments. Special thanks to Dr. Chang Hwa for teaching me X-Ray crystallography. I want to thank Gabriela for her timely support and encouragement. I owe a special thanks to Chithra for generating the reagents required to work on my second project. At this moment, I would like to thank all the Dr. D'Amours lab members Dr. Yogitha, Dr. Roger, Dr. Guillaume, Mirela and friends especially, Dr. Rahul and Dr. Praveen and Pranesh for their constant support and advice.

Finally, I would like to thank my parents, my mom (Saraswathi), father (Thillai Villalan) and in laws (Poorani, Shanmugaraj) for their constant encouragement and support throughout my life. I owe a special thanks to my wife (Amirthavarshini) for her endless love and support in every way imaginable. A special thanks to my son (Rudhra) who allowed me to write my thesis without disturbing me much. A huge thanks to all the teachers, relatives and friends who have inspired and supported me in my life.

Table of contents

List of figures

Chapter 1

Chapter 2

Chapter 3

Chapter 4

List of tables

Chapter 2

Chapter 3

List of abbreviations

AF6	Afadin
AKT	Protein kinase B
ASPP	Apoptosis stimulating protein of p53
ATM	Ataxia telangiectasia mutant
BSA	Bovine serum albumin
C1	Cysteine rich domain
CaM	Calmodulin
CaMKII	Calmodulin-dependent kinase II
cAMP	Cyclic adenosine monophosphate
CDC24	Cell division control protein 24
CK	Casein kinase
co-IP	Co-immunoprecipitations
COSMIC	Catalogue Of Somatic Mutation In Cancer
C-RASSF	C-terminal RASSF / classical-RASSF
CRD	Cysteine rich domain
DAG	Diacylglycerol
DAPI	4',6-diamidino-2-phenylindole
DMEM	Dulbecco's Modified Eagle Medium
DNA	Deoxyribonucleic acid
dRASSF	*Drosophila* RASSF
DTT	Dithiothreitol
EDTA	Ethylenediaminetetraacetic acid
EGTA	Ethylene glycol tetra acetic acid
EGF	Epidermal growth factor
EGFP	Enhanced green fluorescent protein
EGFR	Epidermal growth factor receptor
ERK	Extracellular signal-regulated kinases
FTase	Farnesyltransferase

GAP	GTPase-activating-proteins
GDP	Guanosine diphosphate
GEF	Guanine nucleotide exchange factors
GGTase1	Geranylgeranyltransferase 1
GMPPNP	5'-Guanylyl imidodiphosphate
GPCR	G-protein coupled receptors
GPPNHP	5'-Guanylyl imidodiphosphate
GST	Glutathione S-transferase
GTP	Guanosine-5'-triphosphate
GTPγS	Guanosine 5'-O-[gamma-thio] triphosphate
HCl	Hydrochloric acid
HeLa	HeLa Henrietta Lacks
HEPES	4-(2-hydroxyethyl)-1-piperazine ethane sulfonic acid
HRP	Horse radish peroxidase
HSQC	Heteronuclear single quantum coherence/ correlation
HVA	High voltage-activated channels
HVR	Hypervariable region
ICMT	Isoprenylcysteine carboxylmethyltransferase
IDX	Intron D exon
ITC	Isothermal Titration
kDa	Kilodalton
LVA	Low voltage-activated channels
MAPK	Mitogen-activated protein kinase
MAPs	Microtubule-binding-proteins
MEK	Mitogen-activated protein kinase kinase
MLL	Mixed-lineage leukemia
MOAP-1	Modulator of apoptosis 1
MST1/2	Mammalian STE-20-like kinases 1 and 2
MTOC	Microtubule-organizing center
NaCl	Sodium chloride

NFκB	Nuclear factor kappa-light-chain-enhancer of activated B
Ni-NTA	Nickle-Nitrilotriacetic acid
NLS	Nuclear localization signal
NMR	Nuclear magnetic resonance
NO	Nitric Oxide
NP-40	Nonyl phenoxypolyethoxylethanol-40
N-RASSF	N-terminal RASSF
PAGE	Polyacrylamide gel electrophoresis
PAR4	Apoptosis response protein 4
PBS	Phosphate buffer saline
PDB	Protein data bank
PDK1	Phosphatidyl inositol-dependent kinase 1 (PDK1
PEI	Polyethylenimine
PFA	Paraformaldehyde
PH	Pleckstrin homology domain
pH	Potential of hydrogen
PI	Propidium iodide
PI3K	Phosphoinositide 3-kinases
PIP2	Phosphatidylinositol-4,5-bisphosphate
PIP3	Phosphatidylinositol-3,4,5-trisphosphate
PLC	Phospholipase C
PTB	Phosphotyrosine binding domain
PTKs	protein tyrosine kinase
RA	RAS Association domain
RASGDS	RAL guanine nucleotide dissociation stimulator
RASL12	RAS-like 12
RASSF1	RAS Association family of protein 1
RASSF10	RAS Association family of protein 10
RASSF2	RAS Association family of protein 2
RASSF3	RAS Association family of protein 3

RASSF4	RAS Association family of protein 4
RASSF5	RAS Association family of protein 5
RASSF6	RAS Association family of protein 6
RASSF7	RAS Association family of protein 7
RASSF8	RAS Association family of protein 8
RASSF9	RAS Association family of protein 9
RBD	RAS binding domain
RCE	RAS converting enzyme 1
RGK	RRAD, GEM, Kir
RNA	Ribonucleic acid
RPT	Palmitoyl transferase
RTK	Receptor tyrosine kinase
SARAH	Salvador-RASSF-Hippo
SDS	Sodium dodecyl sulfate
SH2	Src homology domain - 2
SH3	Src homology domain – 3
SIMIBI	Signal recognition particle, MinD and BioD
SOS	Son of sevenless
TAO	Thousand-and-one
TIAM	T-lymphoma invasion and metastasis protein 1
TNFα	Tumor necrosis factor α
TRAFAC	Translation factor association
TRAIL	TNF-related apoptosis-inducing ligand
TxRED	Texas Red
VGCC	Voltage-gated Ca^{2+} channels

1.   Chapter 1: General Introduction

1.1   Cell Signalling

To respond to fluctuations in their external or internal environments, cells must be able to sense, receive and process signals. Multiple signals are often received in parallel, and cells must integrate these and respond accordingly. The entire cell signalling apparatus consists of numerous components, including: ligands or other initiating signals, receptors, signal transducers and adapter proteins and finally effectors **(Figure 1)**.

1.1.1 Signals or ligands

Cells must respond to various signal stimuli including mechanical, electrical or chemical. Prokaryotic cells, for example, sense and detect nutrients and migrate towards higher concentration of nutrient conditions. Eukaryotic cells can respond to a variety of complex signalling molecules or ligands including hormones, cytokines, growth factors, and neurotransmitters in a highly complex way. This signalling can be broadly classified into two different forms; intercellular signalling and intracellular signalling. Intercellular signalling occurs between two different cells. These events are achieved through extracellular messengers (hormones and other factors), gap junctions, surface proteins and electrical impulses. Various modes of intercellular communication by hormones are determined based on the range of signal transmission: autocrine (acts on the same cell that produced the signal), paracrine (short range signalling between cells), or endocrine (long range signalling). Intercellular signalling through cell-cell contact of surface proteins is called juxtacrine (contact-dependent signalling) **(Figure 1)**. The nature of the signal molecules is highly diverse and includes proteins (hormones, peptides, cytokines, chemokines, growth factors etc.), lipids (steroids, prostaglandins), sugars and their polymers (glucans, zymosans), and nucleic acids. Even a gaseous substance such as nitric oxide (NO) can act as a signal molecule, as either autocrine or paracrine that can easily diffuse through the plasma membrane and regulate pathways related to immune response, vasodilation and cardiac effects [1-3]

In contrast, intracellular signalling events occur within the cells in response to external cues. Upon external stimulation, a signal must cross the plasma membrane and be relayed to specific subcellular locations that produce an appropriate response, e.g. gene expression, messenger ribonucleic acid (mRNA) splicing, protein translation or modification, etc. The external stimuli are usually sensed by the receptors present on the cell surface. The detailed description of types and functions of receptors is expanded in sections below.
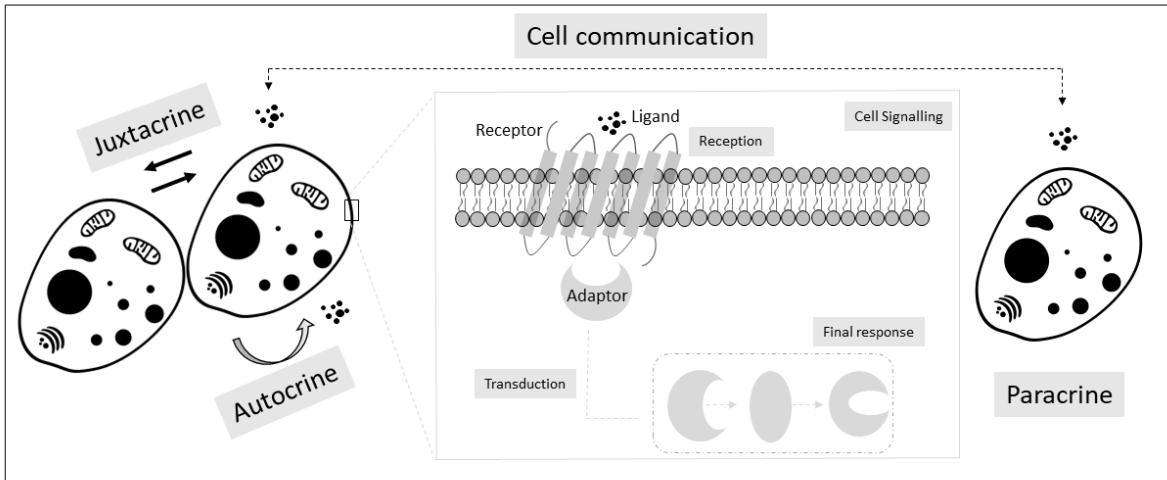
Figure 1: **Schematic of cell signalling components.**

Image shows various components involved in intracellular and intercellular cell signalling process.

1.1.2 Receptors

Cells recognise and respond to stimuli using specialized surface receptors. Cell surface receptors generally span the plasma membrane and comprise an extracellular ligand binding site, a hydrophobic transmembrane domain, and a cytosolic domain. The signalling process starts immediately as the first messenger (ligand) binds a receptor and the receptors transmit this signal to a cytosolic domain. This process commonly includes a conformational change in the protein or oligomerization of several ligand-bound receptors. The cytosolic domains are typically associated with complex enzyme-linked machinery, particularly kinases and phosphatases, and associated with a variety of adaptor and scaffolding-proteins. These

machineries generate secondary messengers that amplify and transduce the signals to downstream effectors. The cell surface receptors are broadly classified into many types, including, G-protein coupled receptors (GPCRs) [4], enzyme linked receptors and receptor tyrosine kinases (RTKs) [5], ionotropic receptors [6], cytokine receptors [7], tumor necrosis factor (TNF) family of receptors [8], etc., are reviewed in detail on [9].

1.1.3 Modular Domains

Receptors are highly specific in nature and bind ligand with high affinity. As with most signalling proteins, receptor specificity is due to the composition of its modular protein domains. A domain is a structurally folded protein region that plays a crucial role in various cellular processes by undergoing highly specific and reversible interaction with partners. Protein domains can be variable in length but are generally comprised of 50 to 250 amino acids [10]. One of the first identified and subsequently most studied domains, the Src homology domain (SH3), consist of approximately 50 amino acids and specifically binds to proteins containing proline rich sequences in PxxP motifs (P being proline and x any amino acid) with left-handed polyproline 2 (PPI) conformations [11]. SH3 domains are frequently present in proteins regulating actin cytoskeleton functions, including phosphoinositide 3-kinases (PI3K), RAS-GTP activating-proteins, CDC24, phospholipase C, myosin, etc. [12, 13]. Another archetypal signalling domain, Src homology 2 (SH2) domains are approximately 100 amino acids and are present in signalling pathways comprising protein tyrosine kinases (PTKs), phospholipases (PLCγ1), protein phosphatases (Shp2, SHIP2), and signal regulator proteins (SOCS). SH2 domains recognize phosphorylated tyrosine (pTyr) residues within specific motifs of target proteins [12, 14]. Indeed, binding specificity is determined by three amino acids carboxy-terminal of the pTyr residue. For example, Src kinase SH2 domains recognizes pYEEI residues while Grb2 SH2 domain binds pYVNV residues [15-17].

The pleckstrin homology domain (PH) consists of approximately 120 amino acids and is known to bind phosphatidylinositol lipids [18], protein kinase C [19] and $\beta\gamma$- subunits of heteromeric G-proteins [20]. The major function of the PH domain is to recruit interacting partners to various membranes and target them to several cellular compartments or assist them

to interact with other proteins of signalling pathways. In addition to above mentioned, one of the most highly studied modular binding domains is the RAS-binding domain (RBD) found in RAS effectors. A description of RBDs is detailed in sections 1.3. The human proteome contains more than 150 interaction domains as listed in Simple Modular Architecture Research Tool (SMART) database and several hundreds in nuclear and extracellular region [21, 22] that are crucial for signalling from different types of cell surface receptors to diverse cellular functions and locales.

1.1.4 Signal Transducers

A diverse and substantial array of cellular machinery is devoted to transmitting signals from cell surface receptors to intracellular responses. As mentioned above, the three major cell surface receptors are: GPCRs, RTKs and ionotropic receptors and the mechanistic operations of signal transduction are generally different in each case [9]. For example, GPCRs, upon ligand binding, undergo a conformational change and recruit a cytosolic adaptor heterotrimeric G-protein that is subsequently activated by GTP-binding [23]. Activated heterotrimeric G-proteins are disassociated into Gα and Gβγ subunits. The Gα subunit in turn stimulates the variety of second messengers such as phospholipase C (PLC) [24], RHOGEFs [25], cAMP [26]. Gβγ activates various ion channels such as, P/Q- and N-type voltage-gated Calcium (Ca^{2+}) channels [27], potassium (K^+) channels [28], and adenylyl cyclase isoforms [26], PLC isoforms [29], and PI3K isoforms [30]. GPCRs are the largest family of cell surface receptors with a range of functions from growth and hormone response to sensations.

In the case of RTKs, these tyrosine kinases undergo ligand-induced dimerization resulting in activation of cytoplasmic kinase domains by transphosphorylation of key tyrosine residues. Subsequent phosphorylation events generate binding sites for various proteins containing SH2 or PTB (phosphotyrosine-binding domains) domains, [5, 13]. Adapter proteins containing serine, threonine and tyrosine are highly likely to undergo phosphorylation themselves, which generates further binding motifs for downstream proteins or can induce conformational changes responsible for activation of downstream target proteins.

Ionotropic receptors, or ligand-gated ion channels, bind ions such as Na^+, K^+, Ca^{2+}, and Cl^-. The transmembrane channel opens and allows influx of these ions. Various ion-binding enzymes respond to the change in local ion concentration to regulate downstream signalling. A detailed mechanism of action for voltage-gated Ca^{2+} channels is explained in section 1.4.6. Though these insights help us understand how various receptor-mediated signal transduction function, these events are highly complex and feed into vast networks responsible for signal response. There remain many avenues to be explored in order to completely understand this multifaceted machinery. In this thesis, I will focus on the transducers of RTKs that activate G-proteins and their downstream effector pathways upon external stimuli.

1.1.5 G-proteins

"G-proteins" are a diverse family of cellular proteins involved in the initiation and relay of signalling cascades. They are named based on an ability to bind the guanine nucleotides guanosine-5'-triphosphate (GTP) or guanosine diphosphate (GDP). G-proteins are classified as larger, heteromeric G-proteins or monomeric small GTPases. Heteromeric G-proteins comprise three distinct subunits (α, β, and γ). The α-subunit of heteromeric G-proteins (Gα) binds either GTP or GDP. Under normal circumstances, Gα- is bound to GDP and the β- and γ-subunits bind Gα to form a Gαβγ inactive trimer. Binding of an external ligand to GPCRs allows inactive Gαβγ trimers to bind the receptor, causing GDP to be replaced with GTP. When GTP bound, Gα dissociates from Gβγ which activates both the subunits, with both Gα and Gβγ subunits binding various downstream effectors to regulate diverse cellular processes.

Monomeric G-proteins, the focus on my thesis, are key switch proteins that transmit signals from activated cell surface receptors. Monomeric or 'small' G-proteins are similar in sequence and structure to a larger family called P-loop GTPases, which all contain a conserved Walker A motif (GxxxxGKS/T); a flexible loop segment [31-33] that functions to properly position the triphosphate moiety of the bound nucleotide. P-loop GTPases can be classified into two major groups: the translation factor association (TRAFAC) group containing GTPases related to translation/elongation factor and a second group containing proteins associated with signal recognition particle, MinD, and BioD (the SIMIBI group). The TRAFAC group of

proteins comprises translation factors, <u>ra</u>t <u>s</u>arcoma (RAS)-like small GTPases, septin GTPases, myosin/kinesins, Dynamins, OBG/HfiX and GNI/RHD3 [34]. The first discovered monomeric G-protein was the RAS small GTPase. RAS GTPases relay signals from receptor kinases to the nucleus using various downstream effector proteins and signalling from these and related small GTPases will be addressed in detail below.

1.2 RAS Small GTPases

1.2.1 The RAS superfamily

The RAS superfamily of small GTPases comprises more than 170 structurally related members that govern a diverse array of signalling pathways and cellular functions [35]. Members of the RAS superfamily are highly evolutionarily conserved with orthologs found in *Drosophila, C. elegans, S. cerevisiae, S. pombe, Dictyostelium,* and plants [35]. RAS superfamily GTPases are broadly classified into five subfamilies; RAS [36], RHO [37], RAB [38], RAN [39] and ARF [40] **(Figure 2)**, which are further classified into various subgroups. Structurally, RAS proteins have five conserved 'G-domains' (G1-G5) that function as a guanine nucleotide-dependent switch. Archetypally, RAS GTPases are in the "active" state when bound to GTP and are "inactive" when GDP-bound. Most members of the small GTPase superfamily have high affinity for GTP and GDP but possess low intrinsic GTP hydrolysis and GTP/GDP exchange rates, though it is not clear if this is true of all members. In the cell, guanine-nucleotide-exchange factors (GEFs) promote GTP loading to activate the protein. GTPase-activating proteins (GAPs) accelerate GTPase activity to promote the formation of the inactive, GDP-bound form. This entire process is called the RAS GTPase cycle **(Figure 3)**. My thesis will primarily focus on two groups in the RAS subfamily of small GTPase proteins: RAS and RGK small GTPases [41, 42].
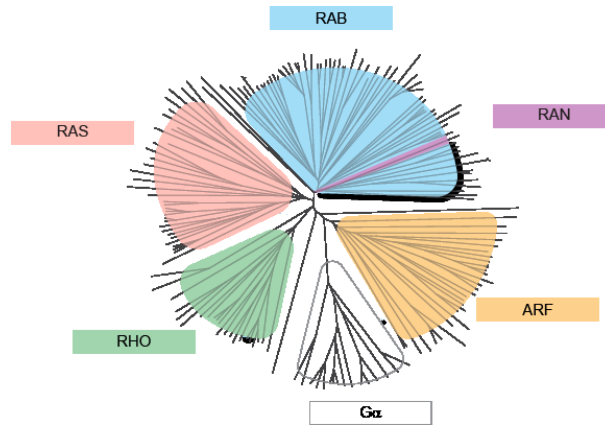
Figure 2:   **The RAS superfamily of GTPase**

The RAS super family of small GTPase consists of five major protein families RAS, RHO, RAN, RAB, and ARF.
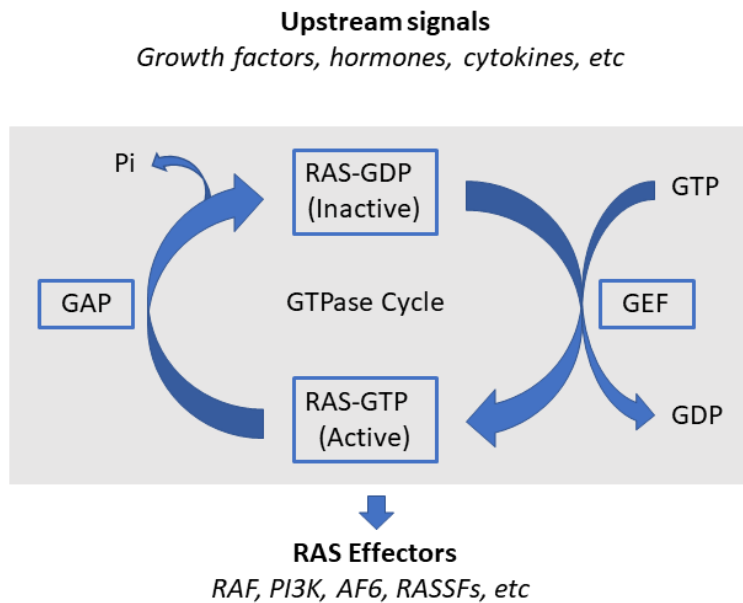
Figure 3:   **The GTPase cycle**

Active RAS is GTP-bound and inactive RAS is GDP-bound. GTP-bound active RAS binds various downstream effectors. GEFs and GAPs assists RAS in its GTP/GDP cycling

1.2.2 RAS discovery

Study of RAS small GTPases has played a crucial role in understanding the fundamental concepts of cell signalling and molecular oncology. Over the course of 30 years, various members of the RAS superfamily have been discovered and characterized. Extensive research on transforming retroviruses isolated from rats, mice, cats, chicken and monkey were conducted throughout the 20th century. As a result, the *RAS* oncogenes were discovered in the late 1960s, the first being the Harvey murine sarcoma virus, discovered by Jennifer Harvey in 1964. Harvey injected Maloney's leukemogenic virus from a leukemic rat into new-born mice, which led to a rapid formation of sarcomas [43]. Kirsten and Mayer, in 1967, discovered the Kirsten murine sarcoma virus. They also observed the development of sarcoma in new-born rats following injection of plasma or spleen filtrates from mice that were infected with an erythroblastosis virus [44]. These oncogenic viruses provided an indication that genetic material has transforming properties. The gene name for *RAS* was coined in the 1970s (after a nomenclature procedure was adapted for retroviral genes) as *HRAS* and *KRAS* based on their ability to form rat sarcomas and along with their discoverer's name. In the late 1970s, Scolnick and colleagues conducted an extensive study that lead to the recognition of a cellular origin for the viral *HRAS* and *KRAS* genes [45, 46]. They later found these genes encode 21 kDa proteins [47] that bind both GTP and GDP [48], and are found associated with the cellular plasma membrane [49]. In the early 1980s, using a DNA transfection assay and mouse fibroblast cells (NIH 3T3), activated oncogenes were detected in genomic DNA of developed tumors. Soon after, it was established that ectopic expression of oncogenic *HRAS* could transform NIH 3T3 cells [50]. Later studies using molecular cloning of wild-type and oncogenic *HRAS* showed the mechanism of *HRAS* gene activation as a single point mutation at position 12, 13 or 61 [51-54]. This made *HRAS* the first gene derived from human cells whose oncogenic properties and mechanism of activation was characterized at a molecular level. In 1983, *NRAS* was discovered by Hall and colleagues [55] and finally, in 1984, the mutated *KRAS* gene was discovered from tumor biopsies [56]. Exhaustive research spanning more than 20 years thus led to the identification and initial characterization of the three RAS oncogenes, however, how RAS signals to activate downstream pathways remained an open question.

1.2.3 RAS isoforms and splice variants

RAS GTPases are now recognized as core components of signal transduction networks governing cell proliferation. Mammalian cells ubiquitously express three RAS proto-oncogenes: *HRAS, KRAS,* and *NRAS*, which share a high degree of sequence homology. Among the three isoforms, *HRAS* (11p15.5) is the smallest gene consisting of 5,046 bp, followed by *NRAS* (1p13.2) at 12,431 base pairs and the largest, *KRAS* (12p12.1), at 46,148 bp. The KRAS gene is comprised of exons -1, -2, -3, -4a and -4b. Alternative splicing of exon 4 results in two mRNA transcripts that are translated into the KRAS-4a and KRAS-4b proteins [51, 57]. Compared to KRAS-4a, KRAS-4b is predominant and ubiquitously expressed in cells [58]. HRAS is encoded by 4 exons (1-4), the HRAS gene also contains an alternative exon that is represented as intron D exon (IDX). Single point mutations in the IDX region are known to increase the translation efficiency of HRAS [59, 60]. NRAS is expressed as five distinct isoforms as a result of alternative splicing. Five transcripts encode proteins of different lengths (20 to 208 amino acids) and expression patterns [61]. Despite these differential expression and translation patters, RAS proteins appear to have a high degree of overlapping biological functions.

1.2.4 Structural details of RAS isoforms

Structural biology studies of RAS small GTPase proteins have provided remarkable insight to the mechanism of its signal relay function. As mentioned above, mammals express four major isoforms of the *RAS* proto-oncogene; HRAS, KRAS (KRAS-4a and KRAS-4b) and NRAS. All of the predominantly expressed proteins are roughly 21 kDa (188/9 amino acid residues) with near-complete sequence homology between residues 1-165. Differences in the sequence are mainly observed in what is termed the hypervariable region (HVR) at the extreme C-terminus of the protein (only 15% sequence similarity in HVR regions among 4 isoforms) [62, 63] **(Figure 4A).** The RAS structure comprises five G domains (G1 to G5) with topology around a central β-sheet of 6 strands (β1-β6) and five surrounding α-helices (α1-α5) [64, 65]. The G1 domain contains the Walker A motif, also known as the P-loop (amino acids 10-17), with the conserved sequence GxxGxGKS/T (x as any amino acid). This region interacts with

the β and γ-phosphates of GTP or the β-phosphate of GDP [33, 65-67]. The P-loop is followed by a switch I region from amino acids 32–38 that form a loop and short β-strand. The G2 domain (xTx) is present in the switch I region. The oxygen atom of the γ-phosphate of GTP hydrogen bonds with a completely conserved threonine residue (T35) in the G2 domain [68, 69]. T35 of RAS also interacts with a Mg^{2+} ion and is essential for GTP hydrolysis **(Figure 4B)**. Upon GTP binding, the switch I region undergoes a conformational change that involves stabilization of the β-strand, resulting in sensing and binding of downstream effectors. The G2 domain is also called the effector loop as it is a primary interaction site for effectors, regulatory GAPs and GEFs (discussed in sections 1.3.2 and 1.3.3). The switch II region spans amino acids 59–67, and forms a helical/loop segment [68] that includes the G3 motif (DxxG). This motif provides several key residues for Mg^{2+} and γ-phosphate binding and undergoes a conformational change dependent on the guanine-nucleotide bound. The final two G domains, G4 (N/TKxD) and G5 (SAK/L), participate in interactions and recognition of the guanosine base [69] **(Figure 4A, B)**. Though the domain architecture of RAS isoforms are highly identical and have overlapping biological functions, the biochemical activities of RAS superfamily proteins can be quite divergent [70].

A)
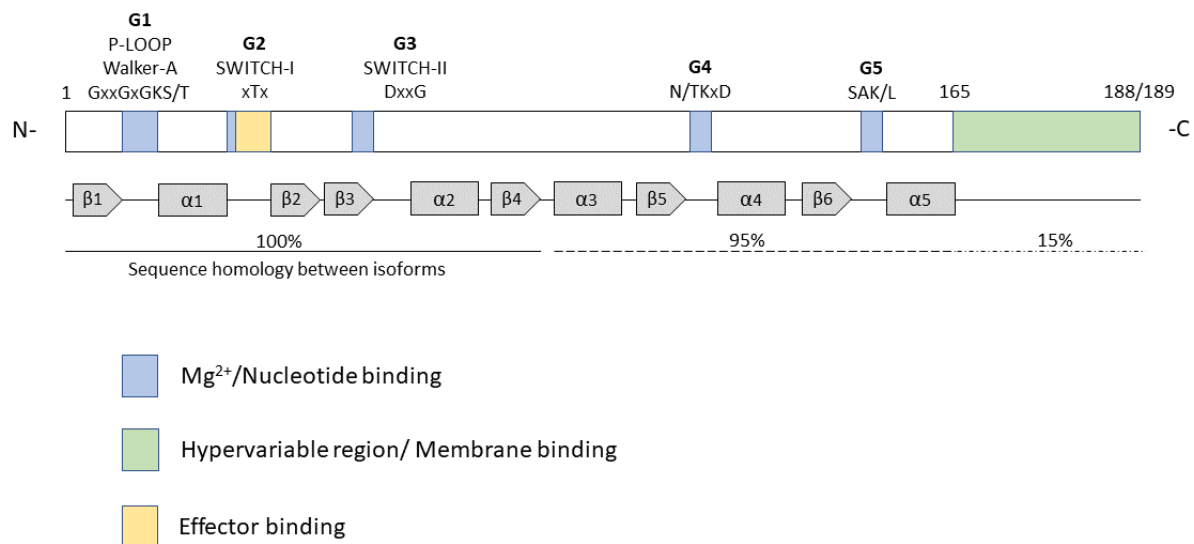
B)
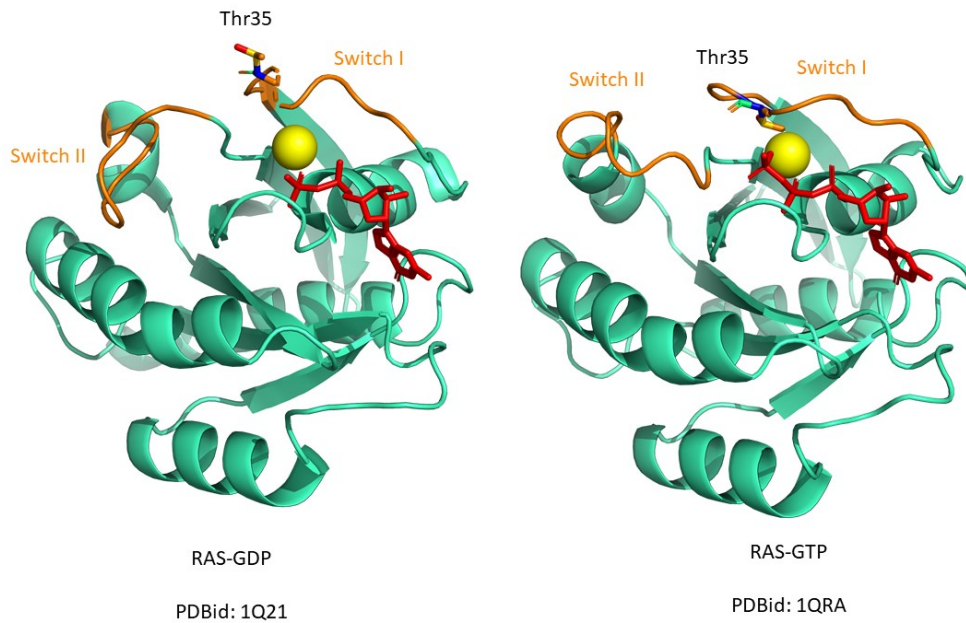
Figure 4: **Domain architecture and structural details of RAS protein**

A) Domain architecture of RAS GTPase. RAS GTPase contains ten loops that interconnects six β-sheets and five α-helices. The major sequence difference among the three major isoforms are at the hypervariable region. **B)** Crystal structure of inactive GDP-bound RAS (PDBid: 1Q21) and active GTP-bound RAS (PDBid: 1QRA). Switch I and switch II regions are highlighted in orange color, bound nucleotide (red) and magnesium ion (yellow). Amino acid (Thr35) shows dramatic change in its interaction with magnesium ion compared between active and inactive RAS

1.2.5 Modifications and membrane localization of RAS GTPases

The RAS HVR comprises approximately 25 amino acid residues and post-translational modification of specific residues is essential for trafficking and membrane anchoring of RAS GTPases [71]. Post-translational modification of HVR residues includes phosphorylation, ubiquitination, sumoylation, acetylation, nitrosylation, farnesylation, palmitoylation, and geranylgeranylation [71]. A motif called CAAx (A is an aliphatic amino acid and "x" is any

amino acid) is present in the C-terminal HVR of many RAS subfamily proteins [72]. The CAAx motif can be modified by three enzymes, farnesyltransferases (FTase), prenyltransferases or geranylgeranyltransferase 1 (GGTase1) [73]. Processing and modification of the CAAx region is essential to anchor RAS GTPases to the plasma membrane [71]. The attachment of a 15-or 20- carbon isoprenyl group is the first step in the CAAx processing. CAAx sequences ending with Ser or Met are modified by FTase and CAAx sequences ending in Leu are modified with GGTase1 [74, 75]. Following CAAx isoprenylation the RAS converting enzyme 1 (RCE), an endoprotease, removes the last 3 amino acids from the CAAx motif (AAx) to create a prenylcysteine as the new C-terminus [76-78]. The final CAAx processing step is performed by isoprenylcysteine carboxylmethyltransferase (ICMT), which methylesterifies the α carboxyl group of C-terminal prenylcysteines [79, 80]. This CAAx modification serves to neutralize negative charges in the C-terminal region and make the hydrophilic C-terminus of RAS hydrophobic for membrane-anchoring. All four major isoforms of RAS undergo modifications at residue Cys corresponding to C186 in HRAS by FTase, however, farnesylation alone is not enough to consistently target RAS to its plasma membrane destination. HRAS undergoes palmitoylation at residues C181 and C184 by palmitoyl transferase (RPT), NRAS has one reported site for palmitoylation at residue C181, and KRAS-4a is palmitoylated at residue C180. KRAS-4b lacks the site for palmitoylation, but in contrast contains a poly-basic region rich in lysine residues. These positively charged amino acids interact with negatively charged lipids at the plasma membrane [72]. Palmitoylation of HRAS, NRAS, and KRAS-4a directs these RAS proteins to exocytic pathways through the Golgi before finally reaching the plasma membrane [81-83]. Once trafficked and anchored to the plasma membrane, RAS can be activated in response to external stimuli. For example, upon epidermal growth factor (EGF) stimulation autophosphorylation of the EGF receptor (EGFR) at multiple tyrosine residues recruits the cytoplasmic, SH2 domain-containing protein GRB2, which in complex with SOS (Son of sevenless) becomes membrane-proximal. SOS, a GEF, activates RAS GTPases adjacent in the plasma membrane to ultimately signal to downstream pathways [84].

1.2.6 RAS signalling: oncogenic mutants and structural differences

Cancer develops by the uncontrolled division of cells. Analysis of human tumors shows that RAS proto-oncogenes are frequently mutated with a compounded mutation rate of 30% [85]. The three ubiquitously expressed RAS proto-oncogenes *HRAS, NRAS* and *KRAS* show single point mutations mainly at positions 12, 13 and 61. The occurrence of these mutations in RAS makes the cell hyper-proliferative. According to the Catalogue Of Somatic Mutation In Cancer (COSMIC) database [86], *KRAS* is most frequently mutated (22% of all cancers), followed by *NRAS* (8%) and *HRAS* (3%). There is a highly intriguing polarity of mutations, with 80% of KRAS mutations occurring at codon 12 and very few at codon 61. For NRAS, 60% of mutations occur at position 61 and only 35% at position 12, and 50% of HRAS mutations are at position 12 versus 40% at position 61. The reason for these divergences is not completely understood. As mentioned above, RAS mutations at position 12/13 are resistant to GAP activity and lock the protein in an active, GTP-bound state. Substitution of the glycine residue at position 12 or 13 with any amino acid will hinder GTPase activity. Substitution of a proline at residue 12 is the only exception that does not render the protein oncogenic [87]. Similarly, mutation at Gln 61 (Q61) of RAS affects its intrinsic catalytic activity.

Structurally, both wildtype and mutant RAS GTPases are highly similar **(Figure 5).** This implies that signalling abnormalities induced by these proteins are instead a result of altered protein dynamics or direct changes in protein interactions. ^{31}P NMR experiments revealed that even wildtype, GTP-bound RAS actually assumes two inter-convertible conformations, specified as state 1 and state 2. These are characterized by altered positioning of the switch I residue Tyr 32 (Y32) relative to the bound nucleotide. In state 1, Y32 is directed away from the nucleotide compared to state 2, where Y32 is found much closer to the γ-phosphate groups [88]. It is believed that wild-type RAS can switch between these two states every few milliseconds. For HRAS-GppNHp, (5'-guanylyl imidodiphosphate, a non-hydrolysable GTP analog) the population in state 1 is 36% [89] but for mutant RAS proteins, this equilibrium shifts significantly. In RAS G12D, a mutant that frequently drives pancreatic cancer, both states are still observed, but state 1 dominates due to an abnormal hydrogen bond between Y32, Q61 and the mutant aspartate that exposes Pro 34 (P34) at the protein surface [87, 90] **(Figure 5).** Slight changes in the orientation of Y32 in RAS G12V and Q61 mutants

also shifts the equilibrium between the two conformational states compared to wild-type [91], with G12V HRAS-GppNHp having a population of 53% in state 1 and Q61L HRAS-GppNHp with 58% state 1 [89]. These differences in the state 1-2 equilibrium between wild-type and mutant RAS are believed to have massive importance to their biological activity.
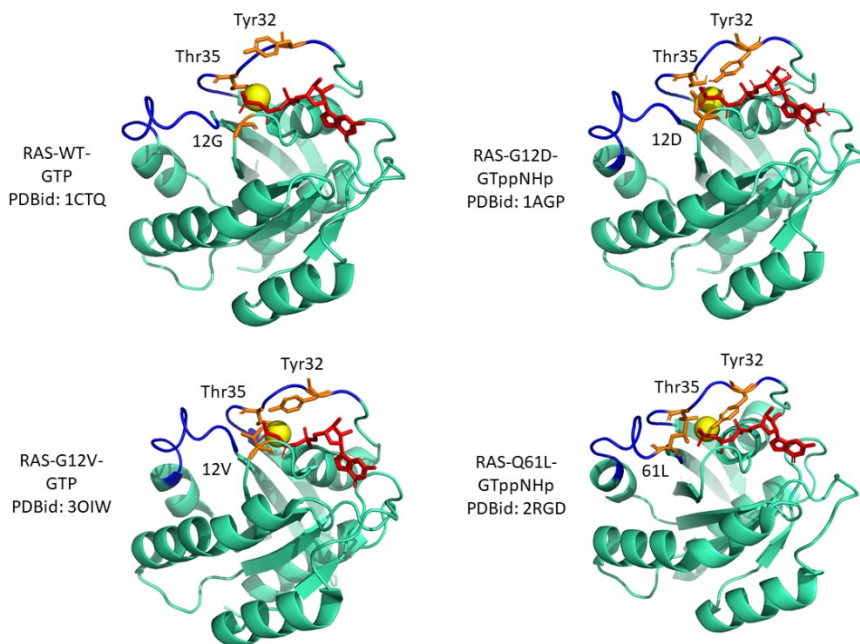
Figure 5: **Image showing the structural difference between major RAS mutants**

Switch regions are highlighted in (blue), bound nucleotide (red) and magnesium (yellow) color. Positioning of amino acids (Thr35, Tyr 32) in response to various RAS mutations (12G, 12D, 12V and 61L) are highlighted.

Furthermore, compared to wildtype RAS, oncogenic mutants show highly divergent binding to guanine nucleotides. For example, wild-type RAS or RAS-G12V has an 8-fold weaker dissociation rate for GTP compared to G12D [92]. Mutant RAS proteins also display impaired intrinsic GTPase activity, with both the G12V and G12D mutants of HRAS retaining just 12% and 43% of wild-type GTPase activity [93]. These differences in enzymatic activity among RAS mutants are reflected in their ability to transform cells. G12V shows a strong ability to transform the cells compared to other HRAS mutants (G12D, G12C, G12A) [94-96], consistent with data showing KRAS G12V induces tumors in nude mice at a shorter time

compared to G12C and G12D [97] . Indeed, codon-specific mutation greatly affects the degrees of tumorigenesis as mutations at codon 12 exhibit much stronger tumorigenic activity compared to mutations at position 13 [95, 98]. In an NIH 3T3 transformation assay, cells expressing KRAS-G12D showed increased colony density and anchorage independency compared to the G13D mutant [99]. Further studies show that, though both G12D and G13D activate ERK to a similar level, G12D activates AKT at a much higher capacity [97]. These structural, biochemical and cellular analyses suggest that though RAS mutants possess a high degree of homology, even minor difference in their underlying biochemical properties could have a massively differential effect on their biological function.

1.3   RAS Signalling: Effectors, GEFs and GAPs

1.3.1 Effectors

Activated RAS transduces signals to 'effector proteins,' which associate directly with RAS using a RAS binding domain (RBD) or RAS association domain (RA). The first identified RAS effector was a Ser/Thr protein kinase, c-RAF (*cellular* RAF or RAF1). RAF1 lies at the top of the *mitogen-activated protein kinases (MAPKs)* cascade, and its binding to RAS activates RAFs kinase activity and the subsequent activation of downstream MAPKs, ERK1 and ERK2 [100, 101].   X-Ray crystallography and NMR-HSQC (Nuclear magnetic resonance - heteronuclear single quantum coherence) characterization reveal that the highly conserved RAF1 RBD is an ordered protein domain spanning residues 55-132 (human CRAF numbering), and that these 77 residues are sufficient to bind active RAS by directly interacting with its switch I region (the Kd of the interaction is 40 nM as measured by NMR binding studies) [102]. The RAF1 RBD has a ubiquitin-like fold that predominantly interacts with RAS *via* an inter-protein β-sheet and surface charge analysis reveals that the RAF1 RBD has a positively charged surface, while its interaction site on the surface of RAS is negatively charged. This complementary drives the RAS-RAF interaction [103, 104], and many of the principals have proven consistent with other RAS-effector complexes.

Numerous alternative RAS effectors have been identified, the first being four RALGDS proteins (RAL guanine dissociation stimulators RGL1, RGL2, RGL3 and RALGDS),

RALGEF and the α, β, and γ PI (3) kinases [105-108]. These effectors contain an RA domain, in spite of low sequence homology among themselves, they have similar secondary structures and protein folds [109-112]. **Figure 6** displays the similarity in protein tertiary structure among several RAS binding RBDs**.** Improvements in techniques used to identify novel protein-protein interactions, such as yeast two-hybrid and mass spectrometric approaches, led to the identification of many new potential RAS effectors. At present, there are more than 50 RA and 20 RBD domain-containing proteins in the human proteome; **Figure 7** shows the schematic flow chart of important RAS effectors and its downstream function [113, 114]. A more recently identified and unique RAS effector family are the RASSF (RAS Association family) proteins [115, 116]. They comprise a total of 10 family members (RASSF1-10) with highly conserved putative RA domains, making up nearly a fifth of the total RAS effector landscape. Most RAS effectors are believed to function in pathways related to cell proliferation or survival, except the RASSF and Apoptosis stimulating protein of p53 (ASPP) families which are, interestingly, putative tumor suppressors presumed to function in pro-apoptotic pathways. X-Ray crystallography studies of a RASSF5-HRAS complex revealed that RASSF5 utilizes a highly unique mode of binding towards RAS compared to the RAF RBD, contacting RAS at both switch regions (switch I - residues 30 to 40 and switch II – residues 60 - 76) [117]. Following, are brief descriptions of various downstream RAS effectors and their putative functions.

c-RAF1: 1RFA   PLCε: 2BYF

RALGDS: 1RAX   AF6: 1W6A   RASSF5: 3DDC
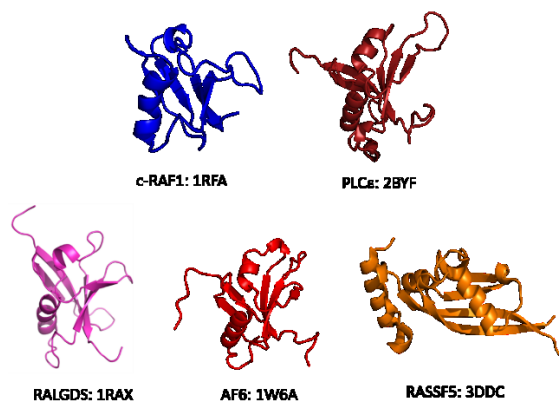
Figure 6:   Crystal structure of RA domains of various RAS effectors

Image shows RA domain of effectors that possess similar ubiquitin fold

RAF/MAP kinases

RAF Ser/Thr protein kinases are crucial to activation of the MAP kinase pathway. There are three highly related RAF homologs; *A-RAF, B-RAF and C-RAF*. All three contain two conserved domains in their N-terminal region called CR1 and CR2, and a third conserved region, CR3, encodes the C-terminal kinase domain. Many genetic and biochemical data demonstrate that GTP-bound RAS binds and activates all three isoforms of RAF. RAS-RAF interactions target RAF to the plasma membrane, and this translocation is crucial for RAF activation [118, 119]. Activated RAF phosphorylates and activates its downstream binding partners, MEK1 and MEK2 (mitogen-activated protein kinase kinases 1 and 2). MEKs are dual-specificity enzymes which in-turn phosphorylate and activate the MAPKs, ERK1 and ERK2. ERKs are extracellular signal-regulated kinases 1 and 2 whose substrates include various nuclear and cytoplasmic proteins, including the nuclear transcription factor ELK1 (ETS Like-1 protein). ELK1 belongs to the ETS family of transcription factors that regulates the transcription of various genes [120]. Phosphorylated ELK1 undergoes conformational change [121] and binds to SRF (Serum response factor) [122], finally the ELK1/SRF complex binds to the promoter of *c-fos* gene and activates the transcription of various genes resulting in the cell-cycle progression and cell proliferation [123]. Gain-of-function mutation in any of the MAPK pathway proteins renders the cells cancerous, reviewed in [124].

PI3K (phosphatidylinositol 3-kinase)

The second well-characterized RAS effector pathway is the PI3K network. PI3K comprises an RBD-containing catalytic p110 subunit and a regulatory p85 subunit. GTP-bound, activated RAS interacts directly with the catalytic p110 subunit of type 1 PI3Ks [125, 126]. Among the three isoforms of RAS, HRAS appears a more potent activator of PI3K [127]. Upon activation, PI3K phosphorylates phosphatidylinositol-4,5-bisphosphate (PIP2) to produce a second messenger phosphatidylinositol-3,4,5-trisphosphate (PIP3). PIP3 binds to a variety of downstream target proteins through their PH domains. There is a major focus on how PIP3 activates its target protein AKT (otherwise called Protein kinase B (PKB)), activated AKT mediates cell survival and tumorigenesis. PIP3 recruits both phosphatidyl inositol-dependent

kinase 1 (PDK1) and AKT to the plasma membrane, whereby PDK1 phosphorylates and activates AKT [128-130]. Activated AKT elicits a strong anti-apoptotic or survival response by phosphorylating numerous downstream targets [131, 132]. Moreover, PI3K activation stimulates the alternative small GTPases RAC and RHO, which regulate the actin-cytoskeleton. Thus, activation of PI3K drives cells towards survival and migration [133].

RALGDS

RALGDS proteins are exchange factors for the RAS-related RAL small GTPases. Many studies demonstrate that RAS stimulates activation of RAL through RALGDS, which in turn activates phospholipase D1 and CDC42/RALBP1. It is believed that the RALGDS pathway works alongside the PKB/AKT pathways, inhibiting factors responsible for apoptosis and cell-cycle arrest [134]. RALGDS also appears to play a crucial role in vesicle trafficking and receptor endocytosis. Further, studies report overactivation of RALA protein in various human malignancies [135].

TIAM

T-lymphoma invasion and metastasis protein 1(TIAM) is a lesser studied binding partner of RAS. It was initially characterized as a GEF for RAC GTPases. TIAM contains an RBD domain by homology, linking RAS directly to RAC signalling. *Tiam1-/-* deficient mouse are resistant to RAS-driven skin tumors caused by dimethylbenzanthracene [136]. Studies by Arthur and colleagues show that TIAM and RAS are involved in RAP1 mediated cell spreading [137], and Tiam1 is also known to facilitate neurotrophin-3 induced cell migration [138]. There is little known of how TIAM signalling downstream of RAS functions in cells.

AF6/Afadin

RAS-AF6 signalling is thought to regulate cell adhesion [139, 140]. AF6 contains two RAS-association domains (RA1 and RA2), and X-Ray crystallography studies show the RA1

domain binds RAS by contacting both switch regions in a manner analogous to RASSF5. Like RASSF5, AF6 also contains the α-helix N-terminal to the core RA1 domain. Structural studies show that αN-helix establishes non-canonical interaction with the RAS switch II region [141]. Various studies report that the *AF6* undergoes rearrangements with the mixed-lineage leukemia gene (*MLL*), and this rearrangement generates a potent leukemia-inducing MLL fusion protein [141, 142]. In general, AF6 expresses at the cytoplasm of healthy bone marrow cells and regulates the RAS-GTP levels. However, in MLL-AF6 rearranged cells, AF6 is found in the nucleus, resulting in the heightened activation of RAS and its downstream effectors [142]. Thus far, the functional significance of wild-type AF6 and its interaction with RAS is not clearly understood. In separate studies, an interaction between AF6 and ZO-1 was found necessary for the formation of tight junctions [143]. Inactivation of the AF6 gene in mice was found to disrupt epithelial cell-cell junctions and cell polarity during development [139].

Phospholipase C

Another downstream effector of RAS, Phospholipase Cε, also contains two RAS-association domains (RA1 and RA2) along with a RAS-GEF domain. X-Ray crystallography studies show that only PLCε RA2 domain interacts with RAS [144]. Phospholipase C promotes the hydrolysis of phosphatidylinositol 4,5 bisphosphate to diacylglycerol and inositol-1,4,5-trisphosphate (Ins(1,4,5)P3) [145], and could link RAS towards PKC and Ca^{2+} signalling. The biological role of PLCε in the context of cancer is not very clear. However, studies by Martins et al 2014, demonstrate the tumor suppressive function of PLCε by showing that mouse strains carrying P*lcε*-/- were more susceptible to tumor formation [146].

RASSF

RAS-RASSF interactions are presumed to drive pro-apoptotic signalling, in contrast to other RAS downstream effectors, making this family highly unique and of great clinical interest. Further detailed descriptions of RAS-RASSF signalling and its biological significance are addressed in sections 1.5.
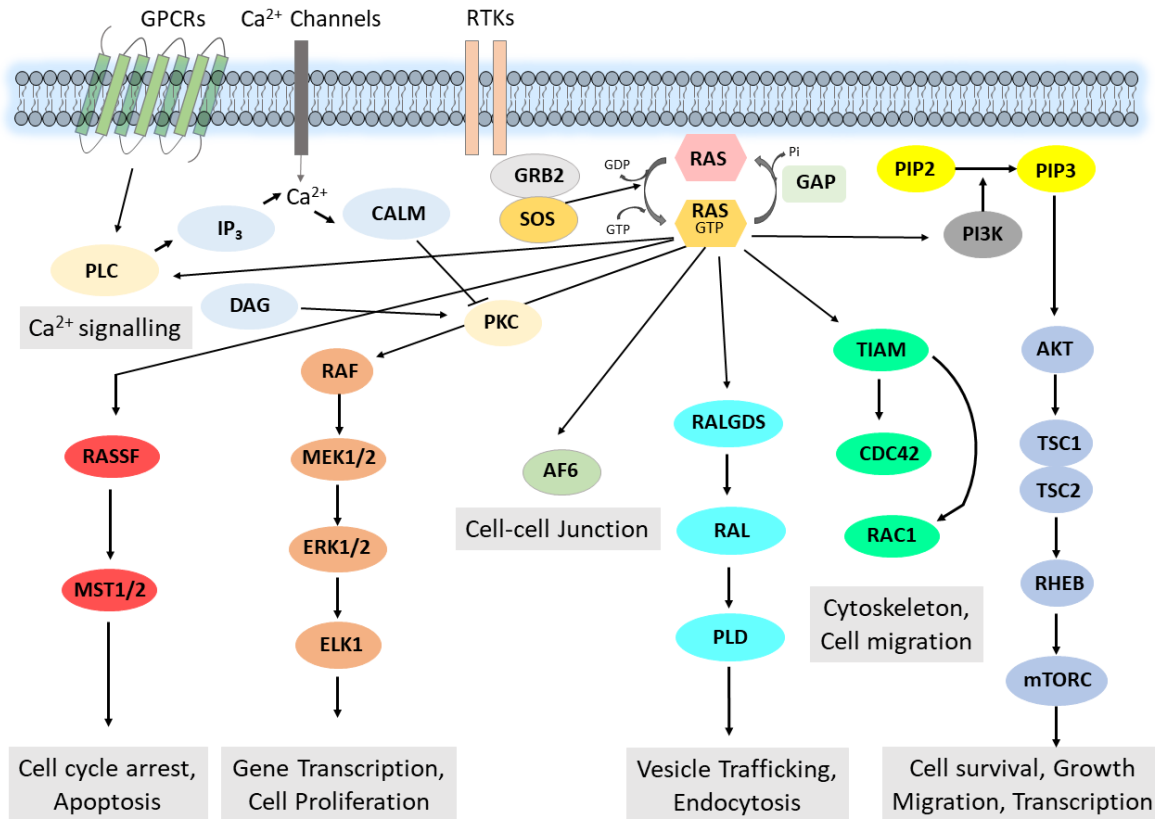
Figure 7:   Overview of major RAS effector signalling pathways

Upon activation, active GTP-bound RAS simulates the cascade of signalling networks such as, RAF-MAP kinase pathway, PI3K pathway, RASSF signalling, RALGDS pathway, AF6 binding and cell adhesion regulation, TIAM-RAC1 activation for cytoskeleton regulation, etc.

Outside of signalling effectors, the other major RAS binding proteins are GEFs and GAPs. The RAS GTP/GDP cycle is tightly regulated in the cell by the coordination of these key regulatory proteins. Members of the various branches of RAS superfamily GTPases have specific GEFs and GAPs that contain structurally distinct catalytic domains. Human cells contain approximately 36 RAS subfamily GTPases proteins that are regulated by approximately 27 GEFs and 27 GAPs [147].

1.3.2 GEFs

RAS small GTPases are involved in nucleotide binding and hydrolysis. The intrinsic nucleotide exchange rate of some RAS GTPase is slow compared to GEF-assisted exchange process. Hence, RAS GTPase uses GEFs to enhance their nucleotide exchange rates. GEFs are RAS regulators that interact with RAS to stimulate the release of GDP and allow GTP binding. GEF proteins possess a conserved Cdc25 domain of approximately 500 amino acids that acts as a catalytic domain [148]. The kinetics of GEF-stimulated nucleotide exchange has been studied in detail for several RAS/Cdc25 proteins. The first step in the exchange process involves low-affinity complex formation between a GEF and GDP bound GTPase, followed by a high-affinity complex forming between the GEF and nucleotide-free GTPase. Generally, GTPases in cell have similar affinities for both GDP and GTP. Since GEF-bound GTPases do not favour GDP rebinding, and GTP is present at a approximately ten-fold higher cellular concentration than GDP, GTP binds to the GTPase thereby displacing GEF, resulting in the formation of active GTPase [69, 149]. The first structure of a nucleotide-free RAS GTPase and a GEF was solved for the RAS complex with its major GEF, SOS1 [148]. The structural details revealed the mechanisms by which GEF assists in the nucleotide exchange process, including GEF interactions with hydrophobic residues near the Mg^{2+} ion binding site of the GTPase. This results in lowered affinity between Mg^{2+} and GTPase and hence GDP, ultimately causing GDP release [148]. Alternatively, RCC1, a GEF for RAN GTPase, inserts an acidic residue into the phosphate-binding region of the GTPase causing a repulsive force to expel bound nucleotide [150], while others bind the switch II region of the GTPase at a conserved Alanine residue and project its CH3 group towards Mg^{2+}, resulting in steric repulsion and removal of Mg^{2+} ion [148]. Although there exist various GEFs and these are not conserved, the common mechanism of action among them is to distort the phosphate-binding pocket of GTPase and reduce their binding affinity for nucleotides. The intrinsic GTP (GTPγS) exchange rates, denoted as (k) for wild-type GTPase H/K/N-RAS are 3.5, 5.7, 3.9 X 10^{-3} min^{-1} respectively. However, the GEF (SOScat) assisted exchange rate for these GTPases are approximately 17, 20, 13 X 10^{-3} min^{-1} respectively. These data were obtained from NMR-multiplexed experiments representing the exchange activity of multiple RAS GTPases at the same time [151]. Due to the robust ability of GEFs to activate GTPases, they are even considered as drug targets to reduce the GTPase activity [152] that plays key role in the tumorigenicity of many RAS GTPase.

1.3.3 GAPs

Although RAS GTPases possesses intrinsic GTPase activity to cleave the gamma-phosphate of GTP, this process is extremely slow. GAPs assist RAS GTPases in hydrolysis by increasing this rate by several orders of magnitude [153]. For instance, the intrinsic hydrolysis rate of H/K/N-RAS are approximately 4.5×10^{-3} min^{-1}, whereas, the GAP (GAP-334) assisted hydrolysis rates are approximately $10\text{-}12 \times 10^{-3}$ min^{-1} [151]. An understanding of the mechanism of GAP-assisted RAS hydrolysis activity was obtained from a crystal structure of RAS in complex with one of its major GAPs, p120GAP. In the absence of GAP, the intrinsic RAS hydrolysis activity develops a partial negative charge during the "transition state", which affects the enzymatic activity. The GTPase activity of RAS proceeds through a "loose transition state", where the hydrolysis of a terminal phosphate monoester of GTP, proceeds through a metaphosphate-like transition state. This state, displays the cleavage of bond between phosphorus and the leaving oxygen but at the same time no bond formation between phosphorus and the nucleophile [154]. To overcome this issue, GAP provides an arginine residue (arginine finger) to stabilize the partial negative charge during the transition state, and optimally positions the conserved glutamine residue (Q61 for RAS, in switch II) to activate the water molecule for nucleophilic attack on the γ-phosphate of GTP. This final configuration of the RAS-RasGAP complex shows very high enzymatic activity of approximately 5-fold higher than intrinsic hydrolysis rate [155]. One of the major RAS mutations found in human tumors, Gln61 (Q61), prevents GAP-induced hydrolysis as the Gln side chain is lost. Other oncogenic RAS mutants (at positions 12 and 13) are also known to sterically hinder the positioning of the arginine finger and glutamine 61[155]. Thus, the main purpose of the GAP is to stabilize the transition state of the GTPase by inserting the catalytic residue.

The extensive genetic, biochemical and biophysical studies performed on RAS small GTPases reveal the extent of complexity these proteins hold in terms of mechanisms of cell signalling. However, the H/K/N-RAS small GTPases are just a few members of the larger RAS subfamily. The next section will focus on an evolutionarily related family of RAS small GTPases, the RGKs.

1.4   RGK Small GTPases

1.4.1 The RGK GTPases

The RGK family of small GTPase comprises four members: RRAD, GEM (mouse homolog also known as Kir), REM1 and REM2. Although the founding members of this family, GEM and RRAD, were discovered more than 25 years ago, the physiological function of these proteins is not well understood. GEM was initially cloned based on differential expression of mitogen-induced T-lymphocytes; similarly, RRAD was cloned based on its over-expression in type II diabetic muscle. The other two members, REM1 and REM2, were later identified based on sequence similarity to the existing RGK proteins [156-159].

Proteins of the RGK family share similar structural features among themselves but differ from typical RAS GTPase on many accounts [160-162]. First, RGK GTPases comprise extended N- and C-terminal regions involved in 14-3-3 binding; second, the presence of many amino acid substitutions within the GTPase core that are involved in nucleotide (GDP/GTP) and Mg^{2+} binding; third, amino acid substitutions in their putative (G2) domains indicate that they may interact with different effectors and regulatory proteins [163]; forth, the presence of a calmodulin-binding site in the C-terminal region; and fifth, an atypical CAAx motif is responsible for membrane targeting [164].

Members of the RGK family are expressed in a tissue-specific manner [163] and undergo both transcriptional and translational regulation depending on the external stimuli. No GEFs or GAPs have been identified for RGK proteins. In an attempt to define a function for RGK GTPases, previous work using yeast two-hybrid screens of protein interactions have identified several direct interactors, particularly that GEM interacts with RHO Kinase β and $Ca_V\beta$ [165, 166]. Subsequent work showed that interaction of RGK proteins with Rho Kinase β modulates actin cytoskeletal remodelling, specifically in neurons, generating retraction of neurites [165], and that RGK GTPases regulate the activity of voltage-gated Ca^{2+} channels (VGCC) by interacting with accessory β or/and α subunits [157, 167]. Another interactor of RGK proteins is calmodulin [168], but the physiological significance of this interaction is not yet clear. This means that RGK GTPases are involved in vast cellular processes, but remain amongst the under-studied GTPases within the RAS subfamily.

1.4.2 RGK primary structure and comparison with RAS GTPases

Members of the RGK GTPases contain several non-conservative substitutions in the G-domain, especially in the region responsible for nucleotide binding and hydrolysis **(Figure 8)** [157, 158]. The first important substitution is within the G1 motif involved in phosphate binding. Gly12 in RAS and many RAS-related proteins is highly conserved. Mutations to G12 result in constitutive activation of RAS GTPases by locking the protein in GTP bound state. This residue is substituted in all four RGK proteins (to glutamine in GEM, proline in REM2 and RRAD and serine in REM1) **(Figure 8)**. Further, Thr35 in the RAS switch I region, responsible for γ-phosphate sensing and nucleotide cycling, is absent in all the four RGK proteins **(Figure 8)**. Phe 28 of RAS, important for capping the guanine ring and establishing high affinity binding to nucleotide, is also substituted in each of the RGK members **(Figure 8)**. In addition to these alterations in the G1 domain, both the G2 and G3 domains of RGK family members have considerable sequence divergence compared to other RAS-related proteins. In the G3 motif (equivalent to RAS DTAGQ) , alanine and glycine are substituted to bulky and charged residues tryptophan and glutamate (DxWEx) [169] **(Figure 8)**. This is significant as glutamine in G3 of RAS (Q61) is required for GTP hydrolysis and in GEM and REM1 this is substituted to asparagine and alanine **(Figure 8)**. The putative G2 domain which is responsible for effector binding and highly conserved in RAS is completely different in individual RGK GTPases. These combined differences suggest that each member of the RGK GTPase family could have specific effector binding properties and underlying nucleotide cycling kinetics.

```
HRAS   ------------------------------------------------------------   0
REM2   MHTDLDTDMDMDTETTALCP-------SGSRRASPPGTPTPEADATLLKKSEKLLAELDR   53
REM1   --------MTLNTEQEAK-------TPLHRRASTPLPLSPRGH---------------   28
GEM    --------MTLNNVTMR--------------QGTVGMQPQQQ---------------   20
RRAD   --------MTLNGGGSGAGGSRGGGQERERRRGSTPWGPAPPLH---------------   36


HRAS   ------------------------------------------------------------   0
REM2   SGLPSAPGAPRRRGSMPVPYKHQ--------L-------RRAQAVDELDWPPQASSSGSS   98
REM1   --------QPGRLSTVPSTQSQH---PRLGQSASLN-PPTQKPSPAPDDWSSESS-----   71
GEM    --------RW----SIPADGRHLMVQKEPHQYSHRNRHSATPEDHCRRSWSSDST-----   63
RRAD   --------RR----SMPVDERDLQAALTPGALTAAA--AGTGTQGPRLDWPEDSE-----   77
                                    |  G1            |      | G2
HRAS   -------------MTEYKLVVVGAGGVGKSALTIQLI--QNHFVDEYDPTIEDSYRKQVV   45
REM2   DSLGSGEAAPAQKDGIFKVMLVGESGVGKSTLAGTFGGLQGDSAHE-PENPEDTYERRIM   157
REM1   DS-------EGSWEALYRVVLLGDPGVGKTSLASLFAGKQERDL--HEQLGEDVYERTLT   122
GEM    DSVIS----SESGNTYYRVVLIGEQGVGKSTLANIFAGVHDSMDSDCEVLGEDTYERTLM   119
RRAD   DSLSSGG--SDSDESVYKVLLLGAPGVGKSALARIFGGVEDGPEAE---AAGHTYDRSIV   132
                        G3  |||
HRAS   IDGETCLLDILDTAGQEE--YSAMRDQYMRTGEGFLCVFAINNTKSFEDIHQYREQIKRV   103
REM2   VDKEEVTLVVYDIWEQGD-AGGWLRDHCLQTGDAFLIVFSVTDRRSFSKVPETLLRLRAG   216
REM1   VDGEDTTLVVVDTWEAEKLDKSWSQESCLQGGSAYVIVYSIADRGSFESASELRIQLRRT   182
GEM    VDGESATIILLDMWENKG-ENEWLHDHCMQVGDAYLIVYSITDRASFEKASELRIQLRRA   178
RRAD   VDGEEASLMVYDIWEQDG--GRWLPGHCMAMGDAYVIVYSVTDKGSFEKASELRVQLRRA   190
                   G4                             G5
HRAS   KDSDDVPMVLVGNKCDLAA-RTVESRQAQDLARSYGIPYIETSAKTRQGVEDAFYTLVRE   162
REM2   RPHHDLPVILVGNKSDLARSREVSLEEGRHLAGTLSCKHIETSAALHHNTRELFEGAVRQ   276
REM1   HQADHVPIILVGNKADLARCREVSVEEGRACAVVFDCKFIETSATLQHNVAELFEGVVRQ   242
GEM    RQTEDIPIILVGNKSDLVRCREVSVSEGRACAVVFDCKFIETSAAVQHNVKELFEGIVRQ   238
RRAD   RQTDDVPIILVGNKSDLVRSREVSVDEGRACAVVFDCKFIETSAALHHNVQALFEGVVRQ   250
                                            Membrane Targeting
HRAS   IRQHKLRKLNPPDESGPGCMS------CKCVLS------------------------   189
REM2   IRLRRGRNHAGGQRPDPGSPEGPAPPARRESLTKKAKRFLANLVPRNAK--FFKQRSRSC   334
REM1   LRLRRRDSAAK---------EPPAPRRPASLAQRARRFLARLTARSARRRALKARSKSC   292
GEM    VRLRRDSKEKNER-------RLAYQKRKESMPRKARRFWGKIVAKNNKNMAFKLKSKSC   290
RRAD   IRLRRDSKEANAR-------RQAGTRRRESLGKKAKRFLGRIVARNSRKMAFRAKSKSC   302


HRAS   ------   189
REM2   HDLSVL   340
REM1   HNLAVL   298
GEM    HDLSVL   296
RRAD   HDLSVL   308
```

■ Sequence identity among RGK GTPase   ■ Sequence similarity among RGK GTPase   ■ Sequence similar among three of four RGK GTPase

Figure 8:   Sequence comparison between HRAS and RGK family of GTPase.

Highlighting the various G domains. G2 domain of RGK GTPase is highly different from RAS GTPase.

1.4.3 RGK structure and nucleotide binding

The presence of substantial amino acid substitutions at positions important for nucleotide (GDP/GTP) binding has given the perspective that RGK GTPases have altered affinity for nucleotide analogs. To-date, atomic resolution structures of RGK G-domains are available in GTP-bound form for only two members, RRAD and REM2. [160-162] **(Figure 9).** The overall G-domain fold of RGK GTPases is highly similar to RAS, involving a central β-sheet of 6 strands (β1-β6) and five surrounding α-helices (α1-α5). A closer look at these structures reveals that the RGK switch I regions are highly disordered or even pointed away from the nucleotide-binding pocket. Sasson et al 2011, attempted to crystalize GTP-bound RGK GTPases using a GNP analog (non-hydrolysable analog of GTP) [170], and were successful in obtaining structures for RRAD and REM2. Their findings suggest that RGK GTPases may not undergo the classical RAS "molecular switching" by exchanging nucleotide [69]. In fact, there is no apparent conformational differences in protein structures of RRAD or REM2 bound to GDP or GTP nucleotides [170]. Moreover, weak electron density in the switch-I region revealed that this loop is highly disordered independent of nucleotide, and has no detectable interaction with nucleotide [170]. In contrast, typical RAS G-domains have a well-defined nucleotide induced conformational exchange in the switch-I region and multiple evident contacts between the loop and nucleotide. The RGK data further resolve that the intrinsic GTP hydrolysis rate of RGK proteins (especially GEM and RRAD) have "no or very little" activity compared to RAS GTPase in a steady-state γ-phosphate release experiments [160]. Studies by De Gunzburg and colleagues have also shown that removal of N-terminal extension or both N- and C terminal regions of GEM reduces its GTPase activity [161], though these segments are not apparently part of the core G-domain fold. Thus, unusual nucleotide cycling ability and lack of conformational change upon nucleotide binding of RGK proteins, make us think how differently these proteins are regulated in the cellular environment.
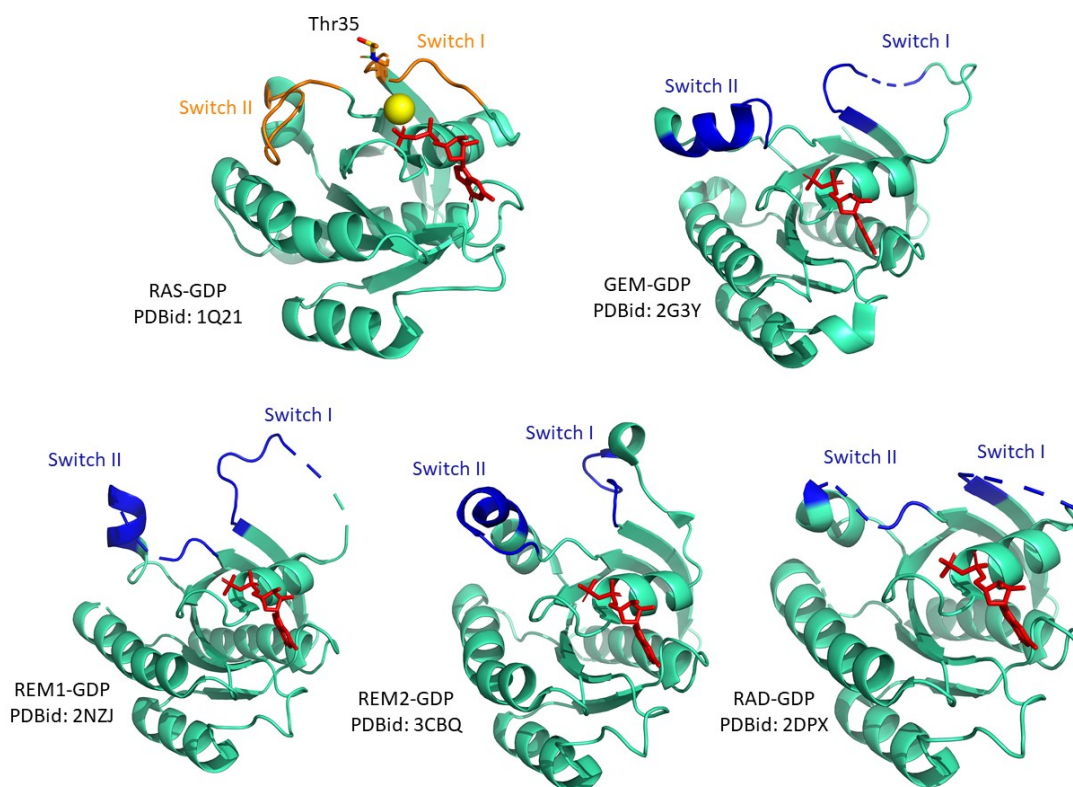
Figure 9:   Crystal structures of RGK GTPase in GDP-bound form

Comparison of structural differences among RGK GTPase and RAS in GDP-bound form. Switch regions are highlighted in blue color for RGK GTPase and orange colour for RAS. Bound GDP is represented in red color

1.4.4 RGK localization

The subcellular localization of these small GTPases is varied and depends on multiple factors. Though the RGK proteins lack canonical lipid modification sites or CAAx motifs, several studies have shown their enrichment at plasma membrane regions, while they also reside in the cytoplasm and nucleus [158, 171-181]. Furthermore, it's been noted that some members can localize on the actin and microtubule cytoskeletal network. Studies by Mahalakshmi et al 2007, demonstrated that Kir/GEM and REM possess three conserved nuclear localization signals (NLS) that mediate nuclear accumulation of GEM and REM

through an importin α5-dependent pathway. RRAD is also thought to bind importin α3, α5 and β through three conserved NLS motif [180, 181]. The highly conserved carboxy terminus of these GTPases plays a key role in regulating their sub-cellular localization, in part due to interaction [168, 180, 181] with the phospholipid bilayer [174-176, 182, 183]. Indeed, a polybasic motif in the C-terminus of RGK proteins apparently anchors them to the plasma membrane though association with phosphatidyl inositol phospholipids (PIP). This is suggested to be essential for regulating Ca^{2+} influx in conjunction with voltage gated Ca channels. Work by Beguin et al 2005, shows that calmodulin (CaM) and 14-3-3 binding abrogates nuclear transport of RGK GTPases, likely due to blocking interaction with importins, but the actual mechanism is yet to be understood. In contrast, mutations that prevent 14-3-3 and CaM binding promote nuclear accumulation of RGK GTPases [175, 177]. While plasma membrane targeting of RGK proteins is significant to Ca^{2+} channel inhibition, a function of nuclear RGK has not been elucidated [163, 165, 176, 182, 183]. Mainly, RRAD of the RGK family is known to bind the transcription factor RelA/p65 and regulates its binding towards DNA [172, 173]. The above knowledge suggests that the localization of RGK GTPases is regulated in multiple layers but the importance of the proteins in various cellular components has not been fully explored.

1.4.5 Post-translational modification of RGK GTPases

Another key aspect of RGK protein regulation is through post-translational modification, primarily phosphorylation. Several kinases, including protein kinase A (PKA), protein kinase C (PKC), casein kinase (CK) and calmodulin-dependent kinase II (CaMKII), are known to phosphorylate RGK proteins [184]. Phosphorylation is proposed to regulate RGK subcellular localization and interaction with partner proteins [171, 175, 177, 180, 181, 184-186]. For example, phosphorylated serine residues in the C-and N-terminal extensions of RGK GTPases are necessary for interaction with 14-3-3 [175, 177, 185, 186]. Several alternative serine phosphorylation sites prevent binding with 14-3-3 [180]. A number of recent studies have demonstrated that phosphorylation of GEM at S261 and S289 is crucial for its regulatory role in Ca^{2+} channel inhibition and cytoskeletal remodelling [186], and phosphorylation of S260, S286 and S288 residue in the C-terminal NLS of GEM prevents its nuclear localization and association with microtubules[181]. Data also suggest that REM1 phosphorylation at S18

by protein kinase D1 prevents REM1 mediated inhibition of Ca^{2+} entry [187]. CaMKII phosphorylation of REM2 targets it to localize at nucleus, required to control dendritic complexity [188]. While phosphorylation is the best studied post-translational modification of RGK GTPases, the existence of other protein modifications could be possible to regulate the RGK GTPase which has multi-functional capacity.

1.4.6 Voltage gated Ca^{2+} channels

By far the best characterized biological function of RGK GTPases is their role in regulating voltage gated Ca^{2+} channels. These channels cross the plasma membrane and transduce electric signals (membrane potential) into increased intracellular Ca^{2+} levels to regulate downstream physiological processes. These include, hormone secretion, excitation-contraction in muscles, gene-transcription and synaptic transmission [189]. Voltage gated ion channels can be classified into two major groups, high voltage-activated channels (HVA) and low voltage-activated channels (LVA) depending on the threshold of activation. HVA Ca^{2+} channels are multiprotein complexes comprised of a pore-forming subunit (Cavα1) and several auxiliary subunits (β, α2δ, or γ subunits), whereas LVA Ca^{2+} channels consists of only Cavα1 subunits [189]. The pore-forming subunits (Cavα1) are large, 190kDa proteins responsible for determining ion selectivity, while the auxiliary β-subunits facilitate cell surface trafficking of α1 subunits. In humans there are 10 genes encoding pore-forming subunits (Cavα1) which can be divided into three major families based on sequence similarity and functional properties. For HVA channels the Cav1 family consists of L-type Ca^{2+} channels Cav1.1 (α1S), Cav1.2 (α1C), Cav1.3 (α1D), and Cav1.4 (α1F). The L-type channels are expressed in skeletal muscle, smooth muscle and osteoblasts in the bone and neuronal dendrites. The Cav2 family contains P/Q-type Ca^{2+} channels Cav2.1 (α1A), the N-type channel Cav2.2 (α1B) and the R-type channel Cav2.3 (α1E). P/Q, N and R-type channels are specifically expressed in the nervous system. A third family of LVA channels is the Cav3 family, containing the T-type channels Cav3.1(α1G), Cav3.2 (α1H) and Cav3.3(α1I). These T-type channels are mainly expressed in osteocytes of bones and neurons [189]. Regulation of Ca^{2+} channel functions are highly essential, because alteration in intracellular Ca^{2+} levels in various organelles has serious physiological impacts on the cell.

Excessive intercellular Ca^{2+} flux is known to induce apoptosis in multiple ways. Cytosolic overload of Ca^{2+} stimulates the uptake of Ca^{2+} into mitochondria, where it activates mitochondrial permeability transition pore (MPTP) causing the release of cytochrome *c* from the mitochondria. Released cytochrome *c* then diffuses into endoplasmic reticulum (ER) and binds to inositol-1,4,5-trisphosphate, resulting in the release of Ca^{2+} from ER. These *vice-versa* events increases the global Ca^{2+} levels, thereby cytosolic cytochrome *c* forms apoptosomes which activates caspases. Caspases and nucleases bind to various downstream substrates generating cell death signals [190]. In another mechanism, increased cytosolic concentrations of Ca^{2+} activates calpains (cysteine proteases) that facilitates cleavage of various BCL2 family members, including pro-apoptotic BID. BID is a cell death triggering protein that activates release of cytochrome *c* form ER. Finally, increased cytochrome *c* generates pro-apoptotic signals as mentioned in above mechanism [191, 192]. Cytosolic Ca^{2+} increase by chemical treatment (A23187 or thapsigargin) are also known to induce apoptosis by activation of calcineurin (phosphatase), which in turn dephosphorylates and activates pro-apoptotic protein BAD [193]. Thus, increase in Ca^{2+} levels in cytoplasm, mitochondria and ER being directly linked to the activation of pro-apoptotic signals, makes it clear that the regulation of Ca^{2+} channels are highly essential in deciding the cell fate. These Ca^{2+} channels are regulated by various proteins and RGK GTPases are among the important ones.

1.4.7 RGK GTPase regulation of Ca^{2+} channels

The first connection between RGK GTPases and voltage gated Ca^{2+} channels was established in MIN6 cells [165]. This work demonstrated that GEM interacts with Cavβ3 and inhibits its function. Following this, subsequent studies on other RGK GTPase have shown that all members act as potent inhibitors of VGCC [167, 194]. Indeed, overexpression of RGK GTPases in many lines of cultured cells has demonstrated their capacity to inhibit the activity of L, P/Q, N and R type of Ca^{2+} channels [163]. Conversely, RGK GTPase expression does not impact T-type channels, as they do not require auxiliary Cavβ expression for function [167, 195]. In addition to overexpression studies demonstrating the inhibitory role of RGK GTPases, RNA interference (RNAi) knockdown of RGK protein levels leads to higher Ca^{2+} channel activity [196, 197].

There are two different proposed mechanisms by which RGK GTPases are known to inhibit Ca^{2+} channel activity **(Figure 10).** A first model suggests that RGK GTPases prevent trafficking of these channel subunits (Cavα1 and Cavβ) to the cell surface [165, 171, 175, 187, 198] **(Figure 10).** Evidence for this model is based on the fact that RGK GTPases are differentially localized in cells, regulated by 14-3-3 and calmodulin binding. RGK mutants that do not bind calmodulin or 14-3-3 are highly localized in the nucleus along with co-expressed Cavβ. A contradictory second model contends that RGK proteins directly inhibit Cavα1 and Cavβ directly at the plasma membrane **(Figure 10).** This model is supported by studies which show that RGK proteins bound to Cavβ do not prevent Cavα1 binding [167, 174, 176, 194, 199-201]. In addition, the affinity between Cavα1 and Cavβ is much higher than that of Cavβ to RGK proteins determined by qualitative radiolabelled pull-down experiments. Thus, it would require significantly high expression levels of RGK protein to sequester Cavβ, yet there is no evidence for this [199]. Currently, most studies on the L-type channels or Cav1 family favour the sequestration model , whereas inhibition of N-type channels supports the inhibition through decreased surface activity model [174, 178, 195]. This implies there could be multiple ways by which RGK proteins inhibit Ca^{2+} channels. Indeed, studies by Yang et al 2010, showed ectopic expression of REM1 in HEK 293 cells inhibits L-type Ca^{2+} channels through multiple mechanisms [202], including: 1) decreased number of channels expressed in the cell surface, 2) inhibition of open channel probability, and 3) preventing voltage sensor movement (Qmax). In contrast, overexpression of REM2 or GEM does not decrease surface localization of channels, suggesting that REM2 and GEM act directly at the cell surface [202].

The C-terminus of RGK proteins appears to play a key role in inhibiting Ca^{2+} channel activity. C-terminus truncated RGK GTPases (truncated before residues 264 in Gem, 265 in Rem, 276 in RRad) are not capable of inhibiting Ca^{2+} channels [167, 200, 202]. It is not clear whether the C-terminus alone may inhibit channel activity. Studies show that a GEM-derived C-terminal peptide can sufficiently inhibit the Ca^{2+} channel, but this is not true of peptides derived from REM1 or REM2. When the C-terminus of REM1 or REM2 was swapped with the C-terminus of KRAS-4b, which contains the poly-basic CAAx motif, membrane inhibition of Ca^{2+} channel activity was restored. In summary, it appears that RGK proteins inhibit Ca^{2+} channels through multiple mechanisms and various domains of RGK proteins are involved in

this inhibitory function. That being said, tight regulation of Ca^{2+} channels are essential considering its crucial role in maintaining cellular homeostasis.
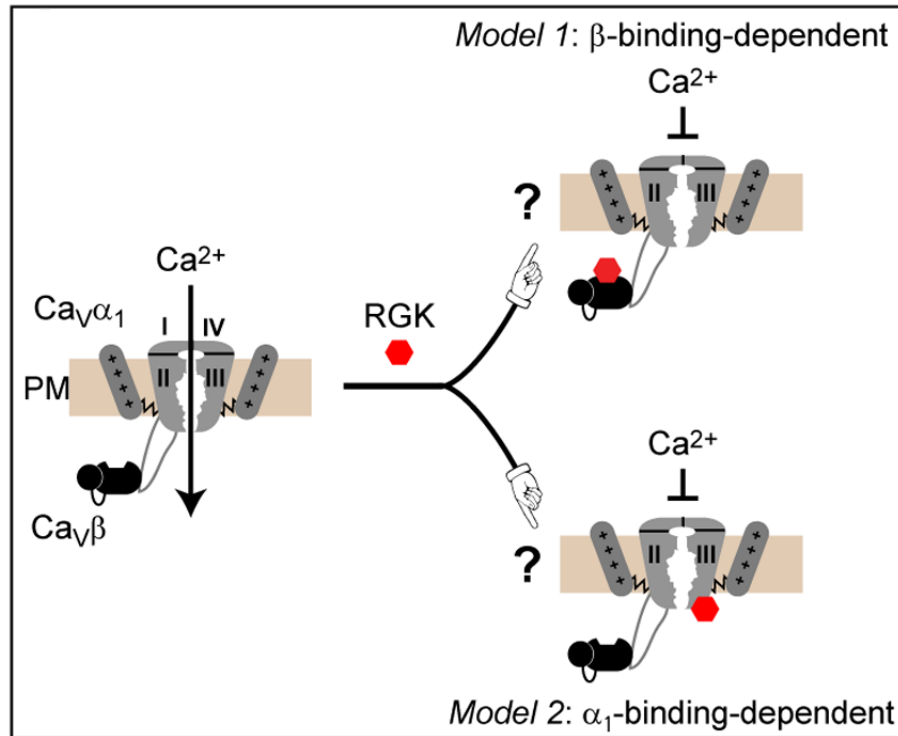
Figure 10: Image showing various models by which RGK GTPase inhibits voltage gated ion channels.

Image adapted from (Yang et al, 2012)

1.5 RASSF proteins

Monomeric small GTPases such as RAS and RGK GTPases have multiple effectors. In the previous sections we introduced two GTPase family (RAS and RGK) and its functions through some of the best studied effectors. In this section, we will focus on one group of the unique and less-studied RAS effectors, RASSF proteins. There are 10 RASSF homologs (RASSF1-10) in the human proteome, each comprising a modular RA domain proposed to bind

specifically to activated RAS GTPases. They are further classified into two groups depending on the position of the RA domain: 'classical' or C-terminal RASSFs (RASSF1-6) and 'N-terminal' RASSFs (RASSF7 - 10) **(Figure 11).** Each of the RASSF family members (except RASSF9 and RASSF10) contain multiple isoforms/splice variants arising either due to alternative splicing or differential promoter usage as mentioned in section 1.5.2 and 1.5.3, direct binding between HRAS and RASSFs has only been reported for RASSF5. In addition to an RA domain, C-RASSFs also contain a SARAH domain that mediates homo and hetero dimerization/interaction with other SARAH domain-containing proteins, namely pro-apoptotic MST kinases of the Hippo pathway. A C1 domain is present in RASSF1 and RASSF5 that is known to bind death receptor complexes. N-RASSFs completely lack both SARAH and C1 domains, instead they have a C-terminal predicted coiled-coil region. Detailed functions of these domains, where known, are addressed in the following sections.
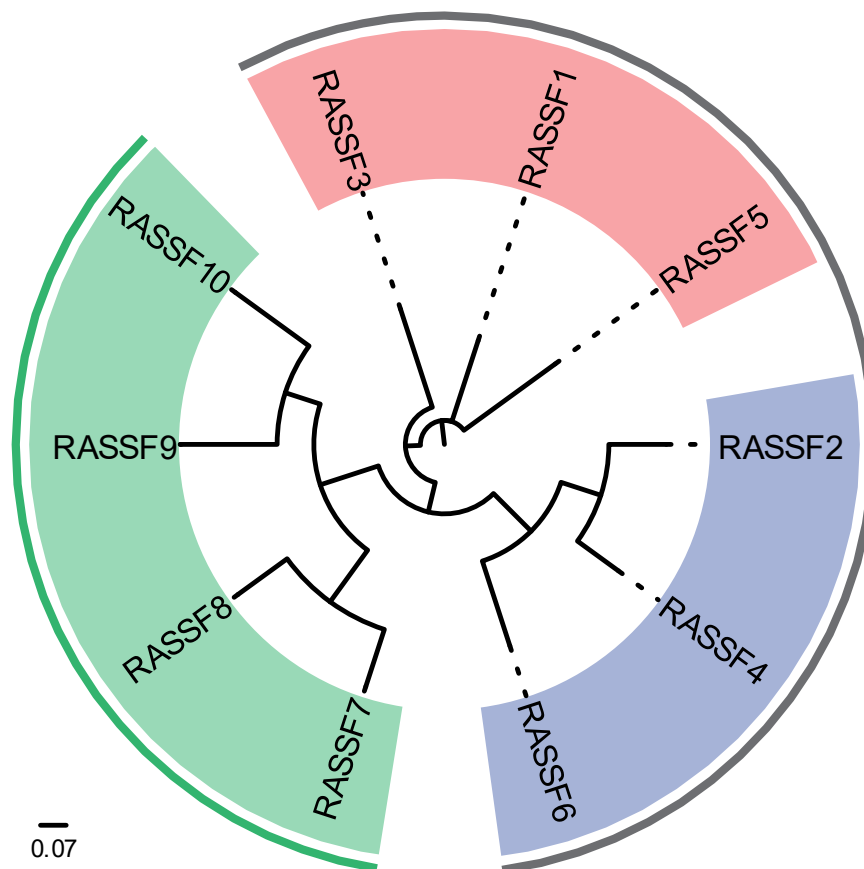
Figure 11:   Schematic representation of RASSF family of proteins.

RASSF proteins are classified into C-Terminal RASSF and N-terminal RASSF proteins. One subgroup of C-RASSFs are represented in red color and other subgroup of C-RASSFs are represented in blue color. N-RASSFs are shown in green color.

1.5.1 Evolution of RASSF family members

RASSF proteins are highly evolutionarily conserved and present across the metazoan kingdom. However, there has been significant sequence divergence as well as the insertion and deletion of multiple domains. A C-RASSF ortholog is present in unicellular choanoflagellates (*Monosiga brevicollis*), and according to secondary structure predictions the *M. brevicollis* RASSF protein (A9V7J7) has well-conserved RA (αN helix, β1, β2, α1, β3, β4, α2 and β5) and SARAH domains. Multicellular metazoans each encode multiple RASSF homologs. The placozoan *Tricoplax adhearens* has three C-RASSF proteins (B3RWW2, B3RTM2 and B3RWM8) with conserved RA and SARAH domains, with the B3RWW2 protein also comprising a C1 domain in the N-terminal region. More complex organisms contain both C-RASSF and N-RASSF proteins, nematodes (*Caenorhabditis elegans*) having a single C-RASSF (RSF-1/T24F1.3a) with an RA, SARAH and C1 domains and an N-RASSF (K05B2.2a) with the N-terminal RA domain and coiled-coil domain towards the C-terminus. Fruit flies (*Drosophila melanogaster*) encode a well-conserved N-RASSF (CG5083) ortholog and a single C-RASSF (CG4656) ortholog that is significantly diverged from those in C. elegans or vertebrates (**Figure 12**). The 10 RASSF homologs in humans (six C-RASSFs and four N-RASSFs) are expressed as multiple complex isoforms, RASSF1 being expressed as at least 8 eight distinctive isoforms. **Figure 12** shows a schematic representation of all known isoforms of human RASSF proteins along with their various modular protein domains. Conservation of RASSF proteins through evolution demonstrates the importance of these genes, however, our understanding of their function remains limited. In my thesis, I will focus primarily on the biological functions of RASSF1's and RASSF5.
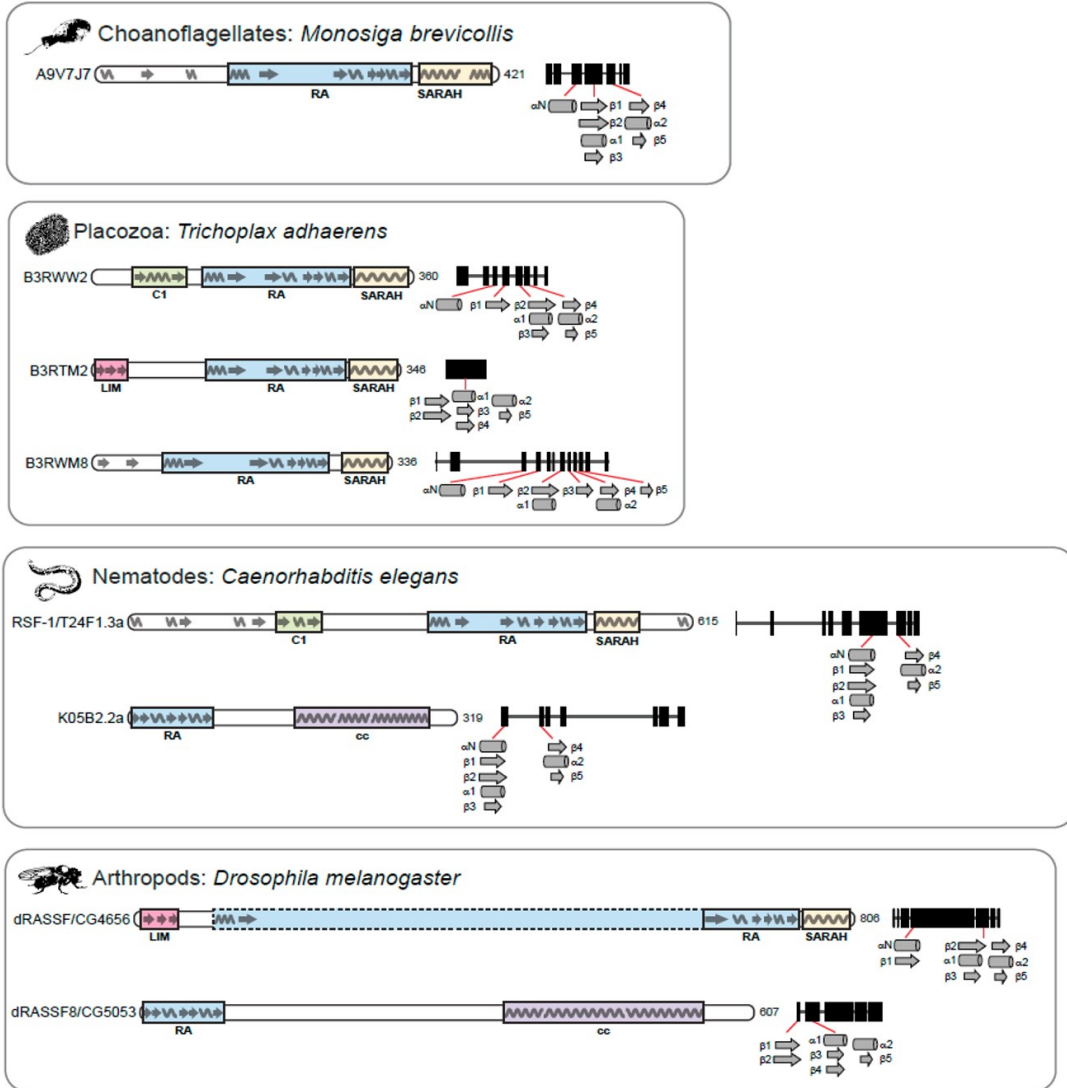
Figure 12: **RASSF proteins in various organisms.**

Unicellular eukaryote (*Monosiga brevicollis*) possess one C-RASSF and metazoans (*Tricoplax adhearens)* contain three C-RASSF proteins. *C. elegans* and *melanogaster* contains both contain C-RASSF and N-RASSF proteins.

1.5.2 C-RASSF proteins

Among the C-RASSF proteins, RASSF1, RASSF3, and RASSF5 form one subgroup of paralogs and have high sequence similarity **(Figure 13).** They appear to be orthologs of *C. elegans* T24F1.3. RASSF2, RASSF4 and RASSF6 forms another subgroup that diverged early in the evolution of metazoans. The two best characterized C-RASSF proteins are RASSF1 and RASSF5, due to the increasing evidence on their role on pro-apoptotic signalling.

Figure 13:   **C-RASSF proteins and their isoforms**

RASSF1

RASSF1 is a tumor suppressor and is frequently downregulated in human cancers. It is found that *RASSF1A* allele is frequently lost in human primary cancer cells and sporadic cancers [203] due to promoter hypermethylation [204, 205], similar observations were found in cervical squamous carcinoma cells [206], bladder carcinoma [207], non-small-cell lung cancer [208]. In addition, *Rassf1a-/-* mice showed increased tumor susceptibility and multiplicity compared to wild-type mice [209]. In the year 2000, Dammann et al, first cloned the *RASSF1* gene, located on chromosome 3p21.3. The eight transcripts of *RASSF1* are classified as A-H (**Figure 13**), of which RASSF1A and RASSF1C are the two best-studied. Despite highly sequence similarity (60% identity), they have highly distinctive biological functions. RASSF1A binds microtubules and is involved in the regulation of growth and migration, whereas RASSF1C is known to promote proliferation in lung and breast cancer cells. **Figure 14** shows the domains of RASSF1A proteins and their proposed functions.
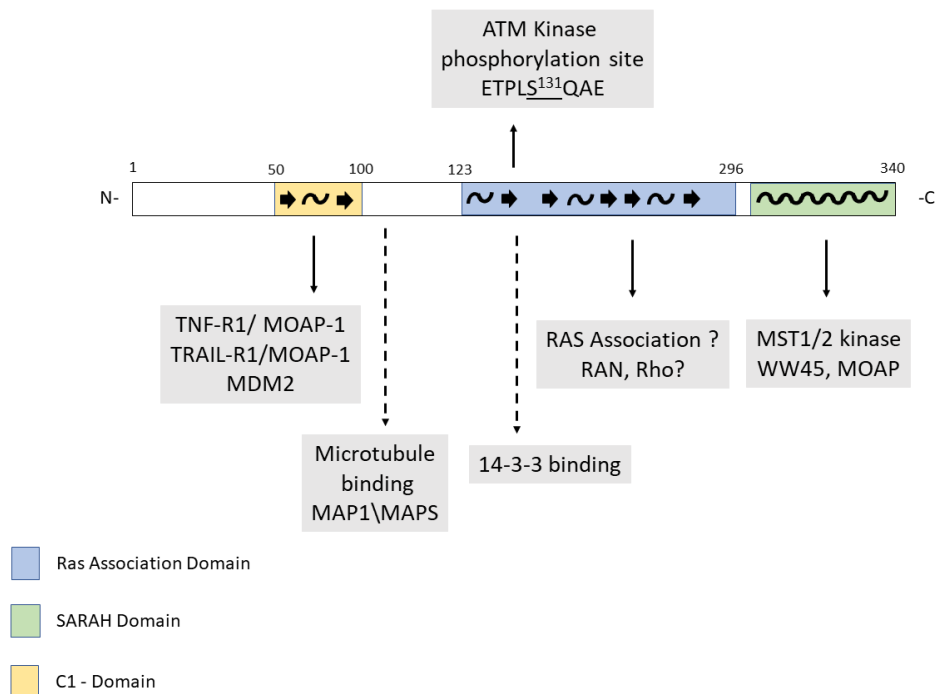
Figure 14:   Domain architecture of RASSF1A protein

Image shows various domains of RASSF1A proteins and their possible functions

RASSF1A encodes a 39 kDa protein harbouring 340 amino acids. The complete protein can be delineated into three major segments: the N-terminal region, the central RA domain and the C-terminal segment. The N-terminal portion comprises a cysteine-rich domain (C1 or CRD) related to the diacylglycerol (DAG) domain of the protein kinase C family. In PKC, this domain is involved in regulating kinase activity by binding to DAG. The RASSF1A C1 domain associates with death receptor complexes TRAIL-R1/MOAP-1 or TNFα-R1/MOAP-1 [210] to inhibit tumour formation and promote cell death (**Figure 15**). The N-terminal region of RASSF1A also contains an ATM (ataxia telangiectasia mutant) consensus site (serine 131) that is phosphorylated by the ATM kinase [211] upon DNA damage, which results in binding to the MST2 Hippo kinase [211] (**Figure 15**). The central RA domain is the largest segment of RASSF1, and due to its high homology to RASSF5 it is believed to associate with activated RAS GTPase [212]. Nevertheless, at least one study has shown that RASSF1A has only weak affinity for RAS [213] compared to RASSF5. The C-terminal region of RASSF1A contains the SARAH domain, a helical coiled-coil structure present only in two other protein families: the serine/threonine kinases MST1 and MST2 (human orthologues of Drosophila Hippo kinase) [214], and the WW45 regulatory protein (human ortholog of the Drosophila protein Salvador). The SARAH domain of RASSF1A protein can both homo- and hetero-dimerize with other SARAH domain-containing proteins (RASSFs and MST-1 kinase) [215, 216], thus playing a crucial role in defining RASSF1s cellular function [216] (**Figure 15**).

There is still much to learn on the *in vivo* function of RASSF1, but its consistently reduced expression in numerous human cancers has made *RASSF1* of increasing clinical interest. Both RASSF1 expression and protein levels are altered during cell-cycle progression [217, 218]. Further, the localization of RASSF1A also varies during different stages of the cell-cycle. RASSF1A is localized at the centrosome in prophase and moves to spindle poles in metaphase and anaphase, while during telophase RASSF1A is found at the midbody [219-221]. It is clear that RASSF1A regulates cell-cycle progression at various stages, inhibiting the G1-S transition by preventing the accumulation of cyclin D1 [222]. RASSF1A also represses synthesis of cyclinA2 through the p120^{E4F} transcription factor [223], during G2 repressing the activity of cyclinA2 and inducing a cell-cycle arrest [219, 224]. Ubiquitination and degradation of RASSF1A by the CUL4A E3 ubiquitin ligase complex is believed to drive the cell-cycle progression through mitosis [218] (**Figure 15**). Thus, RASSF1 is currently proposed to behave

as a scaffolding protein by directly linking RAS, Hippo and apoptotic signalling. How this is specifically accomplished is not known.
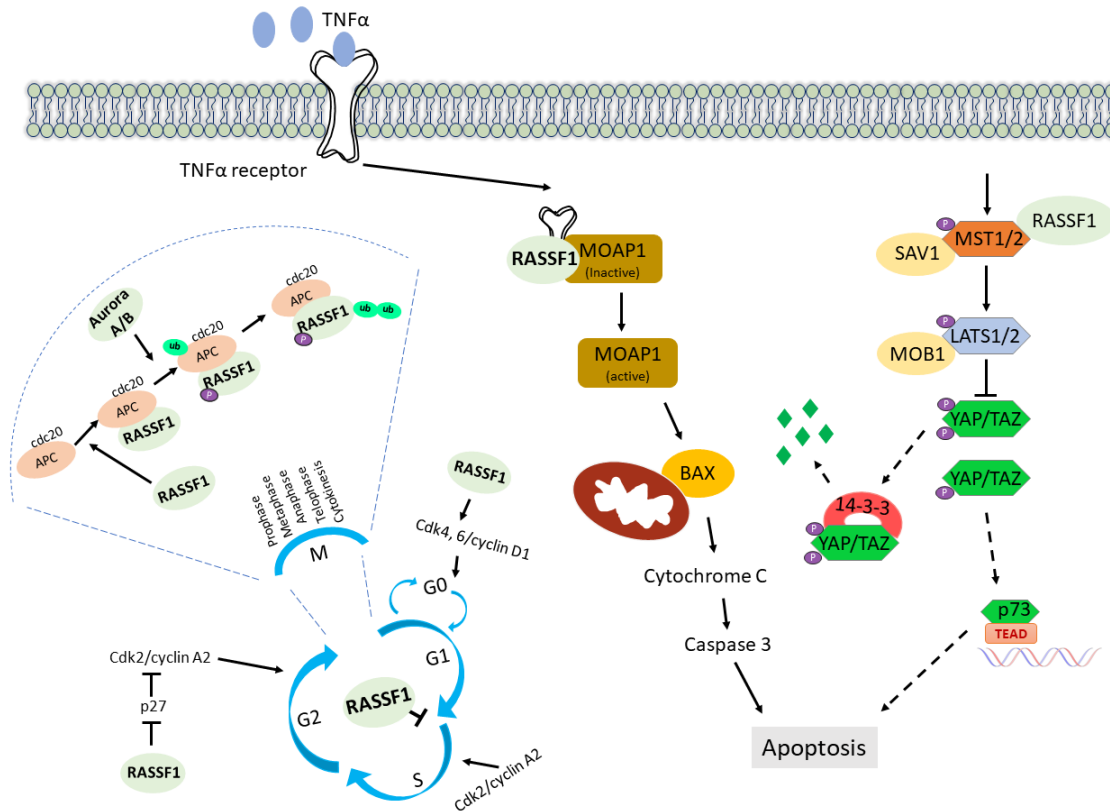
Figure 15: **Schematic representation of RASSF1 signalling network.**

Image shows the activation of RASSF1 in TNFα signalling network, Hippo activation and role of RASSF1 in cell cycle regulation.

RASSF5

Like RASSF1, RASSF5 is also a tumor suppressor and highly downregulated in various human cancers due to promoter hypermethylation [225, 226] and protein degradation in an acetylation-dependent manner [227]. RASSF5 has the same domain architecture as RASSF1 and displays high sequence similarity (60% identity). In humans, RASSF5 is expressed as three separate isoforms defined as RASSF5A, -5B and -5C. Both RASSF5B and RASSF5C are shorter, 5B lacking the entire SARAH domain, and 5C most of the N-terminal region including

54

the C1 domain. RASSF5A is the longest and most studied. Stieglitz et al 2008, solved a crystal structure of HRAS in complex with the RA domain of RASSF5 [117], the only structure to date of a RASSF RA domain. This structure was remarkable in that, while most RAS effectors establish contact with just the switch I region of RAS (e.g. RAF kinase (PDB-4G0N)) [228], RASSF5 contacts both RAS switch regions ((PDB-3DDC) **(Figure 16).** A minimum of 160 amino acid residues (residues 203 to 363 in human sequence) of RASSF5 is required to bind RAS, making its RA domain considerable larger than most other RAS interacting domains. Despite this, the RASSF5 RA adopts a ubiquitin fold similar to the RBDs of other effectors (5-stranded β-sheet, two flanking α-helices and 310-helix). The RASSF5 RBD has an unusually long unstructured loop between strands β1 and β2 and most strikingly an N-terminal helix that is not found in other effectors. The complex shows how RASSF5 recognizes RAS through both the canonical interaction at the switch I region (through the β2 strand of RASSF5), but also through its N-terminal helix (designated αN). The aN-helix is packed tightly against the ubiquitin fold through hydrophobic interaction between β1 strand and α2 helix. The switch II residues M67 and Y64 of RAS establish hydrophobic interactions with residues C220 and L221 of RASSF5. Deletion of amino acids 203 to 219 encoding the RASSF5 aN completely abolish interaction with RAS, verifying the significance of this unique contact [117]. Furthermore, detailed structural analysis of the RA domain of RASSF5 by NMR showed that its interaction with RAS is weakened by direct binding of its C1 domain to the RA domain [229]. Thus, X-Ray structural characterization shows that RASSF5 is a unique RAS effector that contacts HRAS at two distinct regions unlike other common RAS effectors.

The RASSF5 SARAH domain, like RASSF1, can homo- or hetero-dimerize with other SARAH domains. NMR revealed that the RASSF5 SARAH domain folds into an antiparallel helical structure in solution, and that the SARAH domain of RASSF1 (residues 220–270) can hetero-dimerize with the SARAH domain of RASSF5 (residues 366–413). Further, SARAH domains of MST1 and MST2 can also heterodimerize with RASSF5-SARAH [216] **(Figure 16).** From these studies, we can begin to model the complete 3-dimensional structure of RASSF5 and perform a homology model for other similar C-RASSFs.

RASSF5 should be considered a scaffolding protein analogous to RASSF1 and is also involved in pathways related to apoptosis. The specific links between RASSF5 protein in Hippo signal activation and apoptosis are explained in separate sections 1.5.5 and 1.5.6.
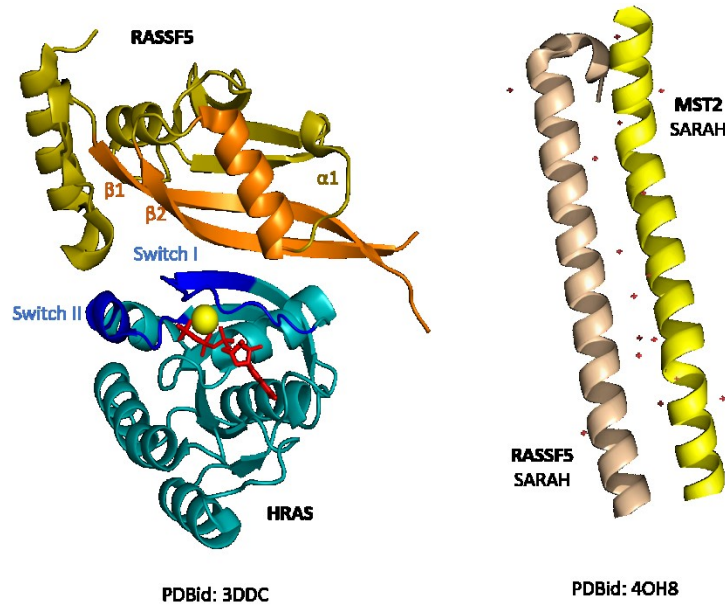
Figure 16:   Structure of RASSF5 domains

Left: Image shows the crystal structure of RASSF5 RBD in complex with HRAS and the image Right: Image shows NMR solution structure of SARAH domain of MST2 and RASSF5

1.5.3 N-RASSF proteins

N-RASSF family members lack both the C1 and SARAH domains found in C-RASSF proteins **(Figure 17).** Instead, they encode a predicted helical region and the overall different domain architectures suggest they belong to an entirely different family. Indeed, I will show in Chapter 2 that N-terminal RASSF proteins are more related to the apoptosis stimulating *protein* of p53 *(ASPP)* family of RAS effectors (Chapter 2).
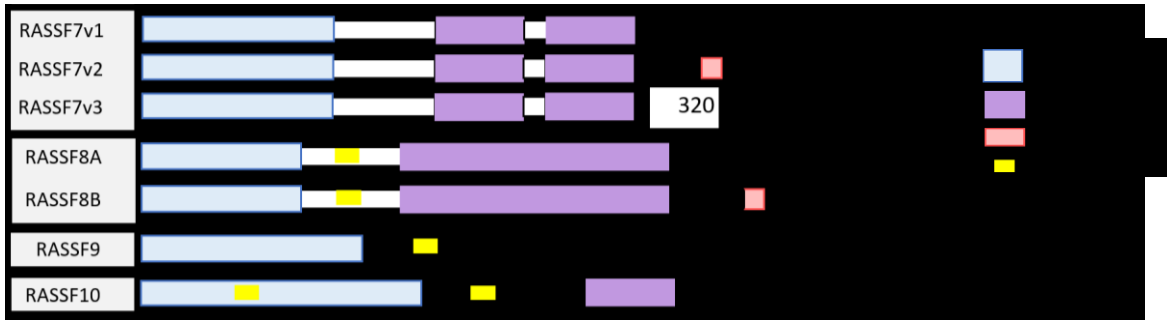
Figure 17: **Domain architecture of N-RASSF isoforms and homologs**

RASSF7

RASSF proteins are generally considered tumor suppressors and their expressions is frequently downregulated in human cancers. However, majority of studies show RASSF7 is not downregulated, in contrast they are upregulated [230-233]. In addition, RASSF7 is not hypermethylated in tumor cells [234] however, this claim is contradicted by others [225] . The *RASSF7* gene is located on chromosome 11p15.5 and is expressed as three major isoforms differentiated by their c-terminal lengths. RASSF7 is ubiquitously expressed but is highly enriched in brain and lung tissues. Yeast-two hybrid experiments identified three interactors of RASSF7: DISC1 (Centrosome-associated protein) [235], CHMP1B (Charged multivesicular body protein 1b) [236] and TSC1 (Tuberous sclerosis protein 1) [237]. The exact function of these interactions in cell is not clear. Studies have shown that RASSF7 regulates cell growth and apoptosis, as depletion of RASSF7 in *Xenopus* embryos results in abnormalities in body axis development, reduction of eye pigmentation and defects in the neuroepithelial cell layer caused by abnormal degradation of tissue architecture [238]. RASSF7 knockdown in neural cells results in mitotic arrest and failure in spindle formation [238], supported by others showing RASSF7 regulates microtubule, cytoskeleton and spindle formation [234]. Thus, until the convincing role of RASSF7 in tumor suppressive function is established, RASSF7 will be a unique protein in the RASSF family member.

RASSF8

RASSF8 is one of the N-RASSF proteins that is considered a tumor suppressor and its expression is downregulated in cancer cells [239]. *RASSF8* is located on chromosome 12p12.3 and is expressed as two isoforms, differing at their C-terminus. An NMR solution structure of the RASSF8 RA domain has been solved by the SGC (PDBid: 2CS4) **(Figure 18)**. *RASSF8* is ubiquitously expressed in murine embryos and human adult tissues [240], and is ostensibly a potent tumor suppressor. Falvella et al 2006, have demonstrated that expression of RASSF8 in lung cancer cell lines completely inhibits anchorage-independent growth [239]. In contrast, the down regulation of *RASSF8* expression in lung cancer lines increases anchorage-independent growth [240]. A role for RASSF8 in cell-adhesion has been proposed in *Drosophila*, demonstrating that dRASSF8 binds dASPP (drosophila apoptotic specific regulator of p53) and co-localizes at adherens junctions of epithelial cells during *Drosophila* eye development [241]. In zebrafish, RASSF8 is essential for the development of blood cells [242] and also necroptotic cell death [243]. With the availability of NMR structure, further work on studying the biological function of RASSF8 will make it a one of the best studied proteins among N-RASSFs.

Outside of their RA domains, the N-RASSFs are completely different from C-RASSFs and should be considered a different family of RAS effectors due to the predicted coiled-coil domain in the C-terminal region of the protein. This region is known to interact with ASPP1/2 (Apoptotic stimulating of p53) proteins and are frequently found with various interactor in proteomics study. However, the biological significance of N-RASSF and ASPP interaction is unclear.
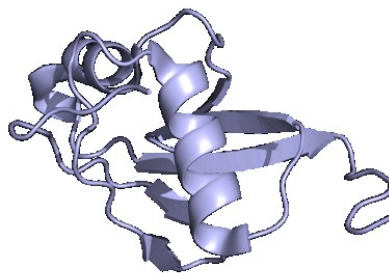
PDBid: 2CS4

Figure 18:   NMR structure of N-terminal domain of RASSF8

1.5.4 Microtubule association of RASSFs

Only RASSF1 among the RASSF family members has been shown to associate with microtubules. It is proposed that one of the primary biological functions of RASSF1A is to stabilize microtubules. Several groups have demonstrated that RASSF1A binds microtubules through microtubule-binding proteins (MAPs), including MAP1B and MAP4 [219, 244, 245]. This localization is dependent on the cell cycle, as during interphase RASSF1A is localized to microtubules, in prophase on centrosomes and during metaphase and anaphase to spindle poles and spindle microtubules. Finally, during early telophase RASSF1A localizes at the midbody and midzone [246]. RASSF1A localization at centrosomes serves as a microtubule-organizing centre (MTOC), and knockdown of RASSF1A results in the formation of multiple centrosomes, Conversely, overexpression of RASSF1A can inhibit centrosome separation [245]. The subcellular localization of other RASSF proteins are not well documented. RASSF5 has been observed quite prominently in the nucleus [247], but also at the plasma membrane. Localization of RASSF1 in microtubules suggests that RASSF1 might be scaffolding proteins to bring the various interactors together.

1.5.5 RAS-RASSF interactions and apoptosis

RAS GTPase activity plays a crucial role in the regulation of growth and proliferation, in tumor development and in cell survival. In mouse melanoma model, withdrawal of doxycycline-inducible HRAS-G12V causes regression of primary and explanted tumors [248] and likewise of oncogenic KRAS-G12D in pneumocytes causes apoptosis [249]. Thus, it is increasingly clear that activated RAS maintains tumorigenesis by evading apoptosis.

Many studies have demonstrated that RAS and other oncogenes counter-intuitively induce both growth and apoptotic signals (reviewed in [250]). Balancing negative and positive signalling activity is dependent on many factors, including cell type, availability of binding partners, kinetics and stoichiometry of binding partners, activation state of other proteins, environmental stimuli, etc. It has been speculated that overexpressed, activated RAS in normal cells could induce a pro-apoptotic signal that would prevent cellular transformation. One study has shown that RAS mediated anti-apoptotic signalling occurs through the activation of PI3K

and the AKT/PKB pathway. AKT phosphorylates pro-apoptotic BAD (Bcl2 members of apoptotic regulators) and sequesters BAD to 14-33, releasing BAD from Bcl2 and initiating an apoptotic response. At the same time, activation of the AKT/PKB pathway results in phosphorylation of IκBα kinase (IKK) and results in the activation of NFκB to promote survival [251, 252]. Thus, the capacity of activated RAS to generate signals towards pro-proliferation and pro-apoptotic pathways is highly context dependent.

One of the major pathways through which RAS is proposed to elicit an apoptotic response is through direct RAS-RASSF effector interactions. While there are scant mechanistic details, the following sections describe RAS-RASSF interactions and their role in apoptosis.

RASSF1

Studies showing a direct interaction between RAS and RASSF1 are highly contradictory. Co-immunoprecipitation studies by Vos et al 2006, showed that RASSF1A forms a complex with KRAS-G12V in HEK 293T cells. They further demonstrated that RASSF1A associates with the Modulator of Apoptosis-1 (MOAP-1) protein in a yeast two-hybrid screen, MOAP1 being a known binding partner of Bax (Bcl2 family member protein). It appears that the interaction between MOAP1 and RASSF1A is enhanced in the presence of KRAS-G12V, resulting in the activation of Bax to induce apoptosis [253]. Others have shown that RASSF1C forms a complex with HRAS-G12V using co-immunoprecipitation assays, and *in vitro* binding experiments show that HRAS binds to RASSF1C in a GTP-dependent manner. Further, they observed that the co-overexpression of RASSF1C and oncogenic HRAS-G12V causes apoptosis in HEK 293T cells [254]. Both of the studies mentioned above are disputed by Ortiz-Vega et al 2002, and they instead hypothesize that RASSF1 binds RAS only through a RASSF5 hetero-dimerization mediated by their SARAH domains [255]. Pull-down studies by Chan et al 2013, also suggest that RASSF1 does not complex with activated HRAS-G12V [256] and fluorescence binding assays by Wohlgemuth et al 2005, reported that the RA domain of RASSF1 shows a very weak affinity of 39 μM for HRAS [213]. Thus, though the biochemical evidence suggests that RASSF1 does not interact with RAS, in the cells they

exhibit pro-apoptotic roles probably due to their interaction with death cell receptors or Hippo kinase (detailed in section 1.5.5).

RASSF2

RASSF2 is one of the least studied RASSF family members. Co-immunoprecipitation studies by Vos et al 2003, show that RASSF2 binds directly to KRAS in a GTP dependent manner. Further, they observe that co-overexpression of KRAS along with RASSF2 induces apoptosis and cell cycle arrest in HEK 293T cells [257]. The biological significance of KRAS interaction with RASSF2 is reported by Donninger et al 2010, where they show that KRAS regulates complex formation between RASSF2 and PAR-4 (prostate apoptosis response protein 4) and RASSF2 assists nuclear translocation of PAR-4 [258]. However, pull-down studies by Chan et al 2013, report that RASSF2 does not forms complex with activated HRAS-G12V [256]. Therefore, convincing biochemical and *in-vivo* studies is required to establish the interaction between RASSF2 and RAS and its significance in inducing apoptosis.

RASSF3

There are no existing studies describing the association of RASSF3 with RAS.

RASSF4

Only one study has directly linked RASSF4 with RAS, Eckfeld et al 2004, observed that RASSF4 associates with activated KRAS-G12V in a GTP dependent manner using co-immunoprecipitation studies. Further, overexpression of RASSF4 with oncogenic KRAS-G12V induces apoptosis in HEK 293T cells [259]. Further work is required to conclusively establish the interaction between RASSF4 and RAS.

RASSF5

Studies on the binding kinetics of the RAS-RASSF5 interaction reveal it binds HRAS with an affinity of 0.08 µM. It must be noted that these experiments were performed in the complete absence of NaCl rather than a more typical physiological salt concentration. Ortiz-Vega et al 2002, reported that RASSF5 binds to several RAS-like GTPase (KRAS, RRAS, MRAS, RRAS3, RAP2A) in a GTP dependent manner[255]. Numerous studies link RASSF5 and RAS in the context of pro-apoptotic signalling. RASSF5 was shown to induce apoptosis in response to death receptor ligand TNF-α, and siRNA depletion of RASSF5 reduces TNF-α-induced apoptosis. The proposed mechanism of this process is direct RASSF5 association with MST1 Hippo kinase, as similar effects were observed when siRNA against MST-1 kinase was used. In mice, depletion of RASSF5 in embryonic fibroblasts results in resistance to TNF-α-mediated apoptosis, RASSF5-null mice cannot activate MST1 and they are highly resistant to TNF-α-induced apoptosis [260]. Finally, Vos et al 2003, show that RASSF5 inhibits the growth of HEK 293T cells in a RAS dependent manner [261]. Therefore, among all RASSF proteins, RASSF5 is the only protein which has been proven to interact with HRAS by X-Ray crystallography techniques and convincingly displayed its role in inducing pro-apoptotic signals in mice models.

RASSF6

RASSF6 was shown to associate with KRAS-G12V by co-immunoprecipitation, and ectopic expression of RASSF6 induces apoptosis in a RAS dependent manner [262]. It was observed that tumorigenicity is enhanced upon siRNA depletion of RASSF6 in human lung cancer cell lines [262], and studies by Chan et al 2012, observed complex formation between RASSF6 and activated HRAS-G12V [256]. Conversely, Ikeda et al 2007, reported little or no interaction between RASSF6 and the small GTPases KRAS, HRAS, NRAS, MRAS, or TC21, yet they found that RASSF6 expression activates BAX and induces the release of cytochrome C followed by apoptosis in HeLa cells [263]. Thus, due to several contradictory claims on the RASSF6 interaction with RAS, convincing evidence is required to establish RASSF6 and RAS interaction.

N-RASSFs

There is no documented evidence showing association of N-RASSFs 7, 8 or 10 with any of RAS isoforms. Interestingly, pull-down experiments with RASSF9 and RAS isoforms shows complex formation, with RASSF9 binding stronger to NRAS then KRAS or HRAS [264].

Chan et al 2013, performed a comparative analysis on all RASSF proteins to check their capacity to bind HRAS using pull-down assay and contradicted most of the above observations, and concluded that except RASSF5, 6 and 7 none of the other RASSF showed interaction with HRAS. However, the study did not show any biological significance of the interaction. It is revealing that there are large contradictions on RAS association with RASSF proteins in the literature, highlighting a near-complete lack of proper *in vitro* characterization of these complexes. However, it is clear that RASSF effectors can generate pro-apoptotic signals, reduce colony formation, and induce cell death.

1.5.6 RASSF and Hippo signalling

Despite RASSF proteins being one of only few direct regulators of Hippo kinases, their role in Hippo signalling has not been well-defined. The Hippo pathway was discovered in *Drosophila*, where the core components are Hippo, Salvador, Mats and Warts. These were identified using a genetic mosaic screen while looking for possible oncogenes and tumor suppressors [265]. Hippo and Warts are kinases, whereas Salvador and Mats are regulators respectively of Hippo and Warts. Loss of function of these components (*Hippo* [266, 267], *Salvador* [268, 269], *Mats* [270] and *Warts* [271, 272]) results in extreme tissue growth in *Drosophila*, where significant work has demonstrated that Hippo, a Ste-20 kinase, phosphorylates and activates the Warts (Wts) kinase. Wts phosphorylates and inactivates its downstream effector, transcriptional coactivator *Yorkie* (Yki) and therefore creates 14-3-3 binding sites that results in cytoplasmic retention of Yki and subsequent degradation [273, 274]. Hippo is also known to phosphorylates Sav and Mats, but this has regulatory functions [275].

Loss of Hippo causes increased transcription of the cell death inhibitor *diap-1* and cell cycle regulator *cycle-E*, resulting in decreased apoptosis and increased cell proliferation [276] **(Figure 19)**.

The mammalian Hippo pathway components are functionally related to their *Drosophila* orthologs. The two mammalian orthologs of *Drosophila* Hippo are Mammalian STE-20-like kinases 1 and 2 (MST1 and MST2). The activation of Hippo signalling in mammals starts with dimerization and auto-phosphorylation of MST1/2 kinases [277]. Other kinases, including thousand-and-one (TAO) amino acids kinase (or TAOK1–3) can regulate Hippo signals by phosphorylating and activating MST1/2 [278, 279]. Activated MST1/2 kinases phosphorylate and complex with SAV1 (mammalian ortholog of Salvador), mediated through their SARAH domains [280]. MST1/2 also phosphorylates the scaffolding protein MOB1 that helps to recruits the LATS1/2 complex (mammalian ortholog of Warts) [281]. MST1/2 directly phosphorylates LATS1/2 on a hydrophobic motif centred on T1079 (LATS1) or T1041 (Lats2), resulting in LATS activation [282]. LATS1/2 phosphorylates and activates the main target of the Hippo pathway, Yes-associated protein (YAP). YAP is the mammalian ortholog of Yorkie, and phosphorylation of YAP results in its inactivation, cytoplasmic retention and degradation [273, 274, 283]. Inactive Hippo signalling means that YAP remains unphosphorylated, translocating into the nucleus and binding to the TEAD transcription factor to promote the expression of genes involved in cell proliferation and inhibition of apoptosis [284-287] **(Figure 19)**. Apart from TEAD, YAP also binds to other transcription factors such as Smad complexes [288-290], RUNX1/2 [291], p63/ p73 [292] and ErbB4 [293]. Over the past two decades, due to extensive research, our understanding of Hippo pathway functions, especially its downstream signals have progressed. However, many questions focusing on the upstream signals that activates Hippo pathway are still elusive.

As mentioned, how RASSF proteins activate Hippo signalling is highly enigmatic. All C-terminal RASSF proteins (RASSF1 - 6) contain a SARAH domain and should bind directly to MST1/2 kinases. The functional significance of this interaction is debatable. Some suggest that RASSF-MST interactions inactivate Hippo signalling, while others propose this has an activating function. *Drosophila* dRASSF competes with Sav for Hippo and recruits a PP2A complex (dSTRIPAK) that appears to dephosphorylate Hippo and antagonize signalling (i.e.

an anti-apoptotic role) [294, 295].   Similarly, Ikeda et al 2009, showed that MST2 kinase inhibited RASSF6-induced apoptosis [296]. In another study, Praskova et al 2004, showed that both RASSF5 and RASSF1 co-immunoprecipitated MST1/2 kinases, but co-expression of RASSF1 and RASSF5 with MST1 kinase suppressed auto-phosphorylation of MST1 (T183), resulting in the abolition of MST1 to undergo Mg-ATP dependent autoactivation [297].

However, others show RASSF proteins activate Hippo pathway by various mechanisms. Overexpression of RASSF1A increases the kinase activity of MST1, suggesting RASSF1 facilitates MST1 activation and promotes death receptor-dependent apoptosis [298]. A recent study by Yee et al 2010, show a completely different mechanism of Hippo activation by RASSF1 in response to DNA damage. Study reports that, upon DNA damage, RASSF1A is phosphorylated at S131 by ATM kinase and phosphorylated RASSF1 activates MST2 and LATS1 complex. Generally, hyper-phosphorylation of YAP displays cytoplasmic retentions and subsequent degradation. However, in this case, under-phosphorylation of YAP by activated LATS1 maintains a pool of YAP in the nucleus that switches its binding partner from anti-apoptotic transcription factor YAP-TEAD complex to pro-apoptotic transcription factor YAP-p73 complex [211, 299]. This observation was further corroborated by Papaspyropoulos et al 2018, where they demonstrated RASSF1 enhances YAP-p73 transcriptional activity and promotes differentiation [300]. Further, they show that RASSF1A acts as a natural barrier for cells' self-renewal capacity by swapping YAP from an β-catenin-TCF pluripotency signalling to an important component that promotes differentiation [300]. In a complex biological system, multiple proteins function in parallel and identifying the precise function of proteins is often context dependent, particularly true for the Hippo pathway. Recent studies also show the involvement of Hippo pathway protein YAP in maintaining RAS driven tumorigenesis [301-303]. Hence, a detailed characterization of RAS-RASSF-MST regulation, might help explain apparent discrepancies in whether RASSFs activate or inactivate Hippo signalling.
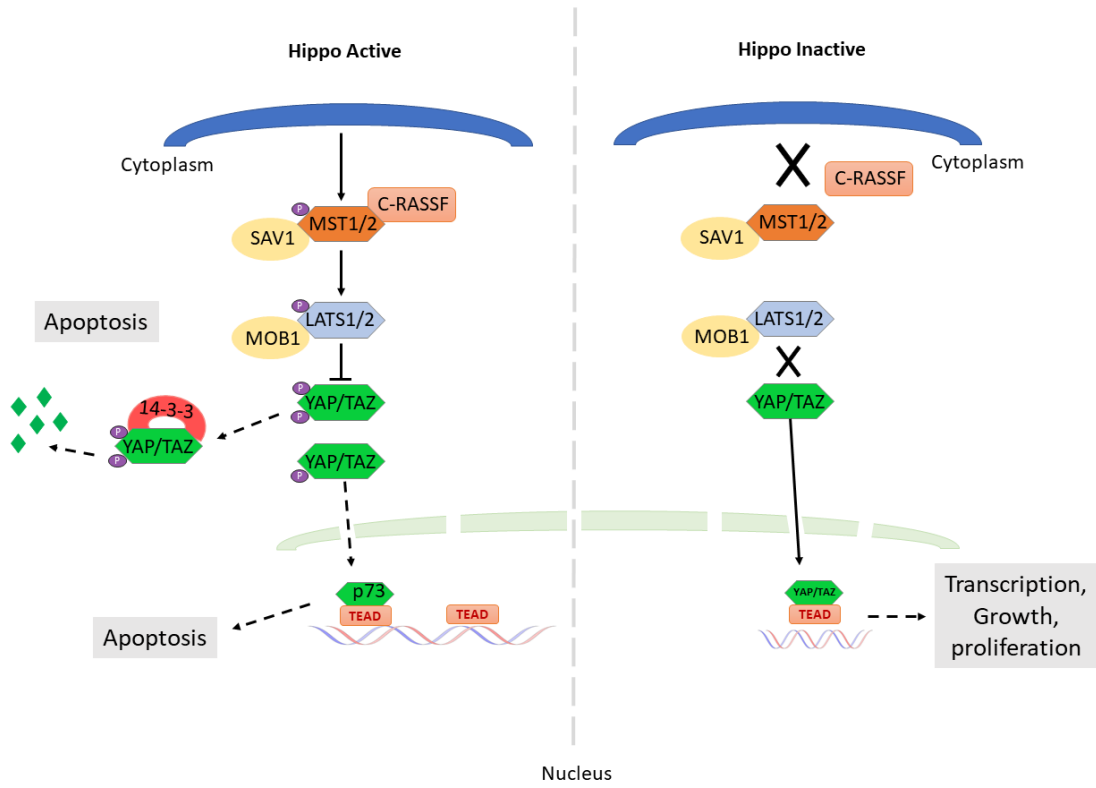
Figure 19: **RASSF protein's involvement in hippo signalling.**

1.6   Hypothesis and Objectives

Since the discovery of RAS and the RAS superfamily of small GTPases, there has been a constant effort to understand their cellular function. A key step was the identification and characterization of effectors of these small GTPases, starting with the MAPK activator RAF. The seemingly diverse biological functions of RAS effectors include both stimulation of cell proliferation and induction of pro-apoptotic signals. There is a considerable gap in our understanding of how RAS may invoke apoptosis, and the physiological role of RAS interactions with RASSF effectors is not entirely understood. Further, there are many RAS family small GTPases whose functions are completely unexplored. For instance, to date there is no direct research article describing a function for the RAS-like small GTPase RASL12, a protein that shares 32% sequence identity with KRAS.

I attempt to answer some of the above questions in the two succeeding chapters. The main objective of my Ph.D. thesis was to better understand how RASSF proteins function in the cell, and how these proteins are linked with RAS small GTPases. Previous studies have not decisively shown how RASSF effectors are linked/regulated by RAS signalling. I show that some RASSF proteins are not direct RAS effectors at all, though they possess a RA domain. Importantly, I focus on how minor differences in their amino acid compositions ultimately make them binding partners for alternative RAS subfamily GTPases. Further, RASSF proteins are known as tumor suppressors and their expression is frequently downregulated in human cancers. RASSF function in pro-apoptotic signals such the Hippo pathway, though not well understood, demonstrates why cancer cells may succeed by down regulating their expression. I wanted to exploit the role of RASSF proteins in inducing apoptotic activity by rewiring RAS signals from the RAF-MAP kinase pathway to the RAS-RASSF pathway.

The foundation of my first hypothesis: not all RASSF proteins are KRAS/HRAS/NRAS effectors and instead interact with other RAS-like small GTPases. To test this, I had the following objectives;

- To biochemically test whether all the RASSF proteins interact with RAS

- To identify other small GTPases to which RASSF1 can interact

- To study the biological significance of interactions between RASSF1 and the newly identified interacting partners

I presented the results of this study in Chapter 2, the manuscript is "under-revision" in a peer-reviewed scientific journal.

My second hypothesis: RAS downstream signals can be rewired from growth-inducing proliferation pathways to the pro-apoptotic Hippo pathway. To accomplish this, I had the following objective;

- To introduce mutation(s) in KRAS that abrogate interaction with RAF and enhance RASSF binding

- To introduce mutation(s) in RASSF proteins to drive stronger RAS binding

- To study the biological outcomes of the designed mutants in cells.

I present the results of this study in Chapter 3 of this thesis. We are preparing the manuscript for publication.

2. Chapter 2: RASSF effectors couple diverse RAS subfamily GTPases to the Hippo pathway

Dhanaraman Thillaivillalan[1], Swati Singh[1], Ryan C. Killoran[1], Anamika Singh[2], Xingjian Xu[1], Julia Shifman[2] and Matthew J. Smith[1,3,*]

[1]Institute for Research in Immunology and Cancer, Université de Montréal, Montréal, Québec, H3T 1J4, Canada
[2]The Hebrew University of Jerusalem, Department of Biological Chemistry, Jerusalem, Israel
[3]Department of Pathology and Cell Biology, Faculty of Medicine, Université de Montréal, Montréal, Québec, H3T 1J4, Canada

[*]To whom correspondence should be addressed:

Matthew J. Smith, Ph.D
Institute for Research in Immunology and Cancer (IRIC)
Department of Pathology and Cell Biology, Université de Montréal
2950 Chemin de Polytechnique, Montréal, Québec, Canada, H3T 1J4
Pavillon Marcelle-Coutu, Rm 4306-11; Tel: (514) 343-5704
email: matthew.james.smith@umontreal.ca

The manuscript is "accepted" in the journal (Science Signalling).

Contributions:

D.T. and M.J.S. designed experiments. D.T., S.S., R.K., X.X. and M.J.S. performed experiments and analyzed data. A.S. and J.S. performed structural modelling. J.S. and M.J.S. supervised studies. D.T. and M.J.S. wrote the manuscript with input from R.K. and J.S.

2.1 Abstract

Activated RAS GTPases signal by directly binding effector proteins. Effectors have a folded RAS association (RA) domain that binds exclusively to GTP-loaded RAS, but the specificity of most RA domains for >150 RAS superfamily GTPases is unknown. RAS-association domain family (RASSF) proteins comprise ten members. It is the largest family of RAS effectors proposed to couple RAS to the pro-apoptotic Hippo pathway. We show that RASSF1-6 complex with Hippo kinase, while RASSF7-10 are a separate family related to p53-regulatory ASPP effectors. Only RASSF5 directly binds activated HRAS and KRAS. Structural modelling reveals that expansion of RASSFs in vertebrates included amino acid substitutions that alter their GTPase binding specificity. We demonstrate that the tumour suppressor RASSF1A complexes with the GTPases GEM, REM1, REM2 and the enigmatic RASL12. Interplay between RASSFs and RAS GTPases can drastically restrict YAP1 nuclear localization. Thus, these simple scaffolds can link activation of diverse RAS proteins to Hippo or p53 regulation.

Keywords: RAS; RASSF; Hippo; ASPP; GTPase; RGK; RASL; apoptosis; Ca^{2+}; RA domain; YAP1

2.2 Introduction

RAS small GTPases are archetypal signalling proteins that control the direction and intensity of signals by acting as 'molecular switches'. The proteins present distinct conformations dependent on a bound nucleotide: when bound to GTP they are 'on' and interact with diverse effector proteins that relay signals downstream. When GDP-bound, they lose their ability to interact with effectors and are considered 'off'. Three RAS proteins (KRAS, NRAS and HRAS) have been intensely studied since the 1980s as key drivers of human cancers [1] . They are members of a GTPase superfamily that consists of >150 proteins divided into the RAS, RHO, ARF, RAB, and RAN branches [2]. The RAS subfamily consists of 35 small GTPases in humans, yet the function of most remains understudied. They can be ostensibly classified into two groups: those that promote cell proliferation or survival (RAS, RAL [3], RIT [4], RHEB [5] and RAP [6]) and those that induce cell cycle arrest or apoptosis (RASD [7], NKIRAS [8], RASL [9], DIRAS [10] and RGK [11]). Comparatively little is known about how these later tumour suppressor RAS GTPases function.

Effector proteins determine where activated GTPase signals are routed, and RAS-induced tumourigenesis is known to depend on multiple effectors [12, 13]. Effectors compete for activated RAS using recognition domains called RAS-Association (RA) or RAS Binding Domains (RBDs) (collectively referred to here as RA domains). There are >50 RA domains in the human proteome by sequence homology [14], and all proteins comprising these domains are currently deemed 'RAS effectors'. Despite this, there is likely extensive plasticity in effector-GTPase interactions whereby each effector signals downstream of multiple GTPases. This idea is supported by data showing PI3K binds to multiple distinct RAS subfamily GTPases [15].

Paradoxically, H/K/N-RAS binding to the poorly studied RAS association domain family (RASSF) of effectors is suggested to promote apoptosis rather than proliferation [16] and the promoters of ten genes encoding RASSF proteins are hypermethylated in numerous cancers [17, 18]. These are amongst the most frequently inactivated tumour suppressors, candidate biomarkers and appealing therapeutic targets. With ten homologous family members, they also comprise one-fifth of the proposed RAS effector landscape. Co-expression of RASSF1 or RASSF5 with oncogenic RAS triggers an apoptotic response [19, 20], and several

RASSF members inhibit proliferation of tumour-derived cells [21-24]. Consistent with a tumour suppressor role, mice lacking RASSF1 are prone to spontaneous tumorigenesis [25]. The proteins are simple scaffolds and can be divided into two groups: C-terminal or classical (C-)RASSFs 1-6 and N-terminal (N-) RASSFs 7-10 (**Figure 1A**). All family members have an RA domain proposed to bind H/K/N-RAS. Some evidence for this exists for RASSF1 [19], RASSF2 [26], RASSF4 [22], RASSF5[16] and RASSF7 [27], but only the RASSF5 interaction is supported by *in vitro* binding data and a structure of its RA domain bound to HRAS [28]. Other studies have linked RASSFs to the small GTPases RAP1A [29], RHEB [30], RHOA [31], and RAN [32]. Conclusive biophysical evidence for these interactions is lacking. Besides an RA domain, C-RASSFs comprise a helical SARAH motif that directly binds the pro-apoptotic Hippo kinases MST1/2 [33-36], which direct the cellular response contact inhibition, mechanical tension and polarity to control organ size and tissue homeostasis *via* coordinated apoptosis. Though RASSFs are one of few direct Hippo interaction partners, their impact on MST1/2 activity or YAP/TAZ nuclear translocation has not been fully investigated. The N-RASSFs lack a SARAH motif and whether they have a role in Hippo signalling is unclear.

A family of tumour suppressors directly linking RAS with apoptotic Hippo signalling is highly intriguing and requires definitive analysis. More generally, the specificity of effector RA domains for RAS or alternative RAS-like GTPases remains unknown. Here, we begin to resolve these questions for the RASSF family of purported RAS effectors. We clarify which RASSF effectors directly complex with activated KRAS and define interaction partners for the associated functional domains in these scaffolds. New RAS subfamily interaction partners are identified for the important RASSF1A tumour suppressor that support a role in cell cycle regulation and Ca^{2+} homeostasis. We reveal that RASSFs do not inherently synergize with oncogenic RAS to promote apoptosis and connect these new data to Hippo activation.

2.3 Results

2.3.1 Delineation and Purification of RASSF RA domains

To investigate RASSF interactions with GTPases we required purified and well-folded RA domains. Only the RASSF5 RA domain has been previously characterised. To define domain boundaries for the other nine RASSFs we used a combination of sequence homology, secondary structure predictions, and the understanding that effector RAS-binding domains share a ubiquitin superfold (ββαββαβ). Additionally, the RA domain of RASSF5 has a distinct N-terminal α-helix that is essential for binding RAS [28]. **Figure 1A** shows the domain architecture of the longest isoform of each RASSF and the boundaries of their RA, C1 and SARAH domains overlaid with secondary structure predictions (JPred). By homology, RA domains from the N-RASSFs (7-10) do not cluster with C-RASSFs, but rather with RA domains from two apoptosis-stimulating proteins of p53 (ASPP) effectors (also PPP1R13B and TP53BP2; **Figure 1B and Supplementary Figure S1A**) [37, 38] . Further, N-RASSFs have a long coiled-coil region analogous to those found in ASPP proteins (**Supplementary Figure S1B**) and do not encode the αN-helix present in RASSF5. We were able to express and purify RA domains from RASSFs 8-10 as recombinant GST-fusion proteins, but the RASSF7 domain proved insoluble under numerous expression and purification conditions and was not considered further (**Supplementary Figure S2**). Amongst the C-terminal RASSF proteins, RASSF1, RASSF3, and RASSF5 form one homology subgroup and RASSF2, RASSF4, and RASSF6 a second. Each of the RASSF1/3/5 RA domains encode an αN-helix critical to RAS binding, and production of recombinant protein using our defined boundaries resulted in RA domains that could be purified to high concentration and homogeneity (**Supplementary Figure S2**). The RASSF2/4/6 subgroup each show a region of predicted secondary structure at their N-termini that bears no homology to RASSF C1 domains. In fact, the sequences encoding these elements are homologous to the αN-helix and β1 strands of RASSF1/3/5 (**Supplementary Figure S3**). Indeed, RASSF2/4/6 RA domains lacking these N-terminal regions proved highly insoluble, but their inclusion stabilized recombinant proteins (**Supplementary Figure S2**). Thus, it appears that long unstructured segments have evolved between strands β1 and β2 of the RASSF2/4/6 RA domains with unknown consequences on protein folding. The analogous region of the *D. melanogaster* ortholog is separated by over 500 amino acids (**Supplementary**

Figure S3). Delineation of these domain boundaries and purification of recombinant RA domains from nine RASSF homologs provided an opportunity to systematically assess their ability to bind RAS GTPases. We also generated vectors to express full-length, FLAG-tagged RASSF proteins in cultured cells, focusing on the longest isoform for each (**Figure 1C**). As with its RA domain we found full-length RASSF7 mostly insoluble, but now had a toolbox to assay interactions for the other nine RASSF effectors and sought to identify binding partners for all functional regions.

2.3.2 Differential RASSF Interactions with KRAS, Hippo Kinase and ASPP Effectors

RASSF effectors are small scaffolds with few recognized domains outside the RA module. An exception is the SARAH motif at the C-termini of all C-RASSFs (**Figure 1A**). Previous studies revealed interactions between the SARAH motifs of RASSF1, RASSF2 and RASSF5 with those of the mammalian Hippo kinases [34, 36, 39, 40]. To ascertain if all RASSF proteins interact with the Hippo kinase MST1 we co-expressed full-length FLAG-RASSF proteins with GFP-tagged MST1 and performed co-immunoprecipitations (co-IPs). This approach established that all six C-RASSF proteins (RASSF1-6) associate with MST1 (**Figure 2A**). Further, we consistently observed increased C-RASSF protein levels upon co-expression with MST1, suggesting the kinase promotes RASSF stability. A RASSF5 construct truncated after the RA domain confirmed that loss of the SARAH motif disrupts MST1 binding. The N-RASSFs 8-10 lack a defined SARAH motif and did not co-precipitate with the Hippo kinase. These data reveal that all C-RASSFs can complex with MST1 and may regulate Hippo signalling.

As N-RASSFs exhibit greater homology to the ASPP family of purported RAS effectors, and these are capable of oligomerization [41], we investigated whether RASSFs 8-10 could complex with ASPP1/2. Indeed, the *Drosophila* ortholog dRASSF8 associates with dASPP to regulate cell adhesion [42]. We co-expressed nine FLAG-RASSF proteins with either HIS-tagged ASPP1 or ASPP2 and performed co-IPs. All three N-RASSFs co-precipitated with both ASPP1 and ASPP2, while none of the C-RASSFs proteins bound (**Figure 2B**).

Interestingly, the ASPP effectors are direct regulators of p53 and known tumor suppressors with a pro-apoptotic function, not unlike RASSFs.

While numerous studies have probed individual interactions between RASSF family members and RAS GTPases, results have been ambiguous and have not employed isolated RA domains. Further, our sequence alignment reveals only RASSF1 has a conserved Lys residue required for RASSF5 binding to HRAS (Lys288; **Supplementary Figure S3**). To resolve whether all RASSF homologs are direct RAS effectors we systematically probed interactions between activated KRAS and the nine purified RA domains. GST-tagged RA domains were added to cell lysates expressing full-length, GFP-tagged WT-KRAS (wild-type), G12V-KRAS (constitutively activated) or GFP alone (control) and complexes isolated on glutathione beads. For a proper comparative analysis, each RA domain was purified by size exclusion chromatography and added to the same batch of cell lysate at a final concentration of 1 µM. GST pull-downs were washed 5X in the identical buffer, and anti-GFP immunoblots exposed in parallel. As expected, we detected strong binding between the RASSF5 RA domain and G12V-KRAS (**Figure 2C**), but no other RASSF complexed with the GTPase. As this approach only assayed interactions with our defined RA domains, we repeated this analysis using the longest isoform of each RASSF. We performed anti-FLAG precipitations following co-expression of FLAG-RASSF proteins with GFP-tagged WT-KRAS, G12V-KRAS or GFP alone. As with the GST binding assays, only RASSF5 interacted with G12V-KRAS (**Figure 2D**). We consistently observed weak association between RASSF1 and G12V-KRAS, and to a lesser extent RASSF4 and RASSF6, but this was only evident upon long exposure of immunoblots. That only RASSF5 is able to bind KRAS contradicts much of the literature, but is consistent with some data suggesting other RASSFs have reduced affinity for RAS [43].

2.3.3 RAS-Induced Apoptosis and RASSF Interactions with RAS Superfamily Small GTPases

The lack of KRAS binding suggested that all RASSF effectors may not elicit an apoptotic response downstream of RAS *via* a direct mechanism, as previously proposed. To test this, we systematically assessed the capacity for RASSF proteins to stimulate cell death.

We measured apoptosis by Annexin V staining of HEK 293T cells expressing FLAG-tagged RASSF proteins alone or together with G12V-KRAS. FACS analysis showed that no RASSF proteins intrinsically stimulate apoptosis over control levels (**Figure 3A/B**). Moreover, we observed no significant increase in Annexin V staining when RASSFs were co-expressed with activated KRAS, which alone stimulated a 4-fold increase in apoptosis (50-60% of KRAS-expressing cells were apoptotic). The homologous HRAS protein (G12V) also induced a significant 3.6-fold increase in apoptosis, but this was not augmented at all by co-expression of RASSF5. These results contradict a model whereby RASSF proteins synergize with oncogenic RAS to induce cell death, and validate that these effectors are not universal RAS-binders.

We presumed that RASSF effectors (other than RASSF5) might associate with distinct members of the RAS superfamily. Using discovery approaches to elucidate GTPase interactions is difficult as the proteins must be highly expressed, be in the active/GTP-bound conformation and not engaged with other high affinity binders. Thus, we took a systematic approach by first selecting six candidate GTPases to perform comparative binding assays: HRAS, RAP1A, RHEB, RAN (all previously proposed to bind RASSFs [29, 30, 32]), and the RHO family GTPases RAC1 and CDC42 (as overexpression of RASSFs alters cell morphology) [31]. HRAS is identical to KRAS across its two RA domain binding sites (switch I and II), while the five other GTPases have amino acid substitutions at several key residues. To examine binding to RASSFs we generated expression constructs for wild-type or activated mutant (based on RAS G12V) variants. Purified, GST-tagged RA domains from the nine RASSFs were added to cell lysates expressing these GTPases, and complexes isolated on glutathione beads. As expected, RASSF5 bound to KRAS and HRAS, and weakly to the homolog RAP1A, but our results did not corroborate a single interaction between other family members and any GTPase (**Figure 3C**). Thus, though RASSFs comprise an RA domain our data suggest upstream GTPase signals feeding into these tumour suppressors, and the cellular manifestation of these signals, are largely unknown.

76

2.3.4 RASSF1 is an Effector of the RGK Family of RAS GTPases

To develop a second set of candidates we considered how residues in RASSF RA domains complement those in small GTPases. RAS effectors share a conserved mode of RAS recognition based on formation of an intermolecular, anti-parallel β-sheet (between β2 and β3 of RAS and β1, β2 and α1 of the RA domain), and RASSF5 has a distinctive αN-helix that contacts the RAS switch II region. Having established positions of secondary structure for all RASSF RA domains (**Supplementary Figure S3**) we used the crystal structure of RASSF5-HRAS (**Figure 4A**) to construct structural models for the six C-RASSF RA domains (**Figure 4B** and **Supplementary Figure S4**). Models for the N-RASSF domains were generated based on an AFDN-HRAS structure [14]. Residues in each αN, β1 and β2 region specify small GTPase interactions based on archetypal RAS-effector binding. Here, we focus on identifying novel GTPase interactors for RASSF1, as it has become an intriguing clinical biomarker and retains most of the key RAS-binding residues from its paralog, RASSF5. The only significant amino acid substitution in RASSF1 is an Asn in the αN-helix. This residue is a Cys in RASSF5 that mediates a key hydrophobic interaction with HRAS (**Figure 4A/B**). To explore the importance of this residue as a specificity determinant, we performed *in vitro* binding experiments using isothermal titration calorimetry (ITC). We measured a dissociation constant (K_d) for wild-type RASSF5 RA domain binding to GMPPNP-loaded KRAS of 1.7 ± 0.1 μM. A C225N mutant of RASSF5, mimicking RASSF1, had a 7-fold weaker K_d of 11.3 ± 0.7 μM (**Figure 4C**). Conversely, wild-type RASSF1 RA domain had no measurable affinity for KRAS but a swapped N149C αN mutation enabled this interaction, with a K_d of 9.6 μM (**Figure 4D**). Taken together, amino acid substitutions in RASSF αN-helices significantly impact binding to small GTPases and, along with residues in β1 and β2, are key specificity determinants.

To identify small GTPase partners for RASSF1 we considered the three contact sites that define a RASSF-GTPase complex. As the RASSF1 β1, β2 and α1 regions are nearly identical to RASSF5 (**Figure 5A**: contact sites 2 and 3), we focused on the αN-helix Cys-Asn substitution (contact site 1). We aligned the amino acid sequences of all 35 RAS subfamily GTPases and considered those with similar switch I regions to HRAS but that diverged in the switch II region (around HRAS Tyr64 and Met67 that contact RASSF5; **Supplementary Figure S5**). Based on this, we selected six candidate GTPases: GEM, REM1, REM2, RASL12,

ERAS and DIRAS3. These are highly conserved around RAS Asp33 and Asp38 but have distinct switch II sequences (**Figure 5B**). To assay interactions with RASSF1 we performed binding experiments using purified RA domain and activated GTPases. Mutational activation of full-length GTPases was based on RAS G12V, though the efficacy of this amino acid substitution in all small GTPases must by interpreted with caution [44]. GST-tagged RASSF1 RA domain was incubated with cell lysates expressing the six activated GTPases or KRAS as a control. Remarkably, we found that all six GTPases could complex with the RASSF1 RA domain while KRAS did not (**Figure 5C**). This was corroborated by co-IP experiments in which FLAG-tagged RA domain (**Figure 5D**) or full-length RASSF1A (**Figure 5E**) were co-expressed with the GTPases. Precipitation with anti-FLAG revealed all six candidate GTPases complex with RASSF1. We consistently noted the RGK family proteins GEM, REM1 and REM2 as strong interactors, but could detect no binding to the fourth RGK GTPase, RRAD (not shown). Thus, a structure and sequence-based informatic approach was able to identify six potential RAS family GTPase partners for RASSF1.

To confirm these proteins directly interact we attempted *in vitro* mixing assays using purified RA domain with the RGK GTPases or RASL12. Unlike most RAS GTPases we've previously isolated, these four proteins were highly unstable under multiple expression and purification conditions. GEM and REM1 proved most stable in solution and were chosen for further study. GST-tagged, wild-type GEM (residues 62-203) and REM1 (residues 76-251) were purified and exchanged with either GDP, GTP, or the non-hydrolyzable analogs GTPγS and GMPPNP. The GTPases had a propensity to precipitate during exchange reactions, possibly due to their low affinity for nucleotide [45]. GEM and REM1 were therefore exchanged using a simplified procedure: incubating for two hours in a 10-fold molar excess of nucleotide and 20 mM $MgCl_2$ [46]. The proteins were then mixed with purified RA domain and complexes isolated on glutathione beads. We observed a strong interaction between RASSF1 and both GEM (**Figure 5F**) and REM1 (**Figure 5G**) that was largely nucleotide independent. This is consistent with previous speculation that RGK GTPases may not behave as canonical switches [44]. As a control, and to explore specificity, we mixed GDP- or GMPPNP-exchanged GEM with the RA domain of RASSF5 but observed no binding (**Figure 5H**). We next attempted to determine an affinity for GEM-RASSF1 using ITC. Purified GEM exchanged with GTP analogs and complexed with RASSF1 RA domain was too unstable for

ITC and could not be analysed. However, we were able to measure a K_d of 9.4 ± 0.3 μM for the interaction between GEM-GDP and RASSF1 (**Figure 5I**), an affinity comparable to other effector-GTPase partners. To summarize, we determined that RASSF1 is an *in vitro* binding partner of six RAS-like GTPases and can speculate the interactions depend on multiple binding hot spots, analogous to the RASSF5-HRAS complex. The promiscuity of effectors for GTPases is not well explored, but PI3K binds 15 distinct RAS family members [15] and we hypothesize most effectors will have several unique GTPase partners. Thus, any of the six RASSF1-interacting GTPases may be functional *in vivo* given the right context.

2.3.5 RASSF1 and Candidate GTPase Binding Partners in Cells

Elucidating a functional role for the identified RASSF1-GTPase complexes is challenging. There are no known guanine nucleotide exchange factors (GEFs) for any of the six small GTPases, and there are no stimulatory conditions under which the endogenous GTPases are known to switch on. We began by resolving if mutationally activated GTPases could co-localize with RASSF1 in cells. Previous work has shown that RASSF1A localizes to microtubules through Microtubule Associated Proteins (MAPs) [47-49]. Other data suggest RASSF1 isoforms are differentially localized and that RASSF1 localization is dynamic and dependent on the cell cycle [50-52]. In HeLa cells we observed FLAG-tagged RASSF1A localized to microtubules. This localization was not dependent on its RA domain, which alone appeared cytoplasmic and enriched around the endoplasmic reticulum (ER) (**Figure 6A**). To determine if the GTPase partners co-localize with RASSF1, we had to consider their spatial restriction to the plasma membrane *via* lipidation. RASL12 and the RGK GTPases GEM, REM1 and REM2 completely lack predicted lipidation motifs, while DIRAS3 and ERAS are predicted to be farnesylated (**Figure 6B**). Expression of GFP-tagged, mutationally activated GTPases in HeLa cells verified that DIRAS3 and ERAS are plasma membrane-localized, like KRAS, while RASL12 was localized diffusely throughout the cell. Despite the lack of predicted lipidation, GEM, REM1 and REM2 were markedly associated with plasma membrane, as has been observed previously [53] (**Figure 6C** and **Supplementary Figure S6A**). When full-length RASSF1A was co-expressed with these GTPases we observed a striking recruitment of the only cytoplasmic GTPase, RASL12, to microtubules (**Figure 6D** and **Supplementary Figure S6A**).

We did not observe significant fractions of the other GTPases on microtubules, consistent with their membrane-restriction. There was, however, a clear propensity for the RGK GTPases to cluster around regions of RASSF1A staining. Thus, RASSF1 can recruit RASL12 to microtubules, but its cytoskeletal attachment in HeLa cells precludes interaction with PM-associated GTPases.

When we expressed activated RGK GTPases in HEK 293A cells they exhibited a completely altered pattern of localization. GEM formed large puncta throughout the cell, while REM1, REM2 and RASL12 aggregated in large, mostly cytoplasmic regions (**Figure 6E** and **Supplementary Figure S6B**). When the GTPases were co-expressed with full-length RASSF1A, these puncta completely disappear (**Figure 6F**). In these cells, RASSF1A and GTPases are co-distributed on microtubules and in the cytoplasm. These data suggest a functional link between RASSF1 and these RAS-like GTPases and highlight complexities to their direct association.

2.3.6 RGK GTPases and RASSF1A Influence the Apoptotic Response and Ca^{2+} Homeostasis

There is not a single paper describing a function for RASL12, while numerous studies have attributed a role for RGK GTPases in regulating voltage-dependent Ca^{2+} channels. As most studies link RASSFs to apoptosis, we first determined if RASL12 or the RGK family members induce apoptosis and whether expression of RASSF1 might be synergistic. We used HEK 293T cells as they do not express detectable levels of endogenous RASSF1 (**Figure S6C**). Annexin V staining revealed that GEM (3.4-fold), REM1 (4-fold) and REM2 (3.8-fold) generate a significant apoptotic response over controls, levels similar to KRAS, while RASL12 induced a modest increase (2-fold) (**Figure 6G** and **Supplementary Figure S6D**). Co-expression with RASSF1 produced a significant decrease in the capacity for GEM (2.1-fold) and REM1 (2.7-fold) to induce apoptosis, while KRAS, REM2 and RASL12 levels were not significantly altered. These results suggest again that RASSF1 is not always a pro-apoptotic effector and may even have a protective function.

As RGK GTPases regulate intracellular Ca^{2+} levels we looked to establish a role for

RASSF1 in Ca^{2+} signalling. We used the Indo-1 AM cell-permeant sensor to measure intracellular Ca^{2+} levels in cells expressing activated RGK GTPases alone, or with RASSF1A. Consistent with previous studies, we observed a significant reduction in free intracellular Ca^{2+} upon overexpression of GEM, and minor decreases when KRAS, REM1 or REM2 were overexpressed (**Figure 6H** and **Supplementary Figure S6E**). When RASSF1A was co-expressed with GEM, Ca^{2+} levels returned to near-normal levels. Conversely, co-expression of RASSF1A with REM1 or REM2 augmented their ability to restrict Ca^{2+} entry. RASSF1 expression had no impact on Ca^{2+} levels in cells expressing KRAS. Taken together, these data link RASSF1-RGK GTPase interactions with Ca^{2+} homeostasis, itself a master regulator of apoptosis and cell death, and begin to elucidate a functional role for the interaction of RASSF1 with the candidate GTPases.

2.3.7 YAP1 nuclear localization is inhibited by RGK GTPases and RASSF effectors

Having established that RASSF1 complexes with both RGK GTPases and MST1 we next considered if the GTPases could regulate Hippo signalling. Immunofluorescent detection of endogenous YAP1 in U2OS cells shows its prominent nuclear localization when cells are sparsely distributed (Hippo off), and sequestration of YAP1 to the cytoplasm in packed cells (Hippo on; **Supplementary Figure S7A**). We thus transfected GFP-tagged, activated RGK GTPases into U2OS cells plated at low density and monitored YAP1 localization. Expression of both GEM and REM1 resulted in abnormally elongated cells that markedly lacked nuclear YAP1, while KRAS had no effect (**Figure 7A**). There was a modest but significant reduction of nuclear YAP1 in cells expressing REM2, while YAP1 remained nuclear in the presence of RASL12 (**Supplementary Figure S7B**). This suggests that RGK GTPases can activate Hippo signalling and sequester YAP1 in the cytoplasm.

The capacity for RASSF proteins themselves to regulate Hippo signalling has not been well explored. We did not observe a significant change in YAP1 localization following expression of FLAG-tagged RASSF1A or RASSF5A alone (**Supplementary Figure S7C**). However, the elongated cell shape phenotype induced by REM1 or GEM was completely

rescued by co-expression with RASSF1A, and YAP1 remained cytoplasmic in these cells (**Figure 7B**). This suggests the irregular cell shape alone was not responsible for Hippo activation. Finally, we sought to answer whether RASSF proteins could regulate Hippo signalling downstream of activated KRAS. We co-expressed FLAG-RASSF1A or RASSF5A with GFP-tagged G12V-KRAS and stained for endogenous YAP1. While neither RASSFs or KRAS alone significantly impacts YAP1 localization, either RASSF1A or RASSF5A co-expressed with KRAS completely blocked YAP1 from the nucleus (**Figure 7C**). Thus, even RASSF effectors that do not directly complex with KRAS have a capacity to stimulate Hippo signalling and inactivate YAP in the presence of activated KRAS.

2.4   Discussion

The distribution of signals to multiple downstream effector pathways is a central component of models describing small G-protein function. The specificity of effectors for GTPases is generally inferred based on homology, but we show that not all RA domain proteins are binding partners of H/K/N-RAS. We determined only one of the pro-apoptotic RASSF effectors can directly complex with these archetypal GTPases, underscoring the need for more stringent biochemical evidence to establish genuine effectors for each RAS family GTPase.

There has been significant interest in RASSF function from both a signalling and clinical standpoint in the past two decades. They represent one of the most highly conserved RAS effector families with orthologs in all metazoans and even single cell choanoflagellates. Tunicates have one N-RASSF ortholog and two C-RASSFs, one clustering with human RASSF2/4/6 by homology and the other with RASSF1/3/5 (**Supplementary Figure S1**). The RASSF family thus expanded significantly in vertebrates, and we show this was accompanied by numerous amino acid substitutions to presumed GTPase binding residues. It is remarkable that relatively minor amino acid changes can significantly alter GTPase specificity, as we've demonstrated with RASSF5 Cys225 and RASSF1 Asn149. Following this, it is unsurprising that most RASSF family members are not true RAS effectors. Their diverse αN, β1, β2 and α1 sequences suggest RASSF effectors evolved to recognize distinct GTPases within the RAS superfamily. We also reveal that N-RASSFs are more highly related to ASPP effectors and

directly complex with these p53-regulatory proteins. Despite this, there appears to be substantial functional overlap between C-RASSFs and N-RASSF/ASPPs, with evidence suggesting each of these scaffolds can respond to changes in cell shape, adhesion or polarity to regulate senescence or apoptosis [35, 54-58]. Indeed, all RASSF and ASPP family members were previously identified as network components that regulate cell growth in tandem with Hippo/STRIPAK, PP1 and polarity modules [59]. It is intriguing to speculate that RASSFs may link the activation of diverse GTPases to these pathways.

There is a peculiar absence of small GTPases in proteomics networks. The explanation for this is likely complex, a combination of restricted expression, competition between effectors, and the requirement for high levels of the activated, GTP-bound conformation in assayed cells. We took a bioinformatic approach to resolve GTPase partners for the RASSF1 effector. As with other *RASSF* genes, expression of *RASSF1* is frequently silenced in numerous human cancers, and its tumour suppressor activity could be related to roles in autophagy [60], Hippo signalling [61-63], cell cycle regulation [50, 64], microtubule dynamics [47, 65], or apoptosis [48, 66]. Though the dominant feature of the RASSF1 protein is its RA domain, its specificity for small G-proteins has not been investigated. Our results suggest that RASSF1 is an effector of the RAS subfamily GTPases GEM, REM1, REM2, RASL12, DIRAS3 and ERAS. We propose that most effectors bind multiple small GTPases rather than a single high affinity partner, and the context in which these specific GTPases are activated and bind RASSF1 must be determined. Also, our work does not exclude the possibility that RASSF1 could signal downstream of H/K/N-RAS, as it forms a heterodimer with RASSF5 *via* a SARAH domain interaction [67]. Nevertheless, future studies should focus on the capacity for RASSF1 to signal from these understudied GTPases and elucidate how these interactions affect morphogenesis and cellular transformation.

The defined function of RGK GTPases is in regulating voltage-dependent Ca^{2+} channels and cell shape. There are multiple data linking RASSFs to Ca^{2+} homeostasis, including a functional interaction between RASSF1 and the Ca^{2+} pump PMCA4B [68] and a role for RASSF4 in regulating store-operated Ca^{2+} entry at ER–PM junctions [69]. Indeed, fluctuations in intracellular Ca^{2+} upon RASSF overexpression may rationalize observations relating to apoptotic induction, as intracellular Ca^{2+} flux can dramatically influence apoptosis. To date,

there is no available literature describing a functional role for the RASL12 GTPase, which we show is cytoplasmic and recruited to microtubules by RASSF1A. This protein clusters by homology with the RAS-like GTPases RERG, RASL11A/B and RASL10A/B (**Supplementary Figure S5**) for which there are also no functional data (despite high evolutionary conservation). Implication of their interaction with RASSF1 thus remains to be elucidated, but the little data available suggest these small G-proteins also have a tumour suppressor role in human cancers [9, 70, 71].

While we did not observe an intrinsic ability for RASSFs to simulate apoptosis, either in the absence or presence of activated RAS, this does not preclude a role. Previous data linking RASSFs to apoptotic pathways suggest this association is complex. As with most Hippo network proteins, further study of RASSFs and apoptosis should employ cells or tissues in native, 3D environments. The strongest evidence for a RASSF-apoptosis connection derives from such studies [20], while those in 2D culture have generally relied on external stimuli to provoke a response (anti-FAS, Trail, etoposide, TNF, staurosporine). This also underscores the strong induction of apoptosis in 2D cultured cells induced by oncogenic RAS, documented here and by many others. We can now postulate this result is not generated by a RAS-RASSF-Hippo signalling axis, but more likely *via* activation of p53 or alternative pathways [72-75].

Numerous recent works suggest KRAS and YAP1 converge to drive oncogenesis. In fact, active YAP1 can bypass KRAS addiction [76] and is required for neoplastic proliferation of numerous RAS-driven cancers [77-82]. Despite this, there is no compelling studies linking RAS to Hippo activation through RASSFs. We detect a near complete loss of nuclear YAP1 in cells co-expressing G12V-KRAS and either RASSF5 or RASSF1. This result could explain the frequent inactivation of *RASSF* genes in human cancers, and the molecular mechanisms directing RASSF control of YAP1 localization warrant further study. This idea is also true of the RGK GTPases, which we demonstrate here are novel Hippo pathway activators.

We have shown how a family of RA domain proteins expanded and diversified in vertebrates. Conserved RASSF interactions with Hippo kinases or ASPP proteins suggest specific RA domain-GTPase interactions may feed into these pathways, which has implications for both normal development and cellular transformation. We require further studies linking

the more obscure RAS-like GTPases with their cognate effectors to help elucidate the full complexity of RAS-effector signalling.

2.5 Methods

2.5.1 Constructs and Antibodies

Table 1:   **Expression constructs generated and used in this study:**

Construct	Backbone	Tag	Region (AA)	Source	Gene ID
GST alone	pGEX4-T2	GST			
GST-RASSF1-RA	pGEX4-T2	GST	123-296	Human	11186
GST-RASSF2-RA	pGEX4-T2	GST	1-271	Human	9770
GST-RASSF3-RA	pGEX4-T2	GST	41-194	Human	283349
GST-Rassf4-RA	pGEX4-T2	GST	1-269	Mouse	213391
GST-RASSF5-RA	pGEX4-T2	GST	199-367	Human	83595
GST-Rassf6-RA	pGEX4-T2	GST	33-312	Mouse	73246
GST-RASSF8-RA	pGEX4-T2	GST	1-87	Human	11228
GST-RASSF9-RA	pGEX4-T2	GST	1-125	Human	9182
GST-Rassf10-RA	pGEX4-T2	GST	1-151	Mouse	78748
GST-RASSF1-RA-	pGEX4-T2	GST	131-288	Human	11186
GST-RASSF1-RA-	pGEX4-T2	GST	131-288	Human	11186
GST-RASSF5-RA-	pGEX4-T2	GST	199-367	Human	83595
RASSF1-N149D/L150D	pGEX4-T2	GST	131-288	Human	11186
RASSF1- N149K/L150K	pGEX4-T2	GST	131-288	Human	11186
RASSF1- N149A/L150A	pGEX4-T2	GST	131-288	Human	11186
GST-GEM	pGEX4-T2	GST	62-203	Human	2669
GST-REM1	pGEX4-T2	GST	76-251	Human	19700
FLAG-RASSF1	pCDNA5-FLAG-5'	FLAG	full-length	Human	11186
FLAG-RASSF2	pDEST-pcDNA5-FLAG-	FLAG	full-length	Human	9770
FLAG-RASSF3	pDEST-pcDNA5-FLAG-	FLAG	full-length	Human	283349
FLAG-Rassf4	pDEST-pcDNA5-FLAG-	FLAG	full-length	Mouse	213391
FLAG-RASSF5	pDEST-pcDNA5-FLAG-	FLAG	full-length	Human	83595
FLAG-Rassf6	pDEST-pcDNA5-FLAG-	FLAG	full-length	Mouse	73246
FLAG-RASSF8	pDEST-pcDNA5-FLAG-	FLAG	full-length	Human	11228
FLAG-RASSF9	pDEST-pcDNA5-FLAG-	FLAG	full-length	Human	9182
FLAG-Rassf10	pDEST-pcDNA5-FLAG-	FLAG	full-length	Mouse	78748
FLAG-RASSF1-RA	pCDNA5-FLAG-5'	FLAG	131-288	Human	11186
GFP alone	pVenus-C1	GFP			
GFP-MST-1	pVenus-C1	GFP	full-length	Human	6789
GFP-KRAS	pDEST-pcDNA3-Venus-	GFP	full-length	Human	3845
GFP-KRAS-G12V	pDEST-pcDNA3-Venus-	GFP	full-length	Human	3845
GFP-HRAS	pDEST-pcDNA3-Venus-	GFP	full-length	Human	3265
GFP-HRAS-G12V	pDEST-pcDNA3-Venus-	GFP	full-length	Human	3265
GFP-RHEB	pDEST-pcDNA3-Venus-	GFP	full-length	Human	6009
GFP-RHEB-Q64L	pDEST-pcDNA3-Venus-	GFP	full-length	Human	6009
GFP-RAP1A	pDEST-pcDNA3-Venus-	GFP	full-length	Human	5906

GFP-RAP1A-G12V	pDEST-pcDNA3-Venus-	GFP	full-length	Human	5906
GFP-RAC1	pDEST-pcDNA3-Venus-	GFP	full-length	Human	5879
GFP-RAC1-G12V	pDEST-pcDNA3-Venus-	GFP	full-length	Human	5879
GFP-CDC42	pDEST-pcDNA3-Venus-	GFP	full-length	Human	998
GFP-CDC42-G12V	pDEST-pcDNA3-Venus-	GFP	full-length	Human	998
GFP-RAN	pDEST-pcDNA3-Venus-	GFP	full-length	Human	5901
GFP-RAN-G19V	pDEST-pcDNA3-Venus-	GFP	full-length	Human	5901
GFP-GEM-Q84V	pDEST-pcDNA3-Venus-	GFP	full-length	Human	2669
GFP-REM1-P89V	pDEST-pcDNA3-Venus-	GFP	full-length	Human	19700
GFP-REM2-S123V	pDEST-pcDNA3-Venus-	GFP	full-length	Human	161253
GFP-RASL12-R29V	pDEST-pcDNA3-Venus-	GFP	full-length	Human	51285
GFP-ERAS-WT	pDEST-pcDNA3-Venus-	GFP	full-length	Human	3266
GFP-DIRAS3-A46V	pDEST-pcDNA3-Venus-	GFP	full-length	Human	9077
HIS-ASPP1	pcDNA3.1/V5-HIS	HIS	full-length	Human	23368
HIS-ASPP2	pcDNA3.1/V5-HIS	HIS	full-length	Human	7159

Table 2:   Antibodies used in this study:

Antibody	Source
anti-FLAG-mouse	Sigma - F3165
anti-FLAG-rabbit	Sigma – F7425
anti-GFP	Abcam - ab290
anti-HIS	Thermo - HIS.H8 - MA1-21315
Goat anti-Mouse IgG-Tx-Red	Sigma - SAB3701076
Annexin-V-Alexa Fluor 350	Life Tech - V13246
anti-RASSF1	Abcam - ab23950
anti-RASSF1	ATLAS Antibodies - HPA040735
anti-YAP1 (63.7)	Santa Cruz biotechnology - 10199
Goat anti-Rabbit IgG-Alexa Fluor-647	Invitrogen - A21244

2.5.2 Protein Expression and Purification

Glutathione *S*-transferase (GST)- or 6xHistidine (HIS)-tagged proteins were expressed in *E. coli* (BL21-DE3-codon+) cells grown in LB media at 37°C. Cells were induced with 250 µM IPTG (isopropyl-β-D-thiogalactopyranoside) at OD 0.7. Following induction, cells were shifted to 16°C for growth overnight. Harvested cells were lysed in buffer (20 mM Tris-HCl (pH 7.5), 150 mM NaCl, 10% glycerol, 0.4% NP-40, protease inhibitors (Roche), and either 1 mM dithiothreitol or 10 mM β-mercaptoethanol) and sonicated. Lysate was clarified by centrifugation and incubated with Ni-NTA (Qiagen) or glutathione (Amersham) resins at 4°C for 1-2 hours. Bound protein was eluted by direct thrombin cleavage (GST) or with elution buffer containing 250 mM imidazole (Bioshop) followed by thrombin cleavage (HIS) or 30 mM reduced glutathione. Eluted proteins were purified by size exclusion chromatography using either an S75 or S200 column (GE).

2.5.3 Nucleotide Exchange and Isothermal Titration Calorimetry

For nucleotide exchange, purified KRAS was incubated with a 10-fold molar excess (nucleotide:protein) of GMPPNP (Sigma) along with 10 mM EDTA and calf intestinal phosphatase at 37°C for 10 min. 20 mM $MgCl_2$ was added, samples were incubated on ice for 10 mins and then dialyzed in the compatible buffer. RGK GTPases repeatedly precipitated using this methodology, so exchange of these GTPases was done with a 2-hour incubation in a 10-fold molar excess of nucleotide (GMPPNP, GTPγS or GTP (Sigma)) and 20 mM $MgCl_2$. GTPase-RA domain interactions were measured using a MicroCal ITC200 (Malvern). Stock solutions were diluted into filtered and degassed 20 mM Tris-HCl (pH7.5), 150 mM NaCl and 1 mM DTT. Experiments were carried out at 25°C. Heats of dilution were determined from control experiments in which domains were titrated into buffer alone. Data were fit using Origin 7 (MicroCal).

2.5.4 Cell Culture, Co-immunoprecipitation and Western Blotting

HEK 293T cells (ATCC CRL-3216) were seeded in six-well plates (at $3x10^6$) and transiently transfected with polyethylenimine (PEI) or Jet Prime. At least 1000 ng of DNA (unless otherwise stated) were transfected for each condition. 48 hours after transfection, cells were harvested and lysed in buffer (20 mM Tris-HCl (pH 7.5), 150 mM NaCl, 10% glycerol, 1% Triton X-100, 1 mM DTT and protease inhibitor P8340) for 10 minutes. Lysates were clarified by centrifugation and supernatant incubated with pre-washed Protein-G Sepharose and immunoprecipitating antibody. After 1 hour of incubation, beads were washed 3 times with lysis buffer. Beads containing bound proteins were reconstituted in SDS-loading buffer, separated using SDS-PAGE and transferred to nitrocellulose membrane for Western blot analysis. Membranes were blocked with TBST containing 5% skim milk. Following blocking, primary antibodies were detected using HRP conjugated anti-mouse Ig or anti-rabbit Ig antibodies (1:10000). Membranes were revealed by ECL reagent (Bio-Rad) and detection done by a Bio-Rad ChemiDoc imaging system equipped with ImageLab software.

2.5.5 GST-RA Pull Downs

Lysates from HEK 293T cells expressing the protein of interest were incubated with GST-RA domain fusion protein or GST alone for 1 hour. Glutathione beads were used to capture GST fusion proteins or GST alone. Beads were washed 5 times with lysis buffer (20 mM Tris-HCl (pH 7.5), 150 mM NaCl, 5 mM $MgCl_2$, 10% glycerol, 1% Triton X-100, 1 mM DTT and protease inhibitor P8340), eluted in SDS loading buffer and resolved by SDS-PAGE. Gels were transferred to nitrocellulose membrane and Western blot analysis performed as above.

2.5.5 Microscopy

HeLa (ATCC CCL-2), HEK 293A (Thermo Fisher) or U2OS (ATCC HTB-96) cells were split in 6-well plates containing coverslips. 48 hours after transfection, cells were washed with phosphate buffered saline (PBS) and fixed with 4% paraformaldehyde (PFA). Fixed cells were permeabilized with 0.05% Tween or 0.1% Triton X100 (for U2OS cells) and blocked with 2%

bovine serum albumin (BSA). Cells were incubated for 1 to 2 hours with primary antibody at 37°C or at RT (for U2OS cells) followed by secondary antibody and Hoechst staining. Finally, cells were treated with 70% then 95% ethanol and air dried before being mounted on glass slides. Slides were imaged using an LSM880 confocal microscope. Three lasers were used for detection (UV, Red and Far-Red). Images were processed using ZEN software.

2.5.6 Structural Modelling

3D models for all RASSF (1-10) effectors were constructed using the automated protein structure homology model building program 'MODBASE' with energy minimization parameters available at the MODWEB server (https://modbase.compbio.ucsf.edu/modweb) [83]. Amino acid sequences based on our alignments were input in FASTA format. The server calculated structural models based on the best available template structures in the Protein Data Bank using MODPIPE, an automated modeling pipeline that relies on MODELLER for fold assignment, sequence-structure alignment, model building and model assessment [84]. Models were evaluated for quality using Ramachandran plots and those with the highest DOPE score and fold reliability were selected for structural analysis.

2.5.7 Measurements for Intracellular Ca^{2+} and Apoptosis

HEK 293T cells were seeded at a confluence of 0.4 million cells/ml/well in a 6 well plate. Following overnight incubation, cells were transfected with 1 µg of plasmid encoding GFP-tagged GTPases and/or FLAG-tagged RASSF along with controls using PEI. For measurements of intracellular Ca^{2+}, 1 hour before harvesting cells they were incubated with 1 µM of Indo-1 AM at 37°C. Following this, cells were harvested by centrifugation and washed twice with PBS. Cells were analyzed using flowcytometry (YETI). In brief, cells were excited with a 350 nM laser and gated for an emission wavelength of 400 nM. Emission wavelength of the dye shifts from 475 nM in the Ca^{2+}-free state to 400 nM when Ca^{2+}-bound. Raw data from the Yeti was analyzed using Flow-Jo software. Apart form quantifying basal intracellular Ca^{2+} levels, Ca^{2+} levels after treatment with Ca^{2+} channel inhibitors (Thapsigargin) were also

analyzed. For apoptosis: after 48 hours cells were harvested by trypsinization and dissolved in Annexin-V/Propidium Iodide (PI) buffer (10 mM HEPES (pH7.4), 150 mM NaCl, and 2.5 mM CaCl$_2$ containing 2 μg of Annexin V 647-Fluor and PI). Samples were transferred to FACS tubes and analyzed using flowcytometry (YETI). Cells were sorted using sequential gating of Annexin, PI, and GFP channels. Raw data were analyzed using Flow-Jo software.

2.6 Acknowledgements

2.7 Author Contributions

D.T. and M.J.S. designed experiments. D.T., S.S., R.K., X.X. and M.J.S. performed experiments and analyzed data. A.S. and J.S. performed structural modelling. J.S. and M.J.S. supervised studies. D.T. and M.J.S. wrote the manuscript with input from R.K. and J.S.

2.8 Declaration of Interests

The authors declare no competing interests.

2.9   References

1. Fernández-Medarde, A. & Santos, E. Ras in cancer and developmental diseases. *Genes Cancer* **2**, 344–58 (2011).

2. Colicelli, J. Human RAS superfamily proteins and related GTPases. *Sci. STKE* **2004**, RE13 (2004).

3. Gentry, L. R., Martin, T. D., Reiner, D. J. & Der, C. J. Ral small GTPase signaling and oncogenesis: More than just 15 minutes of fame. *Biochim. Biophys. Acta - Mol. Cell Res.* **1843**, 2976–2988 (2014).

4. Berger, A. H. *et al.* Oncogenic RIT1 mutations in lung adenocarcinoma. *Oncogene* **33**, 4418–4423 (2014).

5. Mavrakis, K. J. *et al.* Tumorigenic activity and therapeutic inhibition of Rheb GTPase. *Genes Dev.* **22**, 2178–2188 (2008).

6. Rasmussen, N. R., Dickinson, D. J. & Reiner, D. J. Ras-dependent cell fate decisions are reinforced by the RAP-1 small GTPase in C. elegans. *Genetics* **210**, 1339–1354 (2018).

7. Vaidyanathan, G. *et al.* The Ras-related protein AGS1/RASD1 suppresses cell growth. *Oncogene* **23**, 5858–5863 (2004).

8. Fenwick, C. A Subclass of Ras Proteins That Regulate the Degradation of IB. *Science (80-.).* **287**, 869–873 (2000).

9. Finlin, B. S. *et al.* RERG is a novel ras-related, estrogen-regulated and growth-inhibitory gene in breast cancer. *J. Biol. Chem.* **276**, 42259–67 (2001).

10. Sutton, M. N. *et al.* DIRAS3 (ARHI) Blocks RAS/MAPK Signaling by Binding Directly to RAS and Disrupting RAS Clusters. *Cell Rep.* **29**, 3448-3459.e6 (2019).

11. Pan, J. Y., Fieles, W. E., White, A. M., Egerton, M. M. & Silberstein, D. S. Ges, a human GTPase of the Rad/Gem/Kir family, promotes endothelial cell sprouting and cytoskeleton reorganization. *J. Cell Biol.* **149**, 1107–1115 (2000).

12. Hamad, N. M. *et al.* Distinct requirements for Ras oncogenesis in human versus mouse cells. *Genes Dev.* **16**, 2045–2057 (2002).

13. Vandal, G., Geiling, B. & Dankort, D. Ras effector mutant expression suggest a negative regulator inhibits lung tumor formation. *PLoS One* **9**, e84745 (2014).

14. Smith, M. J. *et al.* Evolution of AF6-RAS association and its implications in mixed-lineage leukemia. *Nat. Commun.* **8**, 1–13 (2017).

15. Yang, H. W. *et al.* Cooperative activation of PI3K by Ras and Rho family small GTPases. *Mol. Cell* **47**, 281–90 (2012).

16. Khokhlatchev, A. *et al.* Identification of a novel Ras-regulated proapoptotic pathway. *Curr. Biol.* **12**, 253–265 (2002).

17. Djos, A., Martinsson, T., Kogner, P. & Caren, H. The RASSF gene family members RASSF5, RASSF6 and RASSF7 show frequent DNA methylation in neuroblastoma. *Mol. Cancer* **11**, 40 (2012).

18. Hesson, L., Dallol, A., Minna, J. D., Maher, E. R. & Latif, F. NORE1A, a homologue of RASSF1A tumour suppressor gene is inactivated in human cancers. *Oncogene* **22**, 947–954 (2003).

19. Vos, M. D., Ellis, C. a, Bell, a, Birrer, M. J. & Clark, G. J. Ras uses the novel tumor suppressor RASSF1 as an effector to mediate apoptosis. *J. Biol. Chem.* **275**, 35669–72 (2000).

20. Park, J. *et al.* Tumor suppressor ras association domain family 5 (RASSF5/NORE1) mediates death receptor ligand-induced apoptosis. *J. Biol. Chem.* **285**, 35029–38 (2010).

21. Allen, N. P. C. *et al.* RASSF6 is a novel member of the RASSF family of tumor suppressors. *Oncogene* **26**, 6203–6211 (2007).

22. Eckfeld, K. *et al.* RASSF4/AD037 is a potential Ras effector/tumor suppressor of the RASSF family. *Cancer Res.* **64**, 8688–8693 (2004).

23. Kudo, T. *et al.* The RASSF3 Candidate Tumor Suppressor Induces Apoptosis and G1-S Cell-Cycle Arrest via p53. *Cancer Res.* **72**, 2901–2911 (2012).

24. Li, X. *et al.* Ras association domain family member 10 suppresses gastric cancer growth by cooperating with GSTP1 to regulate JNK/c-Jun/AP-1 pathway. *Oncogene* **35**, 2453–2464 (2016).

25. Tommasi, S. *et al.* Tumor susceptibility of Rassf1a knockout mice. *Cancer Res.* **65**, 92–98 (2005).

26. Vos, M. D. *et al.* RASSF2 is a novel K-Ras-specific effector and potential tumor suppressor. *J. Biol. Chem.* **278**, 28045–28051 (2003).

27. Takahashi, S. *et al.* RASSF7 negatively regulates pro-apoptotic JNK signaling by inhibiting the activity of phosphorylated-MKK7. *Cell Death Differ.* **18**, 645–55 (2011).

28. Stieglitz, B. *et al.* Novel type of Ras effector interaction established between tumour suppressor NORE1A and Ras switch II. *EMBO J.* **27**, 1995–2005 (2008).

29. Verma, S. K., Ganesan, T. S., Kishore, U. & Parker, P. J. The tumor suppressor RASSF1A is a novel effector of small G protein Rap1A. *Protein Cell* **2**, 237–249 (2011).

30. Nelson, N. & Clark, G. J. Rheb may complex with RASSF1A to coordinate Hippo and TOR signaling. *Oncotarget* **7**, 33821–33831 (2016).

31. Lee, M. G. *et al.* RASSF1A directly antagonizes RhoA activity through the assembly of a Smurf1-mediated destruction complex to suppress tumorigenesis. *Cancer Res.* **76**, 1847–1859 (2016).

32. Dallol, A. *et al.* RAN GTPase Is a RASSF1A Effector Involved in Controlling Microtubule Organization. *Curr. Biol.* **19**, 1227–1232 (2009).

33. Avruch, J., Praskova, M., Ortiz-Vega, S., Liu, M. & Zhang, X.-F. Nore1 and RASSF1 regulation of cell proliferation and of the MST1/2 kinases. *Methods Enzymol.* **407**, 290–310 (2006).

34. Cooper, W. N. *et al.* RASSF2 associates with and stabilizes the proapoptotic kinase MST2. *Oncogene* **28**, 2988–2998 (2009).

35. Guo, C. *et al.* RASSF1A Is Part of a Complex Similar to the Drosophila Hippo/Salvador/Lats Tumor-Suppressor Network. *Curr. Biol.* **17**, 700–705 (2007).

36. Hwang, E. *et al.* Structural basis of the heterodimerization of the MST and RASSF SARAH domains in the Hippo signalling pathway. *Acta Crystallogr. D. Biol. Crystallogr.* **70**, 1944–53 (2014).

37. Aylon, Y. *et al.* The Lats2 tumor suppressor augments p53-mediated apoptosis by promoting the nuclear proapoptotic function of ASPP1. *Genes Dev.* **24**, 2420–2429 (2010).

38. Patel, S. *et al.* Molecular interactions of ASPP1 and ASPP2 with the p53 protein family and the apoptotic promoters PUMA and Bax. *Nucleic Acids Res.* **36**, 5139–5151 (2008).

39. Bitra, A., Sistla, S., Mariam, J., Malvi, H. & Anand, R. Rassf proteins as modulators of Mst1 kinase activity. *Sci. Rep.* **7**, 45020 (2017).

40. Hwang, E. *et al.* Structural insight into dimeric interaction of the SARAH domains from Mst1 and RASSF family proteins in the apoptosis pathway. *Proc. Natl. Acad. Sci. U. S. A.* **104**, 9236–9241 (2007).

41. Rotem, S. *et al.* The structure and interactions of the proline-rich domain of ASPP. *J. Biol. Chem.* **283**, 18990–18999 (2008).

42. Langton, P. F. *et al.* The dASPP-dRASSF8 Complex Regulates Cell-Cell Adhesion during Drosophila Retinal Morphogenesis. *Curr. Biol.* **19**, 1969–1978 (2009).

43. Chan, J. J. *et al.* Comparative analysis of interactions of RASSF1-10. *Adv. Biol. Regul.* **53**, 190–201 (2013).

44. Sasson, Y., Navon-Perry, L., Huppert, D. & Hirsch, J. A. RGK family G-domain:GTP analog complex structures and nucleotide-binding properties. *J. Mol. Biol.* **413**, 372–389 (2011).

45. Splingard, A. *et al.* Biochemical and structural characterization of the gem GTPase. *J. Biol. Chem.* **282**, 1905–1915 (2007).

46. Killoran, R. C. & Smith, M. J. Conformational resolution of nucleotide cycling and effector interactions for multiple small GTPases determined in parallel. *J. Biol. Chem.* **294**, 9937–9948 (2019).

47. van der Weyden, L. *et al.* The RASSF1A isoform of RASSF1 promotes microtubule stability and suppresses tumorigenesis. *Mol. Cell. Biol.* **25**, 8356–8367 (2005).

48. Baksh, S. *et al.* The tumor suppressor RASSF1A and MAP-1 link death receptor signaling to bax conformational change and cell death. *Mol. Cell* **18**, 637–650 (2005).

49. Dallol, A. *et al.* RASSF1A Interacts with Microtubule-Associated Proteins and Modulates Microtubule Dynamics. *Cancer Res.* **64**, 4112–4116 (2004).

50. Song, M. S. *et al.* The tumour suppressor RASSF1A regulates mitosis by inhibiting the APC-Cdc20 complex. *Nat. Cell Biol.* **6**, 129–137 (2004).

51. Liu, L., Guo, C., Dammann, R., Tommasi, S. & Pfeifer, G. P. RASSF1A interacts with and activates the mitotic kinase Aurora-A. *Oncogene* **27**, 6175–6186 (2008).

52. Vlahov, N. *et al.* Alternate RASSF1 transcripts control SRC activity, E-cadherin contacts, and YAP-mediated invasion. *Curr. Biol.* **25**, 3019–3034 (2015).

53. Heo, W. D. *et al.* PI (3, 4, 5) P3 and PI (4, 5) P2 lipids target proteins with polybasic clusters to the plasma membrane. *Science (80-.).* **314**, 1458 (2006).

54. Royer, C. *et al.* ASPP2 links the apical lateral polarity complex to the regulation of YAP activity in epithelial cells. *PLoS One* **9**, 14–17 (2014).

55. Sottocornola, R. *et al.* ASPP2 Binds Par-3 and Controls the Polarity and Proliferation of Neural Progenitors during CNS Development. *Dev. Cell* **19**, 126–137 (2010).

56. Samuels-Lev, Y. *et al.* ASPP proteins specifically stimulate the apoptotic function of p53. *Mol. Cell* **8**, 781–794 (2001).

57. Dubois, F. *et al.* RASSF1A Suppresses the Invasion and Metastatic Potential of Human Non-Small Cell Lung Cancer Cells by Inhibiting YAP Activation through the GEF-H1/RhoB Pathway. *Cancer Res.* **76**, 1627–1640 (2016).

58. Donninger, H. *et al.* NORE1A is a Ras senescence effector that controls the apoptotic/senescent balance of p53 via HIPK2. *J. Cell Biol.* **208**, 777–789 (2015).

59. Hauri, S. *et al.* Interaction preoteome of human Hippo signaling. *Mol. Syst. Biol.* **9**, 1–16 (2013).

60. Li, W. *et al.* Suppressor of hepatocellular carcinoma RASSF1A activates autophagy initiation and maturation. *Cell Death Differ.* **26**, 1379–1395 (2019).

61. Papaspyropoulos, A. *et al.* RASSF1A uncouples Wnt from Hippo signalling and promotes YAP mediated differentiation via p73. *Nat. Commun.* **9**, 424 (2018).

62. Pefani, D. E. *et al.* TGF-β Targets the Hippo Pathway Scaffold RASSF1A to Facilitate YAP/SMAD2 Nuclear Translocation. *Mol. Cell* **63**, 156–166 (2016).

63. Del Re, D. P. *et al.* Mst1 Promotes Cardiac Myocyte Apoptosis through Phosphorylation and Inhibition of Bcl-xL. *Mol. Cell* **54**, 639–650 (2014).

64. Donninger, H. *et al.* Cell Cycle Restriction Is More Important Than Apoptosis Induction for RASSF1A Protein Tumor Suppression. *J. Biol. Chem.* **289**, 31287–31295 (2014).

65. Vos, M. D. *et al.* A role for the RASSF1A tumor suppressor in the regulation of tubulin polymerization and genomic stability. *Cancer Res.* **64**, 4244–4250 (2004).

66. Law, J. *et al.* Modulator of Apoptosis 1 (MOAP-1) Is a Tumor Suppressor Protein Linked to the RASSF1A Protein. *J. Biol. Chem.* **290**, 24100–24118 (2015).

67. Ortiz-Vega, S. *et al.* The putative tumor suppressor RASSF1A homodimerizes and heterodimerizes with the Ras-GTP binding protein Nore1. *Oncogene* **21**, 1381–1390 (2002).

68. Armesilla, A. L. *et al.* Novel functional interaction between the plasma membrane Ca^{2+} pump 4b and the proapoptotic tumor suppressor Ras-associated factor 1 (RASSF1). *J. Biol. Chem.* **279**, 31318–31328 (2004).

69. Chen, Y.-J., Chang, C.-L., Lee, W.-R. & Liou, J. RASSF4 controls SOCE and ER–PM junctions through regulation of PI(4,5)P2. *J. Cell Biol.* **216**, 2011 (2017).

70. Zou, H., Hu, L., Li, J., Zhan, S. & Cao, K. Cloning and characterization of a novel small monomeric GTPase, RasL10B, with tumor suppressor potential. *Biotechnol. Lett.* **28**, 1901–1908 (2006).

71. Zhao, W. *et al.* RERG suppresses cell proliferation, migration and angiogenesis through ERK/NF-κB signaling pathway in nasopharyngeal carcinoma. *J. Exp. Clin. Cancer Res.* **36**, 1–15 (2017).

72. Palmero, I., Pantoja, C. & Serrano, M. p19(ARF) links the tumour suppressor p53 to Ras [6]. *Nature* **395**, 125–126 (1998).

73. Mayo, M. W. *et al.* Requirement of NF-κB activation to suppress p53-independent apoptosis induced by oncogenic ras. *Science* **278**, 1812–1815 (1997).

74. Erhardt, P., Schremser, E. J. & Cooper, G. M. B-Raf Inhibits Programmed Cell Death Downstream of Cytochrome c Release from Mitochondria by Activating the MEK/Erk Pathway. *Mol. Cell. Biol.* **19**, 5308–5315 (1999).

75. Joneson, T. & Bar-Sagi, D. Suppression of Ras-Induced Apoptosis by the Rac GTPase. *Mol. Cell. Biol.* **19**, 5892–5901 (1999).

76. Kapoor, A. *et al.* Yap1 activation enables bypass of oncogenic KRAS addiction in pancreatic cancer. *Cell* **158**, 185–197 (2014).

77. Tu, B. *et al.* YAP1 oncogene is a context-specific driver for pancreatic ductal adenocarcinoma. *JCI Insight* **4**, 130811 (2019).

78. Coggins, G. E. *et al.* YAP1 mediates resistance to MEK1/2 inhibition in neuroblastomas with hyperactivated RAS signalling. *Cancer Res.* (2019). doi:10.1158/0008-5472.CAN-19-1415

79. Singh, K. *et al.* Mst1/2 kinases restrain transformation in a novel transgenic model of Ras driven non-small cell lung cancer. *Oncogene* (2019). doi:10.1038/s41388-019-1031-z

80. Mohamed, A. D., Shah, N., Hettmer, S., Vargesson, N. & Wackerhage, H. Analysis of the relationship between the KRAS G12V oncogene and the Hippo effector YAP1 in embryonal rhabdomyosarcoma. *Sci. Rep.* **8**, 1–10 (2018).

81. Lefort, S. *et al.* Initiation of human mammary cell tumorigenesis by mutant KRAS requires YAP inactivation. *Oncogene* (2019). doi:10.1038/s41388-019-1111-0

82. Zhang, W. *et al.* Downstream of mutant KRAS, the transcription regulator YAP is essential for neoplastic progression to pancreatic ductal adenocarcinoma. *Sci. Signal.* **7**, ra42 (2014).

83. Marti-Renom, M. A. *et al.* Modeling Protein Structure from its Sequence. *Curr. Protoc. Bioinforma.* **3**, 5.1.1-5.1.33 (2003).

84. Pieper, U. *et al.* ModBase, a database of annotated comparative protein structure models and associated resources. *Nucleic Acids Res.* **42**, 336–46 (2014).

85. Webb, B. & Sali, A. Comparative protein structure modeling using MODELLER. *Curr. Protoc. Bioinforma.* **2014**, 5.6.1-5.6.32 (2014).

2.10 Figures

Figure 1:   Domain architecture and purification of RASSF effectors.
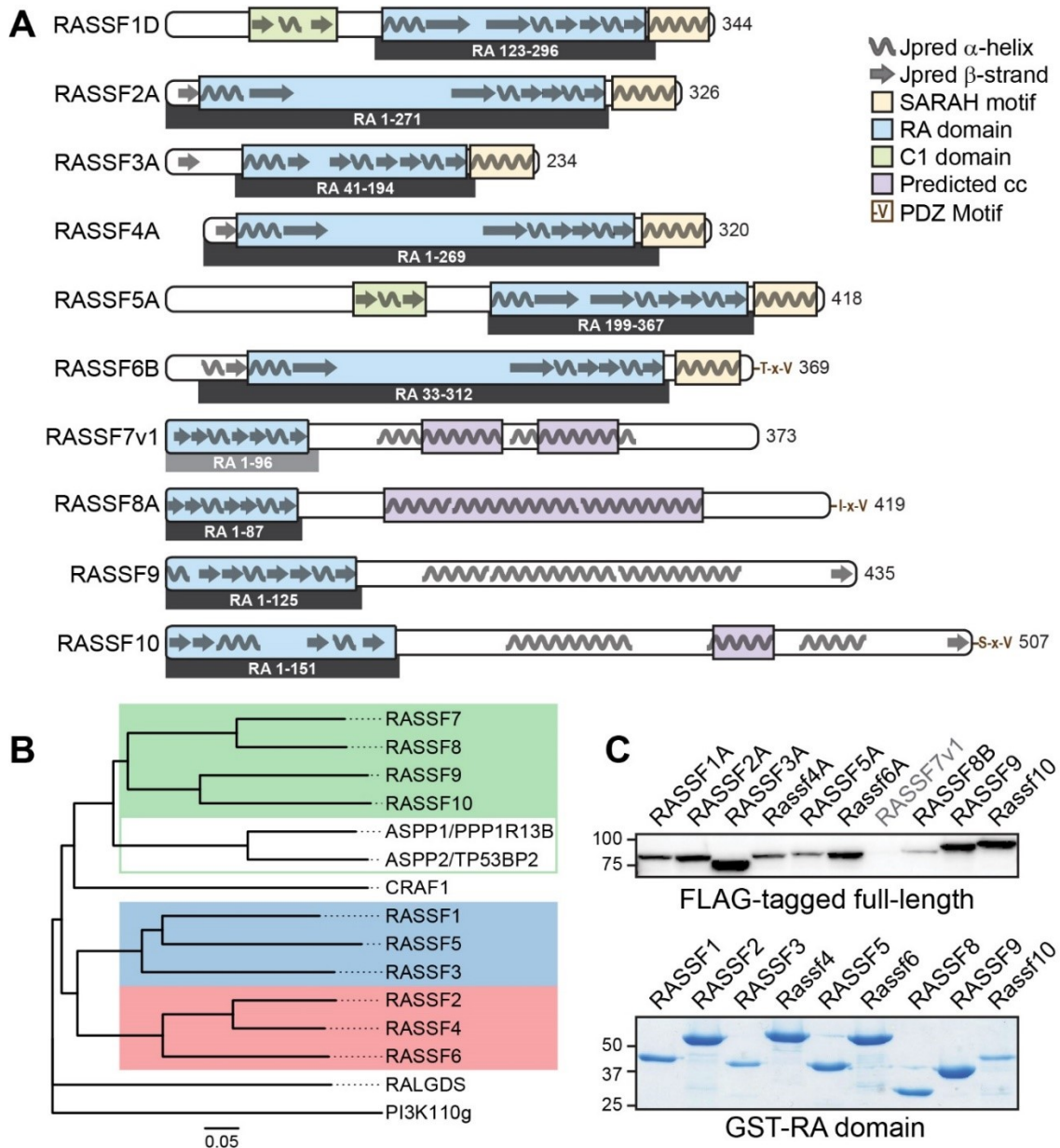
Figure 1: Domain architecture and purification of RASSF effectors.

(A) Schematic representation of the RASSF family members. The longest isoform of each RASSF is depicted, overlaid with secondary structure predictions (Jpred). RA domains are in blue, and amino acid positions of the domain expression constructs are detailed below. C-RASSFs have helical SARAH (Salvador-Rassf-Hippo) motifs, in yellow. RASSF1 and RASSF5 have C1 zinc finger domains, in green. SMART-predicted coiled coil domains of the N-RASSFs are in purple. **(B)** Classification of RASSF homologs based on amino acid sequence similarity. RA domains of the C- and N-RASSFs were aligned with RA domains from ASPP1, ASPP2, CRAF-1, RALGDS and PI3Kγ. The N-RASSF family (green) clusters with the two ASPP domains. Two clusters are evident in the C-RASSF family, one composed of RASSF1/3/5 (blue) and another of RASSF2/4/6 (red). **(C)** anti-FLAG Western blot shows expression of full-length, FLAG-tagged RASSF isoforms (top) and a Coomassie-stained SDS-PAGE gel shows the purified, GST-tagged RA domain proteins (bottom).

Figure 2:   Differential interactions between RASSF effectors and KRAS, MST1 kinase and the ASPP effectors.
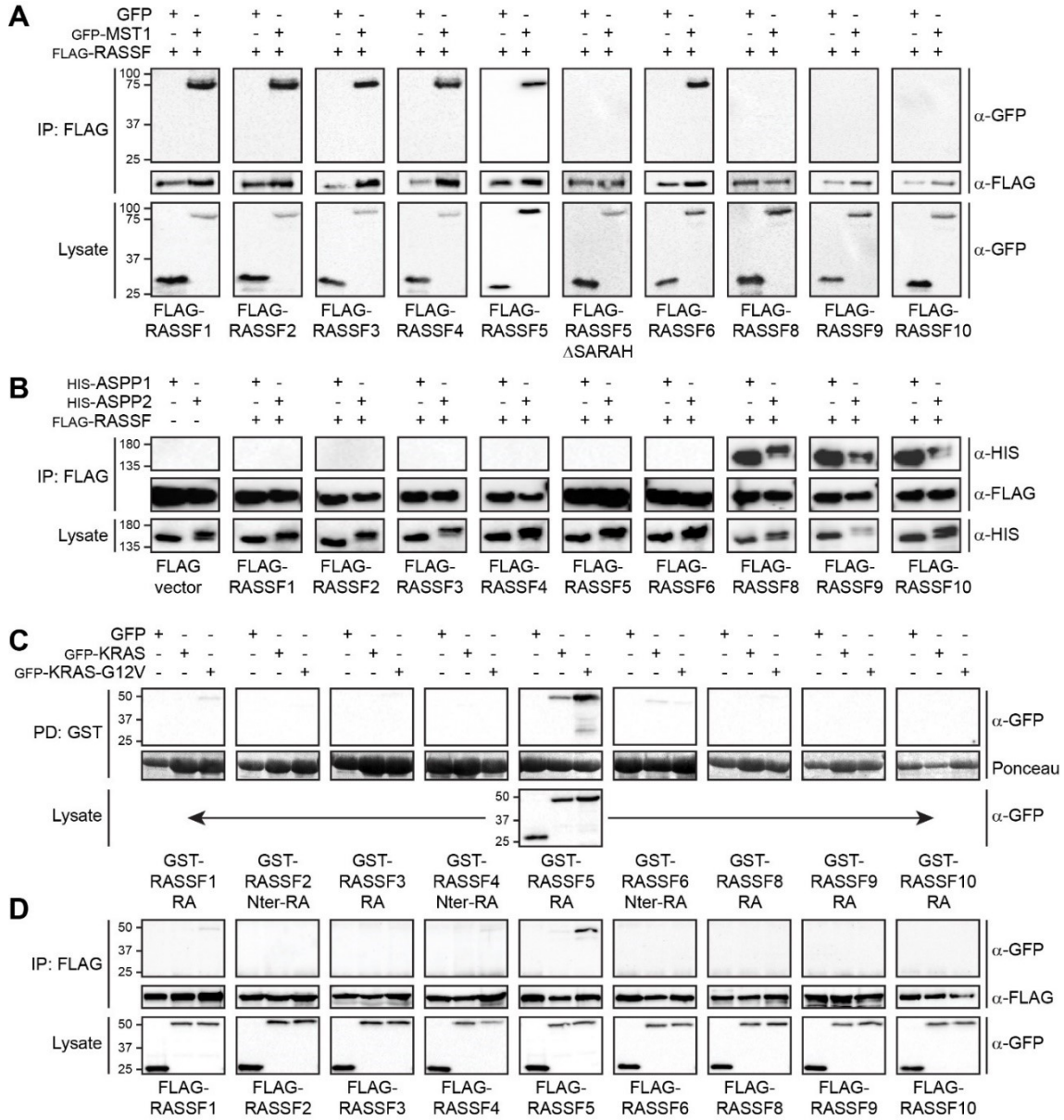
Figure 2:   Differential interactions between RASSF effectors and KRAS, MST1 kinase and the ASPP effectors.

(A) Complex of MST1 kinase and RASSF effectors. Cells were co-transfected with GFP alone or GFP-MST1 and FLAG-RASSF proteins. Anti-FLAG antibodies were used to immunoprecipitate RASSFs and interacting proteins were revealed by anti-GFP immunoblot (top). FLAG-RASSF5 ΔSARAH demonstrates dependency on the SARAH motif. **(B)** Interactions between ASPP1/2 effectors and the RASSF proteins. Cells were co-transfected with HIS-tagged ASPP1 or ASPP2 with FLAG-RASSF proteins. Anti-FLAG immunoprecipitations were probed by anti-HIS immunoblot to reveal interactions (top). **(C)** Binding of purified RASSF RA domains to KRAS. Cells expressing GFP alone, GFP-KRAS-WT or GFP-G12V-KRAS were lysed and incubated with purified GST-RA domains. anti-GFP immunoblots (top) revealed bound proteins. A ponceau stain shows GST-RA domains. **(D)** Interaction between KRAS and full-length RASSF proteins. Cells were co-transfected with GFP alone, GFP-WT-KRAS or GFP-G12V-KRAS with FLAG-RASSF proteins. Anti-FLAG antibodies were used to precipitate RASSFs, and anti-GFP immunoblots reveal interacting proteins (top).

Figure 3:   KRAS-induced apoptosis and RASSF RA domain binding to candidate GTPases.
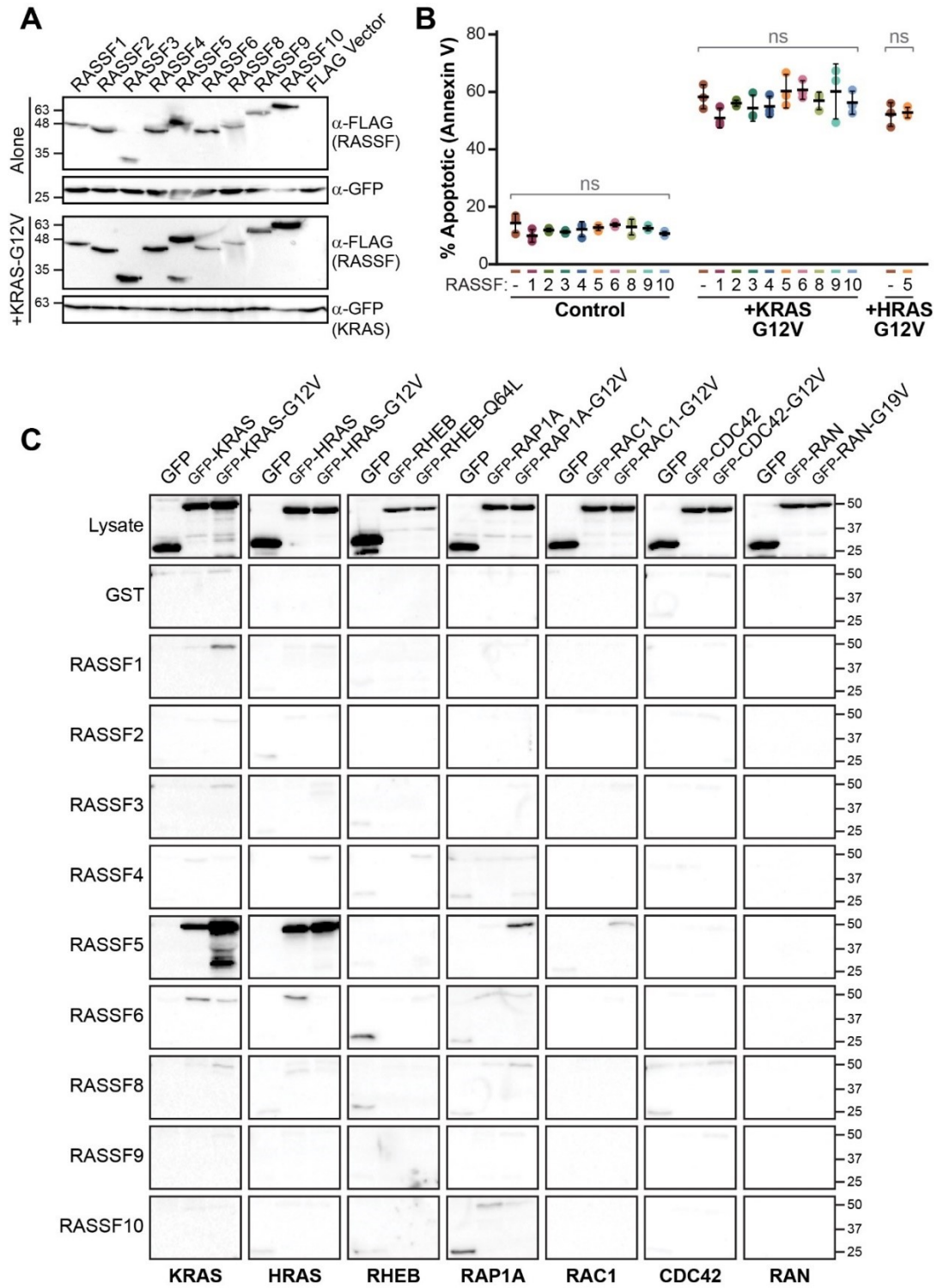
Figure 3: KRAS-induced apoptosis and RASSF RA domain binding to candidate GTPases.

(A) HEK 293T cells expressing full-length FLAG-RASSF proteins alone or with GFP-tagged, activated KRAS or HRAS were assessed for apoptosis using Annexin V staining. A fraction of cells assayed for apoptotic activity verified expression levels of FLAG-tagged RASSF and GFP-tagged GTPase proteins. Immunoblots with anti-FLAG and anti-GFP are shown**. (B)** RASSFs do not intrinsically stimulate apoptosis. RASSFs did not significantly induce apoptosis over controls, nor did they augment the apoptotic response observed in G12V-KRAS or G12V-HRAS expressing cells (ns=not significant as measured by two-way ANOVA). **(C)** Probed interactions between the candidate GTPases and RA domains from nine RASSF homologs. Lysates expressing GFP alone or GFP-tagged wild type/activated mutants of the GTPases KRAS (control), HRAS, RHEB, RAP1A, RAC1, CDC42, or RAN were incubated with purified GST-RA domains. Complexes on glutathione beads were separated by SDS-PAGE and analyzed by anti-GFP immunoblot.

Figure 4: **Structural modelling of RASSF RA domains elucidates specificity-determining substitutions in the αN-helix.**
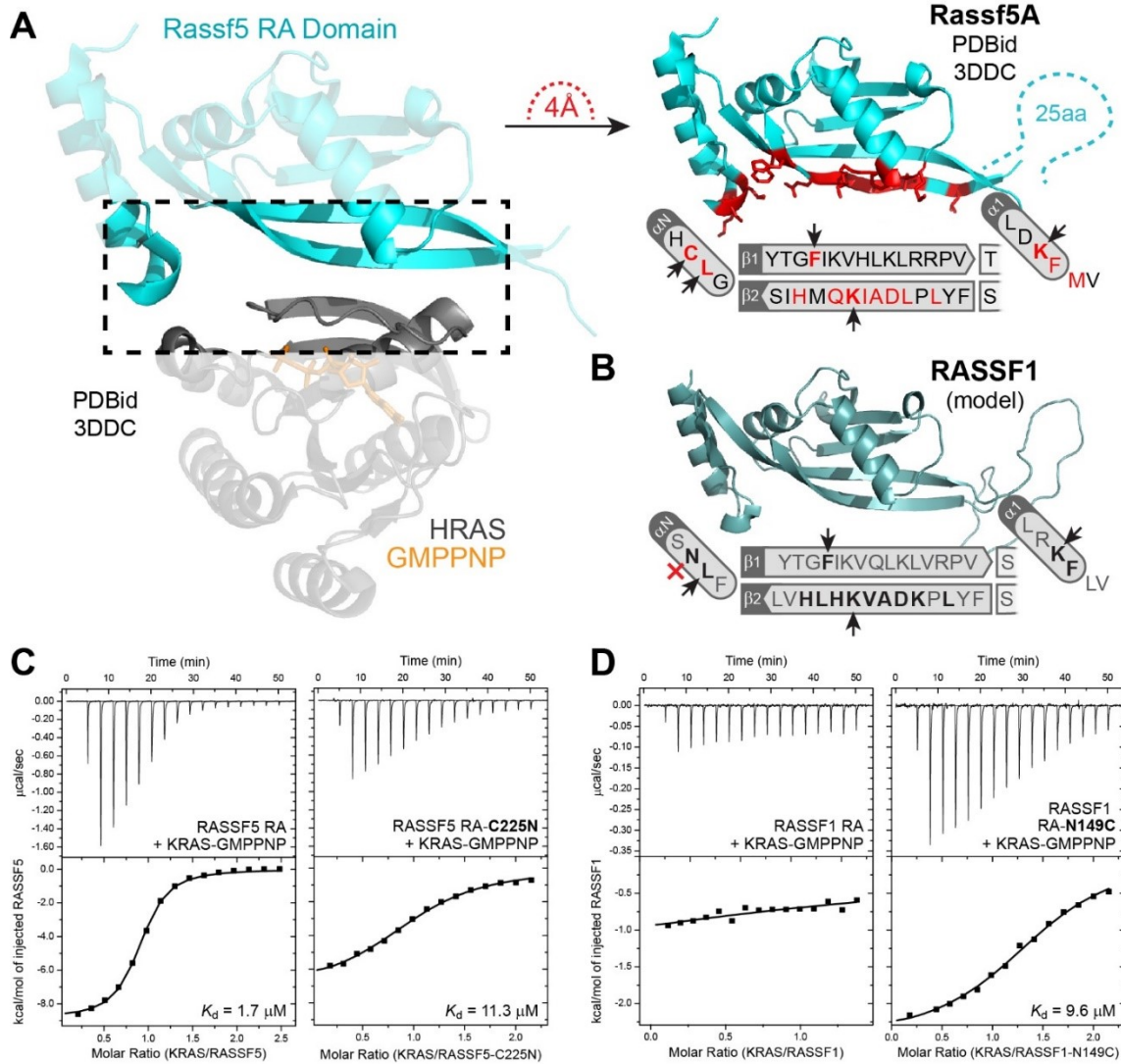
Figure 4: Structural modelling of RASSF RA domains elucidates specificity-determining substitutions in the αN-helix.

(A) Ribbons diagram of the HRAS (grey)-RASSF5 (blue) structure (PDBid 3DDC), highlighting the interface (left). A ribbons diagram of the RASSF5 RA domain and a schematic showing amino acid positions in the β1 and β2 strands, and the αN and α1 helices is at right. Residues within 4 Å of HRAS are highlighted in red. Amino acids indicated by a black arrow are predicted to have side chains that interact with RAS. **(B)** Structural model of the RASSF1 RA domain. Homology modeling based on the HRAS-RASSF5 structure shows the high similarity between RASSF1 and RASSF5 at the GTPase binding interface. RASSF1 residues predicted within 4 Å of HRAS are in bold. Black arrows indicate key conserved amino acids with RASSF5, while a red 'X' denotes a Cys-to-Asn substitution in αN. **(C)** Binding thermodynamics of the RASSF-KRAS interaction. ITC determined the RASSF5 RA domain interaction with KRAS-GMPPNP is 1.7 µM (left). A Cys-to-Asn mutation in RASSF5 αN weakens the interaction 7-fold (right). **(D)** ITC shows the RASSF1 RA domain does not measurably interact with KRAS-GMPPNP (left), but a RASSF5-mimetick Asn-to-Cys αN mutant interacts with a K_d of 9.6 µM (right).

Figure 5: **RASSF1A interacts with several alternative RAS subfamily GTPases.**
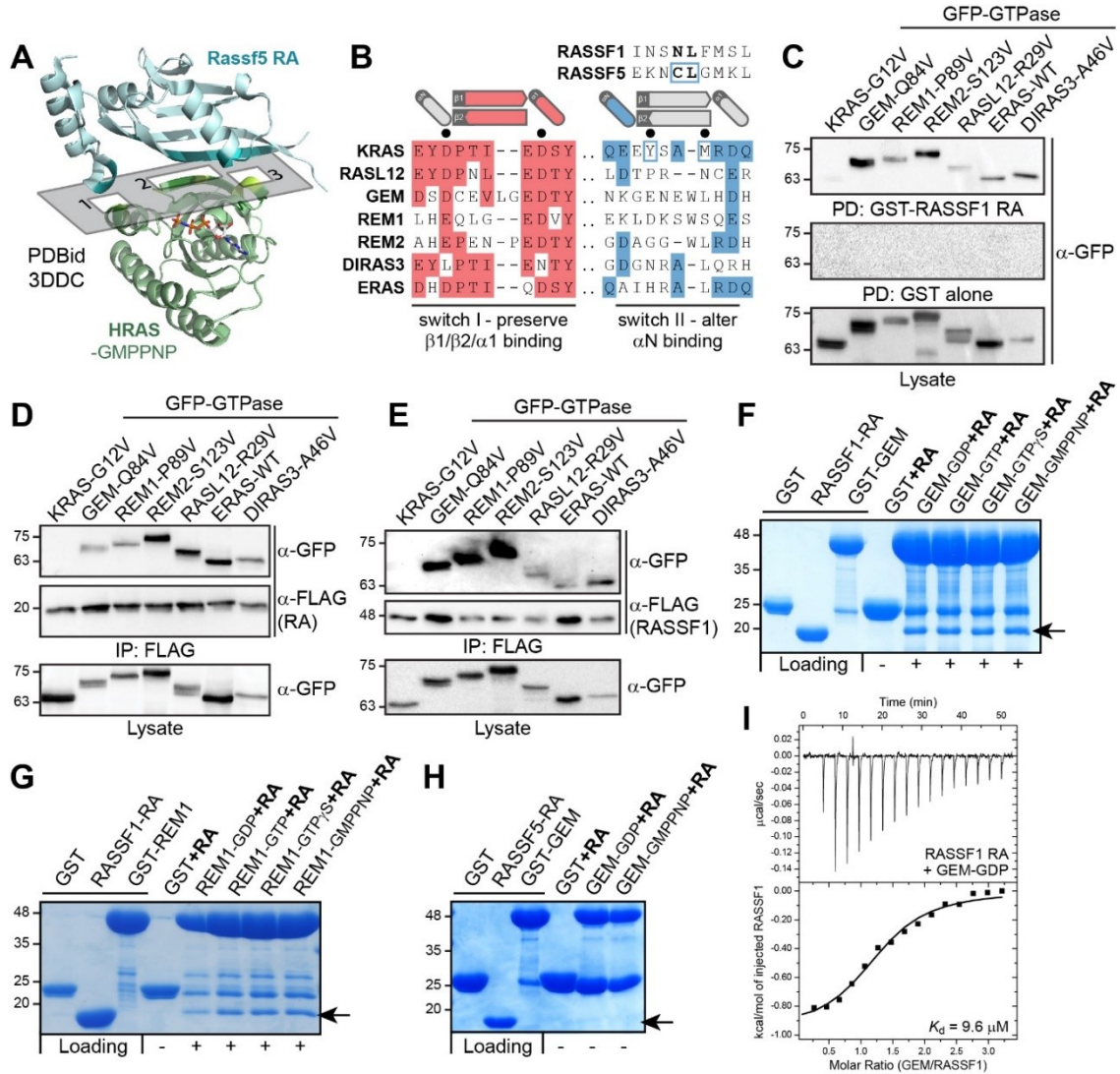
Figure 5: RASSF1A interacts with several alternative RAS subfamily GTPases.

(A) Ribbons representation of the RASSF5-HRAS structure (PDBid 3DDC) reveals three non-linear interaction hot spots between RASSF5 and HRAS. **(B)** Amino acid sequence alignment of KRAS and the six candidate GTPase interactors GEM, REM1, REM2, RASL12, DIRAS3 and ERAS (see also Figure S5). These have high sequence similarity in the switch 1 region (sites 2 and 3 from (A)) but are highly divergent through switch II (site 1 from (A)). Selected candidates preserve key interacting residues for the RASSF β1/β2/α1 interface (schematic at top) but diverge around the αN-helix binding site. **(C)** Interactions between the candidate small GTPases and RASSF1 RA domain. Cells expressing GFP-tagged, activated GTPase mutants were incubated with purified GST-RASSF1 RA domain. Following precipitation on glutathione beads, GTPases interacting with RASSF1 were identified by anti-GFP immunoblot (top). The same lysates were incubated with GST alone as a control. **(D)** Complex between the candidate GTPases and RASSF1 determined by co-IP. Cells were co-transfected with vectors encoding GFP-tagged, activated GTPases and FLAG-RASSF1 RA domain. Anti-FLAG immunoprecipitation followed by anti-GFP immunoblot revealed interacting proteins (top). **(E)** Association of full-length RASSF1A with the candidate GTPases. Cells were co-transfected with vectors expressing GFP-GTPases and full-length FLAG-RASSF1A. Anti-GFP immunoblots of anti-FLAG immunoprecipitations reveal GTPases interacting with RASSF1A. **(F)** Direct binding of the GTPase GEM to the RASSF1 RA domain. Purified RA domain was incubated with purified, GST-tagged GEM exchanged with the nucleotides GDP, GTP, GTPγS or GMPPNP. Complexes were isolated on glutathione beads and washed 3 times. Arrow denotes the RA domain. No binding was observed to a GST alone control. **(G)** Direct binding of the RASSF1 RA domain to REM1. RA domain was incubated with purified, GST-REM1 loaded with GDP, GTP, GTPγS or GMPPNP. Complexes were isolated on glutathione beads and washed 3 times. Arrow denotes the RA domain. No binding was observed to GST alone. **(H)** No interaction was observed between the purified RASSF5 RA domain and either GDP- or GMPPNP-loaded GEM. **(I)** ITC analysis of the RASSF1 RA domain interaction with GEM. GDP-loaded GEM interacted with the RASSF1 RA domain with an affinity of 9.6 µM. The

complex between RASSF1 and GTP-GEM proved highly unstable in solution and could not be measured.

Figure 6: RASSF1 and interacting RAS family GTPases in cells.

HeLa Cells (panel A)

GPS-Lipid Score (panel B)

1) N-Myristoylation: Non-consensus
2) S-Farnesylation: CAAX
3) S-Farnesylation: Non-consensus
4) S-Geranylgeranylation: CAAX
5) S-Geranylgeranylation: CC/CXC
6) S-Geranylgeranylation: Non-consensus
7) S-Palmitoylation: Cluster A
8) S-Palmitoylation: Cluster B

HeLa: Hoechst, Venus-GTPase*, FLAG-RASSF1A

HEK 293A: Hoechst, Venus-GTPase*, FLAG-RASSF1A
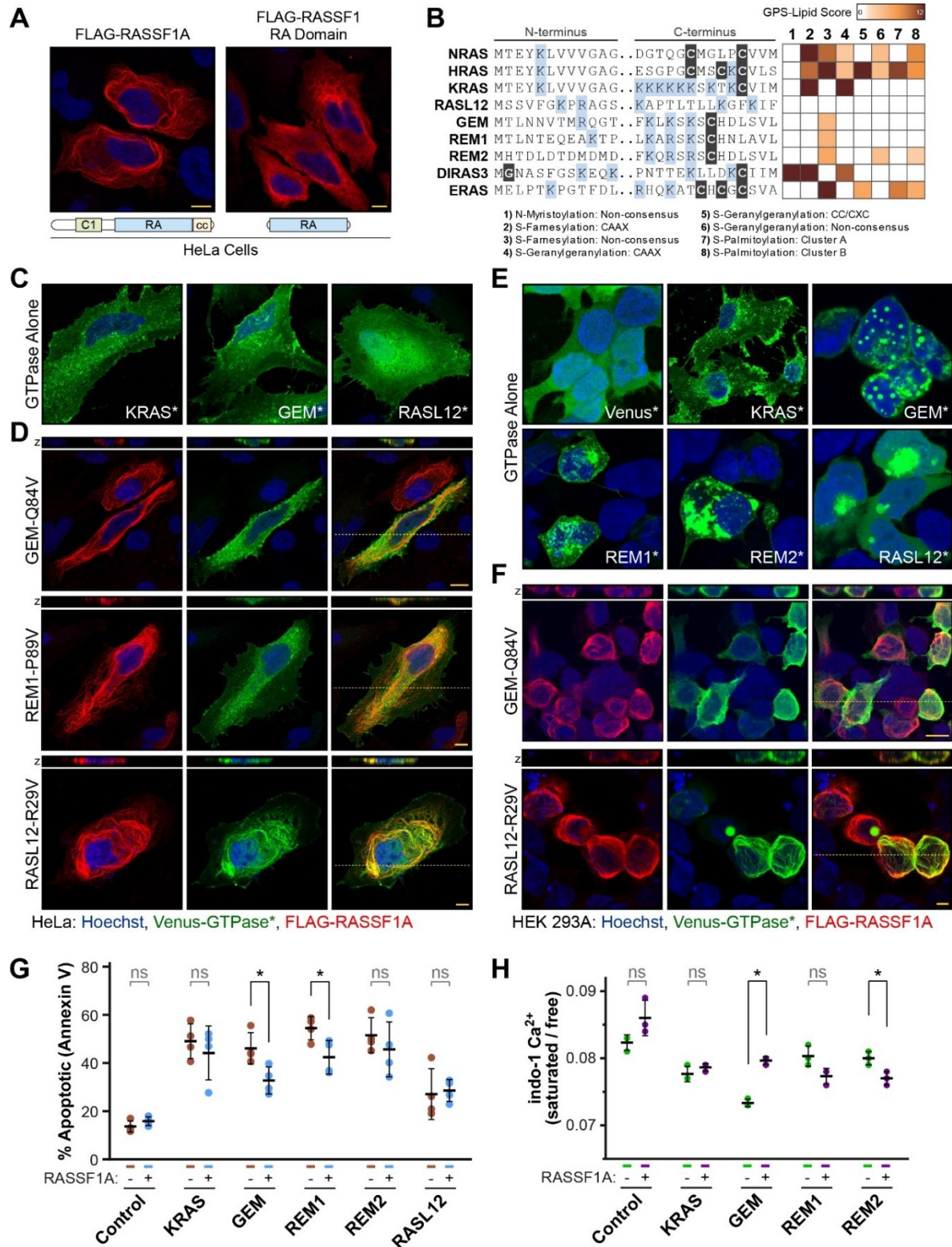
Figure 6:   RASSF1 and interacting RAS family GTPases in cells.

(A) Confocal microscopy shows the localization of full-length FLAG-RASSF1A (left) or the RASSF1 RA domain alone (right) in HeLa cells. **(B)** Prediction of lipidation sites in the candidate GTPases. Highlighted on an amino acid sequence alignment of the GTPase N- and C-termini regions are potential myristoylation or farnesylation sites (black boxes), as well as positively charged Lys and Arg residues (blue boxes). GPS-Lipid scores of potential lipidations are shown in the heat map, at right, colored from a low probability (white) to a high probability (dark brown). **(C)** Localization of GTPases expressed alone in HeLa cells, as determined by confocal microscopy. KRAS and the RGK GTPase GEM localize to the plasma membrane, while RASL12 has a diffuse localization throughout the cell. Asterisk's indicate these are mutationally activated GTPases (based on RAS G12V). **(D)** Localization of the GEM, REM1 and RASL12 GTPases in HeLa cells when co-expressed with RASSF1A. Image shows the localization of mutationally activated, GFP-tagged GTPases (green) and FLAG-tagged RASSF1 (red). The *z*-plane is shown above each image, at a location indicated by the dashed line in the overlay. **(E)** Differential localization of GTPases in HEK 293A cells as detected by confocal microscopy. Asterisk's indicate these are mutationally activated GTPases. **(F)** Co-expression of RASSF1A with these GTPases relieves puncta formation. Images show the localization of GFP-tagged GTPases (green) when co-expressed with FLAG-tagged RASSF1A (red) in HEK 293A cells. The *z*-plane is shown above each image at a location indicated by the dashed line. **(G)** Apoptotic induction by GTPases GEM, REM1, REM2 and RASL12. Annexin V staining and FACS analysis shows a large percentage of RGK expressing cells are undergoing apoptosis. Co-expression with RASSF1A significantly inhibits apoptosis in activated GEM- and REM1-expressing cells (asterisk indicates $p<0.03$). **(H)** Intracellular Ca^{2+} measured by Indo-AM staining and FACS analysis. Indo-AM loaded cells transfected with RGK GTPases have reduced intracellular Ca^{2+}. Co-expression with RASSF1A significantly rescues this phenotype, while it is amplified when RASSF1A is co-expressed with REM2 (asterisk indicates $p<0.025$).

Figure 7:   Hippo activation by RGK GTPases and RASSF effectors.
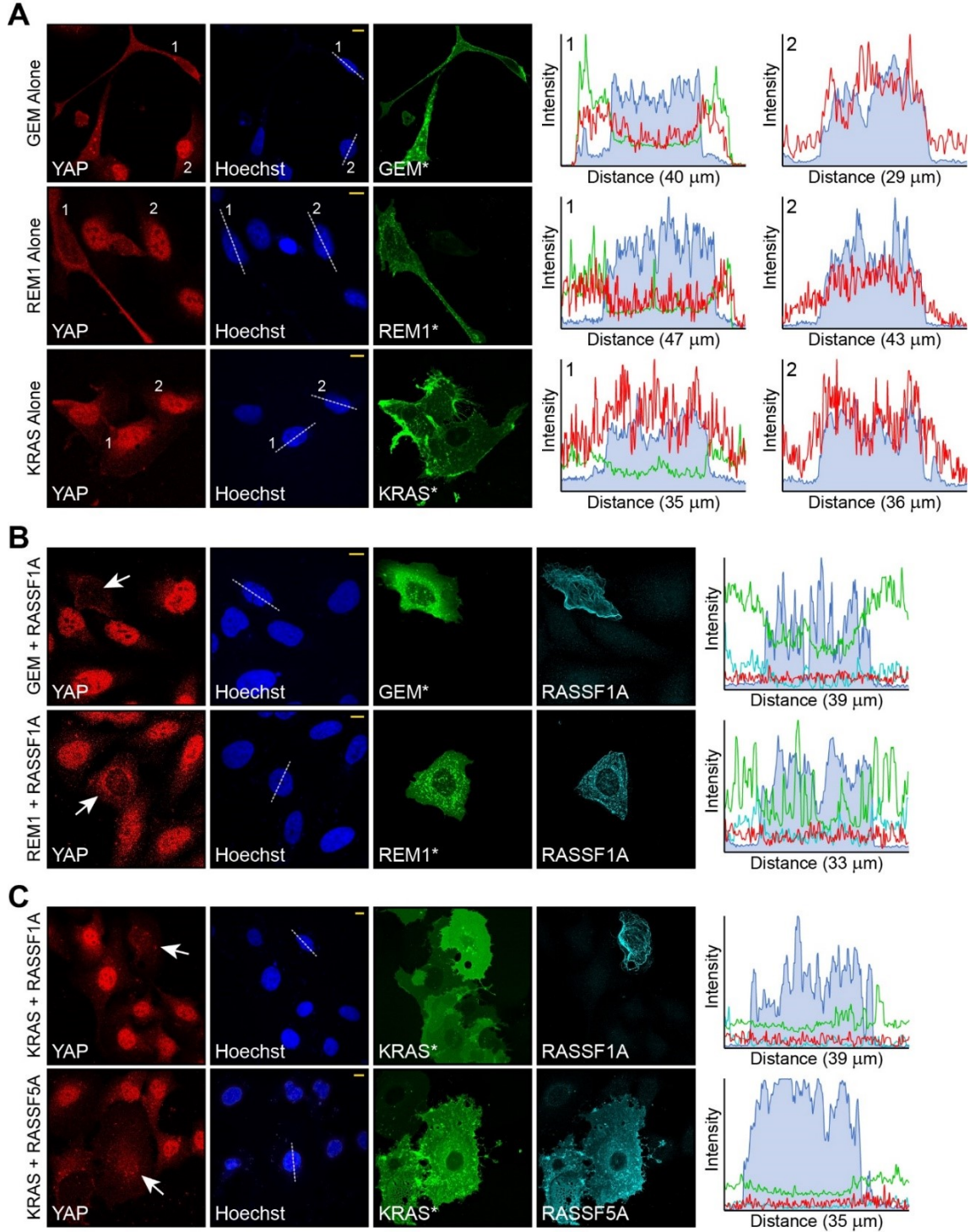
Figure 7:   Hippo activation by RGK GTPases and RASSF effectors.

(A) Confocal images show localization of endogenous YAP1 in U2OS cells expressing GFP-tagged, activated RGK GTPases (GEM or REM1), or KRAS alone. RGK GTPases induce significant cellular elongation and outgrowth. Quantification (right) was performed using *z*-stack fluorescence profiles from a plane through the nucleus (dotted line in Hoechst panel). Nuclei are blue, GTPase green and YAP1 red on the intensity graphs. YAP1 is excluded from the nucleus in cells expressing RGK GTPases (marked with a 1) compared to untransfected cells (marked with a 2). KRAS did not impact YAP1 localization. **(B)** YAP1 in U2OS cells co-expressing the RGK GTPase GEM or REM1 with their binding partner RASSF1A (FLAG-tagged). Quantification by fluorescence profiles is at right. Cells are no longer elongated, and YAP1 remains outside the nucleus. **(C)** Impact of FLAG-tagged RASSF1A or RASSF5A on YAP1 localization in U2OS cells expressing GFP-tagged, oncogenic KRAS. The presence of either RASSF protein restricts YAP1 nuclear localization, not observed when G12V-KRAS is expressed alone. In all panels, scale bar (yellow, Hoechst) represents 10 μm.

2.11 Supplementary Information

Figure S1: Phylogenetic tree and domain architecture of RASSF proteins.
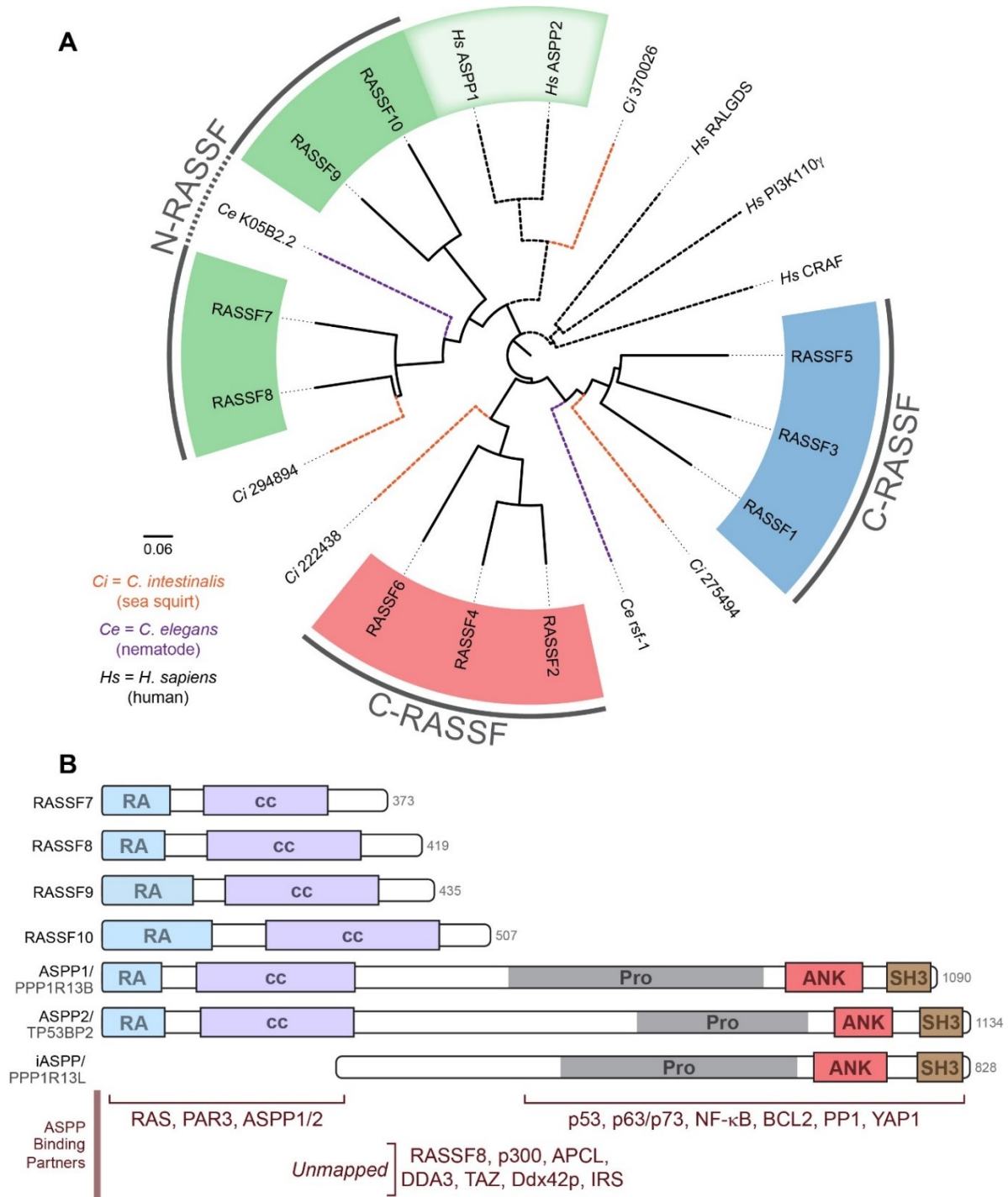
Figure S1: Phylogenetic tree and domain architecture of RASSF proteins.

(A) Phylogenetic relationship between human RASSF proteins, RASSF orthologs in *C. elegans* and *C. intestinalis*, and RA domains from several alternative human RAS effectors. The alignment is based on amino acid sequence conservation of the individual RA domains alone. C-RASSF1/3/5 cluster into one subgroup and C-RASSF2/4/6 into another. RA domains from N-RASSF7-10 are more highly related to those of the ASPP1/2 proteins. Nematodes have single N-RASSF and C-RASSF orthologs but no ASPP protein (APE-1 lacks an RA domain). Sea squirts, a close relative to the ancestral precursor of vertebrates, have single orthologs of the ASSP and N-RASSF effectors. They also have two C-RASSF orthologs, one related to the 2/4/6 cluster and the other to the 1/3/5 cluster. **(B)** A domain architecture schematic reveals similarity between ASPP and N-RASSF effectors. RA domains are in blue. Predicted or known coiled-coil regions are in purple. The ankyrin repeats (red) and SH3 domains (brown) of the ASPP proteins are missing in N-RASSFs. Several interaction partners have been mapped to distinct regions of the ASPP effectors (bottom).

Figure S2:   Purification of recombinant RASSF RA domains.

114
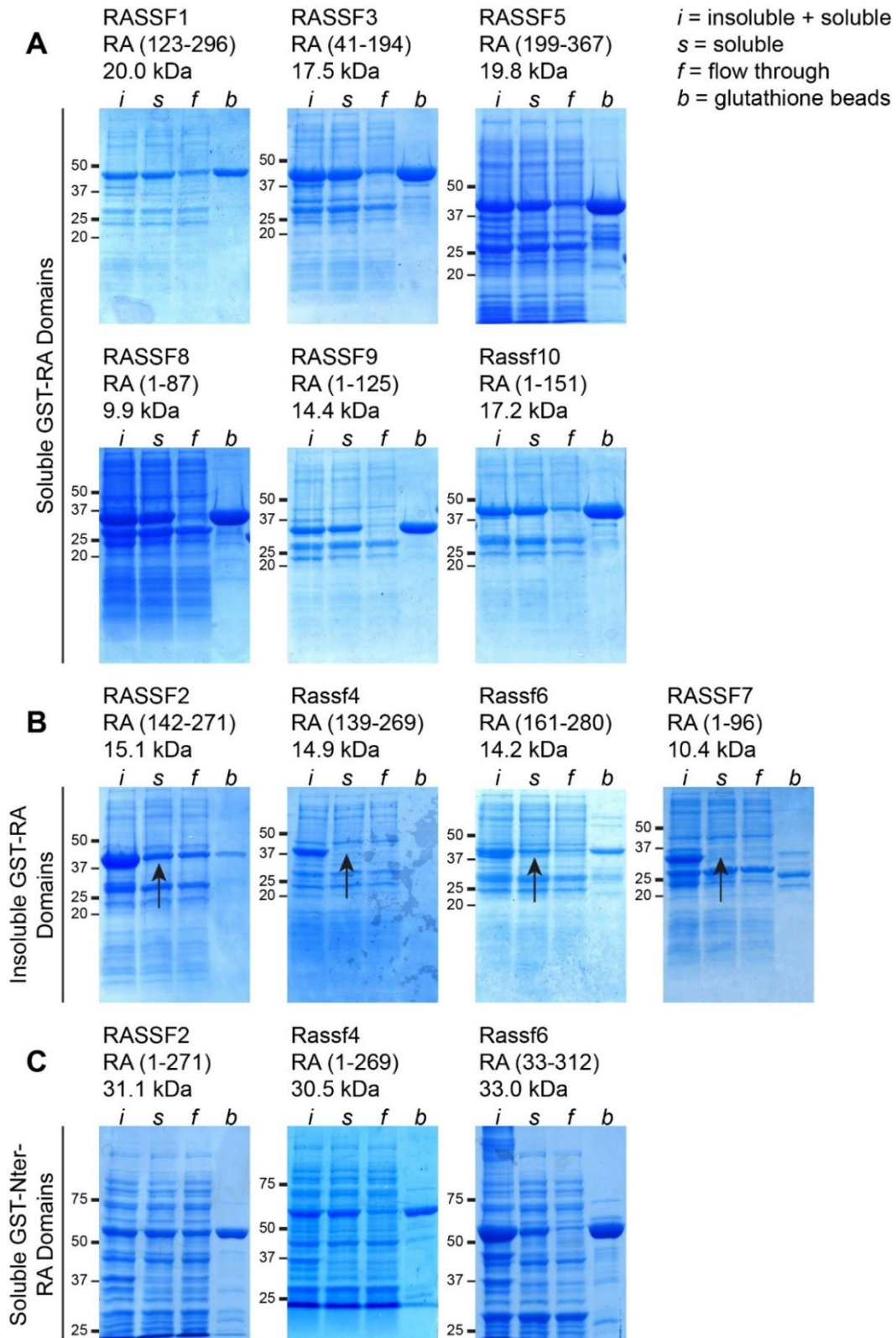
Figure S2: Purification of recombinant RASSF RA domains.

(A) Six RASSF proteins could be expressed and purified to high concentration and high homogeneity using our initial domain boundaries (RASSF1, RASSF3, RASSF5, RASSF8, RASSF9 and RASSF10). Residues defining these boundaries and theoretical molecular weights of the resultant GST-fusion proteins are listed above each Coomassie stained gel. **(B)** Four RASSF proteins proved insoluble using our original boundaries (the related paralogs RASSF2, RASSF4 and RASSF6 as well as RASSF7). Domain boundaries and theoretical molecular weights are above each gel. Arrows indicate an absence of bands in the soluble fraction that were present in the insoluble/soluble fraction. **(C)** Incorporating the predicted secondary structure at the N-termini of RASSFs 2/4/6 significantly improved the solubility of these proteins. The amended domain boundaries and theoretical molecular weights are indicated above each Coomassie stained gel.

Figure S3: Sequence alignment of RASSF proteins.
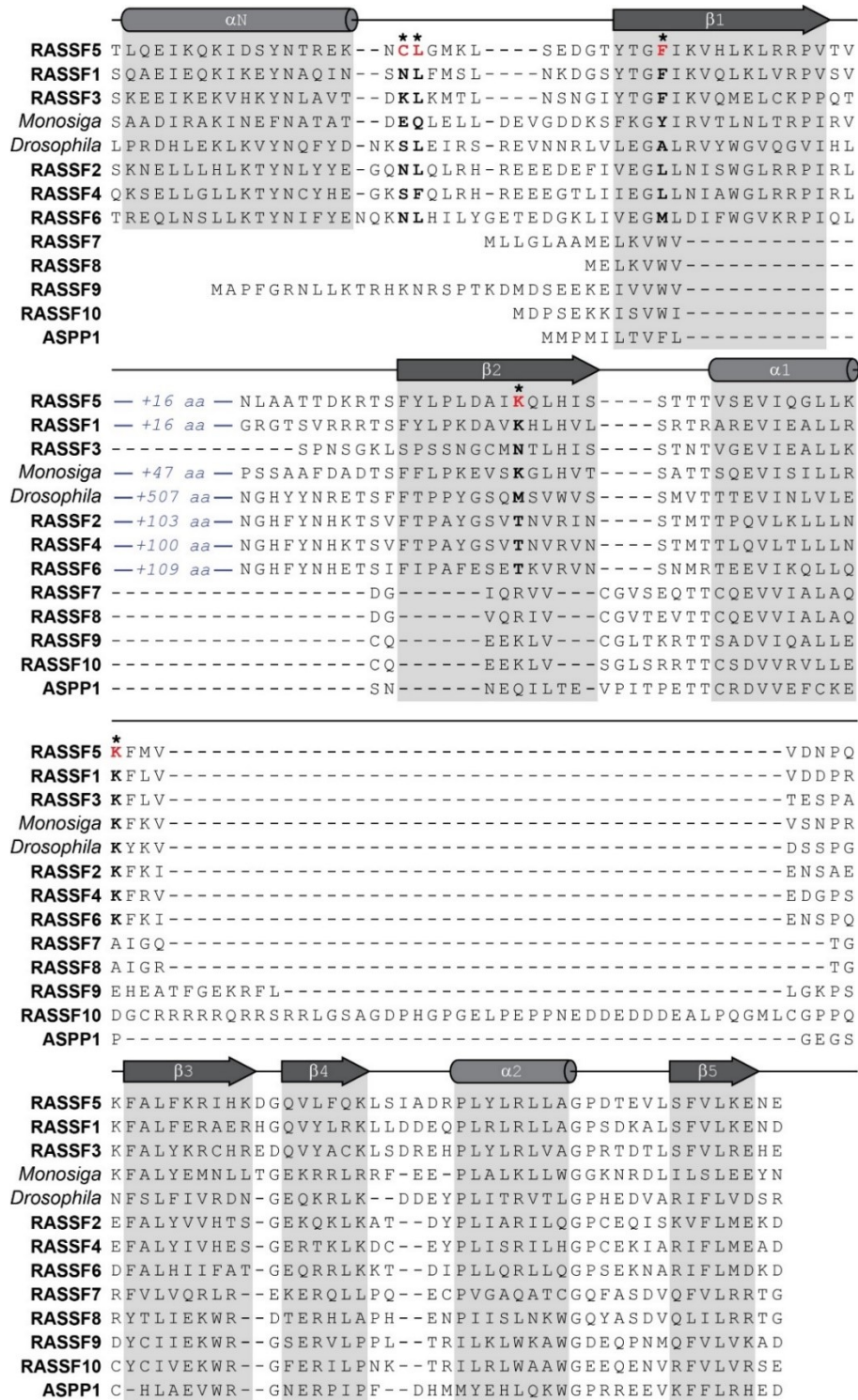
Figure S3: Sequence alignment of RASSF proteins.

Multiple sequence alignment of all ten human RASSF RA domains along with human ASPP1 and RASSF orthologs from the fruit fly *D. melanogaster* and single cell choanoflagellate *M. brevicollis*. Secondary structure regions as derived from the crystal structure of RASSF5 bound to HRAS (PDBid 3DDC) are indicated at top. Amino acid conservation and secondary structure predictions reveal a high degree of homology in all domains from the α1-helix to the C-termini. The β1 and β2 strands of N-RASSFs 7-10 are shorter and they do not encode an αN-helix, analogous to human ASPP1. The RA domain of RASSF5 includes a large, unstructured loop of 29 residues between β1 and β2 that provided no electron density in the published crystal structure. This loop is a similar length in RASSF1 and shorter in RASSF3. The regions of RASSF2, RASSF4 and RASSF6 that are most homologous to the β1 and αN regions of RASSF5 are separated by long insertions of approximately 100 residues from their homologous β2 strands. The IUPred tool (https://iupred2a.elte.hu/) predicts these are intrinsically disordered regions and they are rich in Ser and Arg. This loop is over 50 residues in the lone *M. brevicollis* RASSF ortholog and has expanded to over 500 residues in the single *D. melanogaster* ortholog. Impacts on RA domain folding are unknown, but the domains are insoluble in the absence of the N-terminal homology regions. RASSF5 residues undergoing side chain interactions with HRAS (PDBid 3DD) are in bold red, marked with an asterisk. Corresponding residues in the aligned domains are in bold black.

Figure S4: Structural models of RASSF RA domains.
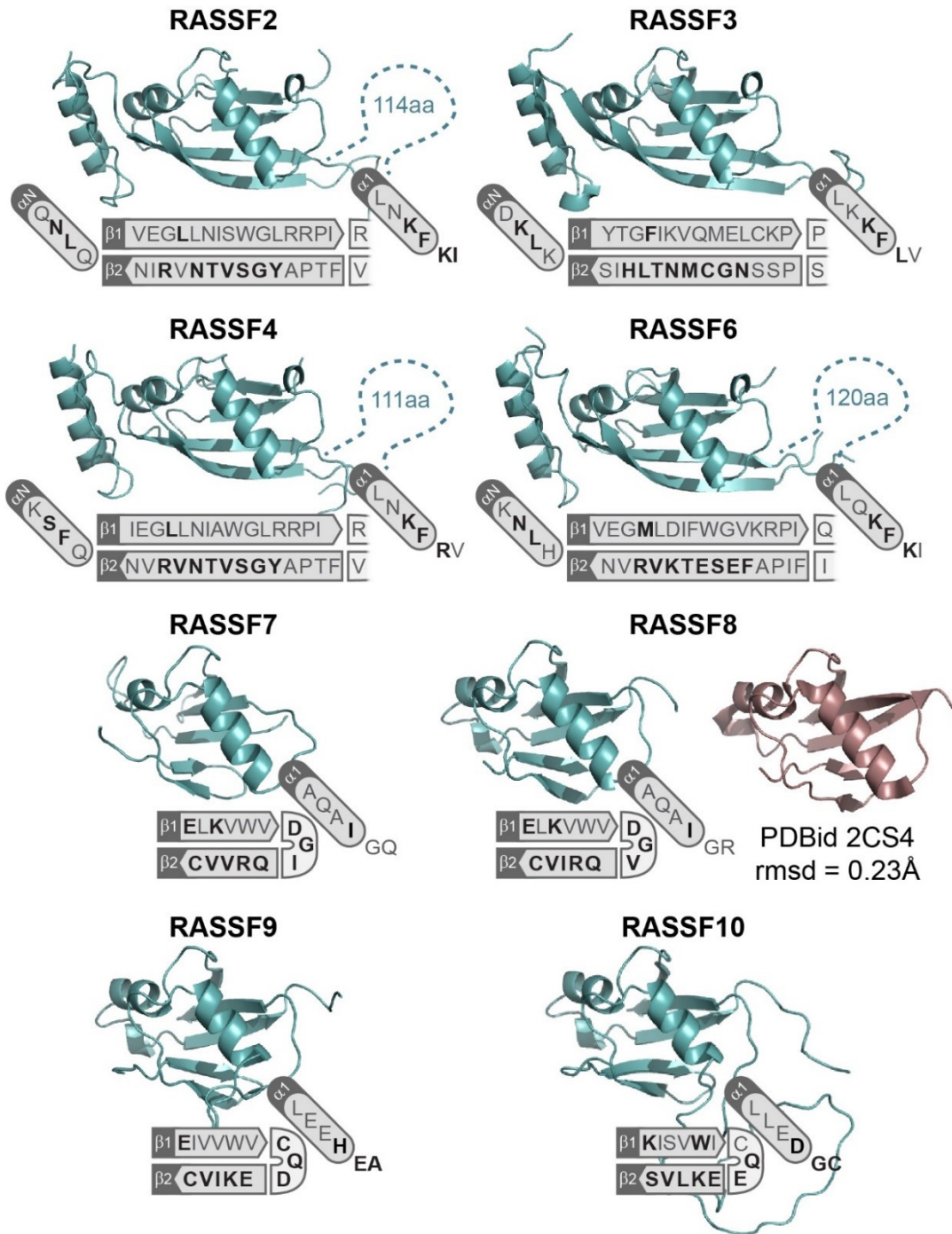
Figure S4: Structural models of RASSF RA domains.

Ribbons representation of homology modelled RASSF RA proteins. Models of domains from C-RASSFs 2/3/4/6 were based on the RASSF5-HRAS structure (PDBid 3DDC). An AFDN-HRAS structure (PDBid 6AMB) served as a template for domains from N-RASSFs 7-10. A solution structure of the RASSF8 RA domain solved by NMR (PDBid 2CS4) has a backbone r.m.s.d. of just 0.23 Å compared with the modelled structure, validating the approach. A schematic showing amino acid positions in the β1 and β2 strands, and the αN (if present) and α1 helices is shown below each structure. Residues within 4 Å of the GTPase are in bold.

Figure S5: Identification of candidate GTPases in the RAS subfamily that could interact with RASSF1.
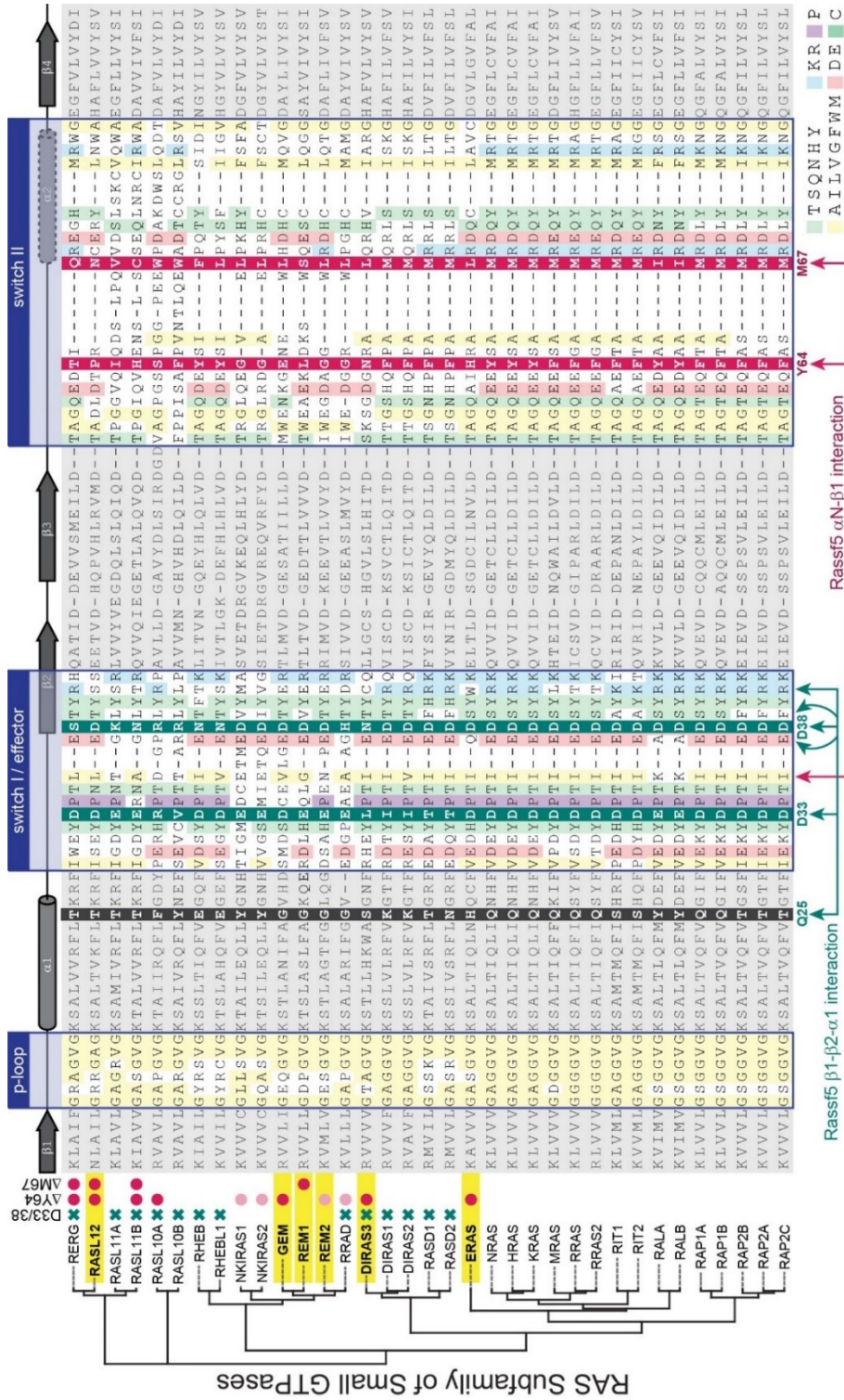
Figure S5: Identification of candidate GTPases in the RAS subfamily that could interact with RASSF1.

Multiple sequence alignment of all 35 RAS subfamily small GTPases. Amino acid sequences starting just upstream of the p-loop and ending after the switch II region are shown. Regions of secondary structure are depicted at top. GTPases are ordered based on their phylogenetic relationship (tree at left). The p-loop, switch I/effector and switch II regions are highlighted while regions outside are in grey. GTPases with significant amino acid substitutions at the RAS Asp33 and Asp38 locations are marked with a green 'X' (left). Those with divergent switch II sequences around RAS Tyr64 or Met67 are marked with a red circle. As candidate RASSF1 interacting proteins we chose six GTPases that were conserved around Asp33 and Asp38 but diverged at Tyr64 and/or Met67: GEM, REM1, REM2, RALS12, ERAS and DIRAS3. These are highlighted yellow.

Figure S6: RASSF1 and candidate GTPases in cells.

HeLa: Hoechst, Venus-GTPase*, Flag-RASSF1A
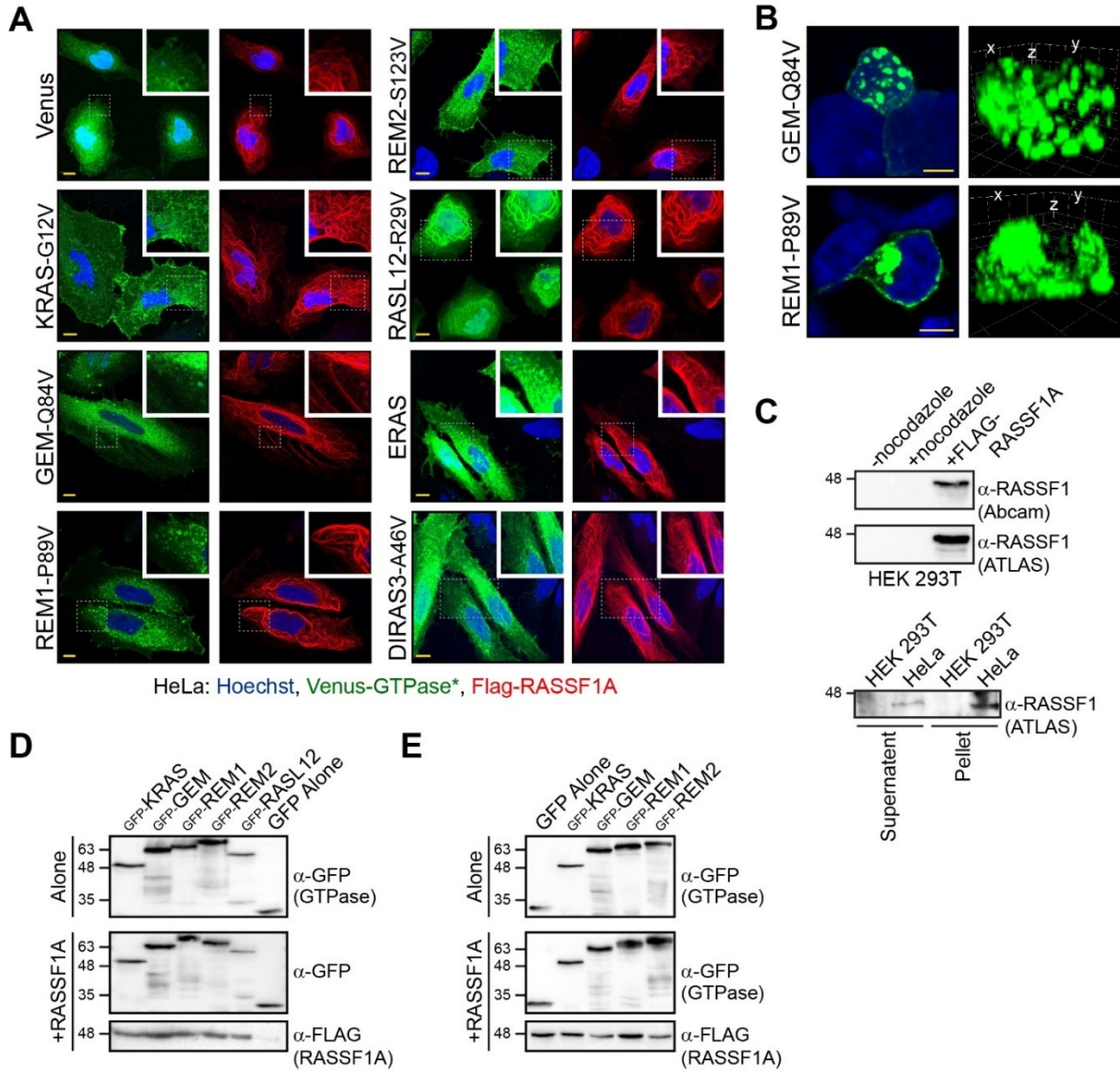
Figure S6: RASSF1 and candidate GTPases in cells.

 (**A**) Co-localization of GTPases and RASSF1 in HeLa cells as detected by confocal microscopy. Images show subcellular localization of GFP-tagged, activated GTPases (green) in the presence of FLAG-tagged RASSF1 RA domain (red, left) or full length RASSF1A (red, right). RASSF1 proteins were detected using anti-FLAG and a TxRed-conjugated secondary antibody. Insets are enlargements of the areas boxed in dotted lines. Scale bar (yellow) represents 10 µm. (**B**) Puncta distribution of activated GEM and REM1 in HEK 293A cells. Shown are both 2D (left) and 3D (right) renders of confocal images taken of GFP-tagged GEM and REM1. The *x*, *y* and *z* planes are labelled on the 3D render. These puncta are observed throughout the cell, while also in the nucleus in GEM-overexpressing cells. (**C**) HEK 293T cells do not express detectable levels of endogenous RASSF1. Two commercial antibodies against RASSF1 (purchased from Abcam and ATLAS Antibodies) were used to probe RASSF1 expression levels. No RASSF1 was present in HEK 293T cell lysates (+/- nocodazole to release protein from microtubules), but overexpressed RASSF1 was positively detected (top). In comparison, a small amount of endogenous RASSF1 was detected in HeLa cell lysates after long exposure (bottom), though much of this protein was found in the insoluble pellet. (**D**) A fraction of cells assayed for apoptotic activity were used to verify expression levels of FLAG-tagged RASSF and GFP-tagged GTPase proteins. Immunoblots with anti-FLAG and anti-GFP are shown for RGK assay. (**E**) A fraction of cells assayed for intracellular Ca^{2+} entry were used to verify expression levels of FLAG-tagged RASSF1A and GFP-tagged GTPases. Immunoblots with anti-FLAG and anti-GFP are shown.

Figure S7: Localization of YAP1 in U2OS cells determines Hippo pathway activation.
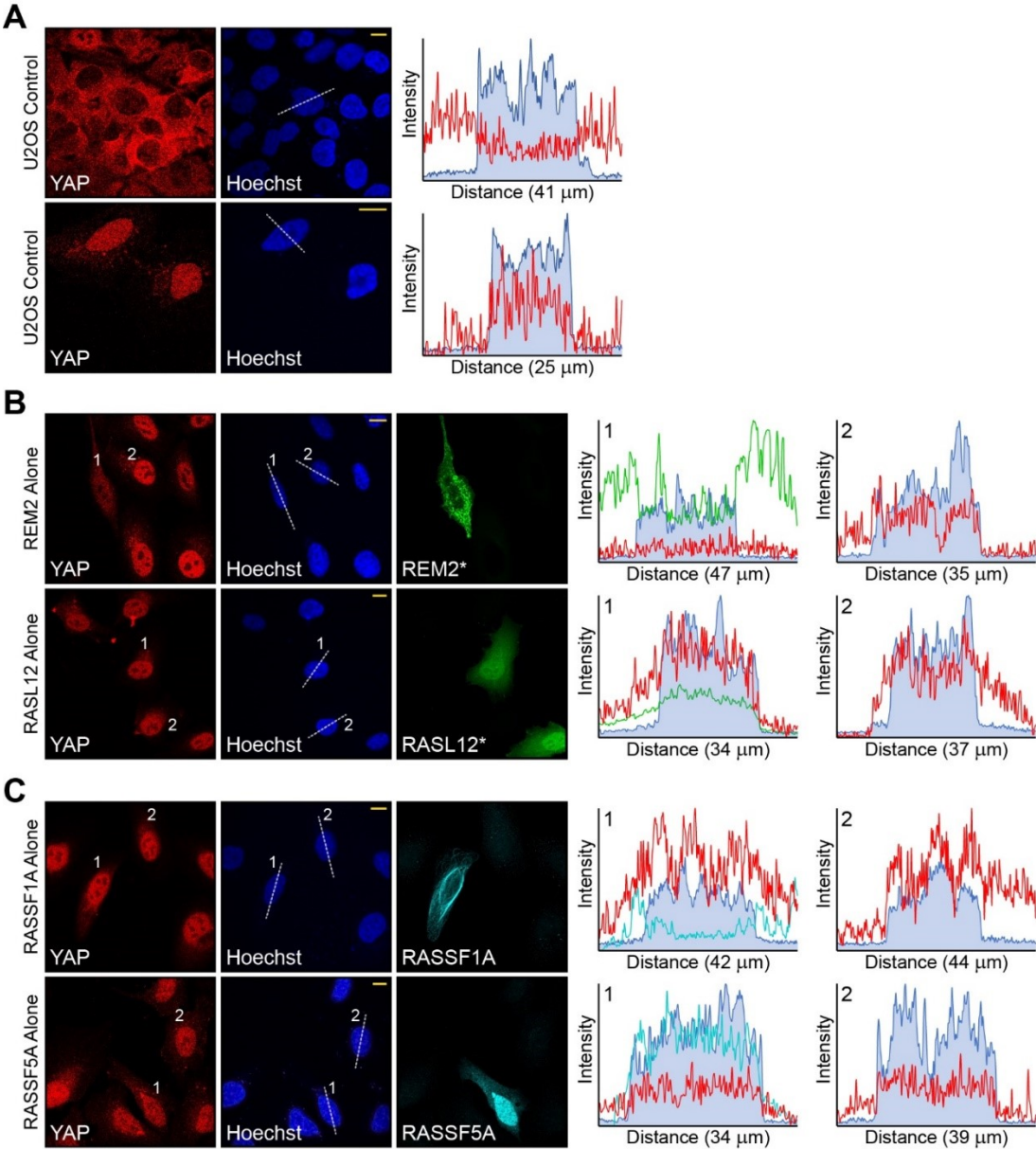
Figure S7: Localization of YAP1 in U2OS cells determines Hippo pathway activation.

(A)   Confocal microscopy shows the localization of endogenous YAP1 in U2OS cells (left). Quantification was performed using fluorescence profiles taken from a plane of *z*-stacks through the nucleus (marked with dotted line on Hoechst panel). On the intensity profiles, blue is from the Hoechst-stained nucleus and red from YAP1. In these cells, YAP1 is localized in the nucleus when they are sparse (30-40% confluent) and is retained in the cytoplasm when cells are dense (80-100% confluent). **(B)** Expression of the RGK GTPase REM2 reduces YAP1 nuclear localization while RASL12 does not. Quantification of a transfected cell (marked with 1) and a non-transfected cell (marked with 2) is at right. **(C)** Expression of either RASSF1A or RASSF5A alone does not activate the Hippo pathway, as YAP1 remains predominantly nuclear. Cells transfected with FLAG-RASSFs are marked with a 1 and quantitated at right, a non-transfected control cell is marked with 2. In all panels, scale bar (yellow, Hoechst) represents 10 µm.

3. Chapter 3: Rewiring mutant KRAS signalling to the proapoptotic RASSF effector pathway

Thillaivillalan Dhanaraman[1], Chitra Muthuramu[1], Ryan C. Killoran[1], Anamika Singh[2], Julia Shifman[2] and Matthew J. Smith[1,3,*]

[1]Institute for Research in Immunology and Cancer, Université de Montréal, Montréal, Québec, H3T 1J4, Canada
[2]The Hebrew University of Jerusalem, Department of Biological Chemistry, Jerusalem, Israel
[3]Department of Pathology and Cell Biology, Faculty of Medicine, Université de Montréal, Montréal, Québec, H3T 1J4, Canada

[*]To whom correspondence should be addressed:

Matthew J. Smith, Ph.D
Institute for Research in Immunology and Cancer (IRIC)
Department of Pathology and Cell Biology, Université de Montréal
2950 Chemin de Polytechnique, Montréal, Québec, Canada, H3T 1J4
Pavillon Marcelle-Coutu, Rm 4306-11; Tel: (514) 343-5704
email: matthew.james.smith@umontreal.ca

The manuscript is "under preparation".

Contributions:

D.T. and M.J.S. designed experiments. D.T., C.M., R.K. and M.J.S. performed experiments and analyzed data. A.S. and J.S. performed structural modelling. J.S. and M.J.S. supervised studies. D.T. and M.J.S. wrote the manuscript with input from J.S.

3.1 Abstract

Interactions between the RAS small GTPases and downstream effectors are highly specific. RAS binds to its effectors through engagement at dynamic switch regions. Previous work has identified single amino acid substitutions within these regions that can alter binding preferences towards specific effectors, which allows detailed study of RAS signalling through more restricted downstream pathways. The functional significance of RAS interactions with effectors varies from induction of cell proliferation to apoptosis, with the RASSF family of effectors believed responsible for activation of the pro-apoptotic Hippo pathway. Here, we derive the first RAS effector mutant that preferentially binds RASSF5 over RAF kinase. Further, using structural modelling we generate a mutant of the RASSF1 effector, typically a partner for atypical RAS GTPases, that is capable of binding KRAS. This rewired RASSF1 phenocopies RASSF5 *in vivo*, co-localizing with activated KRAS at the plasma membrane and activating the Hippo pathway downstream of KRAS-G12V. Thus, we have developed two rewiring approaches that will allow study of KRAS signalling to the RASSF pathway in the absence of strong MAPK activation.

Keywords: RAS; RASSF; BRAF; Hippo; GTPase; RA domain; YAP1; Rewiring; MAP Kinase pathway

3.2   Introduction

The RAS small GTPases regulate various cellular processes ranging from cell growth and differentiation to apoptosis. RAS is a GTP binding protein that acts as a molecular switch, the protein cycling between a GTP-bound "active" state and GDP-bound "inactive" state [1] [2]. GDP-bound RAS at resting state has a high affinity for GDP, and activation is thus regulated by guanine nucleotide exchange factors (GEFs) which stimulate the release of GDP and allow GTP loading. Active, GTP-bound RAS binds diverse downstream 'effector' proteins to turn on a cascade of signalling networks. Termination of signal transduction is assisted by GTPase-activating protein (GAPs). As RAS GTPases have a low intrinsic GTP hydrolysis rate, GAPs help catalyze the GTPase activity of RAS by orders of magnitude, resulting in the inactive, GDP-bound state [3].

The three major isoforms of RAS GTPase; HRAS, KRAS and NRAS, are believed to have overlapping functions and bind a similar set of downstream effectors to induce proliferation, differentiation or even apoptosis [4-6]. Effectors of RAS comprise RAS binding domains (RBD) (or RAS association (RA) domains) that share a ubiquitin-like fold. At present, there are more than 50 RA and 20 RBD domain containing proteins in the human proteome [7, 8]. These include RAF, PI3K, RALGDS, PLCε, RASSF5 and AF6 [8-14]. RAF effectors are Ser/Thr protein kinases, and their activation initiates a phosphorylation cascade known as the MAP kinase pathway, which ultimately activates ERK kinases to phosphorylate transcription factors that mediate gene transcription and induce cellular proliferation [15]. The RAS-PI3K signalling axis regulates cell survival, cell growth, actin-cytoskeleton remodelling and metabolism [16]. RALGDS signalling links RAS to RAS-related RAL GTPases, which regulate cell migration and vesicular trafficking. [17], while PLCε binding is believed to generate the second messengers diacylglycerol (DAG) and inositol trisphosphate (IP$_3$) [18]. RASSF signalling is proposed to activate the Hippo pathway *via* their direct association with the mammalian Hippo kinases MST1/2, leading to cell cycle arrest and apoptosis [19]. Finally, a RAS-AF6 signalling axis is purported to regulate cell-cell adhesion in an unknown manner [20]. While the true biological significance of RAS interaction with RAF is well-understood, comparatively little is known about how many of the alternative RAS effectors function downstream of RAS in cells.

RAS GTPases bind effectors through one or two dynamic switch regions, switch I (amino acids 30-38) and switch II (amino acids 59–67) [21]. The effectors RAF and RALGDS have a similar RA domain fold that binds RAS predominantly at switch I. In contrast, PI3K, PLCε, RASSF5 and AF6 bind *via* a distinct mode and contact both RAS switch I and switch II [8, 22-24]. In addition, RAS binds to effectors with quite varied binding kinetics and thermodynamics [25], and distinct switch 1/2 amino acids determine binding specificity. Landmark studies have identified amino acid substitutions in RAS T35, E37, D38 or Y40 that show preferential binding towards specific effectors [26-28]. These RAS 'effector mutants' offer an opportunity to study RAS signalling to more restricted downstream pathways and delineate their importance to RAS biology and its oncogenic potential. Crucial were a Ser-to-Thr switch at position 35 of HRAS believed to specifically signal to the RAF/MAPK pathway, and a Glu-to-Gly substitution at position 37 of HRAS that abrogates interaction with RAF but retains binding to RALGEF effectors [26]. Currently, there are no RAS effector mutants that specifically signal to the RASSF pathway.

Our previous work has revealed that RASSF5 binds KRAS with an affinity of 1.7 μM and binding assays with the related RASSF1 determined it does not bind KRAS [29-31] (Chapter 2). Despite this, both RASSF5 and RASSF1 activate Hippo signalling downstream of mutationally activated KRAS. Others have shown that siRNA depletion of RASSF5 reduces TNF-α mediated apoptosis in U2OS cells, and inactivation of Rassf5 in mouse embryonic fibroblasts results in resistance to TNF-α mediated apoptosis. These data link RASSFs to Hippo signalling and apoptosis downstream of RAS oncogenes, and we therefore sought to design a RAS 'effector mutant' that specifically rewires RAS to RASSF effectors by identifying amino acid substitutions in the RAS switch regions.

A rewiring approach would provide, for the first time, a system to fully characterize RAS output to RASSF effectors in the absence of high RAF binding or MAPK activity. Using a combination of biophysical approaches, we here identify a RAS mutant with enhanced affinity for RASSF5 and reduced affinity for BRAF. In parallel, a rewired RASSF1 mutant was developed that can interact with activated KRAS. We validate these rewiring approaches both *in vitro* and *in vivo*, demonstrating a potential strategy for rewiring RAS signalling to the pro-apoptotic RASSF pathway.

3.3 Results

3.3.1 Structural modelling and mutational analysis of KRAS mutants to RASSF and RAF proteins

Interactions between RAS and RAF kinases are known to promote cellular proliferation. In contrast, RAS interaction with RASSF5 activates the Hippo pathway and may potentially induce apoptosis. RAS binds with approximately 30-fold higher affinity to BRAF (K_d of 60 nM) than to RASSF5 (1700 nM) (see Chapter 2). To rewire this interaction, we sought to identify mutations in KRAS that weaken affinity to RAF and increase affinity to RASSFs, in line with previously identified RAS 'effector mutants'.

To select RAS residues for mutation, we compared crystal structures of RAS in complex with either RAF (PDBid: 6E6C) or RASSF5 (PDBid: 3DDC) (**Figure 1A).** RAS contacts RAF primarily *via* its switch I region, whereas the RAS-RASSF5 complex involves both RAS switch I and switch II (**Figure 1B**). We identified all key interface residues and designed point mutants based on computational predictions intended to disrupt the RAS-RAF interaction but augment interaction with RASSF5. Five residues were identified as more important for RAS interaction with RAF: I36, E37, A66, M67 and Q70. Four residues were identified as more significant to the RAS-RASSF5 interaction: I21, Q25, N26 and H27. Our designed rewiring mutations focused on several of these residues, designated here as hotspot-1 mutants (A66D, E37D, M67W) or hotspot-2 mutants (I21F, Q25Y, H27R) (**Figure 1B**). Thus, with a structure based informatic approach we were able to identify mutations in RAS-effector interaction interfaces that could potentially abrogate RAS engagement with RAF.

As a parallel strategy to rewire RAS to the RASSF pathway we considered the RASSF1 effector protein, which is highly homologous to RASSF5 but does not bind directly to KRAS or HRAS (Chapter 2). We hypothesized that relatively minor amino acid substitutions in RASSF1 could increase its affinity to RAS and provide a secondary RASSF effector pathway with which we could investigate oncogenic RAS signalling. To design mutations in RASSF1, we used a homology model of the RASSF1 RA domain based on the crystal structure of RASSF5 (see Chapter 2 and **Figure 1C**). We postulated that introduction of N-to-C (N149C) and K-to-L (K208L) mutations in the RASSF1 RA domain may augment RAS binding (**Figure**

1C), as they are the only major primary sequence variations within the RASSF1 and RASSF5 RA domains. The N149C mutation is in the αN-helix and K208L in the β2 strand of the RA domain. This cysteine in RASSF5 forms an essential hydrophobic interaction with Y64 in HRAS switch II and we believe K208L in RASSF1 protein surface might remove the steric hinderance caused by the bulky charged residue lysine. Together, the designed RAS effector mutations and the RASSF1 N149C/K208L mutant (hereafter referred to as RASSF1^{KRAS}) provided two potential avenues to functionally rewire RAS signalling to RASSF effectors.

3.3.2 Mutant KRAS binds to RASSF5 with improved affinity

To biochemically assess the designed rewiring mutants of RAS for their capacity to bind RASSF5 and RAF, we first performed GST pull-down assays. HIS-tagged, wild-type KRAS and GST-tagged RA domains of RASSF5 and BRAF were expressed in *E. coli* and purified to homogeneity. Purified, GST-tagged RASSF5 RA and BRAF-RBD were incubated with GMPPNP-exchanged KRAS on glutathione beads. The mixture was washed three times to remove nonspecific interactions and complexes were resolved on Coomassie-stained SDS-PAGE gels. Densitometric analysis showed that activated KRAS (RAS-GMPPNP) binds approximately 2-fold better to BRAF than to RASSF5 (**Figure S1A**). To investigate the designed KRAS mutants we included GST-alone as a control and the previously identified RAS effector mutants E37G (proposed to disrupt RAF binding) and T35S (proposed to specifically bind RAF) [26] (**Figure 2A**). All KRAS variants were purified and mixed with GST-BRAF RBD or GST-RASSF RA. Densitometric analysis of the pull-down assays revealed that hotspot-1 KRAS mutants (A66D, E37D, M67W and the double mutant E37D/M67W) had a reduced binding profile for RASSF5 as compared to wild-type RAS (**Figure 2A**). Hotspot-2 KRAS mutants, however, showed altered binding affinity for both BRAF and RASSF5 (**Figure 2A**). Notably, the two KRAS mutants I21F and H27R precipitated more RASSF5 compared to other RAS mutants. These findings suggest that these designed hotspot-2 KRAS mutants might have rewiring capacity.

To obtain the binding affinities of these KRAS mutants to RASSF5 RA and BRAF RBD, we performed isothermal titration colorimetric (ITC) experiments **(Figure S1B).** Both

KRAS I21F and H27R mutants showed approximately 2-fold reduced affinity towards the BRAF RBD compared to wild-type KRAS, while having a 2-fold increased affinity for the RASSF5 RA (**Figure S1B**). We combined these two mutations into a I21F/H27R RAS double mutant (hereafter designated as KRAS^RASSF). KRAS^RASSF showed a 4.5-fold reduced affinity towards BRAF and 2-fold augmented affinity for RASSF5, as determined by ITC. The differential in binding affinity of wild-type KRAS for RAF and RASSF5 is 30-fold, versus the rewired mutant KRAS^RASSF which has just a 3-fold difference (**Figure 2B**). To examine the thermodynamic binding parameters of these KRAS mutants bound to RAF or RASSF5, we compared the free energy (ΔG), enthalpy (ΔH), and entropy (ΔS) of binding but observed no significant difference between wild-type KRAS and KRAS^RASSF (**Figure S1C**). To confirm whether introduction of these mutations affects protein stability or folding, we used NMR spectroscopy. ^{1}H-^{15}N-HSQC spectra were acquired of mutant KRAS^RASSF and wild-type KRAS, and these spectra presented no major chemical shift differences, confirming the mutant protein is thermally stable and folded in solution (**Figure S1D**). Thus, the rewired mutant of KRAS has altered interactions with BRAF and RASSF5, yet appears folded to the same extent as wild-type KRAS and interacts with binding partners using a similar mechanism.

We further assessed the capacity for BRAF and RASSF5 to compete for wild-type or the rewired KRAS^RASSF mutant using NMR spectroscopy. In this assay, equal concentrations (200μM) of unlabelled RAS binding domains (RASSF5-RA and BRAF-RBD) are mixed with 100 μM of ^{15}N-labelled, wild-type KRAS or KRAS^RASSF. Peak intensities from ^{1}H-^{15}N-HSQC-derived chemical shifts quantitate the bound ratio of the KRAS variants, informing on the capacity for each RAS binding domain to compete for the GTPase [32]. Results demonstrated that RASSF5 can compete with BRAF for KRAS^RASSF, but is completely outcompeted by BRAF for wild-type KRAS. Weak chemical shift perturbations indicating RASSF5 binding are visible only with the rewired mutant. Chemical shift quantification revealed that BRAF binding to KRAS^RASSF is reduced 37%, while RASSF5 binding to KRAS^RASSF is increased approximately 50% (compared to wild-type KRAS; **Figure 2C).** This approach thus verifies an improved binding affinity of KRAS^RASSF towards RASSF5 when the GTPase is in the presence of both effectors in solution. These data confirm that small amino acid substitutions in RAS have the capacity to shift its binding preference for RAF vs RASSF5.

3.3.3 Mutant RASSF1 binds to KRAS

We next sought to assay whether our designed RASSF1 rewired mutant (RASSF1^{KRAS}) had the capacity to interact with KRAS. We purified the N149C/K208L RA domain mutant as a GST-fusion protein from *E. coli*, along with GST-tagged, wild-type RASSF1 RA domain. We first tested binding of these proteins to KRAS using overexpressed, mutationally activated KRAS in whole cell lysates. Either GFP-KRAS-G12V or GFP alone were mixed with GST (negative control), GST-RASSF1 RA or the N149C/K208L (RASSF1^{KRAS}) mutant. We included several related RASSF1 mutants: RASSF1^{N149C} (single αN helix mutation), RASSF1$^{N149D/L150D}$ (αN negative charged predicted to abrogate RAS binding), RASSF1$^{N149A/L150A}$ (αN small side chain substitutions predicted to abrogate RAS binding), and RASSF1$^{N149K/L150K}$ (αN positive charged predicted to abrogate RAS binding). The purified GST-RASSF1 RA domain variants were precipitated on glutathione beads and complexes with KRAS-G12V were detected by immunoblotting. This analysis revealed that RASSF1^{KRAS} is able to interact with KRAS-G12V. In addition, weak binding was observed between the single mutant RASSF1^{N149C} and KRAS-G12V. We did not observe interaction between wild-type RASSF1 RA and KRAS-G12V, nor any of the alternative αN RASSF1 RA mutants (**Figure 3A**). To further validate this interaction using full length proteins, we performed co-immunoprecipitation assays. Wild-type, FLAG-tagged RASSF1 or mutant RASSF1^{KRAS} were co-expressed with GFP-tagged, wild-type KRAS or KRAS-G12V and complexes were immunoprecipitated with α-FLAG. This analysis corroborated that full length RASSF1^{KRAS} binds to activated KRAS-G12V and not to wild-type KRAS **(Figure 3B).** Taken together, amino acid substitutions in the RASSF1 αN-helix and β2 strand that mimick RASSF5 residues can impart RASSF1 binding to KRAS.

To assess the interaction between KRAS and RASSF1^{KRAS} *in vitro*, we examined the capacity for RASSF1^{KRAS} to co-elute with activated KRAS (KRAS-GMPPNP) using size-exclusion chromatography. 100μM of purified, wild-type RASSF1 RA or RASSF1^{KRAS} RA were run an a Sephadex-G75 10/300 column alone or following mixture with 100μM of purified KRAS-GMPPNP. We clearly observed RASSF1^{KRAS} co-elution with activated KRAS (KRAS-GMPPNP), while wild-type RASSF1 RA domain did not. (**Figure 3C**). As a control, a mixture of KRAS-GDP and the mutant RASSF1$^{N149C/K208L}$ did not complex, suggesting that

the interaction is nucleotide-dependent (**Figure S2**). Thus, KRAS(GMPPNP) can complex with RASSF1^{KRAS} with relatively high affinity compared to wild-type RASSF1.

To ensure the mutant RASSF1 RA domain was properly folded in solution, we collected ^{1}H^{15}N-HSQC spectra of ^{15}N-labelled RASSF1 RA domains (wild-type, single and double mutants). The NMR data show well-overlapped patterns of chemical shift dispersion, indicating no significant differences between the wild-type and mutant RA domains and that all domains are well-folded in solution **(Figure 3D)**. These data further confirm that our *in silico*-designed mutants of RASSF1 have affinity to RAS GTPases, and along with the KRAS^{RASSF} effector mutant we have two functioning RAS-RASSF rewiring systems to study RASSF-Hippo signalling downstream of RAS.

3.3.4 RASSF proteins co-localizes with KRAS

To determine if the KRAS^{RASSF} and RASSF1^{KRAS} mutants were functional when expressed in cells, we used microscopy to study GTPase-effector engagement. It has been established that wild-type RASSF1A localizes on microtubules when overexpressed in a wide variety of cell types. RASSF5 demonstrates a prominent nuclear localization and is also diffusely spread throughout the cytoplasm **(Figure 4A).** In our previous study, we revealed that RASSF1 does not bind and co-localize with either wild-type KRAS or the activated KRAS-G12V mutant), while RASSF5 completely co-localized with a KRAS-G12V oncoprotein at the plasma membrane (Chapter 2). To determine whether rewired KRAS^{RASSF} would co-localize with RASSF5, wild-type RASSF1 or rewired RASSF1^{KRAS} effectors we performed co-localization experiments using FLAG-tagged RASSF proteins and Venus-tagged KRAS variants (wild-type KRAS, constitutively activated KRAS-G12V, or rewired KRAS^{RASSF}-G12V) in HeLa cells. Texas Red immunostaining was used to visualize FLAG-tagged proteins. Confocal micrographs demonstrate that wild-type RASSF1A shows a prominent microtubular localization when expressed alone or with any of the KRAS variants. RASSF5, however, completely co-localizes at the plasma membrane with KRAS-G12V or the rewired KRAS^{RASSF}-G12V, which appears to properly traffic to the plasma membrane and effectively recruit RASSF5. RASSF5 did not co-localize with wild-type KRAS. Surprisingly, the rewired

RASSF1^{KRAS} displayed a prominent nuclear localization, comparable to RASSF5, when expressed alone. Co-expression of RASSF1^{KRAS} with either KRAS-G12V or KRAS^{RASSF}-G12V resulted in complete relocation of RASSF1^{KRAS} to the plasma membrane **(Figure 4B).** Taken together, these data suggest that KRAS^{RASSF} and RASSF1^{KRAS} are functional in cells, capable of interacting with their designed targets.

3.3.5 Hippo signal activation by RASSF in the presence of KRAS

RASSF effectors are presumed to couple activated GTPases to Hippo signalling by direct interaction between the SARAH domains of RASSF proteins and those in MST kinases. We have observed significantly decreased levels of nuclear YAP specifically induced by expressing activated RAS with RASSF1 or RASSF5 (Chapter 2). To test whether our rewired KRAS^{RASSF} retains the capacity to activate Hippo signalling, we stained for endogenous YAP localization in U2OS cells. We observed that, comparable to KRAS-G12V, a KRAS^{RASSF}-G12V mutant activates Hippo signalling only when co-expressed with either wild-type RASSF1, rewired RASSF1^{KRAS} or RASSF5. This result agrees with our previous data which established that RASSF1 can restrict YAP nuclear localization downstream of KRAS even in the absence of direct binding. A quantitative analysis shows that un-transfected cells or cells expressing only RASSF proteins do not alter nuclear YAP levels (**Figure 5**). Thus, the rewired mutant KRAS^{RASSF} maintains a capacity to activate Hippo signalling in the presence of RASSF effectors.

3.3.6 Rewired KRAS has reduced affinity for BRAF in cells

Finally, we sought to test whether rewired KRAS^{RASSF} has an altered effector binding landscape in cells. Previously designed RAS effector mutants have demonstrated biased binding *in vivo*, including HRAS-T35S which preferentially binds RAF and HRAS-E37G which has reduced affinity for RAF and augmented binding to RALGEF effectors [26]. We tested rewired KRAS^{RASSF} for complex with both RASSF5 and BRAF using co-immunoprecipitation. FLAG-tagged RASSF effectors (wild-type RASSF1 or RASSF5 and rewired RASSF1^{KRAS}) and Venus-tagged KRAS variants (wild-type KRAS, constitutively active KRAS-G12V, or rewired KRAS^{RASSF}-G12V) were ectopically expressed in HEK 293T cells. Venus-tagged KRAS variants were immunoprecipitated and complexes were identified

by immunoblotting for FLAG-RASSF effectors or endogenous BRAF. Western blots revealed that rewired KRAS[RASSF]-G12V immunoprecipitates RASSF5 to a similar extent as KRAS-G12V **(Figure 6)**, while the capacity for KRAS[RASSF] to bind BRAF is severely abrogated. Moreover, both wild-type RASSF1 and rewired RASSF1[KRAS] associated with rewired KRAS[RASSF], and RASSF1[KRAS] also interacted strongly with KRAS-G12V. These data demonstrate that our designed mutants have the potential to rewire KRAS signalling from RAF-induced proliferation pathways to the pro-apoptotic RASSF-Hippo pathway.

3.4   Discussion

The RAS small GTPases govern a wide variety of cellular functions by associating with diverse downstream effectors. Functional relay by these effectors can range from induction of cell proliferation to stimulation of apoptosis. Though biophysical and biochemical studies over the past 30 years have shed light on how RAS binds to several effector binding domains, there is a significant gap in our understanding of how RAS GTPases select which effector to engage in a spatiotemporal fashion, and further what are the biological outcomes of RAS engagement with numerous less-studied effectors. To answer this, it is important to dissect specific roles for each effector downstream of activated RAS.

In a previous attempt to compartmentalize the function of specific RAS effector pathways, White *et al,* and others developed a mutational approach [26, 33, 34]. They found that substitution of specific amino acids in the effector loop region of HRAS (switch 1) can differentiate its capacity to interact with certain downstream effectors [26]. For instance, the RAS mutants T35S and D38E binds to RAF but not interact with PI3K or RALGDS. The E37G mutant binds to RALGDS but not interact with RAF or PI3K and the Y40C mutant is highly specific to PI3K. Extensive studies using these RAS mutants led to the critical observation that in human cells, RAF/MAPK signalling alone is not sufficient to induce cellular transformation. In addition, activation of other pathways, mainly PI3K signalling is essential for RAS transformation of mammalian cells and RAS-induced cytoskeleton reorganization. However, thus far there is no RAS mutant that specifically channelize the RAS downstream signals towards RASSF pro-apoptotic pathways. We used here computational approaches to design rewired KRAS$^{\text{RASSF}}$ proteins able to activate Hippo signalling *via* RASSF effector proteins. RASSF proteins have gained significant attention over the past decade due to their tumor-suppressive functions and increasing evidence for a role in activating apoptotic signals. Among the RASSF family members, RASSF5 and RASSF1 are the best-studied [30, 35-38] and we have previously demonstrated that their co-expression with activated KRAS can alter nuclear YAP localization (Chapter 2).

RASSF1 is highly similar to RASSF5, yet shows divergence at several key residues in the RA domain making it a poor RAS effector. Nevertheless, they possess differential interacting partners, differential localization and functions. For instance, RASSF5 is known to

bind RAS GTPase [24] and this interaction recruits RASSF5 to plasma membrane (Chapter 2), while we show that RASSF1 is highly localized at microtubules and does not bind to KRAS and interact with RGK family of GTPase (Chapter 2). Functionally, though RASSF1 and RASSF5 contain SARAH domain and binds MST1/2 Hippo kinases, their mechanism of Hippo kinase activation is not fully understood. The RASSF1^{KRAS} mutant, designed based on homology modelling, shows binding to KRAS and completely phenocopies RASSF5 in U2OS cells. Hence, it will be interesting to compare and quantitate the Hippo signal activation using both the approaches (RASSF1^{KRAS} and RAS^{RASSF}).

As RAS is a major driver of cell proliferation and tumorigeneses, further definition of its role in apoptotic induction is greatly required. Rewiring activated RAS signals towards RASSF cell death effectors may be a novel clinical strategy in the absence of direct RAS inhibitors. KRAS^{RASSF} appears rewired in the presence of both BRAF and RASSF5 effectors *in vitro* and in cells, and retains the capacity to induce Hippo signalling. The significance of this in terms of MAPK activation and cell proliferation needs to be studied. In addition, it will be essential to consider the capacity for KRAS^{RASSF} to transform cells in mouse tumor models or 3D cell cultures. Significantly, several recent reports suggest YAP signalling is vital for RAS induced proliferation of cancer cells and tumorigenesis [39-42]. YAP ostensibly provides resistance to MEK1/2 inhibition in neuroblastomas with hyperactivated RAS signalling [43] and it is reported that the YAP/Tead2 complex drives KRAS-G12D-independent tumor maintenance [39]. Further, it is found that tumorigenicity of pancreatic ductal adenocarcinoma is suppressed upon depletion of YAP [44]. Regardless, there are no direct studies that couple RAS signalling to Hippo pathway regulation through RASSFs.

Detailed analysis of downstream signalling using rewired KRAS or RASSF1 mutants should provide insights on Hippo-RASSF-RAS biology. There are long-standing efforts to inhibit KRAS signalling by targeting downstream effectors, particularly the RAF/MAPK and PI3K pathways, and further network details on KRAS signalling to RASSF pathways could aid the design of RAS inhibitors.

3.5 Methods

3.5.1 Constructs and antibodies

Table 1:   **Expression constructs generated and used in this study:**

Construct	Backbone	Tag	Region	Source	Gene ID
HIS-KRAS-WT	pET-15b	HIS	1-171	Human	3845
HIS-KRAS^{I21F}	pET-15b	HIS	1-171	Human	3845
HIS-KRAS^{Q25Y}	pET-15b	HIS	1-171	Human	3845
HIS-KRAS^{H27R}	pET-15b	HIS	1-171	Human	3845
HIS-KRAS$^{I21F/H27R}$	pET-15b	HIS	1-171	Human	3845
HIS-KRAS$^{D30E/E31K}$	pET-15b	HIS	1-171	Human	3845
HIS-KRAS^{T35S}	pET-15b	HIS	1-171	Human	3845
HIS-KRAS^{E37D}	pET-15b	HIS	1-171	Human	3845
HIS-KRAS^{E37G}	pET-15b	HIS	1-171	Human	3845
HIS-KRAS^{A66D}	pET-15b	HIS	1-171	Human	3845
HIS-KRAS^{M67W}	pET-15b	HIS	1-171	Human	3845
HIS-KRAS$^{E37D/M67W}$	pET-15b	HIS	1-171	Human	3845
GST alone	pGEX4-T2	GST	150-233	Human	
GST-RASSF5 RA	pGEX4-T2	GST	199-367	Human	83595
GST-BRAF RBD	pGEX4-T2	GST	150-233	Human	673
GST-RASSF1 RA	pGEX4-T2	GST	123-296	Human	11186
GST-RASSF1 RA^{N149C}	pGEX4-T2	GST	131-288	Human	11186
GST-RASSF1 RA$^{N149C/K208L}$	pGEX4-T2	GST	131-288	Human	11186
GST-RASSF1 RA$^{N149D/L150D}$	pGEX4-T2	GST	131-288	Human	11186
GST-RASSF1 RA$^{N149K/L150K}$	pGEX4-T2	GST	131-288	Human	11186
GST-RASSF1 RA$^{N149A/L150A}$	pGEX4-T2	GST	131-288	Human	11186
FLAG-RASSF5	pCDNA5-FLAG-5'	FLAG	full-length	Human	83595
FLAG-RASSF1	pCDNA5-FLAG-5'	FLAG	full-length	Human	11186
FLAG-RASSF1$^{N149C/K208L}$	pCDNA5-FLAG-5'	FLAG	full-length	Human	11186
GFP alone	pVenus-C1	GFP			
GFP-KRAS	pDEST-pcDNA3-Venus-	GFP	full-length	Human	3845
GFP-KRAS-G12V	pDEST-pcDNA3-Venus-	GFP	full-length	Human	3845
GFP-KRAS$^{G12V/I21F/H27R}$	pDEST-pcDNA3-Venus-5'	GFP	full-length	Human	3845

Table 2: Antibodies used in this study:

Antibody	Source
anti-FLAG-mouse	Sigma - F3165
anti-FLAG-rabbit	Sigma – F7425
anti-GFP	Abcam - ab290
Goat anti-Mouse IgG-Tx-Red	Sigma - SAB3701076
anti-BRAF	Santa Cruz RAF-B (F-7) sc-5284
anti-YAP1 (63.7)	Santa Cruz biotechnology - 10199
Goat anti-Rabbit IgG-Alexa Fluor-647	Invitrogen - A21244

3.5.2 Protein expression and purification

6 x Histidine (HIS)- and Glutathione *S*-transferase (GST)- tagged proteins were expressed in *E. coli* (Bl21-DE3-codon+) cells grown in LB media at 37ºC. Cells were induced at the OD - 0.8 with 250 µM IPTG (isopropyl-β-D-thiogalactopyranoside) and moved to 16ºC for overnight growth. Bacterial culture was harvested by centrifugation and pellet was dissolved in ice-cold lysis buffer (20 mM Tris-HCl (pH 7.5), 150 mM NaCl, 10% glycerol, 0.4% NP-40, protease inhibitors (Roche), and either 1 mM dithiothreitol or 10 mM β-mercaptoethanol) which were later lysed by sonication. The Lysate was further centrifuged, and the supernatant was incubated with pre- glutathione (Amersham) or equilibrated (Qiagen) resins at 4°C for 1-2 hours. Unbound protein was washed using 20 mM imidazole (for HIS-tagged protein) or 500mM NaCl (for GST-Tagged protein). Protein bounds on beads were eluted by direct thrombin cleavage (GST) or with elution buffer containing 250 mM imidazole (Bioshop) followed by thrombin cleavage (HIS) or 30 mM reduced glutathione. Finally, the eluted proteins were purified by gel filtration chromatography using either an S75 or S200 column (GE).

3.5.3 Nucleotide Exchange and Isothermal Titration Calorimetry

For nucleotide exchanges of RAS GTPase, purified protein was incubated with 10-fold molar excess of (nucleotide: protein) GMPPNP (sigma) along with 10mM EDTA and CIP (calf intestinal phosphatase). The mixture was incubated at 37°C for 10 min. After cooling down the mixture at 4°C, 20 mM MgCl2 was added and the sample was incubated on ice for 10 mins.

For further usage, the exchanged protein was dialyzed accordingly in the respective buffers. ITC experiments were performed using a MicroCal ITC200 (Malvern). Protein stocks were diluted, filtered and degassed into 20 mM Tris-HCl (pH7.5), 150 mM NaCl and 1 mM DTT. Calorimetry titration experiments were performed at 25°C. Heats of dilution were determined from control experiments in which proteins were titrated into buffer alone. Origin 7 (MicroCal) software was used for curve fitting.

3.5.4 NMR

Wild-type and mutants KRAS proteins were grown in ^{15}N labelled M9 media. Effector proteins (BRAF and RASSF variants) were grown on unlabelled LB media. Following protein purification (as explained above) the effectors and RAS protein were mixed in the mentioned ratio and NMR HSQC experiments were performed. For competition assay, protocol was performed as explained in [32]. Spectra were collected and quantified for the interaction.

3.5.5 Cell Culture, Co-immunoprecipitation and Western Blotting

HEK 293-T (ATCC CRL-3216) were cultured in DMEM (Dulbecco's Modified Eagle Medium) medium supplemented with 10% fetal bovine serum. For co-immunoprecipitation experiments, cells were seeded on 6-well plate at the confluence of 0.5million/ml. Overexpression plasmids were transiently transfected at the concentration of 1ug using polyethylenimine (PEI) reagent. For transfection in U2OS and HeLa cells, jetPRIME (Polyplus) transfection reagent was used. 48 hours after the transfection, cells were harvested and lysed in the ice-cold lysis buffer (20 mM Tris-HCl (pH 7.5), 150 mM NaCl, 10% glycerol, 1% Triton X-100, 1 mM DTT and protease inhibitor P8340) for 10 mins. Lysate was clarified and incubated with the pre-washed Protein-G Sepharose beads and immunoprecipitating antibody for 1-2 hours. The beads were thoroughly washed for 3 times using the lysis buffer. Finally, bound proteins from the beads were denatured using the 6X SDS loading buffer, boiled and resolved using SDS PAGE. SDS Gels were transferred into the nitrocellulose membrane for Western blot analysis. Membranes were blocked using 3% skim milk followed by

incubation with primary antibody for overnight. Primary antibodies were detected using HRP conjugated secondary antibody. Finally, membranes were revealed using ECL reagent (Bio-Rad) and detection done by a Bio-Rad ChemiDoc imaging system equipped with ImageLab software.

3.5.6 GST-RA Pull Downs

HEK 293T lysates expressing the protein of interest were incubated with GST alone or GST-RA domain fusion protein for 1 hour. Glutathione beads were used to capture GST fusion proteins or GST alone. Beads were washed 5 times with lysis buffer (20 mM Tris-HCl (pH 7.5), 150 mM NaCl, 5 mM $MgCl_2$, 10% glycerol, 1% Triton X-100, 1 mM DTT and protease inhibitor P8340), eluted in SDS loading buffer and separated by SDS-PAGE. Gels were transferred to nitrocellulose membrane and Western blot analysis was performed as above.

3.5.7 Microscopy

U2OS (ATCC HTB-96) cells and HeLa (ATCC CCL-2) and were split in 6-well plates containing coverslips at the confluence of $50X10^3$ cells per well. 48 hours after transfection, cells were washed with phosphate buffered saline (PBS) and fixed with 4% paraformaldehyde (PFA). Fixed cells were permeabilized with 0.05% Tween or 0.1% Triton X100 (for U2OS cells) and blocked with either 10% FBS or 2% bovine serum albumin (BSA). Cells were incubated for 1 to 2 hours with primary antibody at 37°C or at RT (for U2OS cells) followed by secondary antibody and Hoechst staining. Finally, cells were treated with 70% then 95% ethanol and air dried before being mounted on glass slides. Slides were imaged using an LSM880 confocal microscope. Three lasers were used for detection (UV, Red and Far-Red). Images were processed using ZEN software.

3.5.8 Structural Modelling

3D models for all RASSF was constructed using the automated protein structure homology model building program 'MODBASE' with energy minimization parameters available at the MODWEB server (https://modbase.compbio.ucsf.edu/modweb). Amino acid sequences based on our alignments were input in FASTA format. The server calculated structural models based on the best available template structures in the Protein Data Bank using MODPIPE, an automated modeling pipeline that relies on MODELLER for fold assignment, sequence-structure alignment, model building and model assessment. Models were evaluated for quality using Ramachandran plots and those with the highest DOPE score and fold reliability were selected for structural analysis.

3.6 Acknowledgements

3.7 Author Contributions

D.T. and M.J.S. designed experiments. D.T., C.M., R.K. and M.J.S. performed experiments and analyzed data. A.S. and J.S. performed structural modelling. J.S. and M.J.S. supervised studies. D.T. and M.J.S. wrote the manuscript with input from J.S.

3.8 Declaration of Interests

The authors declare no competing interests.

3.9 References

1. Bourne, H.R., D.A. Sanders, and F. McCormick, *The GTPase superfamily: conserved structure and molecular mechanism.* Nature, 1991. **349**(6305): p. 117-27.

2. Bourne, H.R., D.A. Sanders, and F. McCormick, *The GTPase superfamily: a conserved switch for diverse cell functions.* Nature, 1990. **348**(6297): p. 125-32.

3. VetWittinghofer, A., I. R. and . *The guanine nucleotide-binding switch in three dimensions.* Science, 2001. **294**(5545): p. 1299-304.

4. Castellano, E. and E. Santos, *Functional specificity of ras isoforms: so similar but so different.* Genes Cancer, 2011. **2**(3): p. 216-31.

5. Omerovic, J., A.J. Laude, and I.A. Prior, *Ras proteins: paradigms for compartmentalised and isoform-specific signalling.* Cell Mol Life Sci, 2007. **64**(19-20): p. 2575-89.

6. Potenza, N., et al., *Replacement of K-Ras with H-Ras supports normal embryonic development despite inducing cardiovascular pathology in adult mice.* EMBO Rep, 2005. **6**(5): p. 432-7.

7. Schultz, J., et al., *SMART, a simple modular architecture research tool: identification of signaling domains.* Proc Natl Acad Sci U S A, 1998. **95**(11): p. 5857-64.

8. Smith, M.J., et al., *Evolution of AF6-RAS association and its implications in mixed-lineage leukemia.* Nat Commun, 2017. **8**(1): p. 1099.

9. Castellano, E. and J. Downward, *Role of RAS in the regulation of PI 3-kinase.* Curr Top Microbiol Immunol, 2010. **346**: p. 143-69.

10. Nakhaei-Rad, S., et al., *The Role of Embryonic Stem Cell-expressed RAS (ERAS) in the Maintenance of Quiescent Hepatic Stellate Cells.* J Biol Chem, 2016. **291**(16): p. 8399-413.

11. Chan, J.J. and M. Katan, *PLCvarepsilon and the RASSF family in tumour suppression and other functions.* Adv Biol Regul, 2013. **53**(3): p. 258-79.

12. Bunney, T.D. and M. Katan, *PLC regulation: emerging pictures for molecular mechanisms.* Trends Biochem Sci, 2011. **36**(2): p. 88-96.

13. Ferro, E. and L. Trabalzini, *RalGDS family members couple Ras to Ral signalling and that's not all.* Cell Signal, 2010. **22**(12): p. 1804-10.

14. Rajalingam, K., et al., *Ras oncogenes and their downstream targets.* Biochim Biophys Acta, 2007. **1773**(8): p. 1177-95.

15. Desideri, E., A.L. Cavallo, and M. Baccarini, *Alike but Different: RAF Paralogs and Their Signaling Outputs.* Cell, 2015. **161**(5): p. 967-970.

16. Castellano, E. and J. Downward, *RAS Interaction with PI3K: More Than Just Another Effector Pathway.* Genes Cancer, 2011. **2**(3): p. 261-74.

17. Gentry, L.R., et al., *Ral small GTPase signaling and oncogenesis: More than just 15minutes of fame.* Biochim Biophys Acta, 2014. **1843**(12): p. 2976-2988.

18. Bunney, T.D. and M. Katan, *Phospholipase C epsilon: linking second messengers and small GTPases.* Trends Cell Biol, 2006. **16**(12): p. 640-8.

19. Feig, L.A. and R.J. Buchsbaum, *Cell signaling: life or death decisions of ras proteins.* Curr Biol, 2002. **12**(7): p. R259-61.

20. Yamamoto, T., et al., *The Ras target AF-6 interacts with ZO-1 and serves as a peripheral component of tight junctions in epithelial cells.* J Cell Biol, 1997. **139**(3): p. 785-95.

21. Vetter, I.R. and A. Wittinghofer, *The guanine nucleotide-binding switch in three dimensions.* Science, 2001. **294**(5545): p. 1299-304.

22. Bunney, T.D., et al., *Structural and mechanistic insights into ras association domains of phospholipase C epsilon.* Mol Cell, 2006. **21**(4): p. 495-507.

23. Pacold, M.E., et al., *Crystal structure and functional analysis of Ras binding to its effector phosphoinositide 3-kinase gamma.* Cell, 2000. **103**(6): p. 931-43.

24. Stieglitz, B., et al., *Novel type of Ras effector interaction established between tumour suppressor NORE1A and Ras switch II.* EMBO J, 2008. **27**(14): p. 1995-2005.

25. Wohlgemuth, S., et al., *Recognizing and defining true Ras binding domains I: biochemical analysis.* J Mol Biol, 2005. **348**(3): p. 741-58.

26. White, M.A., et al., *Multiple Ras functions can contribute to mammalian cell transformation.* Cell, 1995. **80**(4): p. 533-41.

27. Khosravi-Far, R., et al., *Oncogenic Ras activation of Raf/mitogen-activated protein kinase-independent pathways is sufficient to cause tumorigenic transformation.* Mol Cell Biol, 1996. **16**(7): p. 3923-33.

28. Khwaja, A., et al., *Matrix adhesion and Ras transformation both activate a phosphoinositide 3-OH kinase and protein kinase B/Akt cellular survival pathway.* EMBO J, 1997. **16**(10): p. 2783-93.

29. Scheel, H. and K. Hofmann, *A novel interaction motif, SARAH, connects three classes of tumor suppressor.* Curr Biol, 2003. **13**(23): p. R899-900.

30. Praskova, M., et al., *Regulation of the MST1 kinase by autophosphorylation, by the growth inhibitory proteins, RASSF1 and NORE1, and by Ras.* Biochem J, 2004. **381**(Pt 2): p. 453-62.

31. Ortiz-Vega, S., et al., *The putative tumor suppressor RASSF1A homodimerizes and heterodimerizes with the Ras-GTP binding protein Nore1.* Oncogene, 2002. **21**(9): p. 1381-90.

32. Smith, M.J. and M. Ikura, *Integrated RAS signaling defined by parallel NMR detection of effectors and regulators.* Nat Chem Biol, 2014. **10**(3): p. 223-30.

33. Rodriguez-Viciana, P., et al., *Role of phosphoinositide 3-OH kinase in cell transformation and control of the actin cytoskeleton by Ras.* Cell, 1997. **89**(3): p. 457-67.

34. Rodriguez-Viciana, P., C. Sabatier, and F. McCormick, *Signaling specificity by Ras family GTPases is determined by the full spectrum of effectors they regulate.* Mol Cell Biol, 2004. **24**(11): p. 4943-54.

35. Guo, C., et al., *RASSF1A is part of a complex similar to the Drosophila Hippo/Salvador/Lats tumor-suppressor network.* Curr Biol, 2007. **17**(8): p. 700-5.

36. Hwang, E., et al., *Structural insight into dimeric interaction of the SARAH domains from Mst1 and RASSF family proteins in the apoptosis pathway.* Proc Natl Acad Sci U S A, 2007. **104**(22): p. 9236-41.

37. Oh, H.J., et al., *Role of the tumor suppressor RASSF1A in Mst1-mediated apoptosis.* Cancer Res, 2006. **66**(5): p. 2562-9.

38. Park, J., et al., *Tumor suppressor ras association domain family 5 (RASSF5/NORE1) mediates death receptor ligand-induced apoptosis.* J Biol Chem, 2010. **285**(45): p. 35029-38.

39. Kapoor, A., et al., *Yap1 Activation Enables Bypass of Oncogenic Kras Addiction in Pancreatic Cancer.* Cell, 2019. **179**(5): p. 1239.

40. Zhang, W., et al., *Downstream of mutant KRAS, the transcription regulator YAP is essential for neoplastic progression to pancreatic ductal adenocarcinoma.* Sci Signal, 2014. **7**(324): p. ra42.

41. Singh, K., et al., *Mst1/2 kinases restrain transformation in a novel transgenic model of Ras driven non-small cell lung cancer.* Oncogene, 2020. **39**(5): p. 1152-1164.

42. Mohamed, A.D., et al., *Analysis of the relationship between the KRAS G12V oncogene and the Hippo effector YAP1 in embryonal rhabdomyosarcoma.* Sci Rep, 2018. **8**(1): p. 15674.

43. Coggins, G.E., et al., *YAP1 Mediates Resistance to MEK1/2 Inhibition in Neuroblastomas with Hyperactivated RAS Signaling.* Cancer Res, 2019. **79**(24): p. 6204-6214.

44. Tu, B., et al., *YAP1 oncogene is a context-specific driver for pancreatic ductal adenocarcinoma.* JCI Insight, 2019. **4**(21).

3.10 Figures

Figure 1: **Structural modelling and mutational analysis of RAS and RASSF1 proteins**
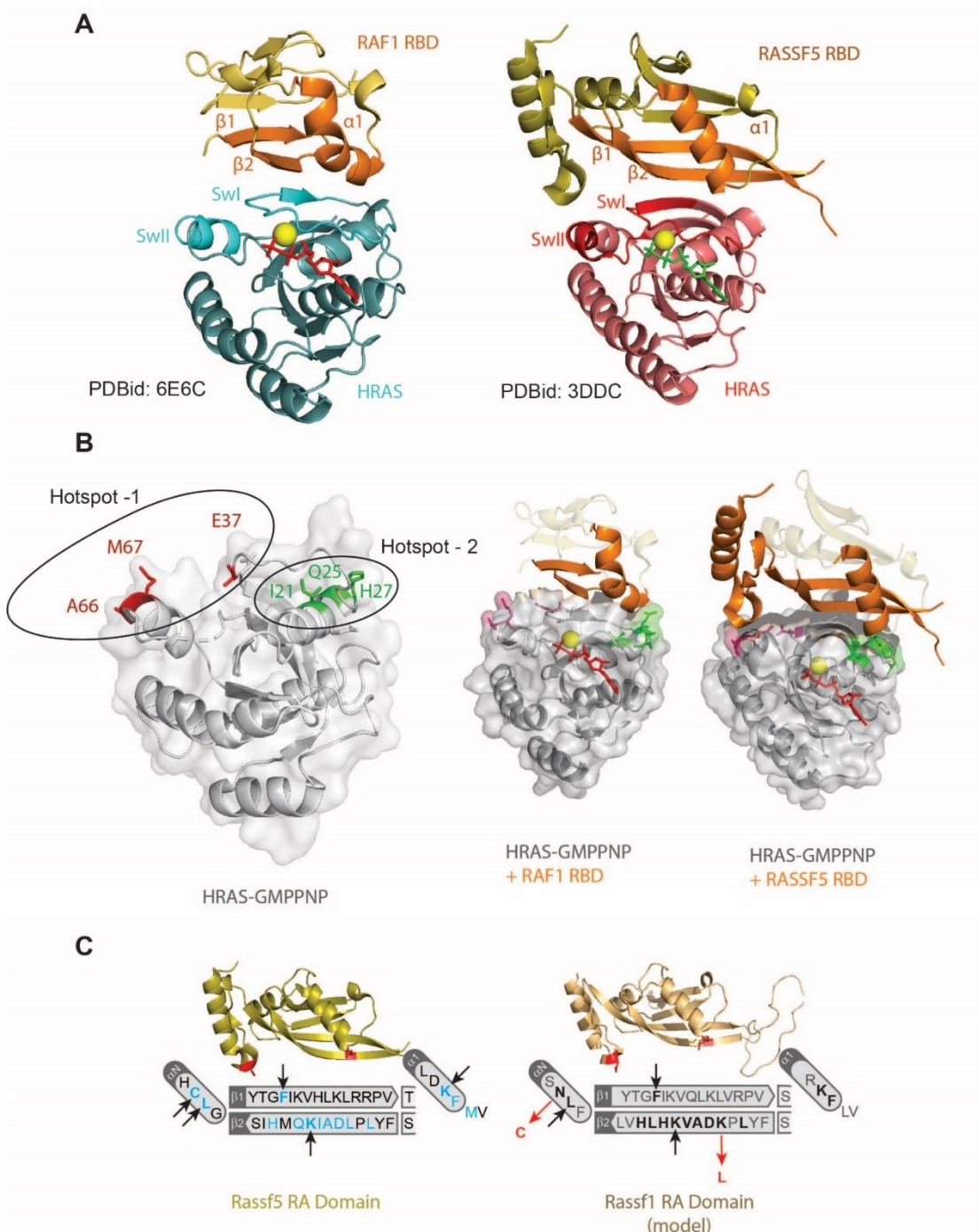
Figure 1: Structural modelling and mutational analysis of RAS and RASSF1 proteins

A) (Left) Cartoon representation of the crystal structure complex of RAF1 RBD with HRAS (PDBid: 6E6C). (Right) Cartoon representation of the crystal structure complex of RASSF5 RBD with HRAS (PDBid: 3DDC). Representational image showing the interaction region between the switch (switch I and II) domains of RAS and α helical and β strand region of the effectors (RAF1 and RASSF5). **B)** Structure of RAS showing the mutational hotspots (left most image). The mutations are in the two clusters of RAS protein, indicated as hotspot-1 and hotspot-2. Hotspot 1 is present in switch II region, which can be seen interacting with RASSF5 (right most image). Hotspot-2 is present in switch I region, which can be seen interacting with both RAF1 and RASSF5 (middle image and rightmost image). **C)** (Left) Cartoon representation of the crystal structure complex of RASSF5 RBD (PDBid: 3DDC). Amino acids of RASSF5 RBD from α1, αN helical and β1, β2 strands are highlighted. Amino acids shown in blue color are within 4Å distance from HRAS. Black arrow mark indicates residues that interact with HRAS. (Right) Homology model of RASSF1 RBD based on the crystal structure of RASSF5. Amino acids of RASSF1 RBD from α1, αN helical and β1, β2 sheet domains are highlighted. Residues represented in bold black color are presumed to be within 4Å distance from RAS. Residues marked with black arrow indicates that they might interact with RAS. Amino acid marked with red arrow represents the residues where the mutations on RASSF1 is made to bind with KRAS, RASSF1-N149C, K208L.

Figure 2: Mutant KRAS binds to RASSF5 with improved affinity
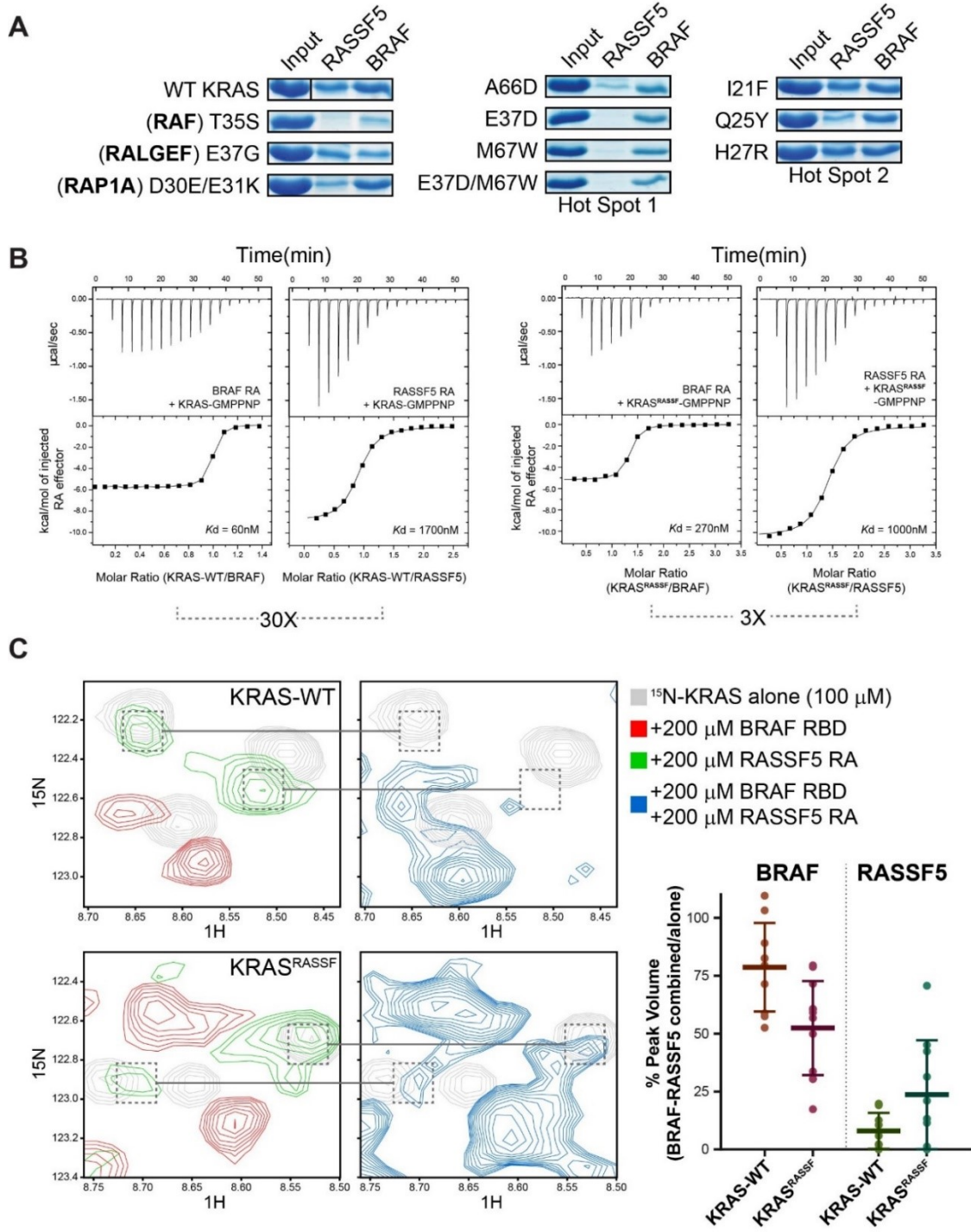
Figure 2:   Mutant KRAS binds to RASSF5 with improved affinity

A) GST Pull down assays. Coomassie gel representation of the intraction between KRAS mutants and its effectors (BRAF and RASSF5). Leftmost image shows the previously described RAS mutations (T35S, E37G and D30E/E31K) that have specific affinities for its effectors. Middle image shows the hotspot-1 KRAS mutations and its interaction with RASSF5 and BRAF. Rightmost image shows the hotspot-2 KRAS mutations and its interaction with RASSF5 and BRAF. **B)** Measurement of binding kinetics for KRAS and its effectors (BRAF and RASSF5) using isothermal titrations calorimetry. (Left) ITC determined the affinity of interaction between KRAS and BRAF RBD is 60 nM measured with 150 mM NaCl concentration Whereas, the affinity of interaction between KRAS and RASSF5 RA is 1700 nM. The difference between the affinities for KRAS-WT and its effectors (BRAF and RASSF5) is approximately 30-fold. (Right) ITC determined the affinity of interaction between KRAS^{RASSF} and BRAF RBD is 270 nM measured with 150 mM NaCl concentration. Whereas, the affinity of interaction between KRAS^{RASSF} and RASSF5 RA is 1000 nM. The difference between the affinities for KRAS^{RASSF} and its effectors (BRAF and RASSF5) is approximately 3-fold. **C)** NMR HSQC competition assay illustrates the switching of KRAS interaction from BRAF towards RASSF5. Quantitative analysis shows that, in comparison with wild-type KRAS, KRAS^{RASSF} mutant displays reduced affinity for BRAF and increased affinity for RASSF5.

Figure 3:   Mutant RASSF1 binds to KRAS
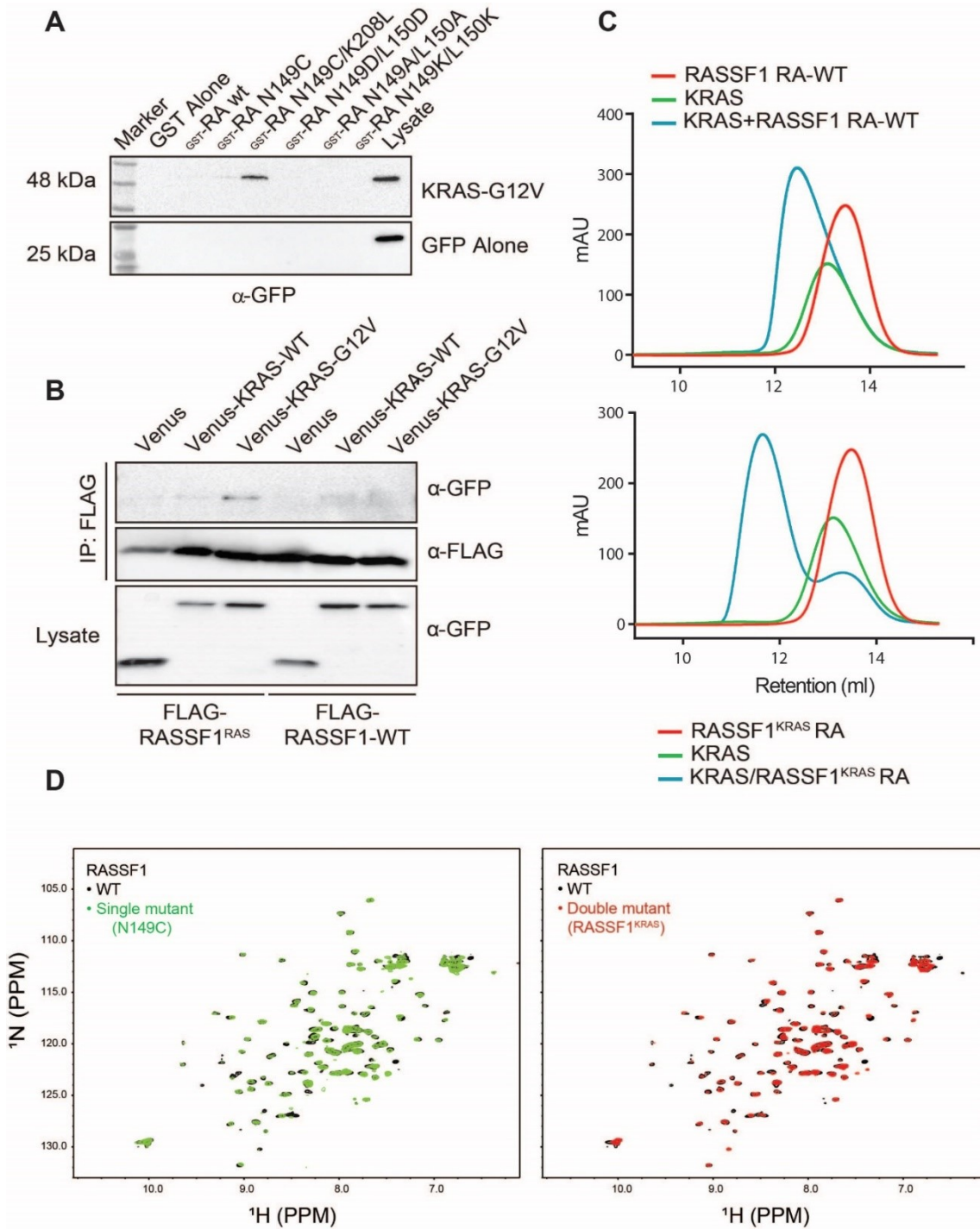
Figure 3:   Mutant RASSF1 binds to KRAS

A) Pull down interaction between the mutant RASSF1 RA variants and KRAS-G12V. Glutathione beads with immobilized RASSF1 RA variants were incubated with cell lysate expressing activated KRAS (KRAS-G12V). Following precipitation on glutathione beads, KRAS-G12V interacting with RASSF1 RA variants were identified by anti-GFP immunoblot. The same mutants were incubated with GFP alone as a control. **B)** Co-immunoprecipitation interaction between the RASSF1 variants and KRAS-G12V. Cell lysate expressing GFP-tagged wild-type or activated mutant of KRAS and FLAG tagged wild-type RASSF1 or RASSF1^{KRAS} were passed through beads contaiing immobilized FLAG antibody. Following precipitation on FLAG-immobilized beads, KRAS interacting with RASSF1 variants were identified by anti-GFP/anti-FLAG immunoblot. **C)** Gelfiltration profile show co-elution of RASSF1^{KRAS} with KRAS-GMPPNP. **(**Top) chromatography profile of KRAS alone (green), RASSF1-WT alone (red) and KRAS-GMPPNP + RASSF1-WT (blue). (Bottom) chromatography profile of KRAS alone (green), RASSF1^{KRAS} alone (red) and KRAS-GMPPNP + RASSF1^{KRAS} (blue). **D)** NMR-HSQC spectra shows that single and double RASSF1 RA mutants have similar spectra as compared to wild-type.

Figure 4:   RASSF proteins co-localizes with KRAS
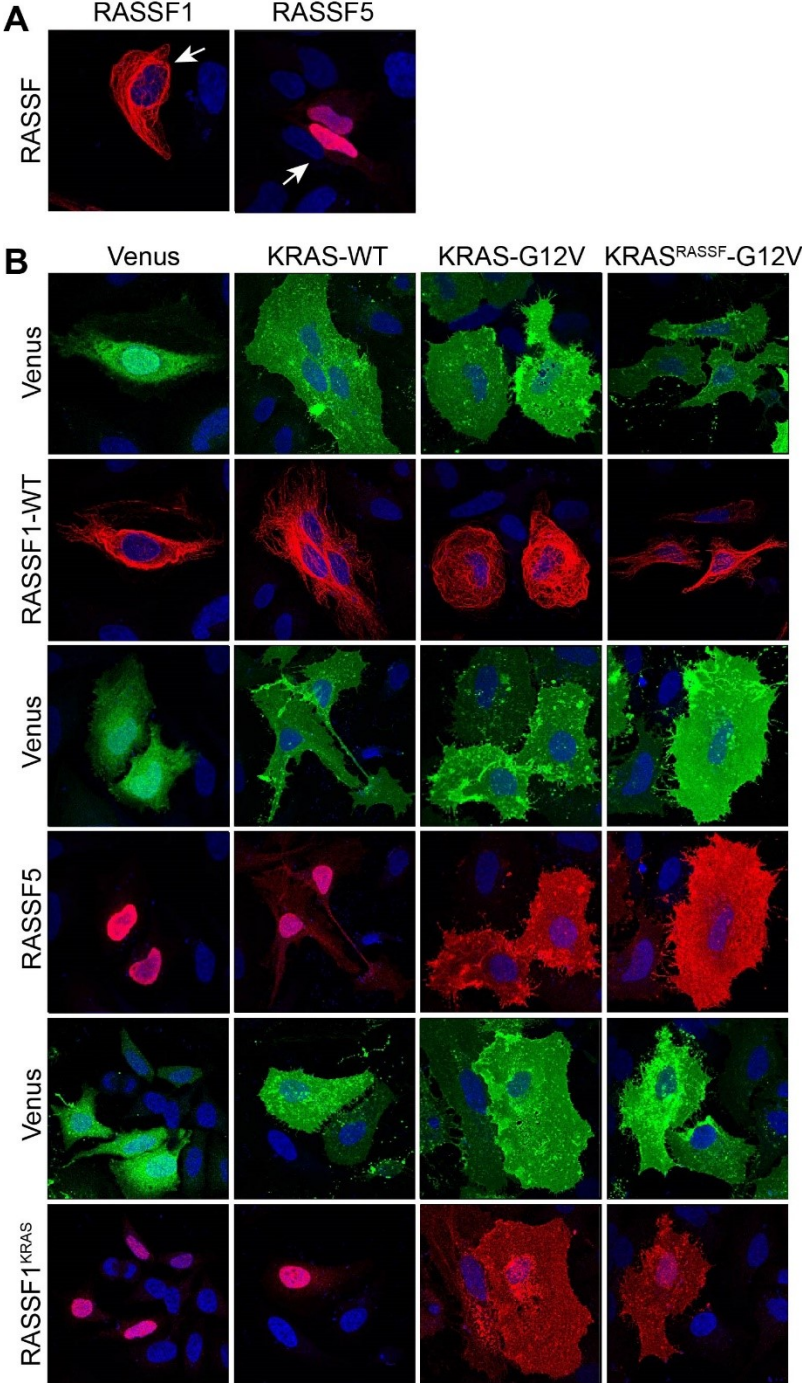
HeLa: Hoechst, Venus-GTPase, FLAG-RASSF

Figure 4:   RASSF proteins co-localizes with KRAS

A) Localization of RASSF1 and RASSF5. Confocal micrographs of RASSF1A protein expressed in HeLa cells show microtubular localization. Similarly, confocal micrographs of RASSF5 protein expressed in HeLa cells show nuclear localization. FLAG-tagged RASSF constructs was transfected in HeLa cells and immunostained using primary (anti-FLAG antibody) and secondary (Texas Red). **B)** Co-localization of KRAS and RASSF proteins. Co-expression of FLAG-tagged RASSF and Venus-tagged KRAS variants show that RASSF5 does not co-localize with wild-type KRAS, but colocalize with KRAS-G12V and KRAS^{RASSF} mutants. Whereas, RASSF1 does not co-localize with KRAS-WT or mutants. Surpraisingly, RASSF1^{KRAS} shows phenotype similart to RASSF5. RASSF1^{KRAS} lacks microtubular localization and instead shows nuclear localization when expressed alone. RASSF1^{KRAS} does not co-localize with wild-type KRAS, but co-localize with KRAS-G12V and KRAS^{RASSF}.

Figure 5: Hippo signal activation RASSF in presence of KRAS
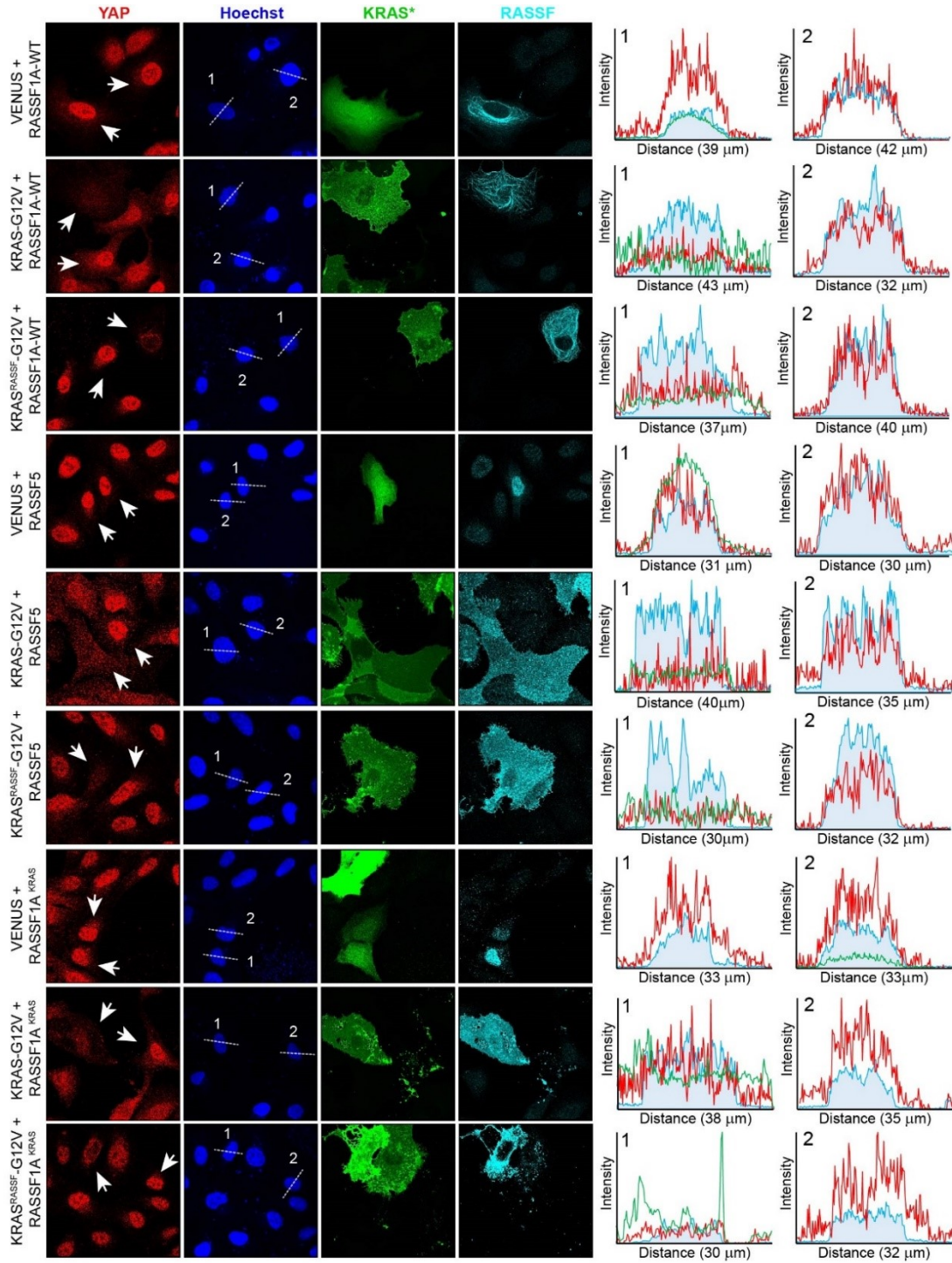
Figure 5:   Hippo signal activation RASSF in presence of KRAS

Confocal images show localization of endogenous YAP1 in U2OS cells co-expressing Venus, Venus-tagged KRAS-G12V and Venus-tagged KRAS^{RASSF} with FLAG-tagged RASSF1, FLAG-tagged RASSF5 and FLAG-tagged RASSF1^{KRAS}. Expression of RASSF1, RASSF5 and RASSF1^{KRAS} alone does not impact YAP localization. However, YAP1 remains outside the nucleus or disappears in U2OS cells co-expressing the either KRAS-G12V and RASSF1 or KRAS-G12V and RASSF5 or KRAS-G12V and RASSF1^{KRAS} or KRAS^{RASSF} and RASSF1, or KRAS^{RASSF} and RASSF5 or KRAS^{RASSF} and RASSF1^{KRAS}. Quantification (right) was performed using z-stack fluorescence profiles from a plane through the nucleus (dotted line in Hoechst panel). Nuclei are blue, GTPase green and YAP1 red on the intensity graphs. YAP1 is excluded from the nucleus in cells expressing KRAS (marked with a 1) compared to untransfected cells (marked with a 2).

Figure 6: Rewired KRAS has reduced affinity for BRAF in cells
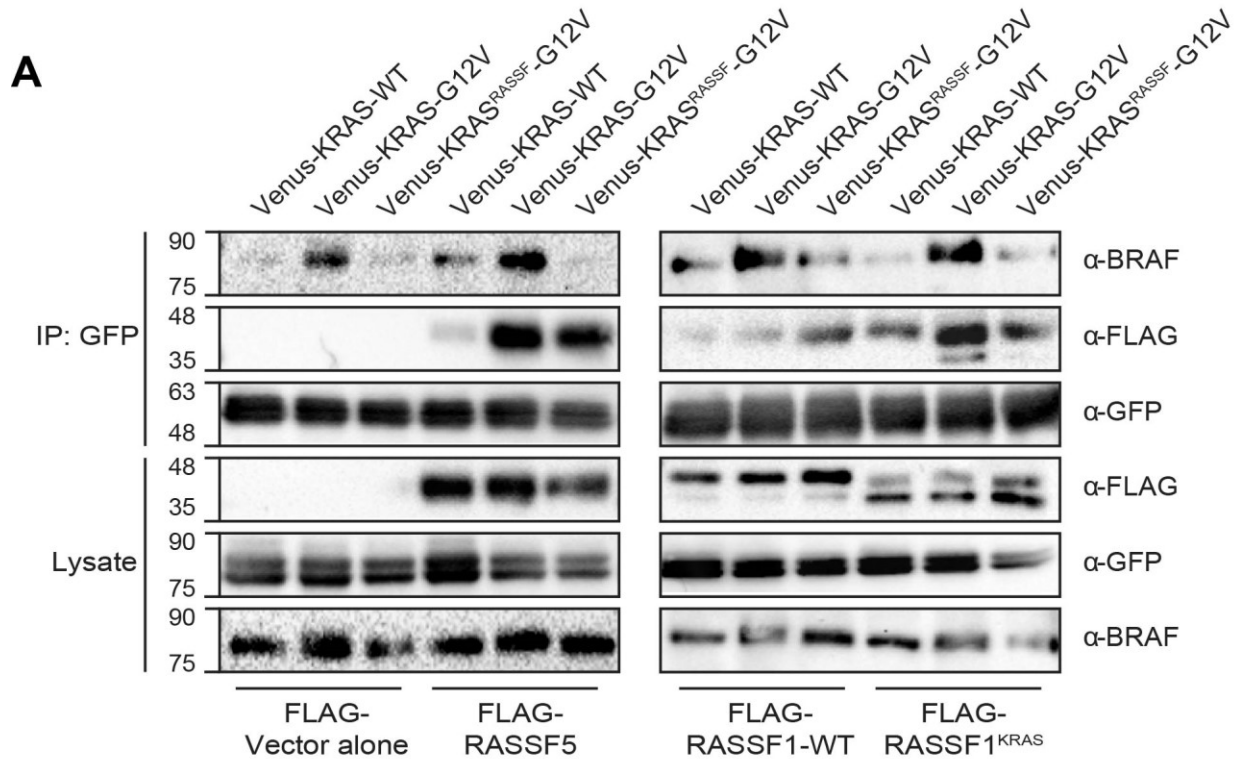
Figure 6:   Rewired KRAS has reduced affinity for BRAF in cells

Co-immunoprecipitation experiments reveal the capacity of KRAS^{RASSF} to bind BRAF is severely impaired. HEK293K cells were co-transfected with various constructs of KRAS and RASSF expressing proteins as indicated above. Cell lysates were immunoprecipitated using anti-GFP antibody. Immunoprecipitants were probed against anti-FLAG, anti-BRAF and anti-GFP antibodies to detect KRAS, RASSF and BRAF protein's occupancy.

3.11 Supplementary Information

Figure S1: Biophysical characteristics of KRAS mutants.

A

B

	BRAF		RASSF5	
	Kd	N	Kd	N
	nM	sites	nM	sites
KRAS (WT)	60	0.705	1704.5	0.875
KRAS (I21F)	161	0.73	1281	0.945
KRAS (H27R)	155	1.28	910.5	1.095
KRAS (I21F, H27R)	270	1.29	1000	1.34
KRAS (M67W)	21	1.4	NA	NA

C

D
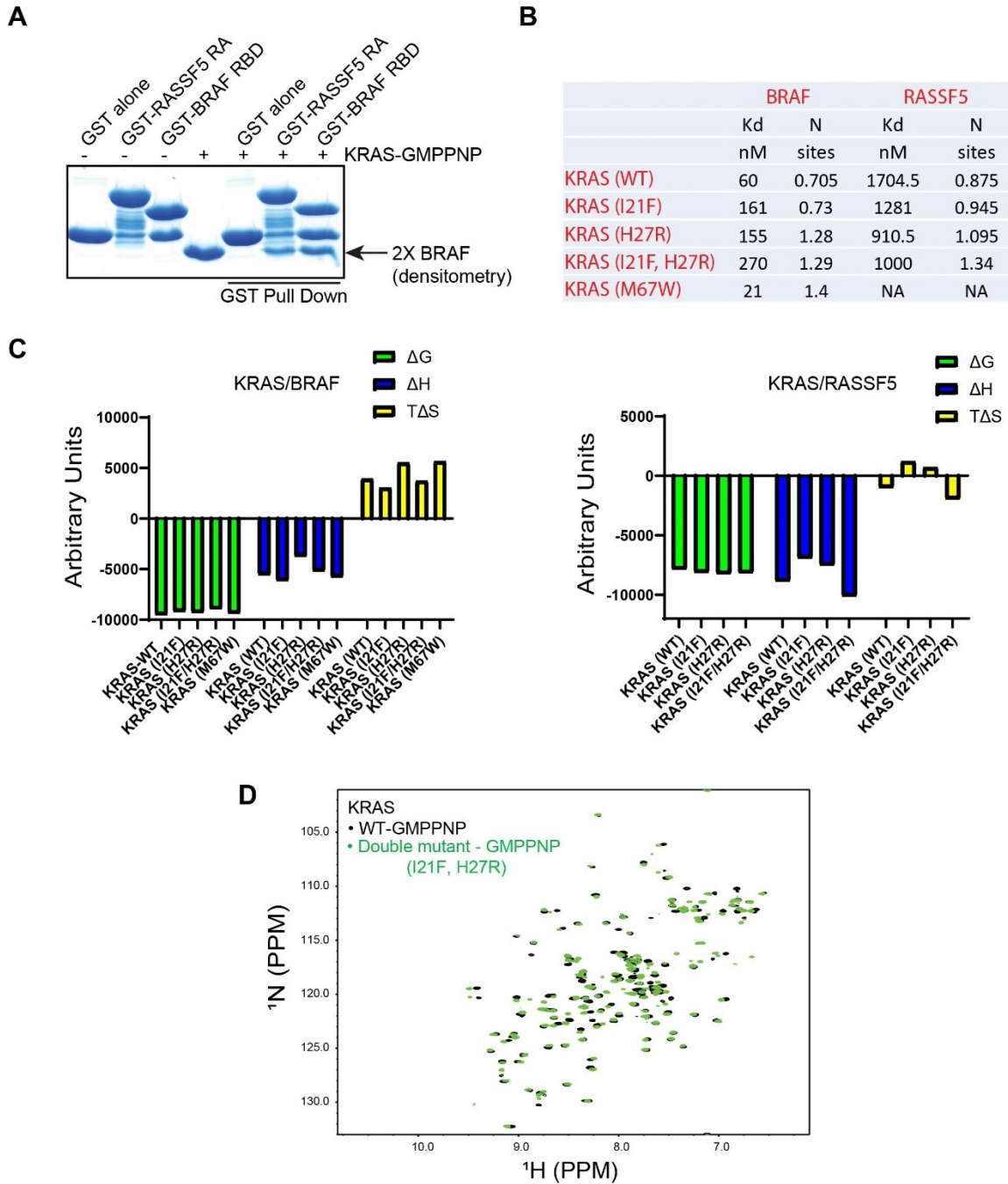
Figure S1:   Biophysical characteristics of KRAS mutants.

A) Control GST Pull down assay. Coomassie gel representation of the intraction between KRAS mutants and its effectors. Purified KRAS-GMPPNP protein is passed through GST-immobilized RAS effectros (BRAF RBD and RASSF5 RA). **B)** Table showing binding affinities determined by ITC for KRAS mutants and its comparision with wild-type. **C)** Thermodynamic binding parameters determined by ITC for various KRAS mutants and its comparision with wild-type. **D)** Comparision of NMR-HSQC spectra of KRAS -WT and KRAS[RASSF].

Figure S2: Nucleotide dependency of KRAS in complex formation with RASSF1

+GMPPNP

+GDP

— RASSF1^{KRAS} RA
— KRAS
— KRAS/RASSF1^{KRAS} RA
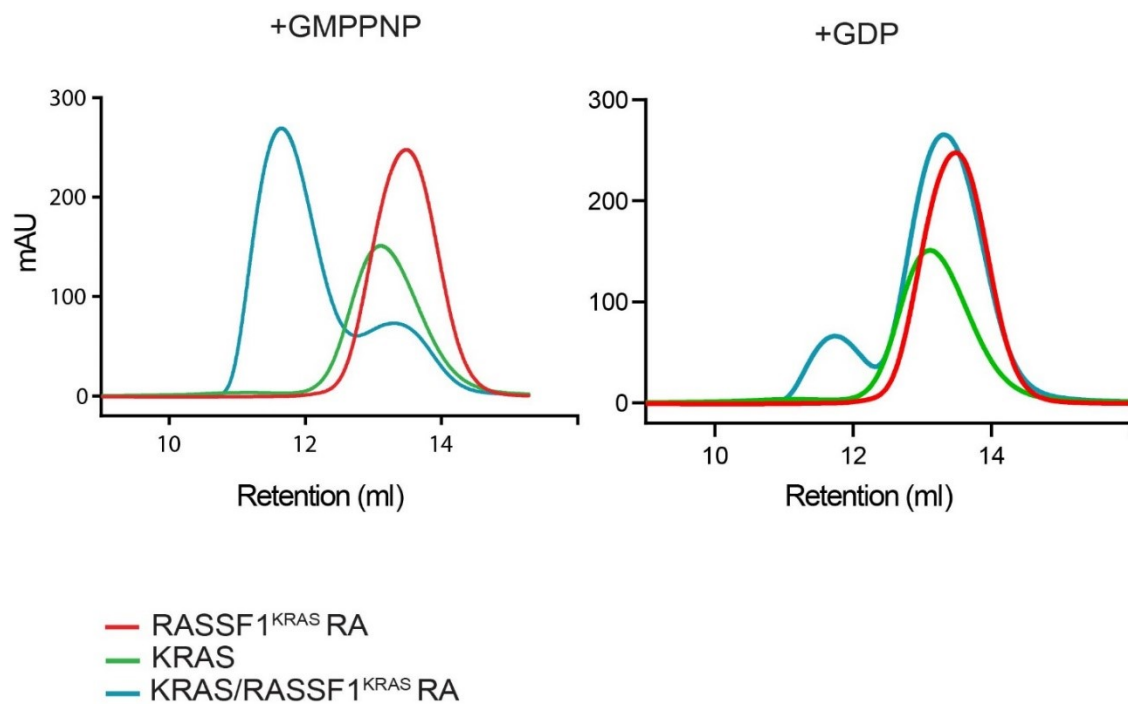
Figure S2. Nucleotide dependency of KRAS in complex formation with RASSF1

Gelfiltration profile show co-elution of RASSF1^{KRAS} with KRAS-GMPPNP. (Left) chromatography profile of KRAS alone (green), RASSF1^{KRAS} alone (red) and KRAS-GMPPNP + RASSF1^{KRAS} (blue). **(**Top) chromatography profile of KRAS alone (green), RASSF1^{KRAS} alone (red) and KRAS-GDP + RASSF1^{KRAS} (blue).

4.   Chapter 4: Discussion and conclusions

Well-regulated signalling is essential for normal cells to proliferate. The RAS small GTPases play a crucial role in regulating cell proliferation and survival through their regulation of two important pathways: MAP kinase and PI3K. In the past few decades, many new putative RAS effectors have been identified with diverse cellular functions, including cell adhesion scaffolds, regulators of vesicular trafficking, and inducers of pro-apoptotic signal activation. While a proliferative and cell survival role for RAS is well characterized, its capacity to stimulate pro-apoptotic signals remains enigmatic. The alleged transducer of these signals downstream of RAS is the RASSF family of effectors, proposed as direct activators of the pro-apoptotic Hippo pathway.

The RASSF family consists of 10 homologs containing putative RAS Association (RA) domains and are known tumor suppressors. Though RASSF proteins each comprise an RA domain, direct engagement with RAS had been verified only for RASSF5. Claims of direct interaction between RAS and other RASSF proteins were prevalent, but debatable. Further, a pro-apoptotic role for RASSF proteins has not been completely established, and most RASSFs have only been shown to induce apoptosis when overexpressed in 2D culture systems in the presence of external stimuli (TNFα, TRAIL, staurosporine, etoposide). An intrinsic ability of RASSF proteins to stimulate apoptotic signals is unclear, except for RASSF5, which shows that *RASSF5* deficient mouse embryonic fibroblasts are resistant to TNFα related apoptosis. Similarly, the capacity for RASSF effectors to regulate Hippo kinase activity is contentious, as data have shown that RASSF proteins can both activate and deactivate Hippo kinase activity. Despite these inconsistencies, it is clear that RASSF expression is heavily down regulated in numerous human cancers due to promoter hypermethylation. It is therefore crucial to better understand the function of each RASSF family member, to identify genuine interacting partners, to probe the ability of RASSF RA domains to bind RAS family GTPases, and to elucidate how these interactions feed into apoptotic or Hippo pathways.

Here, I attempted to answer some of these questions, focusing especially on the two RASSF family members RASSF1 and RASSF5. I show that most RASSF effectors do not interact with the HRAS/KRAS/NRAS GTPases, and that RASSF1 binds with the related RGK

family of small G-proteins. Further, I have demonstrated that RASSF5 activates the Hippo pathway upon co-expression with activated KRAS, and that RASSF1 plays a similar role despite not binding directly to KRAS. I have further identified the Ca^{2+}-regulatory RGK small GTPases as novel Hippo pathway activators. In Chapter 3, I described the design of rewiring KRAS and RASSF1 mutants that specifically channel KRAS downstream signals to RASSF proteins, which will eventually permit the study of apoptotic signals downstream of oncogenic RAS.

4.1   Not all RASSF are direct RAS effectors

Since the discovery of RASSF proteins, numerous studies have attempted to characterize their interaction with RAS GTPase. While previous data have concluded that RASSF1 is capable of interacting with RAS, this is arguable. Studies by Vos et al 2007, show that non-farnesylated KRAS does not interact with RASSF1A using co-immunoprecipitation techniques, however, they observed that RASSF1A preferentially binds to farnesylated KRAS compared to HRAS [246]. In my co-immunoprecipitation and pull-down experiments, using either full length KRAS and RASSF1 or the purified GTPase and RA domains alone, respectively, I did not observe an interaction between RASSF1A and either activated KRAS or HRAS. In addition, co-localization experiments in three different cell lines (HEK 293A, HeLa and U2OS) using full-length RASSF1A and activated KRAS-G12V showed RASSF1A is not recruited to the plasma membrane, where KRAS is localized. Instead, I observed RASSF1A at microtubules, consistent with previous RASSF1 localization studies [244, 304]. My work therefore corroborates the previous observation by Ortiz-Vega et al 2002, that shows RASSF1A and RASSF1C do not bind with seven distinct RAS-like GTPases (including KRAS and HRAS [255]). I suggest that under certain contexts, depending on cell-type and expression level, RASSF1 might co-precipitate weakly with RAS due to hetero-dimerization between the SARAH domains of RASSF1 and RASSF5 (as RAS binds strongly with RASSF5). Thus, I believe RASSF homologs are not just evolved to bind RAS GTPase, instead their RA domain might be utilized to bind other interacting partners.

4.2 RASSF1 diverged to bind RGK GTPases

RASSF1A has been deemed an effector of several small GTPases besides the RAS proteins. However, some studies have shown that few small GTPases can function downstream of RASSF1A. Dallol et al 2009, reported that RAN GTPase is an effector of the RASSF1A, involved in controlling microtubule organization [305]. In addition, O'Neill and colleagues have demonstrated that RASSF1A is required to maintain nuclear actin levels downstream of RAN GTPase signalling [306].

Here, I used an informatics approach to identify interactors of the RASSF1A protein. I have shown that the RASSF1 RA domain is highly similar to the RA domain of RASSF5 and we proposed a structural model of the RASSF1 RA domain using a homology modelling approach. There are only minor amino acid substitutions in each of the αN, β1 and β2 secondary structure regions of RASSF1 that differentiate it from RASSF5, and I resolved that these residues play a crucial role as specificity determinants towards GTPases. The two most significant amino acid substitutions in RASSF1 are an Asn in the αN-helix and Lys in β2-strand. These residues are Cys and Leu in RASSF5, and the Cys in αN mediates an essential hydrophobic interaction with HRAS switch II. Swapping the RASSF1 residues to mimic RASSF5 dramatically improved binding towards KRAS. This result illustrates how divergent residues in αN, β1 and β2 regions of RASSF effectors may allow binding to GTPases other than RAS.

We predicted that RASSF1 might instead interact with the RAS subfamily RGK GTPases (GEM, REM1 and REM2), the completely unstudied RAS-like GTPase RASL12, DIRAS3 and ERAS. I hypothesized that the diverged residues in αN, β1 and β2 of the RASSF1 RA domain could accommodate these RAS-like GTPases, and this was corroborated by both biochemical and cell-based assays. Additionally, I hypothesize a possible mechanism of RGK GTPase-RASSF1 binding that is suggested by NMR structural analysis of RASSF5, which shows an intramolecular interaction between its C1 and RA domains [229]. Interestingly, this intramolecular contact is disrupted in the presence of RAS, which was proposed to promote a more "open" conformation of RASSF5. As RASSF1 is highly homologous to RASSF5, and their C1 domains are highly similar [210], I can speculate the presence of a similar intramolecular association between the C1 and RA domains of RASSF1. Perhaps, in the context

of full length RASSF1, this intramolecular contact is disrupted in the presence of RGK GTPase and promotes a "open" conformation of RASSF1 to bind RGK GTPase. But this hypothesis must be validated by mutational and NMR binding studies as performed previously [229]. In brief, after assigning the peaks for RASSF1 C1 and RA domains, ^{15}N-HSQC spectra of full length RASSF1 protein can be obtained before, during, and after the addition of GMPPNP activated RGK GTPases (particularly GEM). In the spectrum of RASSF1 protein, resonances corresponding to free C1 domain should display chemical shifts completely different from those of C1-RA domain. Addition of GEM-GMPPNP should display a chemical shift in the HSQC spectra progressively toward the free C1 domain. Such observation would suggest the presence of an intramolecular interaction between the C1 and RA domain for RASSF1, and disruption of C1-RA intramolecular interaction upon addition of GEM-GMPPNP. This experiment would further corroborate the existence of an interaction between GEM-GMPPNP and RASSF1. Furthermore, key residues involved in the intramolecular interaction between C1 and RA domain of RASSF1 can also be identified to validate the interaction using mutational analysis.

Finally, I propose that RASSF proteins are effectors of multiple small GTPases rather than binding a single high-affinity partner. However, the specific functions and biological significance of RASSF1 interactions with these small GTPases must yet be determined, primarily focusing on the expression and activation state of endogenous GTPases and RASSFs.

4.3 Biological implications of RASSF1 and RGK GTPase interaction

4.3.1 RGK GTPase interactions with RASSF1

The RGK GTPase family is comprised of four members: GEM, REM1, REM2 and RRAD. These proteins differ from typical RAS GTPases mainly in their G2 domain and HVR, but also contain several additional domains and amino acid substitutions. Structural details of RGK GTPases in the GDP-bound form are well characterized. Conversely, solved structures of GTP-bound RGKs are available only for RRAD and REM2. These data suggest that RGK

GTPases may not operate as classical RAS "molecular switches" [69], as there is no apparent conformational change in RRAD or REM2 that correlates with the bound nucleotide [170]. In addition, the weak electron density for the switch I region implies that the effector-binding switch I region is disordered and not highly engaged with nucleotide [170]. Other evidence shows that RGK GTPase have poor intrinsic GTP-hydrolysis rate (especially GEM and RRAD) [170] and preferential binding towards GDP [161]. These data corroborate our experimental results. I have shown that there is no nucleotide-dependent binding of RGK GTPase with RASSF1 proteins in pull-down studies, and that the nucleotide exchange process for these GTPases (especially GEM) results in protein precipitation. This result is consistent with RGK GTPases having poor affinity for nucleotides. Thus, I speculate that due to the differences of the G2 and G3 domain of RGK GTPase that are highly substituted and lack critical residues such as T35 (in G2), which are required for GTP hydrolysis and effector binding for RAS superfamily GTPase, RGK GTPase have evolved not to bind typical RAS effectors, instead they are evolved to interact with RASSF family members and other effectors proteins.

In general, RAS small GTPase with poor nucleotide cycling are assisted by GEFs and GAPs to activate and deactivate them. Nevertheless, this is not yet proven for RGK GTPases as GEFs and GAPs are not yet identified for these proteins. Several previous attempts to estimate the rates of nucleotide cycling for RGK GTPase revealed that compared to RAS, the ability of GTP hydrolysis and exchange for RGK GTPase is "very slow". These results raises important questions, such as, how do RGK proteins function in cell and what are their activation states. Thus, I propose that future studies should emphasize on identification of GEFs and GAPs for RGK GTPases, which could help facilitate nucleotide cycling and enhance interaction with their effectors.

4.3.2 Localization of RGK GTPases and RASL12

As stated in the section 1.4.4, RGK GTPases localize differentially at the plasma membrane, in the cytoplasm, nucleus and on microtubules. In accordance with the literature, I also observed differential localization of RGK GTPases in different cell types, GEM being located in the cytoplasm and plasma membrane in HeLa and U2OS cells, while showing a

punctate nuclear pattern in HEK 293T cells. Similarly, REM1 showed cytoplasmic aggregation in HEK 293T cells, whereas the same is located ubiquitously in cytoplasm and plasma membrane in HeLa cells.

The sub-cellular localization of RGK GTPases is highly dynamic, and I propose it may depend on their activation state and other stimuli that activate RGK proteins. Thus far, there is no information in the literature on how RGK GTPases are activated in cells, unlike well characterized RAS proteins that are turned on by EGF and other factors. Stimulus dependent localization of RGK GTPase and RASSF1 could be tested using various factors, including serum, EGF, calcium, TGFβ or stress inducing factors such as hydrogen peroxide, nocodazole, etc. This would provide insights on the functional significance of the interaction between RASSF1-RGK GTPase. For instance, our studies show that the interaction of GEM GTPase and RASSF1 is required to maintain the calcium hemostasis in the cell (see Chapter 2). Hence, we can perform immunofluorescence experiments to show localization of GEM and RASSF1 upon change in the intracellular calcium conditions. We also show that RASSF1 is highly localized on microtubules (see Chapter 2 and 3) and treatment of cells with high concentrations of nocodazole disrupts microtubules and thus RASSF1 localization (data not shown). It will be interesting to assess the localization of RASSF1 interacting partners such as RGK GTPases and RASL12 under similar conditions (i.e. nocodazole treatment). RASL12 completely colocalizes with RASSF1 at the microtubules in both Hela and HEK293 cells lines. However, the functional significance of the interaction between RASL12 and RASSF1 is not yet known. Studying the localization of RASL12-RASSF1 in the presence of nocodazole and other related stimuli would unravel whether RASL12 plays a protective role by colocalizing with RASSF1 at the microtubules and evading microtubule disruption by microtubule destabilizing agents.

4.3.3 Ca^{2+} channels and RASSF1

RGK GTPases play a well characterized role in regulating voltage-gated Ca^{2+}channels. RASSF proteins have also been associated with Ca^{2+} signalling, with RASSF4 regulating store-operated Ca^{2+} entry at ER–PM junctions [307]. Only two reports link RASSF1 to Ca^{2+} signalling: 1) Armesilla et al 2004, reported a functional interaction between RASSF1 and the

Ca^{2+} pump PMCA4B [308], and 2) an interaction was observed in cardiomyocytes between RASSF1A and components of TNF receptor implicated in maintaining intracellular Ca2+ hemostasis [309]. I have shown a relationship between RGK GTPases and RASSF1, as overexpression of RGK GTPase alone inhibits Ca^{2+} entry while co-expression of RASSF1 with RGK GTPases repressed the inhibitory role of RGK proteins, partially restoring intracellular Ca^{2+} levels. Previous studies have demonstrated a mechanism for RGK GTPase-driven inhibition of Ca^{2+} channels [202, 310], and below is a schematic representation of the proposed mechanism by Yang et al, 2012.
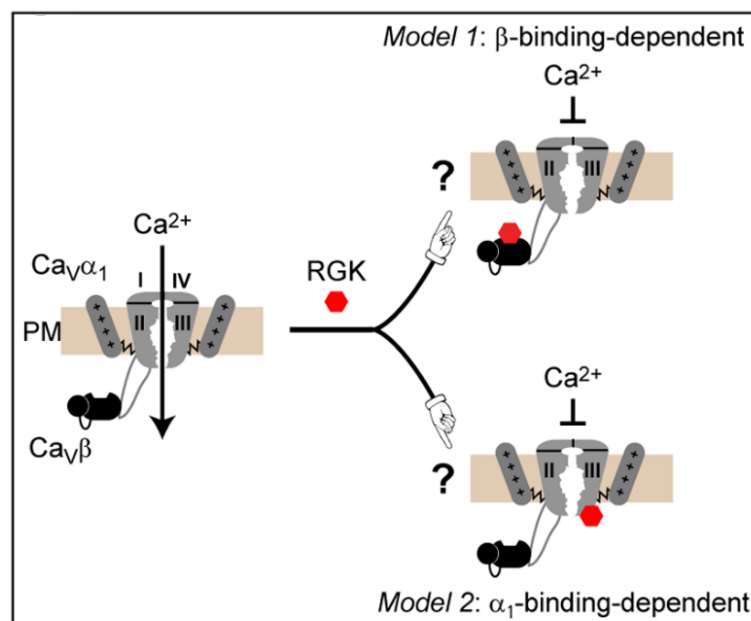
Figure 1: **Image showing various models by which RGK GTPase inhibits voltage gated ion channels.**

Image adapted from (Yang et al, 2012)

The above model suggests that, for proper functioning of VGCC, both $Ca_v\alpha_1$ and $Ca_v\beta$ subunits must form a complex for Ca^{2+} influx. RGK GTPase would inhibit this complex formation by binding directly to the $Ca_v\alpha_1$ or $Ca_v\beta$ subunit. I hypothesize that, in our overexpression experiments, RASSF1 titrates out RGK GTPases and prevents binding to the $Ca_v\alpha_1$ and $Ca_v\beta$ subunits, restoring channel activity. This hypothesis must be tested

appropriately to elucidate the mechanism of how RASSF1 inhibits the function of RGK GTPase.

It will be essential to study the biological significance of RGK-RASSF1 interactions in the context of apoptosis. Our preliminary study shows that overexpression of RGK GTPases causes cells to undergo apoptosis, but that co-expression of RGK GTPases with RASSF1 rescues this. There is a clear connection between apoptosis and subcellular Ca^{2+} levels in the literature. One of the many mechanisms of Ca^{2+} induced apoptosis in the cell suggests that, cytosolic overload of calcium causes release of cytochrome *C* from mitochondria and eventual caspase activation leads to the generation of pro-apoptotic response [190, 192, 193]. I reason that the apoptosis induced in HEK 293T cells upon overexpression of RGK GTPase in my experiments could be due to a similar mechanism, given that overexpression of RGK GTPase inhibited the function of Ca^{2+} channel thereby altering subcellular calcium levels, resulting in the cell undergoing apoptosis. Also, co-expression of RGK GTPase with RASSF1 repressed the Ca^{2+} channel inhibitory role of RGK proteins causing the rescue of cells from apoptosis. An interesting observation is that, RASSF1 being a tumor suppressor and pro-apoptotic inducing protein showed an opposite effect and rescued the cell from apoptosis. A recent paper shows that RASSF1A interaction with hypoxia inducible factor-1α (HIF-1α) drives the Warburg effect in cancer cells [311], suggesting that RASSF1A can have a survival role. Thus, it seems that the signalling mechanism of RASSF1 is highly context dependent. Therefore, it must be addressed appropriately by performing specific experiments and choosing the right cell lines that express RASSF1 and its interacting partners. A more optimal solution would be to perform *in vivo* experiments using a model system where RGK GTPases and other interacting proteins of RASSF1 will be available endogenously at the right stoichiometry, concentration and probably in their activation states.

4.4   RASSF proteins, apoptosis and the Hippo pathway

RASSF proteins are tumor suppressors thought to induce pro-apoptotic signalling, at least in some contexts. Studies show that *Rassf1a-/-* deficient mice have a higher incidence of tumor formation and are more susceptible to tumorigenesis [209]. Further, *Rassf5-/-* mice are

resistant to TNFα induced apoptosis [260]. Yet, a direct mechanistic role for RAS-RASSF complexes to induce apoptosis has not yet been demonstrated, and it is unclear how RASSF proteins in general regulate apoptosis downstream of diverse upstream signals. Early studies report that RASSF proteins induce cell death in HEK 293T cells when co-expressed with oncogenic RAS-G12V [254, 259]. However, this analysis was using early apoptosis detection techniques such as cell detachment and crystal violet staining. Recent studies using sensitive detection methods show that RASSF proteins alone do not induce apoptosis. Instead, an apoptotic effect in RASSF overexpressing cells must be stimulated by apoptosis stimulating reagents (anti-FAS, TNFα, TRAIL, etoposide, or staurosporine) [210, 260, 312]. I used a sensitive Annexin V/Propidium Iodide staining followed by flow cytometry and did not observe apoptosis in cells expressing RASSF1 "alone" or in cells expressing RASSFs and KRAS-G12V. Not all the cell types express all the proteins required to activate the apoptosis or Hippo pathway activation machineries. For instance, we have shown that endogenous expression of RASSF proteins vary between HEK 293T, U2OS and HeLa cells. Therefore, I believe that the ability of RASSF to induce apoptosis must be assessed in more complex systems such as 3D culture, tumor models or mouse studies.

While I did not observe apoptosis induction directly, my investigation on signalling did resolve that co-expression of KRAS-G12V or RGK GTPases with RASSF1 or RASSF5 significantly alters nuclear retention of YAP. This represents the first study to demonstrate Hippo pathway activation only in the context of KRAS-RASSF co-expression, suggesting that RASSF proteins activate Hippo signalling downstream of KRAS or RGK GTPase. Previous studies have demonstrated that active HRAS precipitates along with RASSF5-MST1 complex and HRAS co-expression stabilizes RASSF5-MST1 complex formation [116]. With these observations, I hypothesize that active KRAS or RGK GTPase somehow stabilize the Hippo pathway proteins and activate them. Simultaneously, recent reports suggest that the key Hippo pathway protein, YAP, is vital for signalling during RAS-induced proliferation of cancer cells and tumorigenesis [301, 303, 313, 314]. YAP also provides resistance to MEK1/2 inhibition in neuroblastomas with hyperactivated RAS signalling [315]. Together, these explanations confirm the previous claim that active RAS can be both pro-proliferative as well as pro-apoptotic. However, to understand and predict the outcome of RAS downstream signalling (either pro-proliferative or pro-apoptotic) can be dependent on many factors such as, the

availability of interacting partners, their endogenous expression levels, activations states, stoichiometry of interaction and kinetics, etc. Hence, to dissect and understand the balancing effect of RAS, it is essential to compartmentalize and study each of the RAS downstream signalling separately using RAS mutants that selectively activate specific downstream pathways. Our rewired RAS and RASSF1 mutants can be one of the best candidates for such analysis. Together, the down regulation of RASSF expression in human cancers and their dependence on YAP activity suggest a RAS-RASSF-Hippo signalling axis could be of significant clinical interest.

4.5   N-RASSFs are not close homologs of C-RASSFs

Based on their domain architecture, N-RASSF proteins form a separate family of RA domain-containing effectors. I have shown that N-RASSF complexes with the ASPP1 and ASPP2 (apoptosis stimulating protein of p53) proteins and have significant sequence homology to these effectors, but the functional significance of this interaction is not yet clear. As *Drosophila* dRASSF (ortholog of human RASSF8) complexes with dASPP to regulate retinal morphogenesis, this interaction appears to be evolutionarily conserved [241]. ASPP effectors also complex with PP1 (a serine/threonine phosphatase) to regulate various cellular process [316], and PP1-ASPP2 binds and regulates YAP1 [317]. Alternatively, ASPP proteins are also known to interact with the tumor suppressor p53. Upon external stress, p53 stimulates a wide variety of signalling network. The common among them is external death receptor pathway, which triggers the activation of caspase cascade and pro-apoptotic signalling [318] and intrinsic pathways of activating Bcl2 family members towards pro-apoptotic members, leading to the formation of apoptososme and subsequent caspase activation [319]. A seminal study shows that the apoptotic effect of p53 increases five-fold when it is co-expressed with ASPP1/2 [320]. Therefore, it will be interesting to study the apoptotic effect of p53 in presence of both N-RASSF and ASPP1/2. I hypothesis that N-RASSF, through interaction with ASPP, can activate both Hippo and p53 signalling. However, this claim must be tested appropriately in both these contexts.

4.6 Rewiring mutants compartmentalize RAS signalling to RASSF effectors

RAS functions through various complex pathways to control cellular processes, making it difficult to understand its whole function. The third chapter of my thesis focused on generating KRAS and RASSF1 mutants to channel RAS downstream signals towards RASSF effectors. Previous studies have generated RAS 'effector mutants' that specifically channel RAS downstream signals to either the MAP kinase pathway (RAS-T35S) or RALGEF pathway (RAS-E37G) [321]. These data show that RAS-E37G is deficient in binding RAF1 and this attenuates its transformation capacity in mammalian cells. This example shows how restricting RAS to one downstream pathway can alter its function and perhaps allow study of less potent effectors. Our RAS mutant has a diminished interaction with RAF but augmented interaction with RASSF5, and while the rewired RASSF1 mutant interacts with KRAS, wild-type RASSF1 does not. I postulate that with these mutants, I can begin to dissect how RAS signals channel through RASSF proteins to the Hippo pathway by analyzing downstream signalling using proteomics approaches.

As previously mentioned, in order to fully understand RASSF signalling, it will be necessary to perform experiments in 3D-culture systems as mentioned in [322] or mouse models. 3D culture would represent more accurately the tissue models compared to normal 2D culture. To study RASSF biology it will be essential to take into account the complexity of signals from various factors as it can affect the results. For instance, RASSF proteins are implicated in the Hippo signalling and proteins of the Hippo pathway are variably affected by cell density, cell contact, cell stretching, cell shape, cell adhesion and matrix stiffness, shear stress, polarity, etc. [323]. Such complexity can only be attained on 3D-culture systems or animal models. Thus, it will be interesting to observe the real effect of rewired KRAS mutants towards RASSF proteins in the context of activating other proteins in the pathways in such systems.

4.7 Conclusions and future perspective

Our study was carried out to understand the biological function of the presumed RASSF family of RAS effectors. Our biochemical assays demonstrate that RASSF family members, except RASSF5, do not bind KRAS or HRAS. These studies further lead to the identification of novel small GTPase interactors for the RASSF1 protein, and these proved to be novel activators of the Hippo pathway. Indeed, our data reveal that RASSF1-6 all interact with MST1/2 hippo kinases, while RASSF8-10 are a separate family related to p53-regulatory ASPP effectors. We built homology models of the RASSF RA domains based on available structures and used these to show how RASSF1 divergence at just a few key residues alters specificity for RAS subfamily small GTPases. Importantly, reverting these residues to mimic RASSF5 improves the binding affinity of RASSF1 to KRAS and provides a novel RASSF effector through which we can study RAS signalling.

RASSF1 binds to three of the four RGK family of small GTPases: GEM, REM1, and REM2. Ectopic expression of RGK GTPase in HEK 293T cells induces apoptosis and alters intracellular Ca^{2+} levels, while co-expression of RGK GTPases with RASSF1 rescues both these observed phenotypes. I identified a novel interaction of RASSF1 with the RAS-like small GTPase RASL12, and RASL12 completely co-localizes with RASSF1 on microtubules in several cell types. The functional significance of this interaction is yet to be elucidated. Perhaps most importantly, I have shown for the first time that co-expression of KRAS with RASSF effectors activates Hippo signalling and alters nuclear YAP1 retention.

In chapter 3, I derived a rewired KRAS mutant with reduced affinity for BRAF and increased affinity for RASSF5. In parallel, I generated a rewired RASSF1 mutant with robust binding to KRAS. The rewired mutants co-localize with their selected interacting partners in cells, and I have shown that co-expression of rewired KRAS with RASSF1, RASSF5 or rewired RASSF1^{KRAS} activates Hippo signals and alters levels of nuclear YAP1.

As a future perspective, I would focus on three major points: first, a functional significance of the interaction between RASSF1 and RASL12 must be further studied. RASSF1 is localized at microtubules and enhances their stability, acting essentially like paclitaxel [324]. I would assess the effects of RASL12 co-localization with RASSF1 on microtubule stability by

using microtubule destabilizing agents such as nocodazole, colchicine, etc. Little evidence suggests that RASL12 is a tumor suppressor, and I hypothesize that RASL12 interaction with RASSF1 is to protect the pro-apoptotic function of RASSF1 by preventing RASSF1 degradation since the expression of RASSF1 is highly downregulated in cancer cells. Indeed, several studies show that RASSF1 undergoes ubiquitination-mediated degradation upon TGFβ stimulation [325]. Thus, studying the role of RASL12 in the context of protecting RASSF1 and imparting stability to microtubules would be interesting.

Secondly, I would focus on solving a crystal structure of the RASSF1 RA domain in complex with KRAS **(Figure 2).** Our rewired RASSF1 mutant co-elutes with KRAS on size-exclusion chromatography columns, and I have used the purified complex to set up crystal screens. I have successfully optimized crystallization conditions, and these can now be scaled up for X-Ray diffraction. Thus far, RASSF5 is the only RASSF family member whose structure has solved by crystallography. Solving the structure of RASSF1[KRAS] in complex with KRAS will provide insights on the mode of interaction between RASSF family proteins and KRAS. This information can be used to reason why the RASSF family of proteins have diverged to bind other small GTPases.
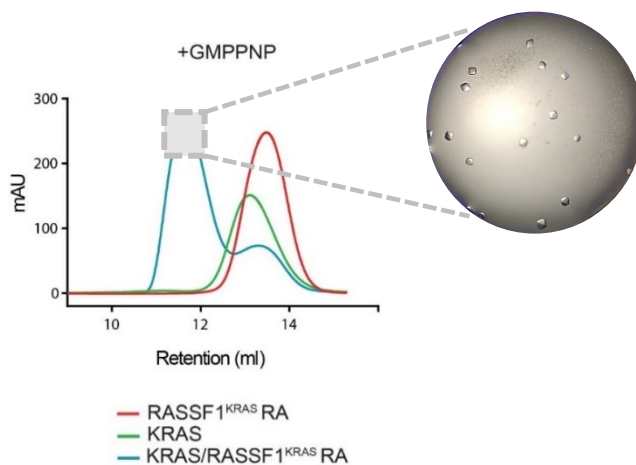
Figure 2:   **Image showing the crystals of RASSF1-KRAS complex**

Crystals were obtained by screening the concentrate of gel filtration co-elution peak (indicated in blue) containing RASSF1-RA and KRAS-GMPPNP.

Third, downstream signalling of the rewired KRAS and RASSF1 mutants and the mechanism by which they activate the Hippo signalling needs to be studied in detail using tumor models and proteomics approaches. Specifically, we should investigate the up and down regulations, posttranslational modifications of all the downstream proteins of the Hippo pathway under the rewired KRAS/RASSF conditions. This analysis can provide insights on the enigma of how RASSF activates the Hippo signalling downstream of activated KRAS.

I believe my thesis addresses several key questions in the field of RAS and RASSF biology, at the same time unravelling new avenues of study which need to be answered to understand RASSF signalling. The knowledge acquired from my doctoral work can help in future studies to target RAS signalling during oncogenesis. Most of the studies pertaining to oncogenic KRAS mutations have always focused on developing inhibitors against KRAS downstream signalling proteins of MAPK and PI3K pathways. My study will provide a new avenue to divert the hyperproliferative oncogenic KRAS signals towards tumor suppressive network such as the Hippo pathway.

References

1. Cooper, G.M., *The Cell: A Molecular Approach*. 2000, Sunderland (MA): Sinauer Associates.
2. Nair, A., et al., *Conceptual Evolution of Cell Signaling.* Int J Mol Sci, 2019. **20**(13).
3. Karp, G., J. Iwasa, and W. Marshall, *Karp's Cell and Molecular Biology: Concepts and Experiments*. 2015, Wiley.
4. Weis, W.I. and B.K. Kobilka, *The Molecular Basis of G Protein-Coupled Receptor Activation.* Annu Rev Biochem, 2018. **87**: p. 897-919.
5. Lemmon, M.A. and J. Schlessinger, *Cell signaling by receptor tyrosine kinases.* Cell, 2010. **141**(7): p. 1117-34.
6. Unwin, N., *Neurotransmitter action: opening of ligand-gated ion channels.* Cell, 1993. **72 Suppl**: p. 31-41.
7. Grotzinger, J., *Molecular mechanisms of cytokine receptor activation.* Biochim Biophys Acta, 2002. **1592**(3): p. 215-23.
8. Smith, C.A., T. Farrah, and R.G. Goodwin, *The TNF receptor superfamily of cellular and viral proteins: activation, costimulation, and death.* Cell, 1994. **76**(6): p. 959-62.
9. Heldin, C.H., et al., *Signals and Receptors.* Cold Spring Harb Perspect Biol, 2016. **8**(4): p. a005900.
10. Xu, D. and R. Nussinov, *Favorable domain size in proteins.* Fold Des, 1998. **3**(1): p. 11-7.
11. Musacchio, A., *How SH3 domains recognize proline.* Adv Protein Chem, 2002. **61**: p. 211-68.
12. Pawson, T., G.D. Gish, and P. Nash, *SH2 domains, interaction modules and cellular wiring.* Trends Cell Biol, 2001. **11**(12): p. 504-11.
13. Schlessinger, J. and M.A. Lemmon, *SH2 and PTB domains in tyrosine kinase signaling.* Sci STKE, 2003. **2003**(191): p. RE12.
14. Huang, H., et al., *Defining the specificity space of the human SRC homology 2 domain.* Mol Cell Proteomics, 2008. **7**(4): p. 768-84.
15. Waksman, G., et al., *Binding of a high affinity phosphotyrosyl peptide to the Src SH2 domain: crystal structures of the complexed and peptide-free forms.* Cell, 1993. **72**(5): p. 779-90.
16. Nolte, R.T., et al., *Crystal structure of the PI 3-kinase p85 amino-terminal SH2 domain and its phosphopeptide complexes.* Nat Struct Biol, 1996. **3**(4): p. 364-74.
17. Nioche, P., et al., *Crystal structures of the SH2 domain of Grb2: highlight on the binding of a new high-affinity inhibitor.* J Mol Biol, 2002. **315**(5): p. 1167-77.
18. Wang, D.S. and G. Shaw, *The association of the C-terminal region of beta I sigma II spectrin to brain membranes is mediated by a PH domain, does not require membrane proteins, and coincides with a inositol-1,4,5 triphosphate binding site.* Biochem Biophys Res Commun, 1995. **217**(2): p. 608-15.
19. Yao, L., Y. Kawakami, and T. Kawakami, *The pleckstrin homology domain of Bruton tyrosine kinase interacts with protein kinase C.* Proc Natl Acad Sci U S A, 1994. **91**(19): p. 9175-9.
20. Wang, D.S., et al., *Binding of PH domains of beta-adrenergic receptor kinase and beta-spectrin to WD40/beta-transducin repeat containing regions of the beta-subunit of trimeric G-proteins.* Biochem Biophys Res Commun, 1994. **203**(1): p. 29-35.

21. Hurley, J.H., et al., *Structural genomics and signaling domains.* Trends Biochem Sci, 2002. **27**(1): p. 48-53.

22. Yu, J.W. and M.A. Lemmon, *Genome-wide analysis of signaling domain function.* Curr Opin Chem Biol, 2003. **7**(1): p. 103-9.

23. Trzaskowski, B., et al., *Action of molecular switches in GPCRs--theoretical and experimental studies.* Curr Med Chem, 2012. **19**(8): p. 1090-109.

24. Kadamur, G. and E.M. Ross, *Mammalian phospholipase C.* Annu Rev Physiol, 2013. **75**: p. 127-54.

25. Siehler, S., *Regulation of RhoGEF proteins by G12/13-coupled receptors.* Br J Pharmacol, 2009. **158**(1): p. 41-9.

26. Hanoune, J. and N. Defer, *Regulation and role of adenylyl cyclase isoforms.* Annu Rev Pharmacol Toxicol, 2001. **41**: p. 145-74.

27. Zamponi, G.W. and K.P. Currie, *Regulation of Ca(V)2 calcium channels by G protein coupled receptors.* Biochim Biophys Acta, 2013. **1828**(7): p. 1629-43.

28. Dascal, N., *Signalling via the G protein-activated K+ channels.* Cell Signal, 1997. **9**(8): p. 551-73.

29. Lyon, A.M. and J.J. Tesmer, *Structural insights into phospholipase C-beta function.* Mol Pharmacol, 2013. **84**(4): p. 488-500.

30. Vanhaesebroeck, B., L. Stephens, and P. Hawkins, *PI3K signalling: the path to discovery and understanding.* Nat Rev Mol Cell Biol, 2012. **13**(3): p. 195-203.

31. Milner-White, E.J., J.R. Coggins, and I.A. Anton, *Evidence for an ancestral core structure in nucleotide-binding proteins with the type A motif.* J Mol Biol, 1991. **221**(3): p. 751-4.

32. Walker, J.E., et al., *Distantly related sequences in the alpha- and beta-subunits of ATP synthase, myosin, kinases and other ATP-requiring enzymes and a common nucleotide binding fold.* EMBO J, 1982. **1**(8): p. 945-51.

33. Saraste, M., P.R. Sibbald, and A. Wittinghofer, *The P-loop--a common motif in ATP- and GTP-binding proteins.* Trends Biochem Sci, 1990. **15**(11): p. 430-4.

34. Leipe, D.D., et al., *Classification and evolution of P-loop GTPases and related ATPases.* J Mol Biol, 2002. **317**(1): p. 41-72.

35. Colicelli, J., *Human RAS superfamily proteins and related GTPases.* Sci STKE, 2004. **2004**(250): p. RE13.

36. Zenonos, K. and K. Kyprianou, *RAS signaling pathways, mutations and their role in colorectal cancer.* World J Gastrointest Oncol, 2013. **5**(5): p. 97-101.

37. Schwartz, M., *Rho signalling at a glance.* J Cell Sci, 2004. **117**(Pt 23): p. 5457-8.

38. Schwartz, S.L., et al., *Rab GTPases at a glance.* J Cell Sci, 2007. **120**(Pt 22): p. 3905-10.

39. Joseph, J., *Ran at a glance.* J Cell Sci, 2006. **119**(Pt 17): p. 3481-4.

40. Jackson, C.L. and S. Bouvet, *Arfs at a glance.* J Cell Sci, 2014. **127**(Pt 19): p. 4103-9.

41. Cox, A.D. and C.J. Der, *Ras history: The saga continues.* Small GTPases, 2010. **1**(1): p. 2-27.

42. Malumbres, M. and M. Barbacid, *RAS oncogenes: the first 30 years.* Nat Rev Cancer, 2003. **3**(6): p. 459-65.

43. Harvey, J.J., *An Unidentified Virus Which Causes the Rapid Production of Tumours in Mice.* Nature, 1964. **204**: p. 1104-5.

44. Kirsten, W.H. and L.A. Mayer, *Morphologic responses to a murine erythroblastosis virus*. J Natl Cancer Inst, 1967. **39**(2): p. 311-35.

45. Scolnick, E.M., et al., *Studies on the nucleic acid sequences of Kirsten sarcoma virus: a model for formation of a mammalian RNA-containing sarcoma virus*. J Virol, 1973. **12**(3): p. 458-63.

46. Scolnick, E.M. and W.P. Parks, *Harvey sarcoma virus: a second murine type C sarcoma virus with rat genetic information*. J Virol, 1974. **13**(6): p. 1211-9.

47. Shih, T.Y., et al., *Identification of a sarcoma virus-coded phosphoprotein in nonproducer cells transformed by Kirsten or Harvey murine sarcoma virus*. Virology, 1979. **96**(1): p. 64-79.

48. Scolnick, E.M., A.G. Papageorge, and T.Y. Shih, *Guanine nucleotide-binding activity as an assay for src protein of rat-derived murine sarcoma viruses*. Proc Natl Acad Sci U S A, 1979. **76**(10): p. 5355-9.

49. Willingham, M.C., et al., *Localization of the src gene product of the Harvey strain of MSV to plasma membrane of transformed cells by electron microscopic immunocytochemistry*. Cell, 1980. **19**(4): p. 1005-14.

50. Chang, E.H., et al., *Tumorigenic transformation of mammalian cells induced by a normal human gene homologous to the oncogene of Harvey murine sarcoma virus*. Nature, 1982. **297**(5866): p. 479-83.

51. Capon, D.J., et al., *Activation of Ki-ras2 gene in human colon and lung carcinomas by two different point mutations*. Nature, 1983. **304**(5926): p. 507-13.

52. Reddy, E.P., et al., *A point mutation is responsible for the acquisition of transforming properties by the T24 human bladder carcinoma oncogene*. Nature, 1982. **300**(5888): p. 149-52.

53. Tabin, C.J., et al., *Mechanism of activation of a human oncogene*. Nature, 1982. **300**(5888): p. 143-9.

54. Taparowsky, E., et al., *Activation of the T24 bladder carcinoma transforming gene is linked to a single amino acid change*. Nature, 1982. **300**(5894): p. 762-5.

55. Hall, A., et al., *Identification of transforming gene in two human sarcoma cell lines as a new member of the ras gene family located on chromosome 1*. Nature, 1983. **303**(5916): p. 396-400.

56. Nakano, H., et al., *Isolation of transforming sequences of two human lung carcinomas: structural and functional analysis of the activated c-K-ras oncogenes*. Proc Natl Acad Sci U S A, 1984. **81**(1): p. 71-5.

57. McGrath, J.P., et al., *Structure and organization of the human Ki-ras proto-oncogene and a related processed pseudogene*. Nature, 1983. **304**(5926): p. 501-6.

58. Plowman, S.J., et al., *K-ras 4A and 4B are co-expressed widely in human tissues, and their ratio is altered in sporadic colorectal cancer*. J Exp Clin Cancer Res, 2006. **25**(2): p. 259-67.

59. Cohen, J.B. and A.D. Levinson, *A point mutation in the last intron responsible for increased expression and transforming activity of the c-Ha-ras oncogene*. Nature, 1988. **334**(6178): p. 119-24.

60. Cohen, J.B., S.D. Broz, and A.D. Levinson, *Expression of the H-ras proto-oncogene is controlled by alternative splicing*. Cell, 1989. **58**(3): p. 461-72.

61. Eisfeld, A.K., et al., *NRAS isoforms differentially affect downstream pathways, cell growth, and cell transformation.* Proc Natl Acad Sci U S A, 2014. **111**(11): p. 4179-84.

62. Fiorucci, G. and A. Hall, *All three human ras genes are expressed in a wide range of tissues.* Biochim Biophys Acta, 1988. **950**(1): p. 81-3.

63. Omerovic, J., A.J. Laude, and I.A. Prior, *Ras proteins: paradigms for compartmentalised and isoform-specific signalling.* Cell Mol Life Sci, 2007. **64**(19-20): p. 2575-89.

64. de Vos, A.M., et al., *Three-dimensional structure of an oncogene protein: catalytic domain of human c-H-ras p21.* Science, 1988. **239**(4842): p. 888-93.

65. Pai, E.F., et al., *Refined crystal structure of the triphosphate conformation of H-ras p21 at 1.35 A resolution: implications for the mechanism of GTP hydrolysis.* EMBO J, 1990. **9**(8): p. 2351-9.

66. Pai, E.F., et al., *Structure of the guanine-nucleotide-binding domain of the Ha-ras oncogene product p21 in the triphosphate conformation.* Nature, 1989. **341**(6239): p. 209-14.

67. Valencia, A., et al., *GTPase domains of ras p21 oncogene protein and elongation factor Tu: analysis of three-dimensional structures, sequence families, and functional sites.* Proc Natl Acad Sci U S A, 1991. **88**(12): p. 5443-7.

68. Milburn, M.V., et al., *Molecular switch for signal transduction: structural differences between active and inactive forms of protooncogenic ras proteins.* Science, 1990. **247**(4945): p. 939-45.

69. Vetter, I.R. and A. Wittinghofer, *The guanine nucleotide-binding switch in three dimensions.* Science, 2001. **294**(5545): p. 1299-304.

70. Johnson, C.W., et al., *The small GTPases K-Ras, N-Ras, and H-Ras have distinct biochemical properties determined by allosteric effects.* J Biol Chem, 2017. **292**(31): p. 12981-12993.

71. Hancock, J.F. and R.G. Parton, *Ras plasma membrane signalling platforms.* Biochem J, 2005. **389**(Pt 1): p. 1-11.

72. Hancock, J.F., H. Paterson, and C.J. Marshall, *A polybasic domain or palmitoylation is required in addition to the CAAX motif to localize p21ras to the plasma membrane.* Cell, 1990. **63**(1): p. 133-9.

73. Wright, L.P. and M.R. Philips, *Thematic review series: lipid posttranslational modifications. CAAX modification and membrane targeting of Ras.* J Lipid Res, 2006. **47**(5): p. 883-91.

74. Casey, P.J., et al., *p21ras is modified by a farnesyl isoprenoid.* Proc Natl Acad Sci U S A, 1989. **86**(21): p. 8323-7.

75. Seabra, M.C., et al., *Protein farnesyltransferase and geranylgeranyltransferase share a common alpha subunit.* Cell, 1991. **65**(3): p. 429-34.

76. Boyartchuk, V.L., M.N. Ashby, and J. Rine, *Modulation of Ras and a-factor function by carboxyl-terminal proteolysis.* Science, 1997. **275**(5307): p. 1796-800.

77. Otto, J.C., et al., *Cloning and characterization of a mammalian prenyl protein-specific protease.* J Biol Chem, 1999. **274**(13): p. 8379-82.

78. Freije, J.M., et al., *Identification and chromosomal location of two human genes encoding enzymes potentially involved in proteolytic maturation of farnesylated proteins.* Genomics, 1999. **58**(3): p. 270-80.

79. Clarke, S., et al., *Posttranslational modification of the Ha-ras oncogene protein: evidence for a third class of protein carboxyl methyltransferases.* Proc Natl Acad Sci U S A, 1988. **85**(13): p. 4643-7.

80. Hancock, J.F., K. Cadwallader, and C.J. Marshall, *Methylation and proteolysis are essential for efficient membrane binding of prenylated p21K-ras(B).* EMBO J, 1991. **10**(3): p. 641-6.

81. Lobo, S., et al., *Identification of a Ras palmitoyltransferase in Saccharomyces cerevisiae.* J Biol Chem, 2002. **277**(43): p. 41268-73.

82. Hancock, J.F., et al., *All ras proteins are polyisoprenylated but only some are palmitoylated.* Cell, 1989. **57**(7): p. 1167-77.

83. Choy, E., et al., *Endomembrane trafficking of ras: the CAAX motif targets proteins to the ER and Golgi.* Cell, 1999. **98**(1): p. 69-80.

84. Di Guglielmo, G.M., et al., *Compartmentalization of SHC, GRB2 and mSOS, and hyperphosphorylation of Raf-1 by EGF but not insulin in liver parenchyma.* EMBO J, 1994. **13**(18): p. 4269-77.

85. Prior, I.A., P.D. Lewis, and C. Mattos, *A comprehensive survey of Ras mutations in cancer.* Cancer Res, 2012. **72**(10): p. 2457-67.

86. Forbes, S.A., et al., *The Catalogue of Somatic Mutations in Cancer (COSMIC).* Curr Protoc Hum Genet, 2008. **Chapter 10**: p. Unit 10 11.

87. Franken, S.M., et al., *Three-dimensional structures and properties of a transforming and a nontransforming glycine-12 mutant of p21H-ras.* Biochemistry, 1993. **32**(33): p. 8411-20.

88. Geyer, M., et al., *Conformational transitions in p21ras and in its complexes with the effector protein Raf-RBD and the GTPase activating protein GAP.* Biochemistry, 1996. **35**(32): p. 10308-20.

89. Spoerner, M., A. Wittinghofer, and H.R. Kalbitzer, *Perturbation of the conformational equilibria in Ras by selective mutations as studied by 31P NMR spectroscopy.* FEBS Lett, 2004. **578**(3): p. 305-10.

90. Al-Mulla, F., et al., *Structural differences between valine-12 and aspartate-12 Ras proteins may modify carcinoma aggression.* J Pathol, 1999. **187**(4): p. 433-8.

91. Buhrman, G., G. Wink, and C. Mattos, *Transformation efficiency of RasQ61 mutants linked to structural features of the switch regions in the presence of Raf.* Structure, 2007. **15**(12): p. 1618-29.

92. John, J., et al., *C-terminal truncation of p21H preserves crucial kinetic and structural properties.* J Biol Chem, 1989. **264**(22): p. 13086-92.

93. Trahey, M., et al., *Biochemical and biological properties of the human N-ras p21 protein.* Mol Cell Biol, 1987. **7**(1): p. 541-4.

94. Der, C.J., T. Finkel, and G.M. Cooper, *Biological and biochemical properties of human rasH genes mutated at codon 61.* Cell, 1986. **44**(1): p. 167-76.

95. Fasano, O., et al., *Analysis of the transforming potential of the human H-ras gene by random mutagenesis.* Proc Natl Acad Sci U S A, 1984. **81**(13): p. 4008-12.

96. Seeburg, P.H., et al., *Biological properties of human c-Ha-ras1 genes mutated at codon 12.* Nature, 1984. **312**(5989): p. 71-5.

97. Cespedes, M.V., et al., *K-ras Asp12 mutant neither interacts with Raf, nor signals through Erk and is less tumorigenic than K-ras Val12.* Carcinogenesis, 2006. **27**(11): p. 2190-200.

98.   Bos, J.L., et al., *Amino-acid substitutions at codon 13 of the N-ras oncogene in human acute myeloid leukaemia.* Nature, 1985. **315**(6022): p. 726-30.

99.   Guerrero, S., et al., *K-ras codon 12 mutation induces higher level of resistance to apoptosis and predisposition to anchorage-independent growth than codon 13 mutation or proto-oncogene overexpression.* Cancer Res, 2000. **60**(23): p. 6750-6.

100.   Rapp, U.R., et al., *Structure and biological activity of v-raf, a unique oncogene transduced by a retrovirus.* Proc Natl Acad Sci U S A, 1983. **80**(14): p. 4218-22.

101.   Morrison, D.K., et al., *Signal transduction from membrane to cytoplasm: growth factors and membrane-bound oncogene products increase Raf-1 phosphorylation and associated protein kinase activity.* Proc Natl Acad Sci U S A, 1988. **85**(23): p. 8855-9.

102.   Emerson, S.D., et al., *Solution structure of the Ras-binding domain of c-Raf-1 and identification of its Ras interaction surface.* Biochemistry, 1995. **34**(21): p. 6911-8.

103.   Nassar, N., et al., *The 2.2 A crystal structure of the Ras-binding domain of the serine/threonine kinase c-Raf1 in complex with Rap1A and a GTP analogue.* Nature, 1995. **375**(6532): p. 554-60.

104.   Nassar, N., et al., *Ras/Rap effector specificity determined by charge reversal.* Nat Struct Biol, 1996. **3**(8): p. 723-9.

105.   Wolthuis, R.M., et al., *RalGDS-like factor (Rlf) is a novel Ras and Rap 1A-associating protein.* Oncogene, 1996. **13**(2): p. 353-62.

106.   Stephens, L.R., T.R. Jackson, and P.T. Hawkins, *Agonist-stimulated synthesis of phosphatidylinositol(3,4,5)-trisphosphate: a new intracellular signalling system?* Biochim Biophys Acta, 1993. **1179**(1): p. 27-75.

107.   Kodaki, T., et al., *The activation of phosphatidylinositol 3-kinase by Ras.* Curr Biol, 1994. **4**(9): p. 798-806.

108.   Rodriguez-Viciana, P., et al., *Role of phosphoinositide 3-OH kinase in cell transformation and control of the actin cytoskeleton by Ras.* Cell, 1997. **89**(3): p. 457-67.

109.   Geyer, M., et al., *Structure of the Ras-binding domain of RalGEF and implications for Ras binding and signalling.* Nat Struct Biol, 1997. **4**(9): p. 694-9.

110.   Huang, L., et al., *Three-dimensional structure of the Ras-interacting domain of RalGDS.* Nat Struct Biol, 1997. **4**(8): p. 609-15.

111.   Esser, D., et al., *Structure determination of the Ras-binding domain of the Ral-specific guanine nucleotide exchange factor Rlf.* Biochemistry, 1998. **37**(39): p. 13453-62.

112.   Walker, E.H., et al., *Structural insights into phosphoinositide 3-kinase catalysis and signalling.* Nature, 1999. **402**(6759): p. 313-20.

113.   Schultz, J., et al., *SMART, a simple modular architecture research tool: identification of signaling domains.* Proc Natl Acad Sci U S A, 1998. **95**(11): p. 5857-64.

114.   Letunic, I., et al., *Recent improvements to the SMART domain-based sequence annotation resource.* Nucleic Acids Res, 2002. **30**(1): p. 242-4.

115.   Vavvas, D., et al., *Identification of Nore1 as a potential Ras effector.* J Biol Chem, 1998. **273**(10): p. 5439-42.

116.   Khokhlatchev, A., et al., *Identification of a novel Ras-regulated proapoptotic pathway.* Curr Biol, 2002. **12**(4): p. 253-65.

117.   Stieglitz, B., et al., *Novel type of Ras effector interaction established between tumour suppressor NORE1A and Ras switch II.* EMBO J, 2008. **27**(14): p. 1995-2005.

118. Leevers, S.J., H.F. Paterson, and C.J. Marshall, *Requirement for Ras in Raf activation is overcome by targeting Raf to the plasma membrane.* Nature, 1994. **369**(6479): p. 411-4.

119. Marais, R., et al., *Ras recruits Raf-1 to the plasma membrane for activation by tyrosine phosphorylation.* EMBO J, 1995. **14**(13): p. 3136-45.

120. Pruitt, K. and C.J. Der, *Ras and Rho regulation of the cell cycle and oncogenesis.* Cancer Lett, 2001. **171**(1): p. 1-10.

121. Janknecht, R., et al., *Activation of ternary complex factor Elk-1 by MAP kinases.* EMBO J, 1993. **12**(13): p. 5097-104.

122. Rao, V.N. and E.S. Reddy, *elk-1 domains responsible for autonomous DNA binding, SRE:SRF interaction and negative regulation of DNA binding.* Oncogene, 1992. **7**(11): p. 2335-40.

123. Hipskind, R.A., et al., *Ets-related protein Elk-1 is homologous to the c-fos regulatory factor p62TCF.* Nature, 1991. **354**(6354): p. 531-4.

124. Dhillon, A.S., et al., *MAP kinase signalling pathways in cancer.* Oncogene, 2007. **26**(22): p. 3279-90.

125. Rodriguez-Viciana, P., et al., *Phosphatidylinositol-3-OH kinase as a direct target of Ras.* Nature, 1994. **370**(6490): p. 527-32.

126. Sjolander, A., et al., *Association of p21ras with phosphatidylinositol 3-kinase.* Proc Natl Acad Sci U S A, 1991. **88**(18): p. 7908-12.

127. Yan, J., et al., *Ras isoforms vary in their ability to activate Raf-1 and phosphoinositide 3-kinase.* J Biol Chem, 1998. **273**(37): p. 24052-6.

128. Cully, M., et al., *Beyond PTEN mutations: the PI3K pathway as an integrator of multiple inputs during tumorigenesis.* Nat Rev Cancer, 2006. **6**(3): p. 184-92.

129. Scheid, M.P. and J.R. Woodgett, *Phosphatidylinositol 3' kinase signaling in mammary tumorigenesis.* J Mammary Gland Biol Neoplasia, 2001. **6**(1): p. 83-99.

130. Scheid, M.P. and J.R. Woodgett, *PKB/AKT: functional insights from genetic models.* Nat Rev Mol Cell Biol, 2001. **2**(10): p. 760-8.

131. Datta, S.R., A. Brunet, and M.E. Greenberg, *Cellular survival: a play in three Akts.* Genes Dev, 1999. **13**(22): p. 2905-27.

132. Khwaja, A., et al., *Matrix adhesion and Ras transformation both activate a phosphoinositide 3-OH kinase and protein kinase B/Akt cellular survival pathway.* EMBO J, 1997. **16**(10): p. 2783-93.

133. Fresno Vara, J.A., et al., *PI3K/Akt signalling pathway and cancer.* Cancer Treat Rev, 2004. **30**(2): p. 193-204.

134. De Ruiter, N.D., B.M. Burgering, and J.L. Bos, *Regulation of the Forkhead transcription factor AFX by Ral-dependent phosphorylation of threonines 447 and 451.* Mol Cell Biol, 2001. **21**(23): p. 8225-35.

135. Moghadam, A.R., et al., *Ral signaling pathway in health and cancer.* Cancer Med, 2017. **6**(12): p. 2998-3013.

136. Malliri, A., et al., *Mice deficient in the Rac activator Tiam1 are resistant to Ras-induced skin tumours.* Nature, 2002. **417**(6891): p. 867-71.

137. Arthur, W.T., L.A. Quilliam, and J.A. Cooper, *Rap1 promotes cell spreading by localizing Rac guanine nucleotide exchange factors.* J Cell Biol, 2004. **167**(1): p. 111-22.

138. Yamauchi, J., et al., *Ras activation of a Rac1 exchange factor, Tiam1, mediates neurotrophin-3-induced Schwann cell migration.* Proc Natl Acad Sci U S A, 2005. **102**(41): p. 14889-94.

139. Zhadanov, A.B., et al., *Absence of the tight junctional protein AF-6 disrupts epithelial cell-cell junctions and cell polarity during mouse development.* Curr Biol, 1999. **9**(16): p. 880-8.

140. Zhang, Z., et al., *AF6 negatively regulates Rap1-induced cell adhesion.* J Biol Chem, 2005. **280**(39): p. 33200-5.

141. Smith, M.J., et al., *Evolution of AF6-RAS association and its implications in mixed-lineage leukemia.* Nat Commun, 2017. **8**(1): p. 1099.

142. Manara, E., et al., *MLL-AF6 fusion oncogene sequesters AF6 into the nucleus to trigger RAS activation in myeloid leukemia.* Blood, 2014. **124**(2): p. 263-72.

143. Ooshio, T., et al., *Involvement of the interaction of afadin with ZO-1 in the formation of tight junctions in Madin-Darby canine kidney cells.* J Biol Chem, 2010. **285**(7): p. 5003-12.

144. Bunney, T.D., et al., *Structural and mechanistic insights into ras association domains of phospholipase C epsilon.* Mol Cell, 2006. **21**(4): p. 495-507.

145. Kelley, G.G., et al., *Phospholipase C(epsilon): a novel Ras effector.* EMBO J, 2001. **20**(4): p. 743-54.

146. Martins, M., et al., *Tumor suppressor role of phospholipase C epsilon in Ras-triggered cancers.* Proc Natl Acad Sci U S A, 2014. **111**(11): p. 4239-44.

147. Diez, D., F. Sanchez-Jimenez, and J.A. Ranea, *Evolutionary expansion of the Ras switch regulatory module in eukaryotes.* Nucleic Acids Res, 2011. **39**(13): p. 5526-37.

148. Boriack-Sjodin, P.A., et al., *The structural basis of the activation of Ras by Sos.* Nature, 1998. **394**(6691): p. 337-43.

149. Lenzen, C., et al., *Kinetic analysis by fluorescence of the interaction between Ras and the catalytic domain of the guanine nucleotide exchange factor Cdc25Mm.* Biochemistry, 1998. **37**(20): p. 7420-30.

150. Renault, L., B. Guibert, and J. Cherfils, *Structural snapshots of the mechanism and inhibition of a guanine nucleotide exchange factor.* Nature, 2003. **426**(6966): p. 525-30.

151. Killoran, R.C. and M.J. Smith, *Conformational resolution of nucleotide cycling and effector interactions for multiple small GTPases determined in parallel.* J Biol Chem, 2019. **294**(25): p. 9937-9948.

152. Bos, J.L., H. Rehmann, and A. Wittinghofer, *GEFs and GAPs: critical elements in the control of small G proteins.* Cell, 2007. **129**(5): p. 865-77.

153. Gideon, P., et al., *Mutational and kinetic analyses of the GTPase-activating protein (GAP)-p21 interaction: the C-terminal domain of GAP is not sufficient for full activity.* Mol Cell Biol, 1992. **12**(5): p. 2050-6.

154. Maegley, K.A., S.J. Admiraal, and D. Herschlag, *Ras-catalyzed hydrolysis of GTP: a new perspective from model studies.* Proc Natl Acad Sci U S A, 1996. **93**(16): p. 8160-6.

155. Scheffzek, K., et al., *The Ras-RasGAP complex: structural basis for GTPase activation and its loss in oncogenic Ras mutants.* Science, 1997. **277**(5324): p. 333-8.

156. Reynet, C. and C.R. Kahn, *Rad: a member of the Ras family overexpressed in muscle of type II diabetic humans.* Science, 1993. **262**(5138): p. 1441-4.

157. Finlin, B.S. and D.A. Andres, *Rem is a new member of the Rad- and Gem/Kir Ras-related GTP-binding protein family repressed by lipopolysaccharide stimulation.* J Biol Chem, 1997. **272**(35): p. 21982-8.

158. Finlin, B.S., et al., *Rem2, a new member of the Rem/Rad/Gem/Kir family of Ras-related GTPases.* Biochem J, 2000. **347 Pt 1**: p. 223-31.

159. Maguire, J., et al., *Gem: an induced, immediate early protein belonging to the Ras family.* Science, 1994. **265**(5169): p. 241-4.

160. Opatowsky, Y., et al., *Structure-function studies of the G-domain from human gem, a novel small G-protein.* FEBS Lett, 2006. **580**(25): p. 5959-64.

161. Splingard, A., et al., *Biochemical and structural characterization of the gem GTPase.* J Biol Chem, 2007. **282**(3): p. 1905-15.

162. Yanuar, A., et al., *Crystal structure of human Rad GTPase of the RGK-family.* Genes Cells, 2006. **11**(8): p. 961-8.

163. Correll, R.N., et al., *The RGK family of GTP-binding proteins: regulators of voltage-dependent calcium channels and cytoskeleton remodeling.* Cell Signal, 2008. **20**(2): p. 292-300.

164. Del Villar, K., et al., *C-terminal motifs found in Ras-superfamily G-proteins: CAAX and C-seven motifs.* Biochem Soc Trans, 1996. **24**(3): p. 709-13.

165. Beguin, P., et al., *Regulation of Ca2+ channel expression at the cell surface by the small G-protein kir/Gem.* Nature, 2001. **411**(6838): p. 701-6.

166. Ward, Y., et al., *The GTP binding proteins Gem and Rad are negative regulators of the Rho-Rho kinase pathway.* J Cell Biol, 2002. **157**(2): p. 291-302.

167. Finlin, B.S., et al., *Regulation of voltage-gated calcium channel activity by the Rem and Rad GTPases.* Proc Natl Acad Sci U S A, 2003. **100**(24): p. 14469-74.

168. Fischer, R., et al., *Calmodulin binds to and inhibits GTP binding of the ras-like GTPase Kir/Gem.* J Biol Chem, 1996. **271**(41): p. 25067-70.

169. Bourne, H.R., D.A. Sanders, and F. McCormick, *The GTPase superfamily: conserved structure and molecular mechanism.* Nature, 1991. **349**(6305): p. 117-27.

170. Sasson, Y., et al., *RGK family G-domain:GTP analog complex structures and nucleotide-binding properties.* J Mol Biol, 2011. **413**(2): p. 372-89.

171. Beguin, P., et al., *Nuclear sequestration of beta-subunits by Rad and Rem is controlled by 14-3-3 and calmodulin and reveals a novel mechanism for Ca2+ channel regulation.* J Mol Biol, 2006. **355**(1): p. 34-46.

172. Hsiao, B.Y., et al., *Rad GTPase inhibits the NFkappaB pathway through interacting with RelA/p65 to impede its DNA binding and target gene transactivation.* Cell Signal, 2014. **26**(7): p. 1437-44.

173. Zhang, J., et al., *Rad GTPase inhibits cardiac fibrosis through connective tissue growth factor.* Cardiovasc Res, 2011. **91**(1): p. 90-8.

174. Correll, R.N., et al., *Analysis of the Rem2 - voltage dependant calcium channel beta subunit interaction and Rem2 interaction with phosphorylated phosphatidylinositide lipids.* Cell Signal, 2008. **20**(2): p. 400-8.

175. Beguin, P., et al., *Roles of 14-3-3 and calmodulin binding in subcellular localization and function of the small G-protein Rem2.* Biochem J, 2005. **390**(Pt 1): p. 67-75.

176. Correll, R.N., et al., *Plasma membrane targeting is essential for Rem-mediated Ca2+ channel inhibition.* J Biol Chem, 2007. **282**(39): p. 28431-40.

177. Beguin, P., et al., *14-3-3 and calmodulin control subcellular distribution of Kir/Gem and its regulation of cell shape and calcium channel activity.* J Cell Sci, 2005. **118**(Pt 9): p. 1923-34.

178. Flynn, R., et al., *Activity-dependent subcellular cotrafficking of the small GTPase Rem2 and Ca2+/CaM-dependent protein kinase IIalpha.* PLoS One, 2012. **7**(7): p. e41185.

179. Liput, D.J., et al., *Rem2, a member of the RGK family of small GTPases, is enriched in nuclei of the basal ganglia.* Sci Rep, 2016. **6**: p. 25137.

180. Mahalakshmi, R.N., et al., *Nuclear localization of endogenous RGK proteins and modulation of cell shape remodeling by regulated nuclear transport.* Traffic, 2007. **8**(9): p. 1164-78.

181. Mahalakshmi, R.N., et al., *Nuclear transport of Kir/Gem requires specific signals and importin alpha5 and is regulated by calmodulin and predicted serine phosphorylations.* Traffic, 2007. **8**(9): p. 1150-63.

182. Pang, C., et al., *Rem GTPase interacts with the proximal CaV1.2 C-terminus and modulates calcium-dependent channel inactivation.* Channels (Austin), 2010. **4**(3): p. 192-202.

183. Fan, M., et al., *Direct inhibition of P/Q-type voltage-gated Ca2+ channels by Gem does not require a direct Gem/Cavbeta interaction.* Proc Natl Acad Sci U S A, 2010. **107**(33): p. 14887-92.

184. Moyers, J.S., J. Zhu, and C.R. Kahn, *Effects of phosphorylation on function of the Rad GTPase.* Biochem J, 1998. **333 (Pt 3)**: p. 609-14.

185. Finlin, B.S. and D.A. Andres, *Phosphorylation-dependent association of the Ras-related GTP-binding protein Rem with 14-3-3 proteins.* Arch Biochem Biophys, 1999. **368**(2): p. 401-12.

186. Ward, Y., et al., *Phosphorylation of critical serine residues in Gem separates cytoskeletal reorganization from down-regulation of calcium channel activity.* Mol Cell Biol, 2004. **24**(2): p. 651-61.

187. Jhun, B.S., et al., *Adrenergic signaling controls RGK-dependent trafficking of cardiac voltage-gated L-type Ca2+ channels through PKD1.* Circ Res, 2012. **110**(1): p. 59-70.

188. Ghiretti, A.E., et al., *CaMKII-dependent phosphorylation of the GTPase Rem2 is required to restrict dendritic complexity.* J Neurosci, 2013. **33**(15): p. 6504-15.

189. Catterall, W.A., *Structure and regulation of voltage-gated Ca2+ channels.* Annu Rev Cell Dev Biol, 2000. **16**: p. 521-55.

190. Mattson, M.P. and S.L. Chan, *Calcium orchestrates apoptosis.* Nat Cell Biol, 2003. **5**(12): p. 1041-3.

191. Chen, M., et al., *Bid is cleaved by calpain to an active fragment in vitro and during myocardial ischemia/reperfusion.* J Biol Chem, 2001. **276**(33): p. 30724-8.

192. Gil-Parrado, S., et al., *Ionomycin-activated calpain triggers apoptosis. A probable role for Bcl-2 family members.* J Biol Chem, 2002. **277**(30): p. 27217-26.

193. Wang, H.G., et al., *Ca2+-induced apoptosis through calcineurin dephosphorylation of BAD.* Science, 1999. **284**(5412): p. 339-43.

194. Finlin, B.S., et al., *Regulation of L-type Ca2+ channel activity and insulin secretion by the Rem2 GTPase.* J Biol Chem, 2005. **280**(51): p. 41864-71.

195. Chen, H., et al., *Expression of Rem2, an RGK family small GTPase, reduces N-type calcium current without affecting channel surface density.* J Neurosci, 2005. **25**(42): p. 9762-72.

196. Manning, J.R., et al., *Rad GTPase deletion increases L-type calcium channel current leading to increased cardiac contraction.* J Am Heart Assoc, 2013. **2**(6): p. e000459.

197. Magyar, J., et al., *Rem-GTPase regulates cardiac myocyte L-type calcium current.* Channels (Austin), 2012. **6**(3): p. 166-73.

198. Sasaki, T., et al., *Direct inhibition of the interaction between alpha-interaction domain and beta-interaction domain of voltage-dependent Ca2+ channels by Gem.* J Biol Chem, 2005. **280**(10): p. 9308-12.

199. Finlin, B.S., et al., *Analysis of the complex between Ca2+ channel beta-subunit and the Rem GTPase.* J Biol Chem, 2006. **281**(33): p. 23557-66.

200. Xu, X., S.O. Marx, and H.M. Colecraft, *Molecular mechanisms, and selective pharmacological rescue, of Rem-inhibited CaV1.2 channels in heart.* Circ Res, 2010. **107**(5): p. 620-30.

201. Richards, M.W., A.J. Butcher, and A.C. Dolphin, *Ca2+ channel beta-subunits: structural insights AID our understanding.* Trends Pharmacol Sci, 2004. **25**(12): p. 626-32.

202. Yang, T., et al., *Rem, a member of the RGK GTPases, inhibits recombinant CaV1.2 channels using multiple mechanisms that require distinct conformations of the GTPase.* J Physiol, 2010. **588**(Pt 10): p. 1665-81.

203. Burbee, D.G., et al., *Epigenetic inactivation of RASSF1A in lung and breast cancers and malignant phenotype suppression.* J Natl Cancer Inst, 2001. **93**(9): p. 691-9.

204. Pfeifer, G.P. and R. Dammann, *Methylation of the tumor suppressor gene RASSF1A in human tumors.* Biochemistry (Mosc), 2005. **70**(5): p. 576-83.

205. Agathanggelou, A., et al., *Methylation associated inactivation of RASSF1A from region 3p21.3 in lung, breast and ovarian tumours.* Oncogene, 2001. **20**(12): p. 1509-18.

206. Yu, M.Y., et al., *Hypermethylation of the tumor suppressor gene RASSFIA and frequent concomitant loss of heterozygosity at 3p21 in cervical cancers.* Int J Cancer, 2003. **105**(2): p. 204-9.

207. Chan, M.W., et al., *Frequent hypermethylation of promoter region of RASSF1A in tumor tissues and voided urine of urinary bladder cancer patients.* Int J Cancer, 2003. **104**(5): p. 611-6.

208. Tomizawa, Y., et al., *Clinicopathological significance of epigenetic inactivation of RASSF1A at 3p21.3 in stage I lung adenocarcinoma.* Clin Cancer Res, 2002. **8**(7): p. 2362-8.

209. Tommasi, S., et al., *Tumor susceptibility of Rassf1a knockout mice.* Cancer Res, 2005. **65**(1): p. 92-8.

210. Foley, C.J., et al., *Dynamics of RASSF1A/MOAP-1 association with death receptors.* Mol Cell Biol, 2008. **28**(14): p. 4520-35.

211. Hamilton, G., et al., *ATM regulates a RASSF1A-dependent DNA damage response.* Curr Biol, 2009. **19**(23): p. 2020-5.

212. Ponting, C.P. and D.R. Benjamin, *A novel family of Ras-binding domains.* Trends Biochem Sci, 1996. **21**(11): p. 422-5.

213. Wohlgemuth, S., et al., *Recognizing and defining true Ras binding domains I: biochemical analysis.* J Mol Biol, 2005. **348**(3): p. 741-58.

214. Guo, C., et al., *RASSF1A is part of a complex similar to the Drosophila Hippo/Salvador/Lats tumor-suppressor network.* Curr Biol, 2007. **17**(8): p. 700-5.

215. Hwang, E., et al., *Structural basis of the heterodimerization of the MST and RASSF SARAH domains in the Hippo signalling pathway.* Acta Crystallogr D Biol Crystallogr, 2014. **70**(Pt 7): p. 1944-53.

216. Hwang, E., et al., *Structural insight into dimeric interaction of the SARAH domains from Mst1 and RASSF family proteins in the apoptosis pathway.* Proc Natl Acad Sci U S A, 2007. **104**(22): p. 9236-41.

217. Rong, R., et al., *Mitotic kinase Aurora-A phosphorylates RASSF1A and modulates RASSF1A-mediated microtubule interaction and M-phase cell cycle regulation.* Oncogene, 2007. **26**(55): p. 7700-8.

218. Jiang, L., et al., *Cullin-4A.DNA damage-binding protein 1 E3 ligase complex targets tumor suppressor RASSF1A for degradation during mitosis.* J Biol Chem, 2011. **286**(9): p. 6971-8.

219. Rong, R., et al., *Tumor suppressor RASSF1A is a microtubule-binding protein that stabilizes microtubules and induces G2/M arrest.* Oncogene, 2004. **23**(50): p. 8216-30.

220. Dallol, A., et al., *Depletion of the Ras association domain family 1, isoform A-associated novel microtubule-associated protein, C19ORF5/MAP1S, causes mitotic abnormalities.* Cancer Res, 2007. **67**(2): p. 492-500.

221. Amin, K.S. and P.P. Banerjee, *The cellular functions of RASSF1A and its inactivation in prostate cancer.* J Carcinog, 2012. **11**: p. 3.

222. Shivakumar, L., et al., *The RASSF1A tumor suppressor blocks cell cycle progression and inhibits cyclin D1 accumulation.* Mol Cell Biol, 2002. **22**(12): p. 4309-18.

223. Ahmed-Choudhury, J., et al., *Transcriptional regulation of cyclin A2 by RASSF1A through the enhanced binding of p120E4F to the cyclin A2 promoter.* Cancer Res, 2005. **65**(7): p. 2690-7.

224. Whitehurst, A.W., et al., *The RASSF1A tumor suppressor restrains anaphase-promoting complex/cyclosome activity during the G1/S phase transition to promote cell cycle progression in human epithelial cells.* Mol Cell Biol, 2008. **28**(10): p. 3190-7.

225. Djos, A., et al., *The RASSF gene family members RASSF5, RASSF6 and RASSF7 show frequent DNA methylation in neuroblastoma.* Mol Cancer, 2012. **11**: p. 40.

226. Geli, J., et al., *Assessment of NORE1A as a putative tumor suppressor in human neuroblastoma.* Int J Cancer, 2008. **123**(2): p. 389-394.

227. Suryaraja, R., et al., *The E3 ubiquitin ligase Itch regulates tumor suppressor protein RASSF5/NORE1 stability in an acetylation-dependent manner.* Cell Death Dis, 2013. **4**: p. e565.

228. Fetics, S.K., et al., *Allosteric effects of the oncogenic RasQ61L mutant on Raf-RBD.* Structure, 2015. **23**(3): p. 505-516.

229. Harjes, E., et al., *GTP-Ras disrupts the intramolecular complex of C1 and RA domains of Nore1.* Structure, 2006. **14**(5): p. 881-8.

230. Brandt, R., et al., *DNA microarray analysis of pancreatic malignancies.* Pancreatology, 2004. **4**(6): p. 587-97.

231. Logsdon, C.D., et al., *Molecular profiling of pancreatic adenocarcinoma and chronic pancreatitis identifies multiple genes differentially regulated in pancreatic cancer.* Cancer Res, 2003. **63**(10): p. 2649-57.

232. Soesan, M., et al., *Extramedullary plasmacytoma: clinical behaviour and response to treatment.* Ann Oncol, 1992. **3**(1): p. 51-7.

233. Tan, D.S., et al., *PPM1D is a potential therapeutic target in ovarian clear cell carcinomas.* Clin Cancer Res, 2009. **15**(7): p. 2269-80.

234. Recino, A., et al., *Human RASSF7 regulates the microtubule cytoskeleton and is required for spindle formation, Aurora B activation and chromosomal congression during mitosis.* Biochem J, 2010. **430**(2): p. 207-13.

235. Morris, J.A., et al., *DISC1 (Disrupted-In-Schizophrenia 1) is a centrosome-associated protein that interacts with MAP1A, MIPT3, ATF4/5 and NUDEL: regulation and loss of interaction with mutation.* Hum Mol Genet, 2003. **12**(13): p. 1591-608.

236. Tsang, H.T., et al., *A systematic analysis of human CHMP protein interactions: additional MIT domain-containing proteins bind to multiple components of the human ESCRT III complex.* Genomics, 2006. **88**(3): p. 333-46.

237. Yasui, S., et al., *The TSC1 gene product hamartin interacts with NADE.* Mol Cell Neurosci, 2007. **35**(1): p. 100-8.

238. Sherwood, V., et al., *RASSF7 is a member of a new family of RAS association domain-containing proteins and is required for completing mitosis.* Mol Biol Cell, 2008. **19**(4): p. 1772-82.

239. Falvella, F.S., et al., *Identification of RASSF8 as a candidate lung tumor suppressor gene.* Oncogene, 2006. **25**(28): p. 3934-8.

240. Lock, F.E., et al., *The RASSF8 candidate tumor suppressor inhibits cell growth and regulates the Wnt and NF-kappaB signaling pathways.* Oncogene, 2010. **29**(30): p. 4307-16.

241. Langton, P.F., et al., *The dASPP-dRASSF8 complex regulates cell-cell adhesion during Drosophila retinal morphogenesis.* Curr Biol, 2009. **19**(23): p. 1969-78.

242. Eckfeldt, C.E., et al., *Functional analysis of human hematopoietic stem cell gene expression using zebrafish.* PLoS Biol, 2005. **3**(8): p. e254.

243. Hitomi, J., et al., *Identification of a molecular signaling network that regulates a cellular necrotic cell death pathway.* Cell, 2008. **135**(7): p. 1311-23.

244. Dallol, A., et al., *RASSF1A interacts with microtubule-associated proteins and modulates microtubule dynamics.* Cancer Res, 2004. **64**(12): p. 4112-6.

245. Liu, L., et al., *Control of microtubule stability by the RASSF1A tumor suppressor.* Oncogene, 2003. **22**(50): p. 8125-36.

246. Donninger, H., M.D. Vos, and G.J. Clark, *The RASSF1A tumor suppressor.* J Cell Sci, 2007. **120**(Pt 18): p. 3163-72.

247. Kumari, G., et al., *Nuclear transport of Ras-associated tumor suppressor proteins: different transport receptor binding specificities for arginine-rich nuclear targeting signals.* J Mol Biol, 2007. **367**(5): p. 1294-311.

248. Chin, L., et al., *Essential role for oncogenic Ras in tumour maintenance.* Nature, 1999. **400**(6743): p. 468-72.

249. Fisher, G.H., et al., *Induction and apoptotic regression of lung adenocarcinomas by regulation of a K-Ras transgene in the presence and absence of tumor suppressor genes.* Genes Dev, 2001. **15**(24): p. 3249-62.

250. Hueber, A.O. and G.I. Evan, *Traps to catch unwary oncogenes.* Trends Genet, 1998. **14**(9): p. 364-7.

251. Downward, J., *Ras signalling and apoptosis.* Curr Opin Genet Dev, 1998. **8**(1): p. 49-54.

252. Cox, A.D. and C.J. Der, *The dark side of Ras: regulation of apoptosis.* Oncogene, 2003. **22**(56): p. 8999-9006.

253. Vos, M.D., et al., *The RASSF1A tumor suppressor activates Bax via MOAP-1.* J Biol Chem, 2006. **281**(8): p. 4557-63.

254. Vos, M.D., et al., *Ras uses the novel tumor suppressor RASSF1 as an effector to mediate apoptosis.* J Biol Chem, 2000. **275**(46): p. 35669-72.

255. Ortiz-Vega, S., et al., *The putative tumor suppressor RASSF1A homodimerizes and heterodimerizes with the Ras-GTP binding protein Nore1.* Oncogene, 2002. **21**(9): p. 1381-90.

256. Chan, J.J., et al., *Comparative analysis of interactions of RASSF1-10.* Adv Biol Regul, 2013. **53**(2): p. 190-201.

257. Vos, M.D., et al., *RASSF2 is a novel K-Ras-specific effector and potential tumor suppressor.* J Biol Chem, 2003. **278**(30): p. 28045-51.

258. Donninger, H., et al., *The Ras effector RASSF2 controls the PAR-4 tumor suppressor.* Mol Cell Biol, 2010. **30**(11): p. 2608-20.

259. Eckfeld, K., et al., *RASSF4/AD037 is a potential ras effector/tumor suppressor of the RASSF family.* Cancer Res, 2004. **64**(23): p. 8688-93.

260. Park, J., et al., *Tumor suppressor ras association domain family 5 (RASSF5/NORE1) mediates death receptor ligand-induced apoptosis.* J Biol Chem, 2010. **285**(45): p. 35029-38.

261. Vos, M.D., et al., *The pro-apoptotic Ras effector Nore1 may serve as a Ras-regulated tumor suppressor in the lung.* J Biol Chem, 2003. **278**(24): p. 21938-43.

262. Allen, N.P., et al., *RASSF6 is a novel member of the RASSF family of tumor suppressors.* Oncogene, 2007. **26**(42): p. 6203-11.

263. Ikeda, M., et al., *Ras-association domain family protein 6 induces apoptosis via both caspase-dependent and caspase-independent pathways.* Exp Cell Res, 2007. **313**(7): p. 1484-95.

264. Rodriguez-Viciana, P., C. Sabatier, and F. McCormick, *Signaling specificity by Ras family GTPases is determined by the full spectrum of effectors they regulate.* Mol Cell Biol, 2004. **24**(11): p. 4943-54.

265. Yu, F.X. and K.L. Guan, *The Hippo pathway: regulators and regulations.* Genes Dev, 2013. **27**(4): p. 355-71.

266. Harvey, K.F., C.M. Pfleger, and I.K. Hariharan, *The Drosophila Mst ortholog, hippo, restricts growth and cell proliferation and promotes apoptosis.* Cell, 2003. **114**(4): p. 457-67.

267. Pantalacci, S., N. Tapon, and P. Leopold, *The Salvador partner Hippo promotes apoptosis and cell-cycle exit in Drosophila.* Nat Cell Biol, 2003. **5**(10): p. 921-7.

268. Kango-Singh, M., et al., *Shar-pei mediates cell proliferation arrest during imaginal disc growth in Drosophila.* Development, 2002. **129**(24): p. 5719-30.

269. Tapon, N., et al., *salvador Promotes both cell cycle exit and apoptosis in Drosophila and is mutated in human cancer cell lines.* Cell, 2002. **110**(4): p. 467-78.

270. Lai, Z.C., et al., *Control of cell proliferation and apoptosis by mob as tumor suppressor, mats.* Cell, 2005. **120**(5): p. 675-85.

271. Justice, R.W., et al., *The Drosophila tumor suppressor gene warts encodes a homolog of human myotonic dystrophy kinase and is required for the control of cell shape and proliferation.* Genes Dev, 1995. **9**(5): p. 534-46.

272. Xu, T., et al., *Identifying tumor suppressors in genetic mosaics: the Drosophila lats gene encodes a putative protein kinase.* Development, 1995. **121**(4): p. 1053-63.

273. Huang, J., et al., *The Hippo signaling pathway coordinately regulates cell proliferation and apoptosis by inactivating Yorkie, the Drosophila Homolog of YAP.* Cell, 2005. **122**(3): p. 421-34.

274. Zhao, B., et al., *Inactivation of YAP oncoprotein by the Hippo pathway is involved in cell contact inhibition and tissue growth control.* Genes Dev, 2007. **21**(21): p. 2747-61.

275. Wei, X., T. Shimizu, and Z.C. Lai, *Mob as tumor suppressor is activated by Hippo kinase for growth inhibition in Drosophila.* EMBO J, 2007. **26**(7): p. 1772-81.

276. Wu, S., et al., *hippo encodes a Ste-20 family protein kinase that restricts cell proliferation and promotes apoptosis in conjunction with salvador and warts.* Cell, 2003. **114**(4): p. 445-56.

277. Deng, Y., et al., *Hippo activation through homodimerization and membrane association for growth inhibition and organ size control.* Dev Biol, 2013. **375**(2): p. 152-9.

278. Boggiano, J.C., P.J. Vanderzalm, and R.G. Fehon, *Tao-1 phosphorylates Hippo/MST kinases to regulate the Hippo-Salvador-Warts tumor suppressor pathway.* Dev Cell, 2011. **21**(5): p. 888-95.

279. Poon, C.L., et al., *The sterile 20-like kinase Tao-1 controls tissue growth by regulating the Salvador-Warts-Hippo pathway.* Dev Cell, 2011. **21**(5): p. 896-906.

280. Callus, B.A., A.M. Verhagen, and D.L. Vaux, *Association of mammalian sterile twenty kinases, Mst1 and Mst2, with hSalvador via C-terminal coiled-coil domains, leads to its stabilization and phosphorylation.* FEBS J, 2006. **273**(18): p. 4264-76.

281. Praskova, M., F. Xia, and J. Avruch, *MOBKL1A/MOBKL1B phosphorylation by MST1 and MST2 inhibits cell proliferation.* Curr Biol, 2008. **18**(5): p. 311-21.

282. Chan, E.H., et al., *The Ste20-like kinase Mst2 activates the human large tumor suppressor kinase Lats1.* Oncogene, 2005. **24**(12): p. 2076-86.

283. Oh, H. and K.D. Irvine, *In vivo regulation of Yorkie phosphorylation and localization.* Development, 2008. **135**(6): p. 1081-8.

284. Ren, F., L. Zhang, and J. Jiang, *Hippo signaling regulates Yorkie nuclear localization and activity through 14-3-3 dependent and independent mechanisms.* Dev Biol, 2010. **337**(2): p. 303-12.

285. Wu, S., et al., *The TEAD/TEF family protein Scalloped mediates transcriptional output of the Hippo growth-regulatory pathway.* Dev Cell, 2008. **14**(3): p. 388-98.

286. Vassilev, A., et al., *TEAD/TEF transcription factors utilize the activation domain of YAP65, a Src/Yes-associated protein localized in the cytoplasm.* Genes Dev, 2001. **15**(10): p. 1229-41.

287. Zhao, B., et al., *TEAD mediates YAP-dependent gene induction and growth control.* Genes Dev, 2008. **22**(14): p. 1962-71.

288. Alarcon, C., et al., *Nuclear CDKs drive Smad transcriptional activation and turnover in BMP and TGF-beta pathways.* Cell, 2009. **139**(4): p. 757-69.

289. Varelas, X., et al., *TAZ controls Smad nucleocytoplasmic shuttling and regulates human embryonic stem-cell self-renewal.* Nat Cell Biol, 2008. **10**(7): p. 837-48.

290. Ferrigno, O., et al., *Yes-associated protein (YAP65) interacts with Smad7 and potentiates its inhibitory activity against TGF-beta/Smad signaling.* Oncogene, 2002. **21**(32): p. 4879-84.

291. Yagi, R., et al., *A WW domain-containing yes-associated protein (YAP) is a novel transcriptional co-activator.* EMBO J, 1999. **18**(9): p. 2551-62.

292. Strano, S., et al., *Physical interaction with Yes-associated protein enhances p73 transcriptional activity.* J Biol Chem, 2001. **276**(18): p. 15164-73.

293. Komuro, A., et al., *WW domain-containing protein YAP associates with ErbB-4 and acts as a co-transcriptional activator for the carboxyl-terminal fragment of ErbB-4 that translocates to the nucleus.* J Biol Chem, 2003. **278**(35): p. 33334-41.

294. Polesello, C., et al., *The Drosophila RASSF homolog antagonizes the hippo pathway.* Curr Biol, 2006. **16**(24): p. 2459-65.

295. Ribeiro, P.S., et al., *Combined functional genomic and proteomic approaches identify a PP2A complex as a negative regulator of Hippo signaling.* Mol Cell, 2010. **39**(4): p. 521-34.

296. Ikeda, M., et al., *Hippo pathway-dependent and -independent roles of RASSF6.* Sci Signal, 2009. **2**(90): p. ra59.

297. Praskova, M., et al., *Regulation of the MST1 kinase by autophosphorylation, by the growth inhibitory proteins, RASSF1 and NORE1, and by Ras.* Biochem J, 2004. **381**(Pt 2): p. 453-62.

298. Oh, H.J., et al., *Role of the tumor suppressor RASSF1A in Mst1-mediated apoptosis.* Cancer Res, 2006. **66**(5): p. 2562-9.

299. Yee, K.S. and E. O'Neill, *YAP1--friend and foe.* Cell Cycle, 2010. **9**(8): p. 1447-8.

300. Papaspyropoulos, A., et al., *RASSF1A uncouples Wnt from Hippo signalling and promotes YAP mediated differentiation via p73.* Nat Commun, 2018. **9**(1): p. 424.

301. Kapoor, A., et al., *Yap1 Activation Enables Bypass of Oncogenic Kras Addiction in Pancreatic Cancer.* Cell, 2019. **179**(5): p. 1239.

302. Tu, B., et al., *YAP1 oncogene is a context-specific driver for pancreatic ductal adenocarcinoma.* JCI Insight, 2019. **4**(21).

303. Singh, K., et al., *Mst1/2 kinases restrain transformation in a novel transgenic model of Ras driven non-small cell lung cancer.* Oncogene, 2020. **39**(5): p. 1152-1164.

304. El-Kalla, M., C. Onyskiw, and S. Baksh, *Functional importance of RASSF1A microtubule localization and polymorphisms.* Oncogene, 2010. **29**(42): p. 5729-40.

305. Dallol, A., et al., *RAN GTPase is a RASSF1A effector involved in controlling microtubule organization.* Curr Biol, 2009. **19**(14): p. 1227-32.

306. Chatzifrangkeskou, M., et al., *RASSF1A is required for the maintenance of nuclear actin levels.* EMBO J, 2019. **38**(16): p. e101168.

307. Chen, Y.J., et al., *RASSF4 controls SOCE and ER-PM junctions through regulation of PI(4,5)P2.* J Cell Biol, 2017. **216**(7): p. 2011-2025.

308. Armesilla, A.L., et al., *Novel functional interaction between the plasma membrane Ca2+ pump 4b and the proapoptotic tumor suppressor Ras-associated factor 1 (RASSF1).* J Biol Chem, 2004. **279**(30): p. 31318-28.

309. Mohamed, T.M., et al., *The tumour suppressor Ras-association domain family protein 1A (RASSF1A) regulates TNF-alpha signalling in cardiomyocytes.* Cardiovasc Res, 2014. **103**(1): p. 47-59.

310. Yang, T., A. Puckerin, and H.M. Colecraft, *Distinct RGK GTPases differentially use alpha1- and auxiliary beta-binding-dependent mechanisms to inhibit CaV1.2/CaV2.2 channels.* PLoS One, 2012. **7**(5): p. e37079.

311. Dabral, S., et al., *A RASSF1A-HIF1alpha loop drives Warburg effect in cancer and pulmonary hypertension.* Nat Commun, 2019. **10**(1): p. 2130.

312. Baksh, S., et al., *The tumor suppressor RASSF1A and MAP-1 link death receptor signaling to Bax conformational change and cell death.* Mol Cell, 2005. **18**(6): p. 637-50.

313. Zhang, W., et al., *Downstream of mutant KRAS, the transcription regulator YAP is essential for neoplastic progression to pancreatic ductal adenocarcinoma.* Sci Signal, 2014. **7**(324): p. ra42.

314. Mohamed, A.D., et al., *Analysis of the relationship between the KRAS G12V oncogene and the Hippo effector YAP1 in embryonal rhabdomyosarcoma.* Sci Rep, 2018. **8**(1): p. 15674.

315. Coggins, G.E., et al., *YAP1 Mediates Resistance to MEK1/2 Inhibition in Neuroblastomas with Hyperactivated RAS Signaling.* Cancer Res, 2019. **79**(24): p. 6204-6214.

316. Bertran, M.T., et al., *ASPP proteins discriminate between PP1 catalytic subunits through their SH3 domain and the PP1 C-tail.* Nat Commun, 2019. **10**(1): p. 771.

317. Hauri, S., et al., *Interaction proteome of human Hippo signaling: modular control of the co-activator YAP1.* Mol Syst Biol, 2013. **9**: p. 713.

318. Ding, H.F., et al., *Oncogene-dependent regulation of caspase activation by p53 protein in a cell-free system.* J Biol Chem, 1998. **273**(43): p. 28378-83.

319. Adams, J.M. and S. Cory, *Apoptosomes: engines for caspase activation.* Curr Opin Cell Biol, 2002. **14**(6): p. 715-20.

320. Samuels-Lev, Y., et al., *ASPP proteins specifically stimulate the apoptotic function of p53.* Mol Cell, 2001. **8**(4): p. 781-94.

321. White, M.A., et al., *Multiple Ras functions can contribute to mammalian cell transformation.* Cell, 1995. **80**(4): p. 533-41.

322. Dubois, F., et al., *A role for RASSF1A in tunneling nanotube formation between cells through GEFH1/Rab11 pathway control.* Cell Commun Signal, 2018. **16**(1): p. 66.

323. Ma, S., et al., *The Hippo Pathway: Biology and Pathophysiology.* Annu Rev Biochem, 2019. **88**: p. 577-604.

324. van der Weyden, L., et al., *The RASSF1A isoform of RASSF1 promotes microtubule stability and suppresses tumorigenesis.* Mol Cell Biol, 2005. **25**(18): p. 8356-67.

325. Pefani, D.E., et al., *TGF-beta Targets the Hippo Pathway Scaffold RASSF1A to Facilitate YAP/SMAD2 Nuclear Translocation.* Mol Cell, 2016. **63**(1): p. 156-66.